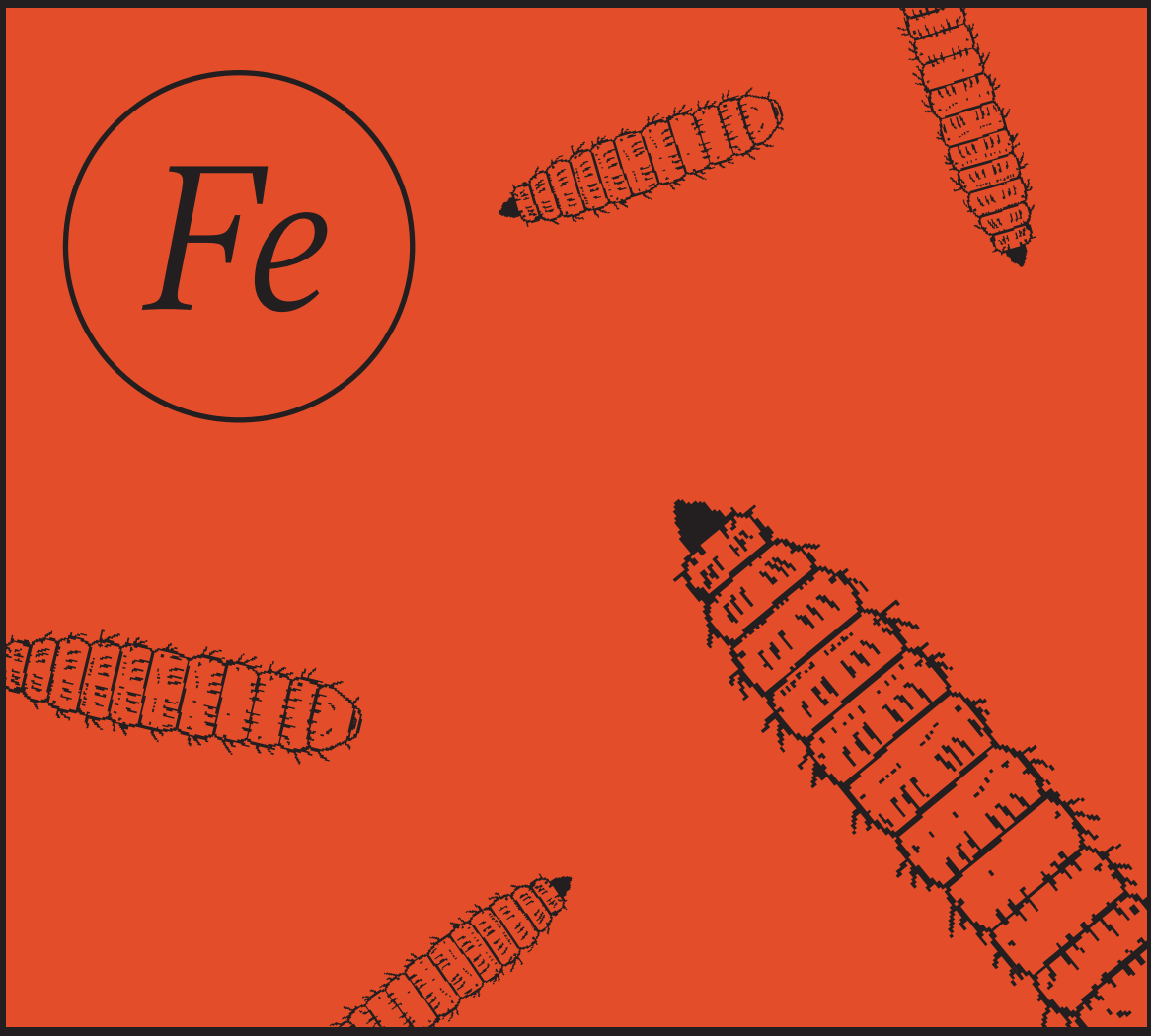


THE POWER OF METALCORE

Iron Biofortification of Black Soldier Fly Larvae as an enhanced micronutrient source

Tomer First

Propositions:

1. The entoferritin-based iron accumulation capacity of black soldier fly larvae will increase their value in feed and food markets.
   (This thesis)

2. Substrate requirements for black soldier fly larvae will be redefined as instruments for nutritional design rather than constraints for growth optimization.
   (This thesis)

3. The success of edible insects in feed markets diverts them from their original purpose as an alternative protein source for food.

4. A meatless future will deepen rather than resolve iron deficiency.

5. In life sciences, the dogma of statistically valid ‘triplicates’ reduces empiricism to ritual rather than scientific necessity.

6. Blind endorsement of traditional practices within food systems undermines innovation and the pursuit of scientific understanding.

7. The rigidity of EU food policies hampers the development of credible solutions to environmental decline.

Propositions belonging to the thesis, entitled:
The Power of Metalcore: Iron Biofortification of Black Soldier Fly Larvae as an Enhanced Micronutrient Source

Tomer First

Wageningen, 29/04/2026

THE POWER OF METALCORE

Iron Biofortification of Black Soldier Fly Larvae
as an enhanced micronutrient source

Tomer First

Thesis comittee:

Promotor
Prof. Dr Vincenzo Fogliano
Professor of Food Quality and Design
Wageningen University & Research

Co-promotor
Dr Maryia Mishyna
Assistant professor in Food Quality and Design
Wageningen University & Research

Other members
Prof. Dr Bregje Wertheim, Wageningen University & Research
Dr Alida Melse-Boonstra, Wageningen University & Research
Dr Ljubinka Francuski, Protix, Bergen op Zoom
Dr Simone Mancini, Università di Pisa, Italy

This research was conducted under the auspices of the VLAG Graduate School (Biobased, Biomolecular, Chemical, Food and Nutrition Sciences).

THE POWER OF METALCORE

Iron Biofortification of Black Soldier Fly Larvae
as an enhanced micronutrient source

Tomer First

Thesis
submitted in fulfilment of the requirements for the degree of doctor
at Wageningen University
by the authority of the Rector Magnificus,
Prof. Dr C. Kroeze,
in the presence of the
Thesis Committee appointed by the Academic Board
to be defended in public
on Wednesday 29 April 2026
at 3:30 p.m. in the Omnia Auditorium.

Tomer First

The Power of Metalcore - Iron Biofortification of Black Soldier Fly Larvae as an enhanced micronutrient source, 204 pages

PhD thesis, Wageningen University, Wageningen, the Netherlands (2026)

With references, with summary in English

http://doi.org/10.18174/681878

"With a little will, and a little skill..."

TABLE OF CONTENTS

Chapter 1: General Introduction *06*

Chapter 2: Entoferritin: an Innovative Iron Source for Human Consumption *28*

Chapter 3: Strike While the Iron Is Hot: Unravelling the Impact of Dietary Iron on Two Edible Insects *50*

Chapter 4: Forged in Iron: Molecular Insights into Iron Tolerance in *Hermetia illucens* *80*

Chapter 5: Built by Iron, Changed by Heat: Mineral Bioaccessibility in Iron-Fortified and Processed *Hermetia illucens* larvae *120*

Chapter 6: General Discussion *150*

Scientific Summary *184*

Appendices *188*

CHAPTER

01

General Introduction

1. A Giant catastrophe

Two interrelated global challenges threaten the long-term sustainability of human societies: climate change and population growth. Climate change, driven by excessive greenhouse gas emissions from anthropogenic activities, has led to rising global temperatures, sea-level rise, and an increased frequency of extreme weather events. These changes place substantial stress on the global food system, compromising its efficiency, stability, and resilience (Wheeler & von Braun, 2013). In parallel, the global population is projected to approach 10 billion by 2050, significantly increasing the demand for food and natural resources. The food supply chain lies at the nexus of both crises, acting as a major contributor to climate change while also being highly susceptible to its impacts. Livestock production alone accounts for nearly 15% of global greenhouse gas emissions. Furthermore, current trends suggest that global meat consumption will double by 2050, exacerbating the environmental pressures associated with conventional animal agriculture (Godfray *et al.*, 2010; Van Eenennaam, 2024). These trends underscore the need to reduce the environmental footprint of animal-source foods while still providing nutrient-rich diets.

2. A tiny solution

1.2.1. Edible insects

One pathway to achieving this involves both the integration of alternative protein sources and the adoption of more sustainable and cost-efficient practices within existing animal-based production systems (Wood & Tavan, 2022). Edible insects have emerged both as a viable alternative protein source for direct human consumption and as a sustainable feed ingredient that can enhance the efficiency of mainstream animal production systems. Insects can be mass-reared under controlled conditions with significantly lower requirements for land, water, and feed compared to traditional livestock as illustrated in Figure 1.1. Many species are also capable of converting organic side streams and waste into high-quality biomass, offering additional advantages in terms of resource efficiency and circularity (van Huis, 2020). Insects can provide protein of comparable quality to conventional livestock, along with beneficial fatty acids and a chitin-rich exoskeleton (Rumpold & Schlüter, 2013). Unlike traditional insect harvesting, modern edible insect production is based on farming systems comparable to those used in conventional animal agriculture, enabling scalability and regulatory integration (van Huis, 2020).

These farming systems are adaptable to both industrial and smallholder contexts. At the

industrial scale, companies operate in automated insect farms that manage the entire production cycle, converting food waste into protein, oil, and frass while contributing to waste reduction and circular agriculture (Facchini *et al.*, 2022; Protix, 2025). At the smallholder scale, insects can be reared on locally available organic waste such as crop residues and animal manure, producing feed for livestock while accelerating fertilizer generation, better disposing of biowaste and supporting local circular farming systems (Madau *et al.*, 2020; Sokame *et al.*, 2024).

Among the species considered suitable for insect farming, mealworms, crickets and black soldier flies have received particular attention. These species exhibit favorable amino acid compositions and are suitable for inclusion in both human diets and the feed of omnivorous livestock such as pigs, poultry and fish (van Huis, 2020). Additionally, certain insect species are rich in micronutrients, including minerals such as iron, further supporting their potential role in sustainable food systems (First *et al.*, 2024; Manditsera *et al.*, 2019; Seyedalmoosavi *et al.*, 2023).

1.2.2. Black soldier fly stands out

Among these farmed species, the black soldier fly (*Hermetia illucens*, BSF) has attracted considerable commercial interest, specifically in organic waste conversion, aquaculture, and feed for poultry and pigs (Bukchin-Peles *et al.*, 2025; Osuch *et al.*, 2024; Radhakrishnan *et al.*, 2023; Siddiqui *et al.*, 2022). Notably, BSF larvae also contain substantially higher iron concentrations than most other commonly reared edible insect species (Mwangi, Oonincx, Stouten, Veenenbos, Melse-Boonstra, Dicke, & van Loon, 2018). Although BSF is currently used almost exclusively as feed, regulatory changes may enable its future entry into the human food sector. To support this potential expansion, consumer research further indicates that BSF larvae as food is viewed as acceptable. In a study conducted in the United States, participants reported being comfortable tasting cookies containing a modest percentage of BSFL flour and French fries fried in oil containing a modest proportion of BSFL fat (Higa *et al.*, 2021).

This combination of environmental sustainability, scalability, and nutritional value has positioned edible insects as an emerging component of future food systems. Yet while their role as alternative proteins is increasingly recognized, their potential as sources of essential micronutrients such as iron has been far less explored.

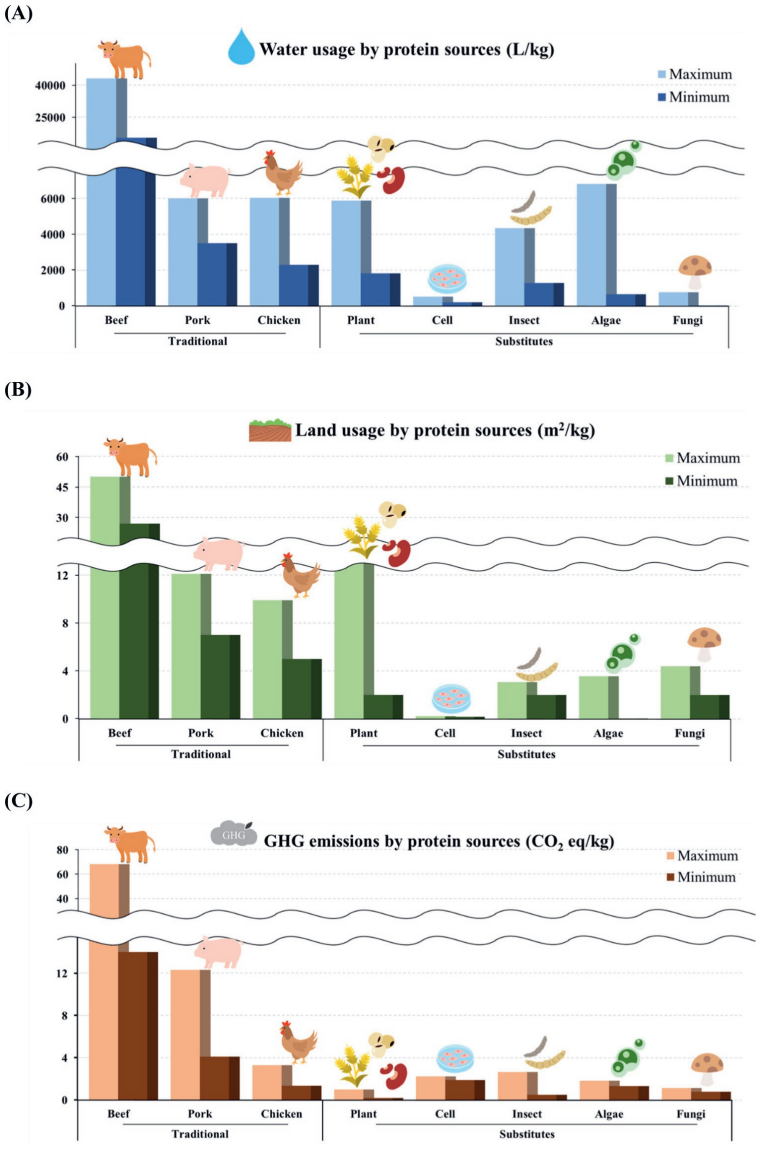


Figure 1.1 (A) Maximum (light blue) and minimum (blue) liters of water required to produce one kilogram of traditional or alternative meat; (B) Maximum (light green) and minimum (green) land area required to produce one kg of traditional or alternative meat; (C) Maximum (peach) and minimum (brown) carbon dioxide equivalent emissions associated with the production of one kilogram of traditional or alternative meat. Data are modeled using production parameters from the following species: Plant: wheat, oats, beans; Cell: cultured meat; Insect: *Tenebrio molitor*, Zophobas morio; Algae: Desmodesmus subspicatus, Arthrospira platensis; Fungi: Fusarium venenatum. Published by Lee *et al.* (2025).

3. Dietary iron

1.3.1. Occurrence

All documented complex life forms cannot exist without the utilization of iron. Due to its redox flexibility, where it can exist either in a reduced form (Fe^{2+}, ferrous) or an oxidized form (Fe^{3+}, ferric), it can act as an efficient electron carrier and catalytic cofactor in numerous biochemical reactions (Wade *et al.*, 2021). This versatility enables iron to participate in essential processes such as cellular respiration, oxygen transport, DNA synthesis, and metabolic regulation. On the other hand, the unique parameters of this element make it so that it can act as a catalyst for reactive oxygen species (ROS) production through the Fenton reaction. These ROS can disrupt many biological processes due to their high reactivity towards DNA, proteins, and other biological targets, a property that stems from their unpaired electrons and strong oxidizing potential (Dev & Babitt, 2017). Given the complexity of handling iron, iron absorption has limited efficiency to both humans and livestock alike. Approximately 25% of the human population suffers from iron deficiency anemia, and the vast majority of farmed pigs are under iron supplementation treatment. The "main" mechanism for iron absorption for both humans and pigs is through the absorption of iron sourced in heme iron. There are specific channels and iron transporters which interact with iron only sourced from heme, making it significantly more bioavailable compared to all other dietary iron sources (Auerbach *et al.*, 2025; Kim *et al.*, 2018). Conventional animal proteins, such as beef, poultry, and pork, are the most widely consumed and contain the most bioavailable form of dietary protein. They are also the best sources of dietary iron due to their high iron content, which in beef meals can reach approximately 60% of the total iron. In these protein sources, heme iron is predominantly found in hemoglobin and myoglobin, which serve as the main oxygen-binding proteins in blood and muscle tissues (Cross *et al.*, 2012). Other heme containing proteins, such as cytochromes, catalases and peroxidases, are also present in edible tissues across a wide range of organisms. However, because they occur in much lower abundance as they are not primarily involved in oxygen transport, their contribution to total dietary iron intake is minimal, making non heme iron the predominant iron source in non-vertebrate based foods (Gallio *et al.*, 2021; Piskin *et al.*, 2022a).

1.3.2. Non heme absorption

Under the umbrella of non-heme dietary iron, two primary pathways contribute to intestinal iron absorption. The predominant mechanism involves the uptake of free

iron ions. In its ferrous form (Fe^{2+}), iron is transported from the intestinal lumen into enterocytes via the divalent metal transporter 1 (DMT1). This form of iron is most commonly found in foodstuff bound to small molecules such as Phytate complexes, organic acids, amino acids, sugars (Zielińska-Dawidziak, 2015). Under the acidic conditions found in the human gastric system, these complexes might dismantle, releasing ferrous iron for absorption (Anderson & Frazer, 2017). Although ferrous iron is soluble under physiological conditions, it is also chemically reactive and prone to oxidation. Ferric iron (Fe^{3+}), the oxidized form of iron, represents the predominant species in most dietary sources. Due to its low solubility under physiological conditions, its bioavailability is considered negligible unless it is first reduced (Anderson & Frazer, 2017). When consumed, non-heme iron is present in the ferric form, it must first be reduced to Fe^{2+} by ferrireductase enzymes (e.g., duodenal cytochrome B) located on the apical surface of enterocytes. This step is essential for its subsequent transport via DMT1 (Dutt *et al.*, 2022; First *et al.*, 2023). Additionally, interactions with dietary inhibitors such as phytates, polyphenols, and certain fibers can further promote precipitation and limit absorption (Piskin *et al.*, 2022b). Thus, diets with low heme content, such as vegetarian diets, make it difficult to absorb adequate amounts of dietary iron, especially in iron deficiency risk groups such as premenopausal women (Hunt, 2003). Moreover, oral iron supplementation, such as with ferrous sulfate, is based on the same reliance on soluble ferrous iron for absorption via DMT1. However, these supplements are often associated with low bioavailability and frequent gastrointestinal side effects (Tolkien *et al.*, 2015).

1.3.3. Ferritins as a dietary iron source

An alternative and potentially more efficient pathway for non-heme iron absorption involves the uptake of iron bound to high molecular weight complexes. This pathway depends on the iron-containing complex being absorbed across the intestinal epithelium while retaining its structural integrity. If the complex remains at least partially intact during gastric and intestinal digestion, it may enable a more controlled and sustained release of iron, potentially bypassing conventional absorption routes. In this process, iron-containing complexes may be internalized via endocytic pathways and trafficked through intracellular compartments such as endosomes and lysosomes. Within these compartments, cellular iron gradient may facilitate the controlled release of iron, providing a gradual and regulated source of bioavailable iron to the cell (Lv *et al.*, 2015).

One such complex which stands out is Ferritin. Ferritins are a major family of high

molecular weight iron-binding molecules involved in iron storage and detoxification across all domains of life. As shown in Figure 1.2, these proteins typically assemble into spherical complexes composed of multiple subunits, forming a hollow interior where iron is sequestered. Iron is taken up in the soluble ferrous form (Fe^{2+}), which is oxidized to ferric iron (Fe^{3+}) at the protein's ferroxidase centers. The ferric ions are then directed into the cavity, where they are mineralized and stored, commonly as ferrihydrite under physiological conditions (Pan *et al.*, 2008). The ferrihydrite mineral core can be readily dismantled in response to cellular iron demands, allowing controlled release of iron when needed. Depending on the organism, ferritin complexes can store hundreds to several thousand iron atoms, with storage capacity varying according to subunit composition, shell structure, and physiological conditions (Pham & Winzerling, 2010). Ferritins are generally stable across a wide range of pH values, and the mineral core of it may keep stable under gastric acidity conditions (Kim *et al.*, 2011). Purified ferritin from both animal and plant sources has been shown to exhibit iron bioavailability comparable to that of commonly used oral iron supplements (Davila-Hicks *et al.*, 2004). Moreover, known dietary iron absorption inhibitors, such as phytates and polyphenols, have limited effect on iron uptake from ferritin, suggesting that as long as the ferritin is intact, its absorption may involve a mechanism independent of the conventional non-heme DMT1-mediated pathway (Lönnerdal, 2007).

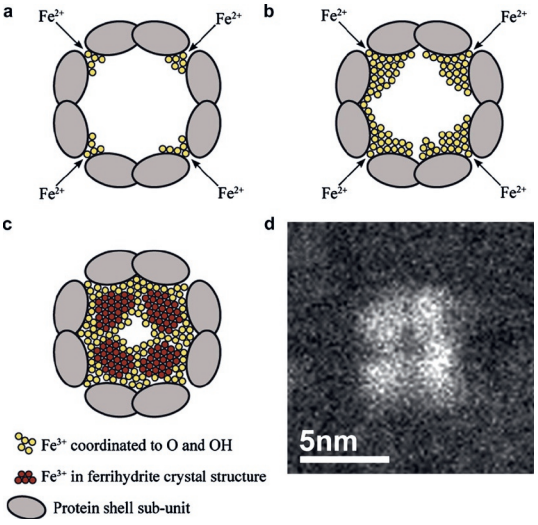


Figure 1.2. Schematic representation of iron uptake and storage in ferritin. (a–b) Ferrous iron (Fe^{2}+) enters the protein shell and is oxidized to ferric iron (Fe^{3}+), coordinated to oxygen and hydroxyl groups at the ferroxidase sites. (c) Ferric iron is subsequently deposited inside the cavity as ferrihydrite, forming a stable mineral core. (d) High-resolution electron microscopy image showing the ferritin shell and its mineralized iron core (~5 nm). Published by Pan *et al.*, (2008).

4. Edible insects in the Iron Equation

1.4.1 Iron in insects

Edible insects are increasingly investigated as sources of dietary iron. The total iron content of several species is higher than that of most plant-based foods and in some cases comparable to or exceeding levels in animal-source foods (Mwangi *et al.,* 2018). This positions insects as potential contributors to reducing the global burden of iron deficiency.

Unlike vertebrates, insects do not transport oxygen via hemoglobin or myoglobin and therefore contain little heme-bound iron. Instead, they rely on insect ferritin, namely entoferritin, as their primary iron storage and transport system. Entoferritin assembles into soluble, iron mineralizing protein complexes capable of storing thousands of iron atoms in a stable ferrihydrite core. In addition to its intracellular role, entoferritin is secreted into the hemolymph (Pham & Winzerling, 2010). From a food and feed perspective, this secreted form suggests increased water solubility, which may enhance its nutritional potential as a dietary iron source compared to conventional ferritin in plants or animals.

Experimental evidence supports the potential dietary value of entoferritin. *In vitro* digestion and absorption studies using human Caco-2 cells demonstrated that iron from grasshoppers, yellow mealworms, lesser mealworms, and crickets was absorbed at levels comparable to beef (Latunde-Dada *et al.*, 2016, Figure 1.3). The high level of absorption is most likely linked to the presence of entoferritin. Once ferritins enter cells, they can act as slow-release reservoirs of iron, delivering a steady supply rather than a rapid, potentially disruptive influx (Theil *et al.*, 2012).

In vivo studies provide additional insight. In one trial, young women with low iron stores consumed porridges fortified with mealworm. Fractional iron absorption from mealworm porridge was comparable to ferrous sulfate supplementation, and mealworm consumption did not impair absorption of supplemental iron (Hilaj *et al.*, 2022). This indicates that despite containing antinutritional factors, mealworms are a suitable and effective dietary iron source. By contrast, a comparable trial using cricket porridge showed lower fractional absorption, and cricket consumption reduced the uptake of supplemental iron (Mwangi *et al.*, 2022). These findings demonstrate that insect species differ not only in their iron content but also in their bioavailability.

Taken together, current evidence indicates that entoferritin is central to the nutritional

potential of insect-derived iron. Its solubility, stability, and capacity to provide controlled intracellular release may explain why insect iron is more bioavailable than would be expected for a non-heme source. However, important gaps remain concerning the contribution of entoferritin across insect species, the presence of alternative storage mechanisms, the influence of rearing and processing conditions, and the pathways governing uptake in the human gut. Entoferritin has not yet been systematically considered as a distinct dietary iron source, and its nutritional relevance remains poorly understood. Addressing these questions is essential to establish edible insects as reliable contributors to bioavailable dietary iron.

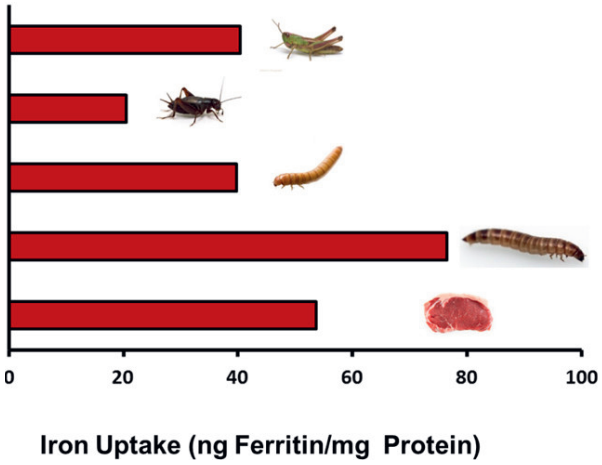


Figure 1.3 *In vitro* bioavailability of edible insects compared to beef using a CACO2 model. The insect meals tested were (from top to bottom) house crickets, grasshoppers, lesser mealworm and yellow mealworm. Published by (Latunde-Dada *et al.*, 2016).

1.4.2. Black soldier fly as an iron source

Such interspecies variation is further illustrated by black soldier fly larvae, which contain more than six times the iron concentration of the lesser mealworm when reared under physiological conditions (Mwangi, *et al.*, 2018). Despite this high iron content, little is known about the molecular organization of entoferritin in BSF, the broader mechanisms of iron storage, and whether additional storage pathways beyond entoferritin are involved. The stability, bioavailability, and behavior of BSF-derived iron during digestion and processing are also largely unexplored. BSF larvae are further recognized for their ability to accumulate heavy metals from their substrate. This trait

is often painted negatively due to the high toxicity of most heavy metals and the strict regulations against their presence in food and feed (Bessa *et al.*, 2021; Cai *et al.*, 2018; Wu *et al.*, 2020). However, while it is not known whether BSF can accumulate iron in a similar manner, their demonstrated capacity for metal uptake and storage suggests potential for exploring iron enrichment. Harnessing this capacity to enrich iron in a protein-bound form such as entoferritin could provide a foundation for targeted iron biofortification strategies.

5. Mineral biofortification

Improving the nutritional quality of foods by enhancing their micronutrient content has become a central goal in efforts to address global malnutrition (Ofori *et al.*, 2022). At the same time, foods with added nutritional value also carry greater commercial appeal, as consumers increasingly seek products that combine health benefits with convenience. Reflecting this dual importance, the global food fortification market was valued at USD 117.3 billion in 2025 and is projected to grow to USD 315.1 billion by 2035, with a compound annual growth rate of 10.4 % (FMI, 2025). In this context, biofortification, the process of increasing the micronutrient content of crops or animals during growth, offers a strategy to create food ingredients that are both nutritionally impactful and commercially competitive.

Plant biofortification has demonstrated clear successes, showing that staple foods can be enriched with essential minerals in a scalable and impactful way (Table 1.1). For example, iron levels in rice were increased by 30–40% through soil supplementation, and by more than 350% using genetic manipulation (Masuda *et al.*, 2012; Utama *et al.*, 2017). Pearl millet enriched through conventional breeding achieved increases of more than 150% in iron concentration, while calcium in carrots has been enhanced by 60% through genetic modification (Jeong & Guerinot, 2008; Kodkany *et al.*, 2013). Zinc levels in wheat have also been boosted by 29–55% via soil and foliar supplementation, and calcium in basil by around 20% through water supplementation. These examples illustrate that plant biofortification is both technically feasible and commercially relevant, with proven nutritional impact. It should be noted, however, that even when biofortified, the absolute iron content of plant foods remains considerably lower than that of animal-derived products or insects. Moreover, the non-heme form of iron in plants is less efficiently absorbed, and have a significant phytic acid content, which is a major antinutritional factor of iron absorption, leading to low iron solubility and iron bioavailability (Hackl *et al.*, 2016). Thus, plant iron biofortification can increase intake but does not fully overcome the issue of low bioavailability. As such, while plant

biofortification is a valuable public health strategy, animal and insect sources of iron continue to provide a distinct nutritional advantage.

By contrast, animal-based biofortification has been far more limited. Fortification of animal diets has not increased the iron content of milk, and no meaningful scalable enrichment of meat, which were also associated with adverse health effects (Lee *et al.,* 2008). Some improvements have been achieved for other minerals, zinc in bovine milk increased by up to 75%, and calcium by about 40% (Klein *et al.*, 2025; Wondater & Ayanie, 2023), though these examples remain exceptions rather than widespread practice.

Table 1.1. Reported examples of mineral biofortification in plants, dairy, and meat. Data include iron, zinc, and calcium enrichment achieved through soil supplementation, foliar application, classical breeding, genetic modification, or feed supplementation.

Mineral/Ingredient	Plant	Dairy	Meat
Iron	**Rice:** 30–40% increase, through soil iron supplementation (Utama *et al.*, 2017) **Rice:** Above 350% increase, through genetic manipulation (Masuda *et al.*, 2012) **Pearl millet:** Above 150% increase, through classical breeding (Kodkany *et al.*, 2013) **Finger millet:** 21% increase, through soil iron supplementation (Teklu *et al.*, 2023)	No report of significant increase	Pig leaver: 20% increase, through feed supplementation (Lee *et al.*, 2008)
Zinc	**Wheat:** 29% increase, through soil zinc supplementation (Hui *et al.*, 2025) **Wheat:** 55% increase, through foliar (Hui *et al.*, 2025) **Finger millet:** 20% increase, through soil zinc supplementation (Teklu *et al.*, 2023)	**Bovine milk:** 75% increase through feed supplementation (Klein *et al.*, 2025) **Goat milk:** a 14% increase through feed supplementation (Witkowska *et al.*, 2015)	No report of significant increase
Calcium	**Basil:** 20% increase through water calcium supplementation (D'Imperio *et al.*, 2016) **Endive:** water calcium supplementation did not affect ingredient calcium content (D'Imperio *et al.*, 2016) **Carrots:** 60% increase through genetic manipulation (Jeong & Guerinot, 2008)	**Bovine milk:** a 40% increase through feed supplementation (Wondater & Ayanie, 2023)	No report of significant increase

Biofortification strategies have shown success in plants, yet their impact remains limited by the inherently low iron content and poor bioavailability of plant-based foods. Comparable approaches in meat have so far failed to achieve meaningful enrichment.

Insects, however, present a novel and potentially more promising avenue. Their unique entoferritin-based iron storage and transport system further distinguishes them from plants and animals and may enhance their suitability for biofortification (Missirlis & Oliveira, 2022; Pham & Winzerling, 2010). Among them, the BSF larva is particularly relevant as it naturally contains high iron levels compared to other insect species and is known for its ability to accumulate metals from the substrate (Seyedalmoosavi *et al.*, 2023; Wu *et al.*, 2020). These characteristics suggest that BSF could be a suitable candidate for mineral biofortification, especially for iron.

6. Rationale thesis outline

Although edible insects are increasingly recognized for their potential to alleviate iron deficiency, several fundamental questions remain unanswered. This thesis addresses four key knowledge gaps. First, while entoferritin is proposed to play a central role in insect iron storage and possibly in human iron uptake, its structure, behavior, and nutritional relevance remain poorly understood. Second, it is unclear to what extent the iron content and composition of edible insects can be modulated through rearing manipulation, including the potential implementation of mineral biofortification strategies, and how these interventions affect yield output and quality. Third, the mechanisms and pathways involved in the absorption of insect-derived iron in the human gut, and the factors that modulate this process, are largely unknown. Fourth, most micronutrient studies have focused on a narrow range of insect species, overlooking others such as the BSF, which is both rich in iron and of high economic relevance. To address these gaps, this thesis employs a multidisciplinary approach, combining literature analysis, ecological physiology, and molecular, biochemical, and nutritional analyses, as illustrated in Figure 1.4.

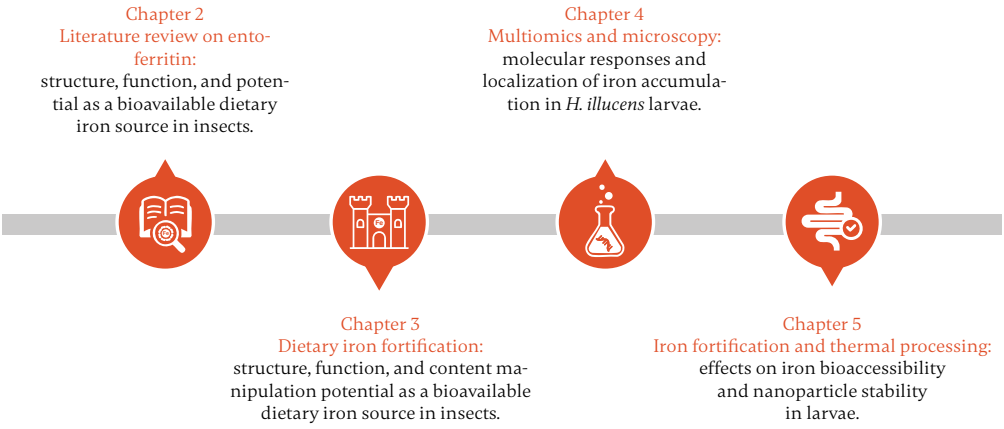


Figure 1.4. Overview of research chapters (2–5). Chapter 2 reviews entoferritin as a dietary iron source, Chapter 3 examines effects of iron fortification on insect performance and composition, Chapter 4 explores molecular responses and iron localization in *H. illucens*, and Chapter 5 assesses fortification and thermal processing effects on mineral bioaccessibility and nanoparticle stability.

Chapter 2 provides an in-depth review of entoferritin and evaluates its potential role as a bioavailable dietary iron source. This chapter utilizes current knowledge on the structure, function, and nutritional implications of entoferritin, with a focus on its presence in farmed edible insects. Additionally, it explores how entoferritin might be leveraged within insect processing and rearing systems to enhance iron delivery in both food and feed applications. This review lays the conceptual groundwork for understanding the molecular mechanisms behind iron storage and mobilization in insects, from a food and feed perspective. **Chapter 3** investigates the impact of dietary iron fortification on two economically relevant edible insect species: the lesser mealworm (Alphitobius diaperinus) and the black soldier fly. By supplementing the insect feed with graded levels of iron, this chapter assesses how iron enrichment influences insect growth performance, survival, and developmental parameters. In addition, changes in the insects' macronutrient and micronutrient composition, including total iron concentration. **Chapter 4** presents an integrated multiomics analysis of black soldier fly larvae reared on diets with varying iron concentrations. Combining transcriptomic and proteomic datasets, this chapter uncovers molecular responses to iron fortification at both the gene and protein levels. Particular attention is given to the expression of iron-binding proteins and stress-related pathways. In

addition, dissection, staining, and light microscopy are used to visualize and localize iron accumulation sites within the larvae, providing spatial context to the molecular findings and offering insights into the mechanisms of iron storage in insect tissues. **Chapter 5** examines how thermal processing affects iron bioaccessibility in iron-fortified black soldier fly larvae. Using *in vitro* digestion models, this chapter evaluates changes in iron solubility and potential bioaccessibility across different cooking treatments. In parallel, nanoparticle analysis is conducted to assess how fortification and processing influence the distribution, form, and stability of iron-containing nanoparticles within insect tissues. This dual approach offers a deeper understanding of the physical and chemical transformations that influence iron availability during food processing. **Chapter 6** offers a reflection on the insights gained throughout this thesis regarding the use of edible insects as a source of dietary iron. Based on the findings from the preceding chapters, this discussion evaluates what has been learned about the biological, nutritional, and technological factors that influence iron content, composition, and bioaccessibility in insects. The chapter then explores the current status of the edible insect industry, examining its trajectory, present challenges, and potential role in addressing nutritional deficiencies. In parallel, the broader field of iron nutrition is considered, including the status and limitations of current food-based and supplemental iron interventions. Finally, the chapter outlines directions for future research, highlighting key gaps in knowledge and identifying areas where further investigation is likely to advance both the scientific understanding and practical application of insect-derived and conventional iron sources.

Reference:

Anderson, G. J., & Frazer, D. M. (2017). Current understanding of iron homeostasis. The American Journal of Clinical Nutrition, 106, 1559S-1566S. https://doi.org/https://doi.org/10.3945/ajcn.117.155804

Auerbach, M., DeLoughery, T. G., & Tirnauer, J. S. (2025). Iron Deficiency in Adults: A Review. Journal of the American Medical Association, 333(20), 1813–1823. https://doi.org/10.1001/jama.2025.0452

Bessa, L. W., Pieterse, E., Marais, J., Dhanani, K., & Hoffman, L. C. (2021). Food Safety of Consuming Black Soldier Fly (*Hermetia illucens*) Larvae: Microbial, Heavy Metal and Cross-Reactive Allergen Risks. Foods (Basel, Switzerland), 10(8). https://doi.org/10.3390/foods10081934

Bukchin-Peles, S., Baker Lozneva, K., Tomberlin, J. K., & Zilberman, D. (2025). From waste management to protein innovation: Black soldier fly as an embodiment of the circular bioeconomy. Future Foods, 11, 100592. https://doi.org/https://doi.org/10.1016/j.fufo.2025.100592

Cai, M., Hu, R., Zhang, K., Ma, S., Zheng, L., Yu, Z., & Zhang, J. (2018). Resistance of black soldier fly (Diptera: Stratiomyidae) larvae to combined heavy metals and potential application in municipal sewage sludge treatment. Environmental Science and Pollution Research, 25(2), 1559–1567. https://doi.org/10.1007/s11356-017-0541-x

Cross, A. J., Harnly, J. M., Ferrucci, L. M., Risch, A., Mayne, S. T., & Sinha, R. (2012). Developing a heme iron database for meats according to meat type, cooking method and doneness level. Food and Nutrition Sciences, 3, 905–913. https://doi.org/10.4236/fns.2012.37120

Davila-Hicks, P., Theil, E. C., & Lönnerdal, B. (2004). Iron in ferritin or in salts (ferrous sulfate) is equally bioavailable in nonanemic women. The American Journal of Clinical Nutrition, 80(4), 936–940. https://doi.org/10.1093/ajcn/80.4.936

Dev, S., & Babitt, J. L. (2017). Overview of iron metabolism in health and disease. Hemodialysis International. International Symposium on Home Hemodialysis, 21 Suppl 1(Suppl 1), S6–S20. https://doi.org/10.1111/hdi.12542

D'Imperio, M., Renna, M., Cardinali, A., Buttaro, D., Serio, F., & Santamaria, P. (2016).

Calcium biofortification and bioaccessibility in soilless “baby leaf” vegetable production. Food Chemistry, 213, 149–156. https://doi.org/https://doi.org/10.1016/j.foodchem.2016.06.071

Dutt, S., Hamza, I., & Bartnikas, T. B. (2022). Molecular Mechanisms of Iron and Heme Metabolism. Annual Review of Nutrition, 42(Volume 42, 2022), 311–335. https://doi.org/https://doi.org/10.1146/annurev-nutr-062320-112625

Facchini, E., Shrestha, K., van den Boer, E., Junes, P., Sader, G., Peeters, K., & Schmitt, E. (2022). Long-Term Artificial Selection for Increased Larval Body Weight of *Hermetia illucens* in Industrial Settings. Frontiers in Genetics, 13, 865490. https://doi.org/10.3389/fgene.2022.865490

First, T., Fogliano, V., & Mishyna, M. (2023). Entoferritin: An innovative iron source for human consumption. Journal of Functional Foods, 108, 105711. https://doi.org/https://doi.org/10.1016/j.jff.2023.105711

First, T., Van Haeften, A. J., Oonincx, D. G. A. B., Van Loon, J. J. A., Fogliano, V., & Mishyna, M. (2024). Strike while the iron is hot: unravelling the impact of dietary iron on two edible insects. Journal of Insects as Food and Feed, 11(7), 1187–1200. https://doi.org/https://doi.org/10.1163/23524588-00001422

FMI. (2025, April). Food Fortification Market Analysis by Type, Process and Application Through 2035. Https://Www.Futuremarketinsights.Com/Reports/Food-Fortification-Market.

Gallio, A. E., Fung, S. S.-P., Cammack-Najera, A., Hudson, A. J., & Raven, E. L. (2021). Understanding the Logistics for the Distribution of Heme in Cells. Journal of the American Chemical Society Au, 1(10), 1541–1555. https://doi.org/10.1021/jacsau.1c00288

Godfray, H. C. J., Beddington, J. R., Crute, I. R., Haddad, L., Lawrence, D., Muir, J. F., Pretty, J., Robinson, S., Thomas, S. M., & Toulmin, C. (2010). Food Security: The Challenge of Feeding 9 Billion People. Science, 327(5967), 812–818. https://doi.org/10.1126/science.1185383

Higa, J. E., Ruby, M. B., & Rozin, P. (2021). Americans’ acceptance of black soldier fly larvae as food for themselves, their dogs, and farmed animals. Food Quality and Preference, 90, 104119. https://doi.org/https://doi.org/10.1016/j.foodqual.2020.104119

Hilaj, N., Zimmermann, M. B., Galetti, V., Zeder, C., Murad Lima, R., Hammer, L., Krzystek, A., Andlauer, W., & Moretti, D. (2022). The effect of dechitinization on iron absorption from mealworm larvae (*Tenebrio molitor*) flour added to maize meals: stable-isotope studies in young females with low iron stores. The American Journal of Clinical Nutrition, 116(4), 1135–1145. https://doi.org/https://doi.org/10.1093/ajcn/nqac210

Hunt, J. R. (2003). Bioavailability of iron, zinc, and other trace minerals from vegetarian diets23. The American Journal of Clinical Nutrition, 78(3), 633S-639S. https://doi.org/https://doi.org/10.1093/ajcn/78.3.633S

Jeong, J., & Guerinot, M. Lou. (2008). Biofortified and bioavailable: The gold standard for plant-based diets. Proceedings of the National Academy of Sciences, 105(6), 1777–1778. https://doi.org/10.1073/pnas.0712330105

Kim, J. C., Wilcock, P., & Bedford, M. R. (2018). Iron status of piglets and impact of phytase superdosing on iron physiology: A review. Animal Feed Science and Technology, 235, 8–14. https://doi.org/https://doi.org/10.1016/j.anifeedsci.2017.11.001

Kim, M., Rho, Y., Jin, K. S., Ahn, B., Jung, S., Kim, H., & Ree, M. (2011). PH-dependent structures of ferritin and apoferritin in solution: Disassembly and reassembly. Biomacromolecules, 12(5), 1629–1640. https://doi.org/10.1021/bm200026v

Klein, G. S., Leal, K. W., Rodrigues, C. A., Draszevski, T. M. R., Brunetto, A. L. R., Vitt, M. G., Klein, M. S., Cauduro, V. H., Flores, E. M. M., da Silva, G. B., Bagatini, M. D., Chitolina, A. B. de M., Baldissera, M. D., & Da Silva, A. S. (2025). Organic Zinc and Selenium Supplementation of Late Lactation Dairy Cows: Effects on Milk and Serum Minerals Bioavailability, Animal Health and Milk Quality. Animals : An Open Access Journal from MDPI, 15(4). https://doi.org/10.3390/ani15040499

Kodkany, B. S., Bellad, R. M., Mahantshetti, N. S., Westcott, J. E., Krebs, N. F., Kemp, J. F., & Hambidge, K. M. (2013). Biofortification of Pearl Millet with Iron and Zinc in a Randomized Controlled Trial Increases Absorption of These Minerals above Physiologic Requirements in Young Children. The Journal of Nutrition, 143(9), 1489–1493. https://doi.org/https://doi.org/10.3945/jn.113.176677

Latunde-Dada, G. O., Yang, W., & Vera Aviles, M. (2016). *In vitro* iron availability from insects and sirloin beef. Journal of Agricultural and Food Chemistry, 64(44), 8420–8424. https://doi.org/10.1021/acs.jafc.6b03286

Lee, D. Y., Mariano Jr, E., Choi, Y., Park, J. M., Han, D., Kim, J. S., Park, J. W., Namkung, S., Li, Q., Li, X., Venter, C., & Hur, S. J. (2025). Environmental Impact of Meat Protein Substitutes: A Mini-Review. Food Science of Animal Resources, 45(1), 62–80. https://doi.org/10.5851/kosfa.2024.e109

Lee, S. H., Shinde, P., Choi, J., Park, M., Ohh, S., Kwon, I. K., Pak, S. Il, & Chae, B. J. (2008). Effects of dietary iron levels on growth performance, hematological status, liver mineral concentration, fecal microflora, and diarrhea incidence in weanling pigs. Biological Trace Element Research, 126 Suppl 1, S57-68. https://doi.org/10.1007/s12011-008-8209-5

Lönnerdal. (2007). The Importance and Bioavailability of Phytoferritin-Bound Iron in Cereals and Legume Foods. International Journal for Vitamin and Nutrition Research, 77(3), 152–157. https://doi.org/10.1024/0300-9831.77.3.152

Lv, C., Zhao, G., & Lönnerdal, B. (2015). Bioavailability of iron from plant and animal ferritins. Journal of Nutritional Biochemistry, 26(5), 532–540. https://doi.org/10.1016/j.jnutbio.2014.12.006

Madau, F. A., Arru, B., Furesi, R., & Pulina, P. (2020). Insect Farming for Feed and Food Production from a Circular Business Model Perspective. Sustainability, 12(13). https://doi.org/10.3390/su12135418

Manditsera, F. A., Luning, P. A., Fogliano, V., & Lakemond, C. M. M. (2019). Effect of domestic cooking methods on protein digestibility and mineral bioaccessibility of wild harvested adult edible insects. Food Research International, 121, 404–411. https://doi.org/https://doi.org/10.1016/j.foodres.2019.03.052

Masuda, H., Ishimaru, Y., Aung, M. S., Kobayashi, T., Kakei, Y., Takahashi, M., Higuchi, K., Nakanishi, H., & Nishizawa, N. K. (2012). Iron biofortification in rice by the introduction of multiple genes involved in iron nutrition. Scientific Reports, 2, 543. https://doi.org/10.1038/srep00543

Mwangi, M. N., Oonincx, D. G. A. B., Hummel, M., Utami, D. A., Gunawan, L., Veenenbos, M., Zeder, C., Cercamondi, C. I., Zimmermann, M. B., van Loon, J. J. A., Dicke, M., & Melse-Boonstra, A. (2022). Absorption of iron from edible house crickets: a randomized crossover stable-isotope study in humans. The American Journal of Clinical Nutrition. https://doi.org/10.1093/ajcn/nqac223

Mwangi, M. N., Oonincx, D. G. A. B., Stouten, T., Veenenbos, M., Melse-Boonstra, A., Dicke, M., & van Loon, J. J. A. (2018). Insects as sources of iron and zinc in human nutrition. Nutrition Research Reviews, 31(2), 248–255. https://doi.org/DOI: 10.1017/S0954422418000094

Mwangi, M. N., Oonincx, D. G. A. B., Stouten, T., Veenenbos, M., Melse-Boonstra, A., Dicke, M., & Van Loon, J. J. A. (2018). Insects as sources of iron and zinc in human nutrition. Nutrition Research Reviews, 31(2), 248–255. https://doi.org/10.1017/S0954422418000094

Ofori, K. F., Antoniello, S., English, M. M., & Aryee, A. N. A. (2022). Improving nutrition through biofortification-A systematic review. Frontiers in Nutrition, 9, 1043655. https://doi.org/10.3389/fnut.2022.1043655

Osuch, B., Barszcz, M., & Tomaszewska-Zaremba, D. (2024). The potential of black soldier fly (*Hermetia illucens* L.) larvae in chicken and swine nutrition. A review. Journal of Animal and Feed Sciences, 33(4), 454–468. https://doi.org/10.22358/jafs/192511/2024

Pan, Y.-H., Sader, K., Powell, J. J., Bleloch, A., Gass, M., Trinick, J., Warley, A., Li, A., Brydson, R., & Brown, A. (2008). 3D morphology of the human hepatic ferritin mineral core: new evidence for a subunit structure revealed by single particle analysis of HAADF-STEM images. Journal of Structural Biology, 166(1), 22–31. https://doi.org/10.1016/j.jsb.2008.12.001

Pham, D. Q. D., & Winzerling, J. J. (2010). Insect ferritins: Typical or atypical? Biochimica et Biophysica Acta - General Subjects, 1800(8), 824–833. https://doi.org/10.1016/j.bbagen.2010.03.004

Piskin, E., Cianciosi, D., Gulec, S., Tomas, M., & Capanoglu, E. (2022a). Iron Absorption: Factors, Limitations, and Improvement Methods. American Chemical Society Omega, 7(24), 20441–20456. https://doi.org/10.1021/acsomega.2c01833
Protix. (2025). Protix about section. https://protix.com/about-us/

Radhakrishnan, G., Liland, N. S., Koch, M. W., Lock, E.-J., Philip, A. J. P., & Belghit, I. (2023). Evaluation of black soldier fly larvae meal as a functional feed ingredient in Atlantic salmon (Salmo salar) under farm-like conditions. Frontiers in Aquaculture, Volume 2-2023. https://doi.org/10.3389/faquc.2023.1239402

Rumpold, B. A., & Schlüter, O. K. (2013). Nutritional composition and safety aspects of edible insects. Molecular Nutrition & Food Research, 57(5), 802–823. https://doi.org/https://doi.org/10.1002/mnfr.201200735

Seyedalmoosavi, M. M., Mielenz, M., Schleifer, K., Görs, S., Wolf, P., Tränckner, J., Hüther, L., Dänicke, S., Daş, G., & Metges, C. C. (2023). Upcycling of recycled minerals from sewage sludge through black soldier fly larvae (*Hermetia illucens*): Impact on growth and mineral accumulation. Journal of Environmental Management, 344, 118695. https://doi.org/https://doi.org/10.1016/j.jenvman.2023.118695

Siddiqui, S. A., Ristow, B., Rahayu, T., Putra, N. S., Widya Yuwono, N., Nisa', K., Mategeko, B., Smetana, S., Saki, M., Nawaz, A., & Nagdalian, A. (2022). Black soldier fly larvae (BSFL) and their affinity for organic waste processing. Waste Management, 140, 1–13. https://doi.org/https://doi.org/10.1016/j.wasman.2021.12.044

Sokame, B. M., Runyu, J. C., & Tonnang, H. E. Z. (2024). Integrating edible insect into circular agriculture for sustainable production. Sustainable Production and Consumption, 52, 80–94. https://doi.org/https://doi.org/10.1016/j.spc.2024.10.015

Theil, E. C., Chen, H., Miranda, C., Janser, H., Elsenhans, B., Núñez, M. T., Pizarro, F., & Schümann, K. (2012). Absorption of iron from ferritin is independent of heme iron and ferrous salts in women and rat intestinal segments. The Journal of Nutrition, 142(3), 478–483. https://doi.org/10.3945/jn.111.145854

Tolkien, Z., Stecher, L., Mander, A. P., Pereira, D. I. A., & Powell, J. J. (2015). Ferrous sulfate supplementation causes significant gastrointestinal side-effects in adults: A systematic review and meta-analysis. Plos One, 10(2). https://doi.org/10.1371/journal.pone.0117383

Utama, M. Z., Sunadi, S., & Haryoko, W. (2017). Bio Fortification Iron for Brown Rice Variety on Paddy Field Gripped Ferrous. Journal of Scientific and Engineering Research, 6(7), 78–84.

Van Eenennaam, A. L. (2024). Addressing the 2050 demand for terrestrial animal source food. Proceedings of the National Academy of Sciences, 121(50), e2319001121. https://doi.org/10.1073/pnas.2319001121

van Huis, A. (2020). Insects as food and feed, a new emerging agricultural sector: a review. Journal of Insects as Food and Feed, 6(1), 27–44. https://doi.org/https://doi.org/10.3920/JIFF2019.0017

Wade, J., Byrne, D. J., Ballentine, C. J., & Drakesmith, H. (2021). Temporal variation of planetary iron as a driver of evolution. Proceedings of the National Academy of Sciences

of the United States of America, 118(51). https://doi.org/10.1073/pnas.2109865118
Wheeler, T., & von Braun, J. (2013). Climate Change Impacts on Global Food Security. Science, 341(6145), 508–513. https://doi.org/10.1126/science.1239402

Witkowska, Z., Michalak, I., Korczyński, M., Szołtysik, M., Świniarska, M., Dobrzański, Z., Tuhy, Ł., Samoraj, M., & Chojnacka, K. (2015). Biofortification of milk and cheese with microelements by dietary feed bio-preparations. Journal of Food Science and Technology, 52(10), 6484–6492. https://doi.org/10.1007/s13197-014-1696-9

Wondater, W. B., & Ayanie, T. D. (2023). Supplementing dairy feed by dicalcium phosphate and effect on dry matter intake, digestibility, milk composition, and blood mineral balances in crossbred dairy cows. PloS One, 18(11), e0282879. https://doi.org/10.1371/journal.pone.0282879

Wood, P., & Tavan, M. (2022). A review of the alternative protein industry. Current Opinion in Food Science, 47, 100869. https://doi.org/https://doi.org/10.1016/j.cofs.2022.100869

Wu, N., Wang, X., Xu, X., Cai, R., & Xie, S. (2020). Effects of heavy metals on the bioaccumulation, excretion and gut microbiome of black soldier fly larvae (*Hermetia illucens*). Ecotoxicology and Environmental Safety, 192, 110323. https://doi.org/https://doi.org/10.1016/j.ecoenv.2020.110323

Zielińska-Dawidziak, M. (2015). Plant Ferritin—A Source of Iron to Prevent Its Deficiency. Nutrients, 7(2), 1184–1201. https://doi.org/10.3390/nu7021184

CHAPTER

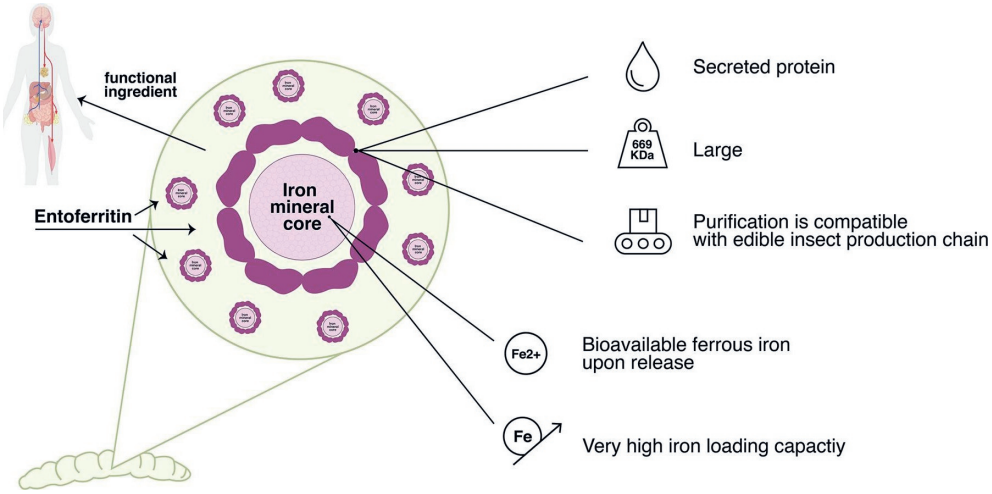
02

Entoferritin: an Innovative Iron Source for Human Consumption

T. First, V. Fogliano, M. Mishyna
Wageningen University and Research, Food Quality and Design group
Published on the "Journal of Functional Foods"

DOI:
https://doi-org.ezproxy.library.wur.nl/10.1016/j.jff.2023.105711

Graphical Abstract



Abstract

The high prevalence of iron deficiency in humans, alongside the lack of sustainable iron sources call for alternatives. Although understudied, edible insects are high in potentially bioavailable iron. Insect ferritin (entoferritin) is thought to make insect-based iron bioavailable. This review examined the use of entoferritin as an iron supplement based on its properties and comparison to mammalian and plant ferritins. Entoferritin is a large, soluble, iron-affine transporting protein complex. These features enable mild entoferritin purification. These purifying methods may not affect other products due to the common structure of edible insect processing chains. The protein complex can accumulate an abundance of bioavailable iron and be absorbed through a human endocytosis mechanism. However, insect ferritin delivery systems into the human iron pool, bioavailability and safety have various possible limits and require further exploration. This paper suggests that entoferritin could help the valorization of edible insects and fight iron deficiency.

1. Introduction

Iron deficiency is currently one of the most frequent form of micronutrient deficit in human populations. It is estimated that over 2.9 billion individuals throughout the globe are affected by iron deficiency anaemia (WHO, 2021).

The human body's capacity to absorb iron is dependent on the amount of bioavailable iron in the diet. Iron bioavailability may be defined as the proportion of an orally administered dosage of iron which reaches the systemic circulation (Wienk *et al.*, 1999). In its most fundamental features, free iron may exist in two forms, ferrous (Fe^{2+}) and ferric (Fe^{3+}), with ferrous being more soluble and absorbable. In addition, even if some ferric iron is absorbed, it will be reduced to ferrous prior to assimilation. Hence, the main reason for the lack of adequate iron absorption is that upon exposure to oxygen, iron forms highly insoluble oxides, which are unavailable for absorption in the human gastrointestinal tract (Wienk *et al.*, 1999). Gastric iron oxidation can be lowered by inhibiting iron-oxygen interaction in the gastric system by placing an iron-binding protein "shield" surrounding the iron atoms (López & Martos, 2004).

The most noteworthy of these "shield" complexes is heme iron. Heme iron consists of an iron ion bound to a porphyrin molecule and is exclusive to animal-derived foods. In animal dietary sources heme iron is obtained from the haemoglobin and myoglobin. In a beef meal, between 60-70% percent of the iron is present in heme form (Cross *et al.*, 2012). During digestion, this complex is taken up by the mucosal cells of the human

intestine and degraded by particular enzymes (Hallberg, 1983). As seen in Fig. 2.1, heme iron may enter the human body iron pool via two primary pathways. The first pathway for endocytosis is the binding of heme to the heme carrier protein 1 (HCP-1). In the intercellular environment, using either Heme oxygenase 1 or Heme oxygenase 2 (named HO-1 and HO-2 respectively), iron will be released from heme, bind to ferroprotein 1 receptor (FPN1), and released into the circulation. In the second pathway, heme iron is directly taken into the cytoplasm by the HCP1 transporter, it is immediately released into the bloodstream by either the feline leukemia virus subgroup C receptor (FLVCR) or the breast cancer resistance protein (BCRP) (West & Oates, 2008, Seyoum *et al.*, 2021) . Due to these specific mechanisms, heme iron is the most bioavailable form of iron that is available today (López & Martos, 2004). However, the direct impact that the meat industry has on the environment, along with the sector's high cost, makes it imperative to find sustainable alternatives also for bioavailable iron (Milford *et al.*, 2019).

Non-heme iron, or inorganic iron, is the predominant iron in alternative protein sources such as plants and insects (Briat *et al.*, 2007, Gorman, 2022). Unlike its heme-based equivalent, the bioavailability of this iron is far more reliant on variables such as enhancers, inhibitors, and its chemical form (ferrous vs ferric) (Lynch *et al.*, 1989). As presented in Fig. 2.1, the human body may acquire inorganic iron by the interaction of divalent metal transporter 1 (DMT1) with the iron on the surface of gut cells (this pathway is shown by the consumption of the commonly used iron supplement FeSO4). The iron absorbed by DMT1 is found in a reduced form, the Duodenal cytochrome B (Dcytb) reduces free ferrous iron atoms. The intercellular iron will be released to the bloodstream via FPN1, similar to the heme originated intercellular iron (Ganz, 2022). This pathway allows the iron absorption by the commonly used iron supplement such as FeSO4 or iron gluconate.

Another interesting group of compounds is the non-heme iron binding proteins that have shown to increase bioavailability of their encapsulated iron (Theil *et al.*, 2012). The iron-binding complex ferritin is a notable example of a non-heme iron-binding protein complex, as its high iron bioavailability has been demonstrated (Lönnerdal, 2009). This iron storage protein complex can be found in a broad variety of organisms, including plants, animals and microbes. In all its variants across different organisms, ferritin is distinguished by its spherical design and the thousands of iron atoms that are found inside its structure. All ferritins share the capacity to accumulate iron via their ferroxidase activity of ionic exchange of ferrous to ferric iron, followed by translocation and hydrolysis to form an inorganic nucleation in the internal cavity (Theil, 1987).

Due to its specific properties, insect ferritin, or entoferritin (a word that was coined in

this publication), has unique characteristics. Comprehensive overview of entoferritin has been previously published by Pham & Winzerling (2010) and detailed illustration of iron homeostasis and metal physiology in insects by Gorman (2022) and Missirlis & Oliveira (2022). However, ferritin is understudied in the field of human consumption. Therefore, the aim of this paper was to offer a novel perspective by examining the potential application of entoferritin as a dietary iron supplement for human consumption. In order to accomplish this, general characteristics of ferritins derived from plants, mammals, and insects, as well as the unique characteristics of entoferritin, were considered in the discussion of entoferritin's potential as a dietary supplement. In addition, a future outlook for this unique approach, designed to valorize the edible insect industry and help combat iron shortage, was examined.

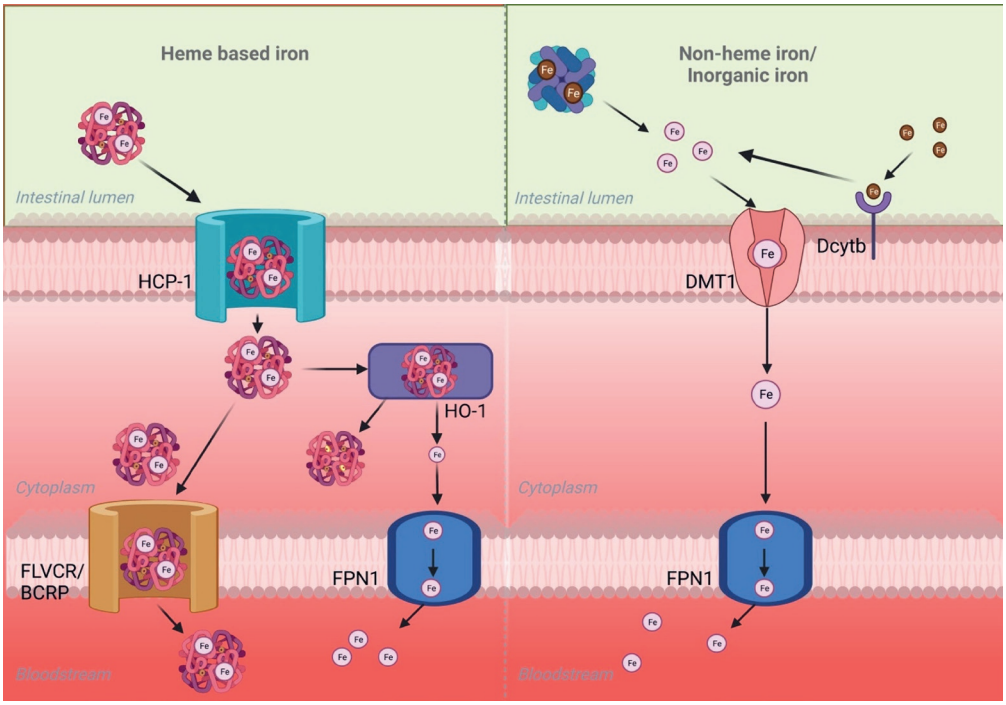


Figure 2.1. Summary of the two primary dietary iron absorption pathways in the human digestive system to the circulation. The pink and brown dots represent iron molecules (Ferrous and ferric respectably). Non-heme iron or inorganic iron, which is the predominant iron in insects, enters the cytoplasm through the divalent metal transporter 1 (DMT1) in a ferric form. DMT1 will only transport the reduced ferrous iron, ferric iron is reduced by the Duodenal cytochrome B (Dcytb). The ferric iron migrates to the bloodstream via the ferroprotein 1 receptor (FPN1). Iron from heme enters the cytoplasm through heme carrier protein 1. (HCP-1). Following that, heme-based iron will enter the bloodstream either with the heme protein through the feline leukaemia virus subgroup C receptor (FLVCR)/breast cancer resistance protein (BCRP) or as free ferrous iron, similar to inorganic iron, following separation from the heme protein with the assistance of the Heme oxygenase (HO) enzyme group. Created with BioRender.com.

2. Ferritins

1. Structural features of ferritin

Ferritin has a structure that is well conserved throughout all living kingdoms, nevertheless, the functions it plays in the control of iron trafficking might vary greatly depending on the organism. Within the centre cavity of ferritin, an inorganic compound containing thousands of iron atoms is allocated. It is a hetero-multimer protein complex that consists of heavy and light chains (named H and L respectively), each of which is encoded by a separate set of genes. Depending on the demand for iron absorption or storage, the ratio of H to L chains fluctuates (Cairo *et al.*, 1991). The L chain contains residues of amino acids that are necessary for the nucleation of iron. The H chain includes amino acid residues that make up the "ferroxidase core", which is responsible for the oxidation of Fe^{2+} to Fe^{3+} using O2 or H2O2, and tyrosine residues, that are responsible for the accelerated biomineralization of iron (Yang *et al.*, 1998). On the ferritin surface, 3-fold hydrophilic ion channels are found. These channels are designed to allows the passive passage of iron atoms in and out of the protein complex (Takahashi & Kuyucak, 2003). Mammalian ferritin is used as a model for the ferritin protein family in most foundational studies on iron loading and release.

2. Iron loading

The iron uptake in ferritin takes place through numerous oxidative reactions. As soon as it has entered the protein complex through the ion channels, the iron will first undergo oxidation, followed by nucleation. Under aerobic conditions, iron (Fe^{2+}) will immediately enter the protein complex and be passively oxidized in the ferroxidase centre. In the ferroxidase centre, it reacts with oxygen to form peroxide, and this peroxide quickly degrades into water and oxidized iron through the reaction (1) (Yang *et al.*, 1998).

$$4Fe^{2+} + O2 + 4H^{+} \rightarrow 4Fe^{3+} + 4H2O \qquad (1)$$

The oxidized ferric iron will go through hydrolysis to form the iron core in the ferritin cavity to form an iron-oxygen mineral structure. Mineralization takes place when the unstable iron state hydrolyzes and releases a proton, while binding to a dioxygen originated from the water molecules. This chemical process is schematized in (2) (Yang *et al.*, 1998).

$$4Fe^{3+} + 8H2O \rightarrow 4FeOOH + 12H^{+} \qquad (2)$$

The complex itself does not attach to the iron core as heme proteins do; rather, the iron mineral structure is kept stable due to the hydrolysis. The extent of the iron biomineralization pathway might vary depending on iron concentration but it always follows the two reaction steps described by Yang *et al.*, (1998) and graphically represented in Fig. 2.2.

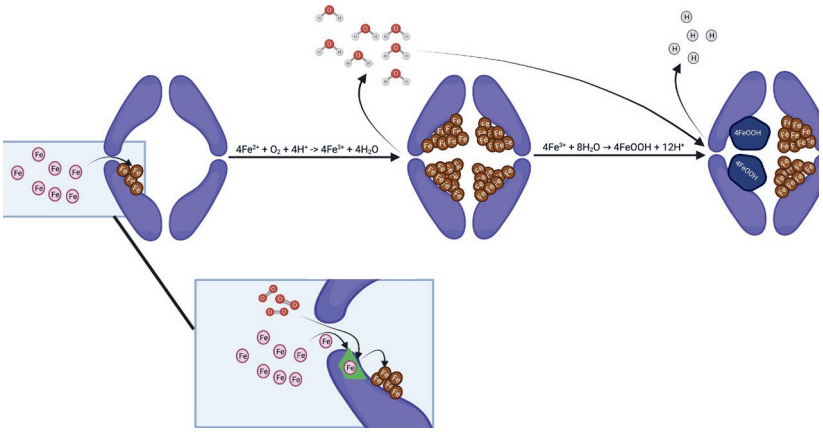


Figure 2.2. A graphical representation of the iron loading process into ferritin. The purple shape is a two-dimensional schematic representation of generic ferritin. Ferrous iron (pink dots labelled Fe) enters the ferritin via the four ion channels. The ferrous iron is oxidized (red dots labelled O) to ferric iron (brown dots labelled Fe) at the ferroxidase (green shape) site. The ferrous iron is subsequently hydrolysed (red and grey dots), resulting in the formation of a mineral with other ferric iron (blue structure labelled 4FeOOH). Created with BioRender.com.

3. Iron release

The reduction of Fe^{3+} with various chemical reductants and chelators is a frequent *in vitro* technique for ferritin iron release. At the cellular level, solubilization of ferric iron through reduction to the ferric state is the primary occurrence of iron release from the ferritin core. This reduction requires a favorable environment to reduction in the cytosol. This environment exists when the thermodynamic activity or electrochemical potential in the cytosol is lower than these parameters inside the ferritin core. The release occurs when the ferritin core interacts by diffusion of an electron donor ligand or an electron acceptor ligand (Badu-Boateng & Naftalin, 2019, Bou-Abdallah *et al.*, 2018) . In Caco-2 cultures, it has been shown that phytoferritin releases iron via an endocytosis mechanism (Lv *et al.*, 2015). This suggests that ferritin derived from exogenous sources

could interact with ferritin receptors found on humanoid cells and release the iron in the most efficient manner.

In gastric acidic conditions, when phytoferritin has been digested by pepsin, iron absorption from phytoferritin and common iron supplements, are essentially equal, indicating that the majority of ferritin may be digested by pepsin in the human digestive tract conditions (Deng *et al.*, 2011). Both mammalian ferritin and phytoferritin have been demonstrated to disassemble into dimeric substructures and release their cavity contents in acidic conditions. Interestingly, when the pH returns to normal, ferritin will reassemble, without its original mineralized core (Kim *et al.*, 2011, Perfecto *et al.*, 2018).

4. Entoferritin

The ferritin found in insects has many different features than its counterparts in plants and mammals, as summarized in Fig. 2.3. The entoferritin crystal structure consists of 12 heavy chain and 12 light chain subunits with tetrahedral symmetry. This protein complex's structural integrity is maintained by a variety of inter-subunit di-sulfide and ionic bridge bonds (Hamburger *et al.*, 2005). One of the most visible differences is the molecular weight: mammalian ferritin ~440 kDa, phytoferritin ~550 kDa and insect ferritin ~669 kDa suggesting a higher heavy to light chain ratio. This ratio vary depending on the function a ferritin complex serves in a specific tissue (Crichton *et al.*, 1973, Nichol & Locke, 1989). A more in-depth outlook of the crystal structures of these ferritins is shown by the work of Hamburger *et al.*, (2005), Lewin *et al.*, (2005) and Masuda *et al.*, (2010). Evidently, these sizes correlates to the subunit size, as the H and L chains of ferritin in mammals weigh 21 kDa and 19 kDa, respectively, but in insects, the H chain weighs 31 kDa and the L chain - 24 kDa (Arosio *et al.*, 1978, Nichol & Locke, 1989) . As such, insect ferritin subunits are often referred to as heavy chain homolog (HCH) and light chains homologous (LCH). The insect HCH contains the same ferroxidase site as other H chains, including those from mammals and plants (Georgieva *et al.*, 2002). The highest amount of mineralized iron in mammalian ferritins is 4,500 Fe atoms per ferritin molecule; while phytoferritin may retain more than 5,000 Fe atoms due to the larger ferritin cavity size (Munro & Linder, 1978, Crichton *et al.*, 1973). As the entoferritin is even bigger than phytoferritin it is probable that the entoferritin cavity has even a greater iron capacity, then it should have a greater iron delivery capability.

The presence of a hydrophobic leader peptide is a further structural distinction specific to insect ferritin. This 20 amino acid-peptide direct the subunits towards

a secretory pathway (Nichol & Locke, 1999), suggesting a significant difference in the protein complex's fundamental functioning. In fact, ferritin in mammals has mostly an intracellular storage function (Arosio *et al.*, 2009). Similarly, phytoferritin serves as the principal iron storage complex in plants, especially in seeds indicating its long-term iron storage ability (Burton *et al.*, 1998). In most insects, iron loaded entoferritin is present in the hemolymph, the insect analogue of blood, as a protein complex secreted from various insect organs. This indicates that in insects, beside storage, ferritin plays a critical role in iron transport (Nichol & Locke, 1990, Strickler-Dinglasan *et al.*, 2006). The structural characteristics of entoferritin suggest a potential use as dietary iron source that is becoming more realistic with the introduction of edible insect consumption as meat alternative. By extrapolating the known data on phytoferritin, mammalian ferritin, and entoferritin, the following chapter evaluates the potential of entoferritin as a functional product.

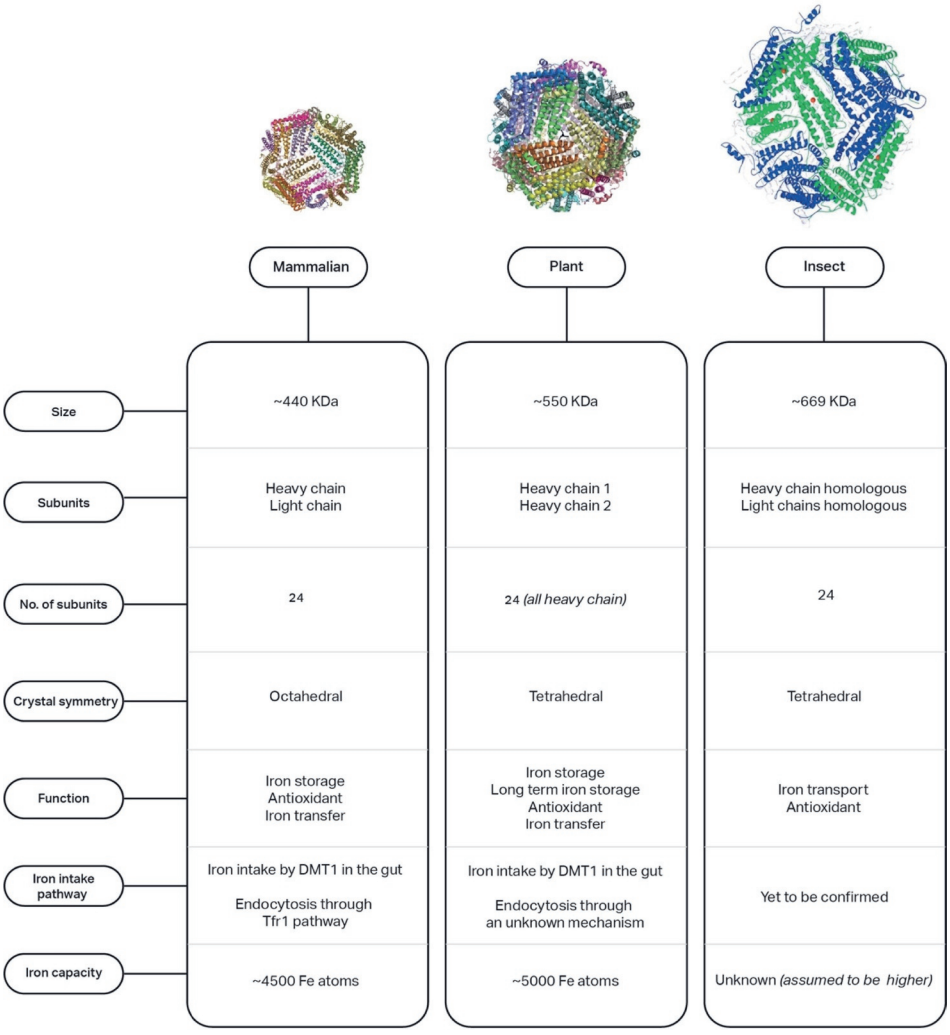


Figure 2.3. Entoferritin versus plant and mammalian ferritin (Hamburger *et al.*, 2005, Masuda *et al.*, 2010, Seong-Gyu *et al.*, 2018). Created with Adobe illustrator.

3. Utilization of entoferritin

1. Entoferritin purification in the edible insects production chain

The diet has a significant effect on the reared insect composition (Bordiean *et al.*, 2022). Specifically, the amount of iron in the insect substrate has a direct influence on ferritin gene expression in insects (Georgieva *et al.*, 1999), implying that increased iron digestion promotes entoferritin production. Furthermore, because iron content varies across insect species and larval stage (Mwangi *et al.*, 2018), entoferritin concentration may vary between edible insect species. The precise amounts of entoferritin present in various species of edible insects remain undetermined.

Prior to processing, edible insects are often starved to empty their digestive tract (Wynants *et al.*, 2017). Recently, Li *et al.*, (2022) demonstrated that starved bee larvae overexpress the ferritin-coding genes. This may indicate that the known ferritin concentrations found in insect hemolymph, which have reached ~0.3 mg/mL, could be enhanced, thereby increasing the yield potential of entoferritin purification from edible insects (Capurro *et al.*, 1996).

The gold standard for entoferritin purification utilizes a KBr density gradient. In recent advances and uses of this technique, insect hemolymph or reconstituted insect proteins were subjected to a series of extensive high-speed density gradient ultracentrifugation (105,000-180,000 g, 36 hours) (Wajnberg *et al.*, 2018, Gutiérrez *et al.*, 2013). However, for both commercial and research purposes, the time and energy invested in this ultracentrifugation process should spur the search for a low-cost alternative. In terms of ferritin purification and production for human consumption, these procedures are very uncommon, and an industrially scalable ferritin purification process may be found only for mammalian recombinant ferritin. In this case, genetically engineered bacteria are being used in order to create recombinant mammalian ferritin for pharmacological usage (Zhen *et al.*, 2013). However, these production procedures are only marginally applicable in the food system.

Entoferritin is found predominantly in the soluble protein fraction of the insect material, and it is usually purified from insect hemolymph for research purposes (Nichol & Locke, 1990). To collect this soluble fraction, the insect material should be grinded, following the collection of liquid fraction. This step is already commonly used at the beginning of insect processing (Tzompa Sosa & Fogliano, 2017) and can be done on industrial scale, and excludes harsh mechanical or enzymatic insect tissue treatments. Selection of protein fractionation and processing methods should consider

possible decrease in efficacy of entoferritin as an iron transporter. For instance, pea ferritin shown to be degraded when exposed to acidic environments (Perfecto *et al.*, 2018). It can be assumed that some procedures used to extract proteins from edible insects break down entoferritin into at least its dimers. As a result, iron is released from the protein complex and rendering it irrelevant as an iron source.

Entoferritin exhibits distinctive features that might facilitate the repurposing of existing protein purification. Its high iron affinity may be employed to recover this protein from the insect-soluble fraction by employing different affinity chromatography methods, as previously shown on mammalian ferritin (Akduman *et al.*, 2013, Uygun *et al.*, 2011). Also, the unusually high molecular weight of entoferritin (669 KDa) suggests the use of protein purification techniques based on protein size (Zielińska-Dawidziak *et al.*, 2012 , Ghirlando *et al.*, 2015).

The position of entoferritin purification step in the processing chain of edible insects would depend on the selected processing approach and target insect-delivered products. Entoferritin purification can occur in the initial steps of protein extraction and fractionation that allow retaining the quality of other insect-delivered products.

2. Entoferritin as an iron supplement

While edible insects offer a source for highly concentrated iron (Mwangi *et al.*, 2018), a recent study demonstrated low *in vivo* iron bioavailability from whole cricket powder. It is assumed that the insect sourced chitin played a main role in the iron absorption inhibition (Mwangi *et al.*, 2022). The House cricket's chitin concentration is comparatively low (4-7%) in comparison to other edible insects such as the yellow mealworm (16-17% chitin) (Rehman *et al.*, 2023). This suggests that the prevalence of this iron inhibitor concentration is present in all manufactured edible insect species. Purified entoferritin may relieve these constraints by facilitating the consumption of insect-derived iron under stricter control of enhancers and inhibitors.

The current gold standard for iron supplements is ferrous sulfate. This is due to the iron salt's affordable production costs more than the established efficacy. Moreover, this common iron salt has widespread adverse effects, which in adults present mostly as significant gastrointestinal issues (Tolkien *et al.*, 2015). Purified entoferritin might give an alternate iron supplement that is safer and more effective. To back it up, women who ingested pure phytoferritin did not report any gastrointestinal symptoms (Theil *et al.*, 2012, Lönnerdal *et al.*, 2006). Due to the presence of conserved sites in both

entoferritin and phytoferritin, it may be presumed that their iron uptake mechanisms in humans are comparable.

Furthermore, a difficulty associated with protein-based products is their allergenic potential. Although understudied, evidence suggests that insects share allergenic properties with their crustacean relatives. Some proteins present in edible insects have been demonstrated to cause allergic reactions when consumed (de Marchi *et al.*, 2021). However, it is known that the ferritin heavy chain of dust mites, another arthropod, is non-allergenic (Epton *et al.*, 2002).

4. The emerging market of edible insects

It is anticipated that the edible insect market would expand by 26.5% per year between 2021 and 2027. This is mainly due to the ability of edible insects to convert organic by-products into high-quality proteins, furthering the adoption of sustainable circular agriculture (van Huis *et al.*, 2021). In relation to the subject of this paper, it has been proposed that a high concentration of iron makes edible insects a good source of this vital element. Comparing *Tenebrio molitor* (Yellow mealworm) to common livestock species revealed that its iron content is higher than that of chicken, pork, and beef (Mwangi *et al.*, 2018). In addition to its high iron content, an *in vitro* iron bioavailability assay using the Caco-2 model showed that the bioavailability of insect iron is equivalent to that of beef, which is widely recognized as the most effective source of iron (Latunde-Dada *et al.*, 2016). Even while earlier studies on iron in entomophagy look to point in a favorable direction, little research has been conducted on this area, and its potential and limitations are not yet completely understood. It is assumed that the origin of iron bioavailability is associated with iron-binding complexes present in insects, namely entoferritin (Latunde-Dada *et al.*, 2016).

Even though the trend toward popular acceptance of entomophagy is reversing, the psychological trait of food neophobia (aversion to novel foods) serves as a significant impediment to the growth of entomophagy in Western nations. Eliminating the public's unfamiliarity with edible insects is a fundamental strategy for combating this adverse perception (Ardoin & Prinyawiwatkul, 2020). This is accomplished by processing and fractionating insects into their component parts of fiber, lipids, and protein meals before incorporating them into traditional dishes like burgers, pasta and baked goods (Tzompa Sosa & Fogliano, 2017). However, this wide range of insect derived food ingredients and foods does not include any iron-based items of any kind.

5. Conclusion

Entoferritin is a unique protein found in edible insects. It has the same basic iron mineralization and storage capacities as mammalian and plant ferritins, but it is larger and more soluble. Introducing an entoferritin based iron source could pave the way for the valorization of edible insect products while also addressing the ubiquitous problem of iron scarcity.

The size, function, and iron affinity of entoferritin, as well as past research on its homologs in other species, imply that a mild, effective, and scalable purification method is achievable. To accomplish this, further studies are required to determine how these characteristics of entoferritin can be harnessed for its purification. Furthermore, the emerging edible insect industry is not yet focused on increasing the iron bioavailability of edible insects or producing iron-rich insect-based food components. However, the structure of the production chain enables the purification of entoferritin without compromising other products.

In terms of the nutritional value of pure entoferritin, research on mammalian and plant ferritin has shown that the fundamental properties of this protein complex make it a highly bioavailable iron source. Entoferritin ought to be purified to improve its human consumption potential and to allow studies to evaluate its bioavailability, optimal intake form, and safety.

Reference:

Akduman, B., Uygun, M., Uygun, D. A., & Antalík, M. (2013). Fe3O4 magnetic core coated by silver and functionalized with N-acetyl cysteine as novel nanoparticles in ferritin adsorption. Journal of Nanoparticle Research, 15(4). https://doi.org/10.1007/s11051-013-1564-y

Ardoin, R., & Prinyawiwatkul, W. (2020). Product appropriateness, willingness to try and perceived risks of foods containing insect protein powder: A survey of U.S. consumers. International Journal of Food Science and Technology, 55(9), 3215–3226. https://doi.org/10.1111/ijfs.14612

Arosio, P., Adelman, T. G., & Drysdale, J. W. (1978). On ferritin heterogeneity further evidence for heteropolymers. Journal of Biological Chemistry, 253(12), 4451–4458. https://doi.org/10.1016/S0021-9258(17)34741-5

Arosio, P., Ingrassia, R., & Cavadini, P. (2009). Ferritins: A family of molecules for iron storage, antioxidation and more. Biochimica et Biophysica Acta - General Subjects, 1790(7), 589–599. https://doi.org/10.1016/j.bbagen.2008.09.004

Badu-Boateng, C., & Naftalin, R. J. (2019). Ascorbate and ferritin interactions: Consequences for iron release *in vitro* and *in vivo* and implications for inflammation. Free Radical Biology and Medicine, 133, 75–87. https://doi.org/10.1016/j.freeradbiomed.2018.09.041

Bordiean, A., Krzyżaniak, M., Aljewicz, M., & Stolarski, M. J. (2022). Influence of Different Diets on Growth and Nutritional Composition of Yellow Mealworm. Foods, 11(19). https://doi.org/10.3390/foods11193075

Bou-Abdallah, F., Paliakkara, J. J., Melman, G., & Melman, A. (2018). Reductive Mobilization of Iron from Intact Ferritin: Mechanisms and Physiological Implication. Pharmaceuticals, 11(4), 120. https://doi.org/https://doi.org/10.3390/ph11040120

Briat, J. F., Curie, C., & Gaymard, F. (2007). Iron utilization and metabolism in plants. Current Opinion in Plant Biology, 10(3), 276–282. https://doi.org/10.1016/j.pbi.2007.04.003

Burton, J. W., Harlow, C., & Theil, E. C. (1998). Evidence for reutilization of nodule iron in soybean seed development. Journal of Plant Nutrition, 21(5), 913–927. https://doi.org/10.1080/01904169809365453

Cairo, G., Rappocciolo, E., Tacchini, L., & Schiaffonati, L. (1991). Expression of the genes for the ferritin H and L subunits in rat liver and heart. Evidence for tissue-specific regulations at pre- and post-translational levels. Biochemical Journal, 275(3), 813–816. https://doi.org/10.1042/bj2750813

Capurro, M. D. L., Iughetti, P., Ribolla, P. E. M., & de Bianchi, A. G. (1996). Musca domestica hemolymph ferritin. Archives of Insect Biochemistry and Physiology, 32(2), 197–207. https://doi.org/10.1002/(SICI)1520-6327(1996)32:2<197::AID-ARCH4>3.0.CO;2-W

Chasteen, N. D., & Harrison, P. M. (1999). Mineralization in ferritin: An efficient means of iron storage. Journal of Structural Biology, 126(3), 182–194. https://doi.org/10.1006/jsbi.1999.4118

Crichton, R. R., Millar, J. A., Cummingt, R. L. C., & Bryce, C. F. A. (1973). The organ-specificity of ferritin in human and horse liver and spleen. Biochemical Journal, 131(1), 51–59. https://doi.org/10.1042/bj1310051

Cross, A. J., Harnly, J. M., Ferrucci, L. M., Risch, A., Mayne, S. T., & Sinha, R. (2012). Developing a heme iron database for meats according to meat type, cooking method and doneness level. Food and Nutrition Sciences, 3, 905–913. https://doi.org/10.4236/fns.2012.37120

de Marchi, L., Wangorsch, A., & Zoccatelli, G. (2021). Allergens from Edible Insects: Cross-reactivity and Effects of Processing. Current Allergy and Asthma Reports, 21(5), 1–12. https://doi.org/https://doi.org/10.1007/s11882-021-01012-z

Deng, J., Li, M., Zhang, T., Chen, B., Leng, X., & Zhao, G. (2011). Binding of proanthocyanidins to soybean (Glycine max) seed ferritin inhibiting protein degradation by protease *in vitro*. Food Research International, 44(1), 33–38. https://doi.org/10.1016/j.foodres.2010.11.020

Epton, M. J., Smith, W., Hales, B. J., Hazell, L., Thompson, P. J., & Thomas, W. R. (2002). Non-allergenic antigen in allergic sensitization: responses to the mite ferritin heavy chain antigen by allergic and non-allergic subjects. Clinical & Experimental Allergy, 32(9), 1341–1347. https://doi.org/10.1046/j.1365-2222.2002.01473.x

Fan, K., Cao, C., Pan, Y., Lu, D., Yang, D., Feng, J., Song, L., Liang, M., & Yan, X. (2012). Magnetoferritin nanoparticles for targeting and visualizing tumour tissues. Nature Nanotechnology, 7(7), 459–464. https://doi.org/10.1038/nnano.2012.90

Ganz, T. (2022). Iron Biology: Metabolism and Homeostasis. In M. B. and M. D. and K. K. Karakochuk Crystal D. and Zimmermann (Ed.), Nutritional Anemia (pp. 19–33). Springer International Publishing. https://doi.org/10.1007/978-3-031-14521-6_2

Georgieva, T., Dunkov, B. C., Dimov, S., Ralchev, K., & Law, J. H. (2002). *Drosophila melanogaster* ferritin: cDNA encoding a light chain homologue, temporal and tissue specific expression of both subunit types. Insect Biochemistry and Molecular Biology, 32, 295–302. https://doi.org/10.1016/S0965-1748(01)00090-X

Georgieva, T., Dunkov, B. C., Harizanova, N., Ralchev, K., & Law, J. H. (1999). Iron availability dramatically alters the distribution of ferritin subunit messages in *Drosophila melanogaster*. In Biochemistry (Vol. 96). https://doi.org/10.1073/pnas.96.6.2716

Ghirlando, R., Mutskova, R., & Schwartz, C. (2015). Enrichment and characterization of ferritin for nanomaterial applications. Nanotechnology, 27(4), 45102. https://doi.org/10.1088/0957-4484/27/4/045102

Gorman, M. J. (2022). Iron homeostasis in Insects. Annual Review of Entomology, 68. https://doi.org/doi.org/10.1146/annurev-ento-040622-092836

Gutiérrez, L., Zubow, K., Nield, J., Gambis, A., Mollereau, B., Lázaro, F. J., & Missirlis, F. (2013). Biophysical and genetic analysis of iron partitioning and ferritin function in *Drosophila melanogaster*. Metallomics, 5(8), 997–1005. https://doi.org/10.1039/c3mt00118k

Hallberg, L. (1983). Iron requirements and bioavailability of dietary iron. Nutritional Adequacy, Nutrient Availability and Needs, 223–244. https://doi.org/10.1007/978-3-0348-6540-1_13

Hamburger, A. E., West, A. P., Hamburger, Z. A., Hamburger, P., & Bjorkman, P. J. (2005). Crystal structure of a secreted insect ferritin reveals a symmetrical arrangement of heavy and light chains. Journal of Molecular Biology, 349(3), 558–569. https://doi.org/10.1016/j.jmb.2005.03.074

He, J., Fan, K., & Yan, X. (2019). Ferritin drug carrier (FDC) for tumor targeting therapy. In Journal of Controlled Release (Vols. 311–312, pp. 288–300). Elsevier B.V. https://doi.org/10.1016/j.jconrel.2019.09.002

Kim, M., Rho, Y., Jin, K. S., Ahn, B., Jung, S., Kim, H., & Ree, M. (2011). PH-dependent

structures of ferritin and apoferritin in solution: Disassembly and reassembly. Biomacromolecules, 12(5), 1629–1640. https://doi.org/10.1021/bm200026v

Latunde-Dada, G. O., Yang, W., & Vera Aviles, M. (2016). *In vitro* iron availability from insects and sirloin beef. Journal of Agricultural and Food Chemistry, 64(44), 8420–8424. https://doi.org/10.1021/acs.jafc.6b03286

Lewin, A., Moore, G. R., & Le Brun, N. E. (2005). Formation of protein-coated iron minerals. Dalton Transactions (Cambridge, England: 2003), 22, 3597–3610. https://doi.org/10.1039/b506071k

Li, Z., Ma, R., Wang, L., Wang, Y., Qin, Q., Chen, L., Dang, X., & Zhou, Z. (2022). Starvation stress affects iron metabolism in honeybee Apis mellifera. Biologia, 1–16. https://doi.org/10.1007/s11756-022-01098-4

Lönnerdal, B. (2009). Soybean ferritin: Implications for iron status of vegetarians. American Journal of Clinical Nutrition, 89(5). https://doi.org/10.3945/ajcn.2009.26736W
Lönnerdal, B., Bryant, A., Liu, X., & Theil, E. C. (2006). Iron absorption from soybean ferritin in nonanemic women. The American Journal of Clinical Nutrition, 83(1), 103–107. https://doi.org/10.1093/ajcn/83.1.103

López, M. A. A., & Martos, F. C. (2004). Iron availability: An updated review. International Journal of Food Sciences and Nutrition, 55(8), 597–606. https://doi.org/10.1080/09637480500085820

Lv, C., Zhao, G., & Lönnerdal, B. (2015). Bioavailability of iron from plant and animal ferritins. Journal of Nutritional Biochemistry, 26(5), 532–540. https://doi.org/10.1016/j.jnutbio.2014.12.006

Lynch, S. R., Skikne, B. S., & Cook, J. D. (1989). Food iron absorption in idiopathic hemochromatosis. Blood, 74(6), 2187–2193. https://doi.org/10.1182/blood.V74.6.2187.2187

Masuda, T., Goto, F., Yoshihara, T., & Mikami, B. (2010). Crystal structure of plant ferritin reveals a novel metal binding site that functions as a transit site for metal transfer in ferritin. The Journal of Biological Chemistry, 285(6), 4049–4059. https://doi.org/10.1074/jbc.m109.059790

Milford, A. B., le Mouël, C., Bodirsky, B. L., & Rolinski, S. (2019). Drivers of meat consumption. Appetite, 141. https://doi.org/10.1016/j.appet.2019.06.005

Missirlis, F., & Oliveira, P. L. (2022). Metal ions in the physiology of insects. Current Opinion in Insect Science, 54, 100965. https://doi.org/https://doi.org/10.1016/j.cois.2022.100965

Munro, H. N., & Linder, M. C. (1978). Physiological reviews ferritin: structure, biosynthesis, and role in iron metabolism. Physiological Reviews, 58(2), 317–396. https://doi.org/10.1152/physrev.1978.58.2.317

Mwangi, M. N., Oonincx, D. G. A. B., Hummel, M., Utami, D. A., Gunawan, L., Veenenbos, M., Zeder, C., Cercamondi, C. I., Zimmermann, M. B., van Loon, J. J. A., Dicke, M., & Melse-Boonstra, A. (2022). Absorption of iron from edible house crickets: a randomized crossover stable-isotope study in humans. The American Journal of Clinical Nutrition. https://doi.org/10.1093/ajcn/nqac223

Mwangi, M. N., Oonincx, D. G. A. B., Stouten, T., Veenenbos, M., Melse-Boonstra, A., Dicke, M., & van Loon, J. J. A. (2018). Insects as sources of iron and zinc in human nutrition. Nutrition Research Reviews, 31(2), 248–255. https://doi.org/10.1017/S0954422418000094

Nichol, H., & Locke, M. (1989). The characterization of ferritin in an insect. Insect Biochemistry, 19(6), 587–602. https://doi.org/10.1016/0020-1790(89)90024-3

Nichol, H., & Locke, M. (1990). The localization of ferritin in insects. In Tissue & cell (Vol. 22, Issue 6, pp. 767–777). https://doi.org/10.1016/0040-8166(90)90042-8
Nichol, H., & Locke, M. (1999). Secreted ferritin subunits are of two kinds in insects molecular cloning of cDNAs encoding two major subunits of secreted ferritin from Calpodes ethlius. Insect Biochemistry and Molecular Biology, 29, 999–1013. https://doi.org/10.1016/S0965-1748(99)00076-4

Organization, W. H. (2021). The urgent need to implement patient blood management: policy brief. World Health Organization.

Perfecto, A., Rodriguez-Ramiro, I., Rodriguez-Celma, J., Sharp, P., Balk, J., & Fairweather-Tait, S. (2018). Pea ferritin stability under gastric pH conditions determines the mechanism of iron uptake in Caco-2 cells. Journal of Nutrition, 148(8), 1229–1235. https://doi.org/10.1093/jn/nxy096

Pham, D. Q. D., & Winzerling, J. J. (2010). Insect ferritins: Typical or atypical? Biochimica et Biophysica Acta - General Subjects, 1800(8), 824–833. https://doi.org/10.1016/j.

bbagen.2010.03.004

Rehman, K. ur, Hollah, C., Wiesotzki, K., Heinz, V., Aganovic, K., Rehman, R. ur, Petrusan, J.-I., Zheng, L., Zhang, J., Sohail, S., Mansoor, M. K., Rumbos, C. I., Athanassiou, C., & Cai, M. (2023). Insect-Derived Chitin and Chitosan: A Still Unexploited Resource for the Edible Insect Sector. Sustainability, 15(6). https://doi.org/10.3390/su15064864

Seong-Gyu, Lee Byungjun, A., Jeong Min, L., Ho Min, K., & Yongwon, J. (2018). RCSB PDB - 5XB1: human ferritin mutant - E-helix deletion. https://doi.org/https://doi.org/10.2210/pdb5XB1/pdb

Seyoum, Y., Baye, K., & Humblot, C. (2021). Iron homeostasis in host and gut bacteria – a complex interrelationship. Gut Microbes, 13(1), 1874855. https://doi.org/10.1080/19490976.2021.1874855

Stefanini, S., Cavallo, S., Wang, C.-Q., Tataseo, P., Vecchini, P., Giartosio, A., & Chiancone, E. (1996). Thermal stability of horse spleen apoferritin and human recombinant H apoferritin. ARCHIVES OF BIOCHEMISTRY AND BIOPHYSICS, 325(1), 58–64. https://doi.org/10.1006/abbi.1996.0007

Strickler-Dinglasan, P. M., Guz, N., Attardo, G., & Aksoy, S. (2006). Molecular characterization of iron binding proteins from Glossina morsitans (Diptera: Glossinidae). Insect Biochemistry and Molecular Biology, 36(12), 921–933. https://doi.org/10.1016/j.ibmb.2006.09.003

Sudarev, V. V, Dolotova, S. M., Bukhalovich, S. M., Bazhenov, S. V, Ryzhykau, Y. L., Uversky, V. N., Bondarev, N. A., Osipov, S. D., Mikhailov, A. E., Kuklina, D. D., Murugova, T. N., Manukhov, I. V, Rogachev, A. V, Gordeliy, V. I., Gushchin, I. Yu., Kuklin, A. I., & Vlasov, A. V. (2023). Ferritin self-assembly, structure, function, and biotechnological applications. International Journal of Biological Macromolecules, 224, 319–343. https://doi.org/https://doi.org/10.1016/j.ijbiomac.2022.10.126

Takahashi, T., & Kuyucak, S. (2003). Functional Properties of Threefold and Fourfold Channels in Ferritin Deduced from Electrostatic Calculations. Biophysical Journal, 84(4), 2256–2263. https://doi.org/10.1016/S0006-3495(03)75031-0

Theil, E. C. (1987). Ferritin: Structure, gene regulation, and cellular function in animals, plants, and microorganisms. Annual Review of Biochemistry, 56(1), 289–315. https://doi.org/10.1146/annurev.bi.56.070187.001445

Theil, E. C., Chen, H., Miranda, C., Janser, H., Elsenhans, B., Núñez, M. T., Pizarro, F., & Schümann, K. (2012). Absorption of Iron from Ferritin Is Independent of Heme Iron and Ferrous Salts in Women and Rat Intestinal Segments. The Journal of Nutrition, 142(3), 478–483. https://doi.org/10.3945/jn.111.145854

Tolkien, Z., Stecher, L., Mander, A. P., Pereira, D. I. A., & Powell, J. J. (2015). Ferrous sulfate supplementation causes significant gastrointestinal side-effects in adults: A systematic review and meta-analysis. In Plos one (Vol. 10, Issue 2). Public Library of Science. https://doi.org/10.1371/journal.pone.0117383

Tzompa Sosa, D. A., & Fogliano, V. (2017). Potential of Insect-Derived Ingredients for Food Applications. In Insect Physiology and Ecology (pp. 215–231). InTech. https://doi.org/10.5772/67318

Uygun, D. A., Öztürk, N., & Akgöl, S. (2011). Methacryloylamidohistidine in affinity ligands for immobilized metal-ion affinity chromatography of ferritin. Biotechnol Bioproc, e (16), 173–179. https://doi.org/10.1007/s12257-009-0162-4

van Huis, A., Rumpold, B. A., van der Fels-Klerx, H. J., & Tomberlin, J. K. (2021). Advancing edible insects as food and feed in a circular economy. Journal of Insects as Food and Feed, 7(5), 935–948. https://doi.org/10.3920/JIFF2021.x005

Wajnberg, E., Alves, O. C., Perales, J., da Rocha, S. L. G., Ferreira, A. T., Cameron, L. C., Esquivel, D. M. S., & de Lourdes Barriviera, M. (2018). Ferritin from the haemolymph of adult ants: an extraction method for characterization and a ferromagnetic study. European Biophysics Journal, 47(6), 641–653. https://doi.org/10.1007/s00249-018-1293-3

West, A. R., & Oates, P. S. (2008). Mechanisms of heme iron absorption: Current questions and controversies. World Journal of Gastroenterology, 14(26), 4101–4110. https://doi.org/10.3748/WJG.14.4101

Wienk, K. J. H., Marx, J. J. M., & Beynen, A. C. (1999). The concept of iron bioavailability and its assessment. European Journal of Nutrition , 38(2), 51–75. https://doi.org/10.1007/s003940050046

Wynants, E., Crauwels, S., Lievens, B., Luca, S., Claes, J., Borremans, A., Bruyninckx, L., & van Campenhout, L. (2017). Effect of post-harvest starvation and rinsing on the microbial numbers and the bacterial community composition of mealworm larvae (*Tenebrio molitor*). Innovative Food Science and Emerging Technologies, 42, 8–15. https://

doi.org/10.1016/j.ifset.2017.06.004

Yang, X., Chen-Barrett, Y., Arosio, P., & Dennis Chasteen, N. (1998). Reaction paths of iron oxidation and hydrolysis in horse spleen and recombinant human ferritins. Biochemistry, 37(27), 9743–9750. https://doi.org/10.1021/bi973128a

Yin, S., Davey, K., Dai, S., Liu, Y., & Bi, J. (2022). A critical review of ferritin as a drug nanocarrier: Structure, properties, comparative advantages and challenges. Particuology, 64, 65–84. https://doi.org/https://doi.org/10.1016/j.partic.2021.04.020

Zhen, Z., Tang, W., Chen, H., Lin, X., Todd, T., Wang, G., Cowger, T., Chen, X., & Xie, J. (2013). RGD-modified apoferritin nanoparticles for efficient drug delivery to tumors. ACS Nano, 7(6), 4830–4837. https://doi.org/10.1021/nn305791q

Zielińska-Dawidziak, M., Błaszak, R., & Piasecka-Kwiatkowska, D. (2012). Influence of magnetic field on aqueous two-phase extraction of horse ferritin in the polyethylene glycol/hydroxyethyl starch system. Analytica Chimica Acta, 716, 11–15. https://doi.org/10.1016/j.aca.2011.02.044

CHAPTER

03

Strike While the Iron Is Hot: Unravelling the Impact of Dietary Iron on Two Edible Insects

T. First[1], A.J. Van Haeften[1], D.G.A.B. Oonincx[2], J.J.A. Van Loon[3], V. Fogliano[1] and M. Mishyna[1]

[1]Wageningen University and Research, Food Quality and Design group, Bornse Weilanden 9, 6708 WG Wageningen, the Netherlands; [2]Wageningen University and Research, Animal Nutrition Group, De Elst 1, 6708 WD Wageningen, the Netherlands; [3]Wageningen University and Research, Laboratory of Entomology, Droevendaalsesteeg 1, 6708 PB Wageningen, the Netherlands.

DOI:
https://doi.org/10.1163/23524588-00001422

Abstract

Edible insects are key players in the alternative protein market. Alongside their high protein content, edible insects contain abundant trace minerals, including iron. Given the lack of sustainable and bioavailable iron sources, edible insects are a promising iron source in both human and livestock diets. However, little is known about how the iron concentration in edible insects can be manipulated. This study aims to investigate the impact of dietary iron at different concentrations on the growth, survival, and nutrient composition of two edible insect species larvae: black soldier fly (BSF, *Hermetia illucens*) and yellow mealworm (YM, *Tenebrio molitor*). Substrate iron content was increased using ferric ammonium citrate (FAC), ranging from 267-563 mg/kg (0 to 10 mM FAC) for YM and 323-6637 mg/kg (0 to 100 mM FAC) for BSF. Larval weight of YM was unaffected by dietary iron content, but survival rates significantly decreased by 4% at the 10 mM diet. In BSF larvae, no differences in body weight or survival were noted between dietary iron treatments, but cuticular lesions potentially indicative of iron overload appeared at 100 mM diet. When exposed to excess dietary iron, both YM and BSF showed significant increases in iron content in a dose-dependent manner, with BSF larvae exhibiting a threefold increase from 372 mg/kg to 999 mg/kg. Both species exhibited significant reductions in zinc on iron-enriched diets. Calcium levels in BSF strongly correlated with dietary iron concentration, rising by over 20% at the 100 mM diet, a phenomenon not previously reported. Finally, across all dietary iron concentrations, no significant effects on protein and fat content or soluble protein composition were observed in either species. All together data suggest that BSF larvae can act as a precious source of both iron and calcium for food and feed formulations through substrate manipulation.

1. Introduction

Iron deficiency is the most prevalent hidden nutrient deficiency worldwide, with more than 24% of the world population suffering from iron deficiency anaemia (GBD, 2023). Similarly, iron deficiency anaemia is also widespread among livestock, particularly pigs, with over 60% of piglets suffering from this condition (Kim *et al.*, 2018).

For human consumption, heme-based iron is currently the most bioavailable form of iron available, which is found mostly in animal-based sources (Schönfeldt and Hall, 2011). However, the production of these animal-based products requires extensive use of water, energy, and land, posing significant global economic and sustainability burdens (Parlasca and Qaim, 2022). Iron supplementation is a common practice for both humans and livestock to combat iron deficiency. Nevertheless, this approach

is associated with health risks and low bioavailability. In humans, iron supplements can lead to various side effects, such as gastrointestinal issues, fatigue and dizziness, and poor iron absorption rates (Tolkien *et al.*, 2015). In piglets, iron supplementation can result in antioxidant deficiency and the induction of hepcidin expression, which reduces iron absorption (Szudzik *et al.*, 2018). These observations underscore the need for novel, sustainable and bioavailable iron sources, for humans and livestock alike.

Edible insects are a viable alternative protein source for both feed and food, owing to their lower requirements for water, land and energy in rearing (van Huis *et al.*, 2021). Many edible insects have an iron content similar to beef, and a Caco-2 iron bioavailability assay suggested similar absorption between insects and beef (Latunde-Dada *et al.*, 2016; Mwangi *et al.*, 2018). There is a knowledge gap regarding the effective utilization of iron from edible insects, given the high levels of antinutritional factors that can inhibit absorption (Mwangi *et al.*, 2022). However, the use of fractionated insect products may offer a promising approach to harness this iron as a viable nutritional source. It is hypothesised that the iron availability potential in insects is rooted in entoferritin, the predominant iron transporter protein in insects (First *et al.*, 2023). Although it is evident that substrate iron content influences iron concentrations in insects (Seyedalmoosavi *et al.*, 2023), little is known about how this affects their development and nutritional profiles. For instance, *Hermetia illucens* larvae reared on different waste streams with varying iron contents have shown increased iron concentrations when reared on a high-iron waste stream (Seyedalmoosavi *et al.*, 2023).

This study investigates how the targeted addition of iron affects the overall development and nutritional content of edible insects. The effects of dietary iron on the growth, survival, macro- and micronutrients content of two key insect species in the food and feed industry: black soldier fly (BSF) and yellow mealworm (YM) larvae were measured under a diet intervention trial.

2. Methods

2.1 Yellow mealworm rearing

Ferric ammonium citrate (FAC, CAS number 1185-57-5) was obtained from Merck (Darmstadt, Germany). The iron salt was dissolved in water (FAC solution) in a concentration 0, 1,2.5, 5 and 10 mM (Table 3.1). Mealworm feed provided by InsectenKwekerij van de Ven V.O.F (Deurne, the Netherlands) was mixed using a

magnetic stirrer with the different FAC solutions at a 1:1, FAC solution feed ratio (v/w). The wet feed was then dried overnight at 50 °C with ventilation set on 100% overnight in an incubator (Binder GmbH, Tuttlingen, Germany). After drying, the substrate was ground with a blender (Waring, Stamford, CT, USA) and returned to the incubator at 50 °C with ventilation set on 100% for another night. Finally, the feed was ground again with a blender into a fine powder with a dry matter (DM) content of approximately 90% to finalize the YM substrate. Final iron content in the substrates varied from 267 to 563 mg/kg DM, including the non-spiked iron content of the feed (Table 3.1). Each YM substrate was sampled for freeze-drying and homogenization prior to mineral analysis as described below.

The YM larvae (InsectenKwekerij van de Ven V.O.F, Deurne, the Netherlands) were reared in a controlled environment at 25°C, dark environment and 50% relative humidity in a rearing container (15.5 x 10.5 x 6 cm). For each diet (Table 3.1), 500 larvae, approximately 1 cm in length and weighing approximately 26 mg each, were placed on 20 g of YM substrate and 15 g of carrots. Every other day, the YM were provided with 10 g of fresh YM substrate and 15 g of fresh carrots. Dead YM were removed at each feeding event to prevent cannibalism. Upon the appearance of the first pupae, 20 days after exposing the larvae to the experimental substrate, the YM were transferred to a control YM substrate diet for two days to clear excess iron-spiked diet from their gut (Figure 3.1). On day 22, the YM larvae were separated from the feed using a sieve (pore size 1 mm), weighed (three sets of 30 random larvae), and individually counted.

For each replicate, 5 g of larvae were sacrificed with CO_2 for further preparation of soluble fractions. The remaining larvae were sacrificed by flash-freezing with liquid nitrogen, followed by freeze-drying and stored at -80°C until proximate and mineral analyses. Each diet was done in triplicate.

2.2 Black soldier fly rearing

Before mixing with FAC solution, chicken feed (Kuikenopfokmeel no. 1, Kasper FaunaFood, the Netherlands) was sieved (pore size 1.0 mm). FAC solutions were prepared by dissolving FAC in water at concentrations of 0, 10, 25, 50 and a 100 mM (Table 3.1). The FAC concentrations incorporated in the BSF diet were tenfold higher than those tested in the YM substrate, as preliminary trials indicated the lower FAC concentrations did not affect larval weight or survival of BSF larvae, whereas at 5 mM FAC YM performance was negatively affected (Figure 3.2). Sieved chicken feed was combined with the FAC solution in a 1:2 ratio (w/v) and mixed with a magnetic stirrer

for 30 min at room temperature to prepare the BSF substrate. Final iron content in the substrates varied from 323 to 6637 mg/kg, including the non-spiked iron content of the feed (Table 3.1). Each BSF substrate was sampled for freeze-drying and homogenization prior to mineral analysis as described below.

Eggs from BSF were obtained from Protix (Bergen op Zoom, The Netherlands). Approximately 10,000 eggs were distributed into 10 rearing containers, each containing 600g of wet BSF substrate, with a feed to water ratio of 1:2 (w/v). The lids of the rearing containers had a window (8.0 × 5.5 cm) covered with nylon mesh to allow ventilation. The day of the first larvae hatching was designated as day zero of the trial. Insect rearing was carried out at 27 °C and a relative humidity of 70% in the dark.

On day 3, any unhatched eggs were removed to ensure uniformity among the larvae. On day 5, a homogeneous group of larvae that were manually chosen and collected, weighing approximately 10 mg each, were introduced to the FAC-spiked BSF substrate (Table 3.1, Figure 3.1. A). For each dietary group, 250 larvae were placed on 105 g of wet BSF substrate per 100 larvae with a feed to water ratio of 1:2 (w/v). Each rearing container held a sample size of 250 larvae. After six days on the iron-spiked diet, the larvae were transferred to a control BSF substrate to clear the iron-spiked diet from their guts. On day 12, the larvae were separated from the substrate using a sieve, washed with room temperature tap water, individually counted and weighed (three sets of 30 random larvae).

For each replica, 5 g of larvae were sacrificed with CO_2 for further preparation of soluble fractions. The remaining larvae were sacrificed by flash-freezing with liquid nitrogen, followed by freeze-drying and stored at -80°C until proximate and mineral analyses. Each diet was done in triplicate.

Table 3.1. Iron concentrations (mg/kg dry substrate) of substrates used for rearing the yellow mealworm larvae and black soldier fly larvae.

Yellow mealworm larvae substrate	**Diet**				
	Control*	1 mM	2.5 mM	5 mM	10 mM
Fe	267	293	350	407	563
Black soldier fly larvae substrate	**Diet**				
	Control*	1 mM	2.5 mM	5 mM	10 mM
Fe	323	943	2300	2740	6637

** Control substrates were not mixed with ferric ammonium citrate; the iron content is based on the starting iron concentrations of the feeds.*

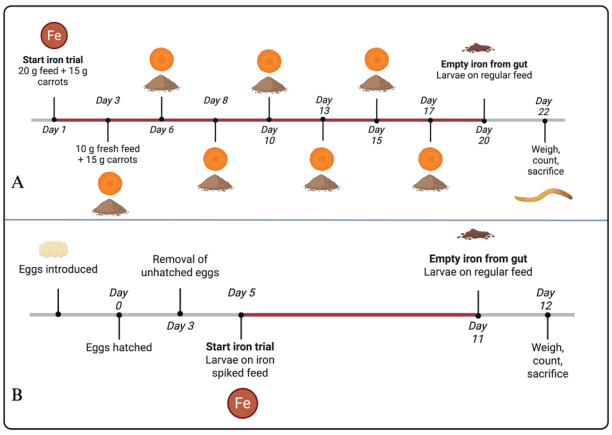


Figure 3.1. Timeline of the rearing period of the yellow mealworm (A) and black soldier fly (B) larvae. Created with BioRender.com.

3. Insect parameters

3.1 Survival

Survival was calculated as described by Oonincx *et al.* (2019). Survival is defined as the percentage of larvae remaining at the end of the rearing period relative to the number of larvae at the beginning of the rearing period.

3.2 Larval weight

Average weight of the larvae was determined by randomly collecting 30 larvae from each rearing container at the end of the rearing period weighing them collectively and dividing the value by 30. This process was repeated three times for each replicate.

3.3 Lesion documentation

Freeze-dried BSF reared on 100 mM FAC diet were visually inspected using an Olympus SZX12 microscope equipped with a Euromex sCMEX-20 camera, using ImageFocus software. Images of specific lesions on the larvae were captured.

4. Proximate composition

4.1 Sample preparation

Firstly, flash-frozen insects were placed in pre-weighed boxes, covered with plastic lids. A hole was cut in each lid and covered with tissue to allow water sublimation. For the substrate samples, approximately 20mL of substrate was placed in 50mL Greiner tubes, covered with tissue, and secured with rubber bands. The insect and substrate samples were freeze-dried with the Super Modulyo freeze dryer (Edwards, Burgess Hill, UK). After freeze-drying, the containers with samples were weighed and immediately transferred to new airtight containers. These containers were then stored in vacuum bags in the freezer at -80°C until sample homogenization.

Insect samples were homogenized using the Freezer/CryoMill® 6775 (SPEX SamplePrep, New Jersey, USA). The CryoMill operated with dual samples under automatic liquid nitrogen filling, with a pre-cool time of 3 min, a run time of 3.5 min, and a cool time of 1 min. Milling was performed in three cycles at a rate of 15 cps. Substrate samples were homogenized by placing 8-10 g of the sample in the Retsch Ball Mill MM400 (Retsch, Haan, Germany) for 45 s at a frequency of 25/s.

Soluble fraction was prepared by grinding CO_2-sacrificed larvae with Milli-Q water at a 1:4 ratio. The resulting slurry was centrifuged at 4,700X g for 45 minutes at 4°C followed by supernatant (soluble fraction) collection. This soluble fraction was then stored at -80°C until further use.

4.2 Dry matter content

The dry matter (DM) content of the freeze-dried larvae was measured using a DAB 200-2 Moisture analyzer (KERN and Sohn GmbH, Balingen, Germany). To determine the DM, one gram of the sample was heated at 120°C until complete dryness. Dry matter content represents the fraction of dried material relative to the fresh weight of the larvae.

4.3 Fat content

Fat extraction was based on the Official AOAC method 920.39 (AOAC, 2023), with minor modifications. The fat content of the larvae was determined using a SOXTHERM® Extraction unit (Gerhardt GmbH and Königswinter, Germany). In this procedure, four g of freeze-dried insect powder were placed into extraction thimbles and covered with

grease-free cotton wool. The fat was extracted using petroleum ether (boiling range 40-60° C) at an extraction temperature of 150°C for a 2 h. Following extraction, the canisters were left in a fume hood overnight to allow any residual solvent to evaporate. The remaining fat content in the canisters was weighed the next day to and calculated as a percentage of the DM.

4.4 Protein content and molecular weight distribution

The nitrogen content of the larvae was quantified using a DUMAS Flash EA 1112 Protein analyser (Thermo Fisher Scientific, USA, Massachusetts, USA). Cellulose (Merck, Darmstadt, Germany) was used as a blank, and D-methionine (Thermo Scientific Chemicals, Waltham, USA) was utilized to construct the calibration curve. The protein content of the samples was calculated assuming a nitrogen-to-protein conversion factor of 4.75 for the yellow mealworm larvae and 4.67 for the black soldier fly larvae as established for these two species respectively (Janssen *et al.*, 2017). The Protein samples were expressed as a percentage of the DM.

Protein composition was assessed using sodium dodecyl sulphate polyacrylamide gel electrophoresis (SDS-PAGE) under reducing conditions. The soluble fraction samples were run on 12-well NuPAGE™ Novex™ 12% Bis-Tris gels. The electrophoresis was carried out using NuPAGE™ MOPS SDS Running Buffer and NuPAGE™ Antioxidant, followed by staining with Coomassie Brilliant Blue R-250 Staining Solution. Thermo Scientific™ Spectra™ Multicolor Broad Range Protein Ladder (10-225 kDa) was used as a molecular weight marker. The gels were scanned using a GS-900 Calibrated Densitometer (Bio-Rad, USA), and ImageLab (version 6.1, Bio-Rad, USA) was employed for documenting the gels.

4.5 Ash content

The total content of non-combustible inorganic elements, called ash, was measured following the AOAC ash determination protocol (Thiex *et al.*, 2012), with minor modifications. In brief, one gram of freeze-dried insect powder was incinerated at 550° C for 5 hours using a Gallenkamp Muffle Furnace (Gemini B.V., Apeldoorn, the Netherlands). Post-incineration, the samples were left to cool overnight in a desiccator before weighting. After weighing, concentrations were calculated and expressed as a percentage of the dry matter.

4.6 Trace mineral analysis

Larvae and substrate mineral quantification was carried out by the Soil Chemistry Laboratory (CBLB, Wageningen University and Research, the Netherlands). Briefly, 300 mg of the insect sample was treated with concentrated nitric acid and hydrochloric acid. The mixture was then heated in a microwave. Following this, hydrogen peroxide was added, and the mixture was reheated in the microwave. After allowing the undissolved silica particles to settle, the supernatant was collected for analysis using Inductively Coupled Plasma Atomic Emission Spectroscopy (ICP-AES, Thermo iCAP-6500 DV; Thermo Fisher Scientific, United states of America). The mineral content was expressed as g/kg DM (Ca, K, Mn and P) or mg/kg (Fe and Zn). Bioaccumulation factor (BAF) is defined by Daş *et al.* (2023) as the larval iron concentration divided by the substrate iron content.

5. Data analysis

Statistical analyses were conducted using RStudio (version 1.3.1073). A one-way ANOVA was performed to evaluate differences among groups, followed by Tukey's Honestly Significant Difference (HSD) post-hoc test for pairwise comparisons with alpha set at 0.05. Pearson correlation analysis was employed to assess the relationship between substrate iron concentration and the mineral contents. Correlations were classified as moderate for Pearson correlation coefficients (r) ranging from 0.75 to 0.9, or from -0.75 to -0.9. Correlations were considered strong when r was ≥ 0.9 or ≤ -0.9.

3. Results and discussion

1. Insect parameters

1.1 Yellow mealworm (YM)

Larvae reared on control diet weighed 134.1 ± 5.3 mg (Figure 3.2A). The observed range of larval weight at this rearing time aligns with values reported in the literature (Kim *et al.*, 2016; Rumbos *et al.*, 2022). The YM reared on substrate with 2.5 mM of FAC reached a similar weight (139.3 ± 3.2 mg) as the larvae on control and 1mM FAC diets. Further increase of FAC concentration to 5 mM significantly decreased larval weight to 131.5 ± 1.5 mg compared to the 2.5 mM Diet. At the highest tested concentration of 10 mM FAC, larval weight (134.2 ± 4.7 mg) was significantly higher than the 5 mM FAC diet but was

similar to that on control, 1 and 2.5 mM FAC diets. Thus, there was no clear trend in the effect of iron concentration on larval weight of YM.

Survival of YM larvae on control diet was the highest (98.6%) compared to all FAC diet reared larvae. Increase in FAC content up to 5 mM resulted in survival of 97.6%. On 10 mM FAC diet, survival dropped to 94.9%, being significantly lower than on control diet (Figure 3.2B). The survival of YM larvae in this study is high compared to other studies. The larvae in this study exhibited survival ranging from 94% to 99%, while previous studies reported survival of 70% to 90% in various feeding experiments (Jamaa *et al.*, 2021; Liu *et al.*, 2020; Rumbos *et al.*, 2022). The high survival rate observed in our study suggests that the larvae were reared under suitable conditions. Prior to this study, the effect of iron excess on YM survival has not been documented. However, exposure to similar excess dietary iron can reduce growth rates, larval size, oviposition, and locomotive functionality in insects such as *Drosophila melanogaster* and *Lymantria dispar* (dos Santos *et al.*, 2024; Keena, 2022). Although those studies did not measure survival, they did demonstrate that excess dietary iron negatively affects larval development and health. This negative impact aligns with the findings reported here on the YM larvae when exposed to excess dietary iron. Given the significant impact of iron supplementation on YM larvae, they were not reared on the tenfold iron diet used for BSF larvae (Table 3.1).

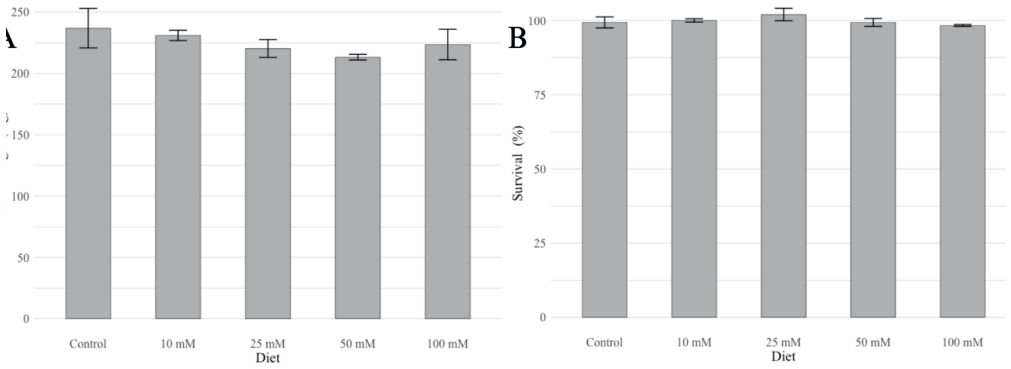


Figure 3.2. A: Average weight (mg) of YM larvae; B: Survival (%) of YM larvae. Both measurements were taken 22 days after larvae were introduced to substrates with varying concentrations of ferric ammonium citrate: control, 1 mM, 2.5 mM, 5 mM, and 10 mM. Bars having no letter in common differ significantly (one-way ANOVA followed by Tukey's HSD test; $p < 0.05$).

1.2 Black soldier fly (BSF)

The weight and survival of BSF larvae did not significantly differ across the FAC concentrations tested (0-100 mM, Figure 3.3). The weight range of BSF larvae at a similar age, between 200-250 mg per larvae, is in line with literature (Kieling *et al.*, 2023; Seyedalmoosavi *et al.*, 2022). Larval weight change in response to increased iron concentrations has not previously been reported for BSF, but the effect of heavy metals is well-documented. In a study conducted by Wu *et al.*, (2020), larvae were reared on diets spiked with copper concentrations ranging from 100 to 800 mg/kg DM and cadmium concentrations from 10 to 80 mg/kg DM. The study demonstrated that BSF larvae do not exhibit significant changes in larval weight when reared on diets with varying levels of cadmium or copper, that is similar to the effect of the excess of dietary iron observed in the current study. However, it should be noted, that biological effects and known lethal or toxic concentrations of different metals vary, making it challenging to directly compare effects of iron concentrations with cadmium or copper (Gupta and Gupta, 1998).

Similar to the larval weight, BSF larval survival was unaffected by dietary iron concentrations (ranging from 99 to 102%). The survival rates slightly exceeding 100% are likely due to human error, as the larvae were counted manually. Survival of nearly 100% during an 11-14 days rearing period is a common in BSF reared in suitable conditions (Cheng *et al.*, 2017). However, survival can vary depending on the feed source. For example, BSF reared on fish-based diets and digested sewage sludge, which are both contaminated with various heavy metals, exhibited survival rates of 47% and 39%, respectively (Lalander *et al.*, 2019; Nguyen *et al.*, 2013). The low survivability of larvae reared on sewage sludge (39%) was associated with a lower protein conversion rate compared to those reared on undigested sewage sludge, which had 79% survival (Lalander *et al.*, 2019). Cai *et al.*, (2018) reared larvae on artificial diets spiked with 11 different heavy metals, mimicking the content found in such waste streams, to investigate the specific effect of heavy metals on BSF larvae survival in contaminated waste streams. Although iron was not included in the study, none of the tested heavy metals affected larval survival when exposed to these artificial diets. These findings align with the current study, indicating that metal content, including iron, has a lesser impact on BSF larval survival compared to factors like substrate processing, moisture content and macronutrient bio-accessibility.

Several BSF larvae reared on the 100 mM diet (6637 mg/kg DM of iron) displayed a dark, three-layered lesions with an approximate diameter of 400 to 800 µm (Figure 3.3). Although this phenomenon has not been previously documented in insects, forensic signs of iron toxicity have been characterized in other animals. For instance, bronze

skin hyperpigmentation and the presence of a black-greyish, rigid pancreas have been observed in humans (de Carvalho Machado and Dinis-Oliveira, 2023). Iron is not known to be directly involved in cuticle formation in BSF larvae, but calcium is. As elaborated below, calcium levels of BSF larvae levels are correlated with dietary iron concentrations in the substrate (Table 3.3). Amorphous calcium carbonate and calcite are abundant in the larval cuticle and their presence increases with larval growth (Rebora *et al.*, 2023). This could explain the appearance of these lesions. This finding could be used as an indication of extreme iron concentrations in waste streams fed to BSF larvae.

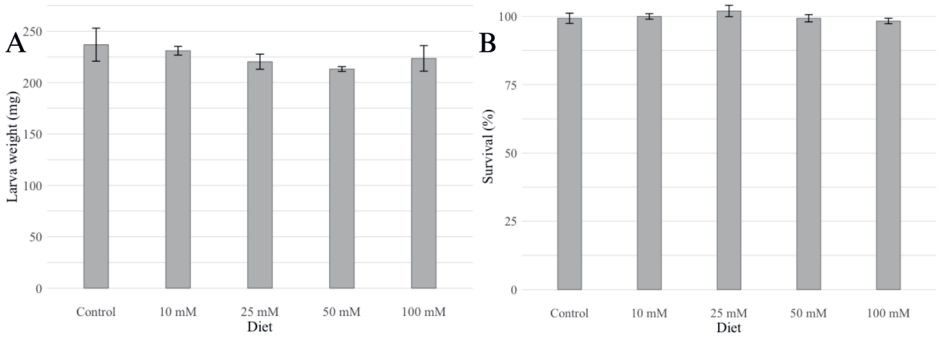


Figure 3.3. A: Average weight (mg) of BSF larvae; B: Survival rates (%) of BSF larvae. Both measurements were taken 6 days after 5 days old homogenous larvae were introduced to substrates with varying concentrations of ferric ammonium citrate: control, 10 mM, 25 mM, 50 mM, and 100 mM. No significant differences between diets were found for either the average weight or survival rate of the BSF larvae.

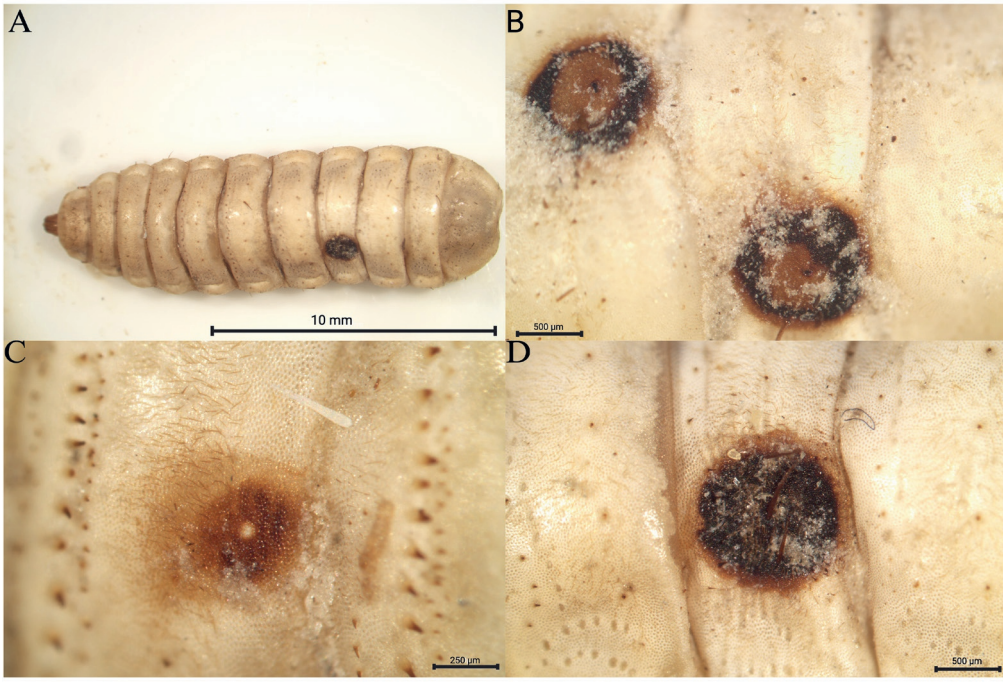


Figure. 3.4. BSF reared in the 100 mM FAC diet. Image captured using an Olympus SZX12 microscope equipped with a Euromex sCMEX-20 camera. The taken pictures focus on the lesions found on the larvae reared on the 100 mM diet. The scale bars in the pictures are 10 mm (A), 500 µm (B), 250 µm (C), and 500 µm (D).

1.3 Proximate composition

Fat content, protein content and soluble protein composition of the two larvae species were not significantly altered by the incorporation of FAC in the substrate. For the BSF larvae, protein content ranged from 32.9% to 33.8% DM, and fat content ranged from 28.5% to 31.1% DM. For the YM larvae, protein content ranged from 38.0% to 38.7% DM, and fat content ranged from 34.8% to 35.9% DM (Table 3.2, Figure 3.4). Protein content, bio-accessibility and fat content have been shown to be the main drivers for protein and fat alteration of both BSF and YM larvae (Fischer and Romano, 2021; Jankauskienė *et al.*, 2024; Wu *et al.*, 2006). These findings further support the conclusion that substrate processing, macronutrient composition and form are the primary determinants of larval macronutrient composition, with iron playing a negligible role.

Ash content of YM larvae did not differ significantly between the different FAC diets,

with 3.4% DM on the 1 mM diet being the lowest and 3.8% DM on the 5 mM FAC diet being the highest. These ash concentrations are aligned with previously reported YM larvae inorganic content ranging from 1% DM to 5% DM. An increase of dietary iron concentration from FAC in this study did not significantly alter the ash content of YM larvae. It is suggested that the relatively low proportion of iron, comprising less than 0.5% DM of the total larval mineral composition (Costa *et al.*, 2020), is insufficient to significantly affect the total ash content.

The ash content of the BSF larvae was highest on the 100 mM FAC diet, at 11.5% DM, was significantly higher compared to all other diets. The ash content reported in this study falls within the previously reported range for BSF larvae, which varies widely from 3% DM to 17% DM depending on factors such as strain, diet and rearing conditions (Boafo *et al.*, 2023; Weko *et al.*, 2023). Unlike protein and fat content, ash is not reported to be dose-dependent on any specific macronutrient (Boafo *et al.*, 2023). Similar to YM larvae, the total iron content in BSF larvae ranks it among microminerals, comprising less than 0.5% of the total mineral content (Chia *et al.*, 2020). Despite this, an increase in ash content by 1.3% DM was observed. Given the small proportion of iron in the total mineral composition of the larvae, it is unlikely that increased iron alone could account for the rise in ash content. Instead, the data suggest that the elevated dietary iron in the BSF substrate may have facilitated the accumulation of other minerals, notably calcium, which contributed to the observed increase in ash content, as mentioned below.

Table 3.2. Protein, fat, and ash content (% dry matter) of YM and BSF larvae reared on diets with different ferric ammonium citrate concentrations. Each nutritional value is compared between the FAC diets within the two insect species.

Yellow mealworm					
	Control	**1.0 mM**	**2.5 mM**	**5.0 mM**	**10.0 mM**
Protein (%/DM)	38.5 ± 0.5	38.1 ± 0.0	38.0 ± 0.1	38.7 ± 0.3	38.3 ± 0.2
Fat (%/DM)	34.8 ± 3.0	35.7 ± 2.3	35.9 ± 1.4	35.7 ± 1.2	35.5 ± 2.0
Ash (%/DM)	3.6 ± 0.1	3.4 ± 0.5	3.7 ± 0.1	3.8 ± 0.2	3.5 ± 0.1
Black soldier fly					
	Control	**1.0 mM**	**2.5 mM**	**5.0 mM**	**10.0 mM**
Protein (%/DM)	32.9 ± 0.8	33.3 ± 0.8	33.6 ± 0.8	33.8 ± 0.1	33.3 ± 0.1
Fat (%/DM)	28.5 ± 1.6	30.8 ± 0.5	30.6 ± 0.6	30.4 ± 1.5	31.1 ± 1.3
Ash (%/DM)	10.3ab ± 0.1	10.2a ± 0.0	10.3ab ± 0.3	10.8b ± 0.2	11.5c ± 0.2

*Different letters indicate significant differences ($p < 0.05$). Mean groups lacking common letters are not significantly different ($p > 0.05$).

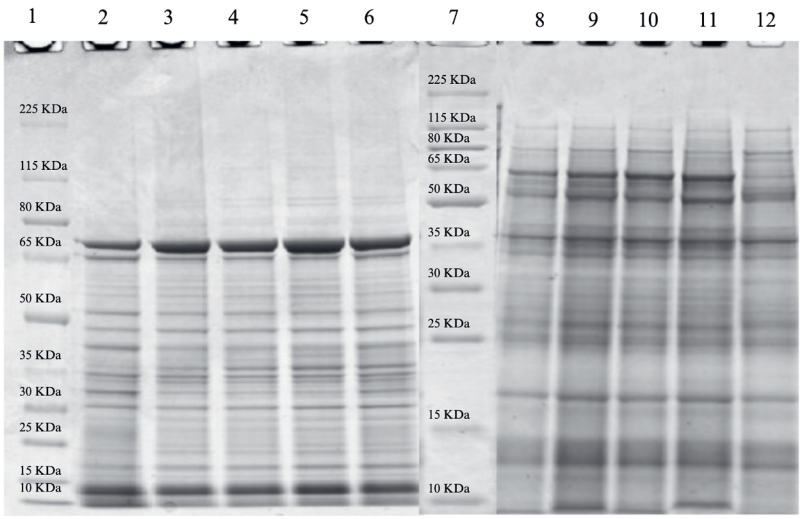


Figure 3.5. Molecular weight distribution of BSF and YM larvae soluble fraction by SDS page under reducing conditions. Lane 1: Marker (10-225 kDa); Lane 2: BSF larvae control; Lane 3: BSF larvae 10 mM; Lane 4: BSF larvae 25 mM; Lane 5: BSF larvae 50 mM; Lane 6: BSF larvae 100 mM; Lane 7: Marker (10-225 kDa); Lane 8: YM larvae control; Lane 9: YM larvae 1 mM; Lane 10: YM larvae 2.5 mM; Lane 11: YM larvae 5 mM; Lane 12: YM larvae 10 mM.

2. Trace minerals

2.1. Iron

A significant dose-dependent positive correlation between iron concentration in the substrate and YM larval iron content was found (Table 3). The YM larvae reared on diets containing up to 5 mM FAC have shown a significant increase of just under 20% in iron content (50.33 to 58.66 mg/kg) without compromising larval growth or survival. Oppositely, a negative dose-dependent trend was observed between the YM substrate iron and the iron BAF of the larvae. Iron bioaccumulation was significantly higher in the control group (0.18) compared to all other treatments, while the 10 mM diet (0.11) showed significantly lower bioaccumulation than all other treatments (Table 3, Figure 3.2). These results suggest that although iron levels in YM larvae can be increased through dietary manipulation, the extent of accumulation is limited due to the low conversion rate.

A significant dose-dependent increase in iron content was also observed in BSF larvae with increasing concentrations of FAC in their substrate (Table 3.3). At the highest dosage (100 mM), the iron content in the larvae nearly tripled, from 372 mg/kg DM to 999 mg/kg DM, while larval size and survival remained similar (Table 3, Figure 3.3). These results are consistent with the study by Seyedalmoosavi *et al.* (2023), who explored rearing BSF larvae on substrates mixed with various fertilizers to simulate sewage waste and resulting in iron content of the substrates between 337 and 5852 mg/kg DM. However, a decrease in iron BAF was observed, with the highest value in the control diet (1.15). Bioaccumulation then plateaued at 25 mM (0.27), showing similar values in the 50 mM and 100 mM treatments. The lack of significant differences among these three highest iron treatments highlights the BSF larvae's capacity to accumulate iron even at very high substrate iron concentrations. The consistent BAF values across diets with more than 25 mM FAC and above may indicate that iron absorption at high concentrations occurs via a passive paracellular pathway, driven by a density gradient. Unlike protein-regulated gut absorption, paracellular transport involves the passive movement of water and charged molecules through tight junctions between epithelial cells (Hollander & Kaunitz, 2020). This phenomenon has not been investigated in edible insects regarding iron and warrants further study. In the work of Seyedalmoosavi *et al.* (2023), larvae reared on substrates with varying iron content showed lower larval iron levels (150-557 mg/kg DM), compared to the current findings (372-999 mg/kg DM). Notably, larvae reared on a substrate mimicking sewage containing 337 mg iron/kg DM, accumulated less than half the iron (150 mg/kg DM) compared to larvae reared on a sewage mimic with 351 mg iron/kg DM, which accumulated 339 mg/kg DM. The latter

treatment is comparable to the iron BAF found in the control diet (1.15). Additionally, larvae reared on a sewage mimic substrate with 5852 mg iron/kg DM resulted in a larval iron content of 557 mg/kg DM, leading to a lower iron BAF when compared to the 100 mM treatment (0.15). Thus, the strong correlation observed in the current study between substrate iron and larval iron content and the higher iron BAF (Table 3), as opposed to the findings of Seyedalmoosavi *et al.* (2023), may be attributed to differences in iron accessibility in the substrates. Missirlis *et al.* (2006) demonstrated that FAC inclusion in the substrate significantly increases iron levels in *Drosophila melanogaster*, another fly species, suggesting that FAC can act as a bioavailable iron source for BSF larvae as well. Thus, it is suggested that the FAC iron is more bioavailable compared to the iron in fertilizer mimics, which may be less soluble and more prone to interactions with anti-nutritional factors, making it less accessible to the larvae. Pre-processing methods might improve the bioavailability of iron in waste materials for BSF larvae, as suggested by this comparison.

2.2. Zinc

Increasing the dietary iron in both the BSF and YM substrate decreased the zinc concentration of the larvae, from 128 (Control) to 117 (10 mM) mg/kg in the YM larvae and from 183 (Control) to 125 mg/kg for the BSF larvae (100 mM, Table 3). The dose-depended relationship between iron intake to zinc levels is not studied in insects but is well known amongst other organisms. Iron is a known antinutritional factor of zinc in mammals (Meadows *et al.*, 1983). For instance, piglets exposed to excessive dietary iron have a dose-dependent zinc decrease (Middleton *et al.*, 2021). This might be as iron and zinc share similar transporters and receptors, such as the ZIP protein family and DMT1 (Hansen *et al.*, 2009, Cousins *et al.*, 2006). Although this relationship in insects has not been investigated, ZIP proteins were identified in insects to deliver both iron and zinc, and the transporter DMT1 is known to interact with both metals in insects (Bettedi *et al.*, 2011; Missirlis, 2021). Therefore, it is possible that excessive dietary iron inhibits zinc absorption due to competition for both DMT1 and ZIP proteins capacity in BSF and YM.

2.3. Calcium

Calcium levels were similar across all diets for the YM (from 1.1 to 1.2g/kg). In mammals calcium is known to decrease iron absorption due to noncompetitive inhibition of the DMT1 transporter (Thompson *et al.*, 2010). The calcium absorption pathway in insects begins primarily in the midgut, where calcium uptake is driven by a calcium concentration gradient (Taylor, 1985). Although the specific mechanisms of calcium

absorption in the insect midgut remain underexplored, evidence suggests that this process may involve passive and active transport pathways. A secondary reabsorption of calcium occurs in the Malpighian tubules, facilitated by calcium-specific channels such as Dmca1A and Dmca1D (Browne and O'Donnell, 2018; Dube *et al.*, 2000). This reliance on specific transporters and calcium concentration might explain the minimal effect on calcium absorption observed in the diets provided, despite the competition on the DMT1 pathway.

Interestingly, a strong correlation was found between substrate iron content to BSF larvae calcium content (from 26.5 to 31.9 g/kg, Table 3) when dietary iron was increased. Notably, this approximate 5.4 g/kg increase in calcium partially explains the 1% significant increase in the total insect ash content (Table 3.2, Table 3.3). There is a gap in literature regarding how increased iron intake affects calcium levels in arthropods. However, calcium has been shown to inhibit iron absorption in humans (Lönnerdal, 2010). Understanding this phenomenon requires further research.

2.4. Phosphorus

No significant differences in phosphorus content were observed within the larvae of the two insect species across the iron treatments. The phosphorus content ranged from 6.8 to 7.2 g/kg in the YM larvae and from 7.6 to 7.8 g/kg in the BSF larvae (Table 3.3). Ferric citrate hydrate is a medicine used for patients suffering from chronic kidney disease to lower phosphorus serum levels (Iida *et al.*, 2013). Ferric iron binds to phosphorus ions, making it insoluble, lowering absorption. Similarly, the free iron in FAC could interact with phosphorus. This potential interaction did not affect YM and BSF larvae phosphorus levels.

2.5. Potassium

The most abundant mineral in the larval body, potassium, was not affected by dietary iron concentrations. The potassium content ranged from 8.3 to 8.7 g/kg in the YM larvae and from 10.9 to 11.5 g/kg in the BSF larvae (Table 3.3). The absorption pathways of potassium occur primarily via a concentration gradient through Na+/K+-ATPase pumps, a conserved mechanism common in all animals. This pathway has minimal connection to the DMT1 and ZIP transporters involved in iron absorption found in insects (Gorman, 2023; Terra and Ferreira, 2020; Thabet *et al.*, 2016).

2.6. Magnesium

The FAC diets did not affect magnesium content in the larvae of either insect species. The magnesium content ranged from 1.9 to 2 g/kg in the YM larvae and 2.5 g/kg in the BSF larvae (Table 3). Iron has not been documented to affect magnesium absorption. Moreover, magnesium increases nonheme iron absorption in humans (Neda *et al.*, 2022).

Table 3.3. Trace mineral composition (W/W dry matter) of YM and BSF reared on diets with different iron (FAC) concentrations. Each value is compared between the iron treatments within each of the two insect species. Different letters indicate significant differences ($p < 0.05$). Mean groups lacking common letters are not significantly different ($p > 0.05$). The Pearson correlation coefficient (r) between the mineral content and the iron in the substrate is defined as follows: *indicates a moderate correlation ($0.7 \leq r < 0.9$ for moderate positive correlation or $-0.9 < r \leq -0.7$ for moderate negative correlation), and xx indicates a strong correlation ($r \geq 0.9$ for strong positive correlation or $r \leq -0.9$ for strong negative correlation).

Yellow mealworm						
Diet	**Control**	**1.0 mM**	**2.5 mM**	**5.0 mM**	**10.0 mM**	Pearson correlation coefficiency (r)
Substrate iron content (mg/kg)	267	293	350	407	563	
Bioaccumulation factor (BAF) of iron	0.18^{a}	0.18^{a}	0.15^{b}	0.14^{b}	0.11^{c}	
Iron* (mg/kg DM)	$50.3^{a} \pm 2.0$	$55.3^{bc} \pm 0.5$	$54.0^{ab} \pm 0.0$	$58.6^{c} \pm 2.3$	$64.0^{d} \pm 1.0$	0.91^{xx}
Zinc* (mg/kg DM)	$128.4^{a} \pm 1.5$	$126.6^{ab} \pm 3.3$	$117.5^{c} \pm 2.6$	$120.3^{bc} \pm 3.2$	$117.3^{c} \pm 2.6$	-0.70^{x}
Calcium (g/kg DM)	1.1 ± 0.0	1.1 ± 0.0	1.1 ± 0.1	1.2 ± 0.2	1.1 ± 0.1	-0.10
Potassium (g/kg DM)	8.6 ± 0.3	8.6 ± 0.1	8.3 ± 0.2	8.7 ± 0.1	8.4 ± 0.2	-0.22
Magnesium (g/kg DM)	2.0 ± 0.1	2.0 ± 0.0	1.9 ± 0.1	2.0 ± 0.0	1.9 ± 0.0	-0.45
Phosphorus (g/kg DM)	7.0 ± 0.3	7.1 ± 0.1	6.8 ± 0.2	7.2 ± 0.2	6.8 ± 0.2	-0.28
Black soldier fly						
Diet	**Control**	**10.0 mM**	**25.0 mM**	**50.0 mM**	**100.0 mM**	Pearson correlation coefficiency (r)
Substrate iron content (mg/kg)	323	943	2300	2740	6637	
Bioaccumulation factor (BAF) of iron	1.15^{a}	0.53^{b}	0.27^{c}	0.21^{c}	0.15^{c}	
Iron* (mg/kg DM)	$372.6^{a} \pm 31.2$	$505.3^{ab} \pm 39.1$	$626.6^{bc} \pm 74.8$	$791.3^{c} \pm 12.5$	$999.3^{d} \pm 125.1$	0.95^{xx}
Zinc* (mg/kg DM)	$183.8^{a} \pm 15.0$	$154.5^{b} \pm 12.1$	$136.3^{bc} \pm 10.1$	$125.8^{c} \pm 2.9$	$125.6^{c} \pm 9.0$	-0.75^{x}
Calcium (g/kg DM)	$26.5^{a} \pm 1.5$	$27.0^{a} \pm 0.53$	$28.1^{ab} \pm 0.5$	$30.1^{bc} \pm 1.3$	$31.9^{c} \pm 0.5$	0.91^{xx}
Potassium (g/kg DM)	11.5 ± 0.2	11.5 ± 0.1	11.2 ± 0.4	10.9 ± 0.3	10.9 ± 0.4	-0.67
Magnesium (g/kg DM)	2.5 ± 0.1	2.5 ± 0.0	2.5 ± 0.03	2.5 ± 0.0	2.5 ± 0.1	0.15
Phosphorus (g/kg DM)	7.6 ± 0.5	7.6 ± 0.5	7.6 ± 0.2	7.8 ± 0.2	7.8 ± 0.5	0.18

4. Conclusion

This study investigated the effects of dietary iron on the growth, survival, and nutritional composition of larvae of the yellow mealworm and the black soldier fly. Survival at high iron concentrations (10 mM) decreased YM survival, indicating sensitivity to iron overload. In contrast, BSF larvae demonstrated resilience across the tested iron levels. Nutritional analysis revealed a dose-dependent increase in iron content in both species, with BSF larvae showing a significant rise from 372 to 999 mg/kg. This increase correlated with a decrease in zinc content in both species of larvae, suggesting competition for absorption. An unexpected rise in calcium levels was observed in BSF larvae across the diets. At the highest iron concentration (100 mM), stress-induced black lesions appeared, suggesting structural modifications of the exoskeleton related to the observed increase in calcium, a crucial mineral for exoskeletal development. Characterization of these lesions and their source could enable the use of BSF larvae as a detection tool for extreme iron conditions in waste streams, warranting further research.

Ferric ammonium citrate (FAC), a commercial iron supplement, was used in this study due to its previous success in enhancing iron content and increasing entoferritin detection in insects. Iron offered as ferric ammonium citrate is likely more bioavailable than naturally occurring iron in substrates. Future research should identify substrate processing methods to enhance the bioavailability of naturally occurring iron in substrates, to further improve the larvae's nutritional profile. The switch to an FAC-free diet in the final days of rearing further supports the effective assimilation of iron by the larvae, as iron was likely retained within the larvae. This suggests an enhancement in the larvae's iron content and potentially improved bioavailability, if bound to iron binding proteins. This still requires further identification of protein expression and concentration.

These findings underscore the potential of dietary manipulation to enhance the nutritional profile of BSF larvae, positioning them as a promising sustainable source of iron and calcium for food and feed applications.

Reference:

AOAC. (2023). Official Methods of Analysis of AOAC International (G. W. Latimer Jr., Ed.). Oxford University Press. https://doi.org/10.1093/9780197610145.001.0001

Bettedi, L., Aslam, M. F., Szular, J., Mandilaras, K., & Missirlis, F. (2011). Iron depletion in the intestines of Malvolio mutant flies does not occur in the absence of a multicopper oxidase. Journal of Experimental Biology, 214(6), 971–978. https://doi.org/10.1242/jeb.051664

Boafo, H. A., Gbemavo, D. S. J. C., Timpong-Jones, E. C., Eziah, V., Billah, M., Chia, S. Y., Aidoo, O. F., Clottey, V. A., & Kenis, M. (2023). Substrates most preferred for black soldier fly*Hermetia illucens* (L.) oviposition are not the most suitable for their larval development. Journal of Insects as Food and Feed, 9(2), 183–192. https://doi.org/https://doi.org/10.3920/JIFF2022.0034

Browne, A., & O'Donnell, M. J. (2018). Calcium transport across the basolateral membrane of isolated Malpighian tubules: a survey of several insect orders. Physiological Entomology, 43(3), 227–238. https://doi.org/https://doi.org/10.1111/phen.12247

Cai, M., Hu, R., Zhang, K., Ma, S., Zheng, L., Yu, Z., & Zhang, J. (2018). Resistance of black soldier fly (Diptera: Stratiomyidae) larvae to combined heavy metals and potential application in municipal sewage sludge treatment. Environmental Science and Pollution Research, 25(2), 1559–1567. https://doi.org/10.1007/s11356-017-0541-x

Cheng, J. Y. K., Chiu, S. L. H., & Lo, I. M. C. (2017). Effects of moisture content of food waste on residue separation, larval growth and larval survival in black soldier fly bioconversion. Waste Management, 67, 315–323. https://doi.org/https://doi.org/10.1016/j.wasman.2017.05.046

Chia, S. Y., Tanga, C. M., Osuga, I. M., Cheseto, X., Ekesi, S., Dicke, M., & van Loon, J. J. A. (2020). Nutritional composition of black soldier fly larvae feeding on agro-industrial by-products. Entomologia Experimentalis et Applicata, 168(6–7), 472–481. https://doi.org/https://doi.org/10.1111/eea.12940

Costa, S., Pedro, S., Lourenço, H., Batista, I., Teixeira, B., Bandarra, N. M., Murta, D., Nunes, R., & Pires, C. (2020). Evaluation of *Tenebrio molitor* larvae as an alternative food source. NFS Journal, 21, 57–64. https://doi.org/https://doi.org/10.1016/j.nfs.2020.10.001

Cousins, R. J., Liuzzi, J. P., & Lichten, L. A. (2006). Mammalian zinc transport, trafficking,

and signals. Journal of Biological Chemistry, 281(34), 24085–24089. https://doi.org/https://doi.org/10.1074/jbc.R600011200

Daș, G., Seyedalmoosavi, M. M., Schleifer, K., Mielenz, M., & Metges, C. C. (2023). The validity of the bioaccumulation index versus the bioaccumulation factor for assessment of element accumulation in black soldier fly larvae. Journal of Insects as Food and Feed, 9(10), 1365–1380. https://doi.org/https://doi.org/10.3920/JIFF2023.0021

de Carvalho Machado, C., & Dinis-Oliveira, R. J. (2023). Clinical and forensic signs resulting from exposure to heavy metals and other chemical elements of the periodic table. Journal of Clinical Medicine, 12(7). https://doi.org/10.3390/jcm12072591

dos Santos, A. B., dos Anjos, J. S., dos Santos, G. G. P., Mariano, M. V. T., Leandro, L. P., Farina, M., Franco, J. L., Gomes, K. K., & Posser, T. (2024). Developmental iron exposure induces locomotor alterations in *Drosophila*: Exploring potential association with oxidative stress. Comparative Biochemistry and Physiology Part C: Toxicology & Pharmacology, 279, 109861. https://doi.org/https://doi.org/10.1016/j.cbpc.2024.109861

Dube, K. A., McDonald, D. G., & O'Donnell, M. J. (2000). Calcium homeostasis in larval and adult *Drosophila melanogaster*. Archives of Insect Biochemistry and Physiology, 44(1), 27–39. https://doi.org/https://doi.org/10.1002/(SICI)1520-6327(200005)44:1<27::AID-ARCH4>3.0.CO;2-I

First, T., Fogliano, V., & Mishyna, M. (2023). Entoferritin: An innovative iron source for human consumption. Journal of Functional Foods, 108, 105711. https://doi.org/https://doi.org/10.1016/j.jff.2023.105711

Fischer, H., & Romano, N. (2021). Fruit, vegetable, and starch mixtures on the nutritional quality of black soldier fly (*Hermetia illucens*) larvae and resulting frass. Journal of Insects as Food and Feed, 7(3), 319–328. https://doi.org/10.3920/JIFF2020.0100

GBD 2021 Anaemia Collaborators. (2023). Prevalence, years lived with disability, and trends in anaemia burden by severity and cause, 1990-2021: findings from the Global Burden of Disease Study 2021. The Lancet. Haematology, 10(9), e713–e734. https://doi.org/10.1016/s2352-3026(23)00160-6

Gorman, M. J. (2023). Iron homeostasis in insects. Annual Review of Entomology, 68(Volume 68, 2023), 51–67. https://doi.org/https://doi.org/10.1146/annurev-ento-040622-092836

Gupta, U. C., & Gupta, S. C. (1998). Trace element toxicity relationships to crop production and livestock and human health: implications for management. Communications in Soil Science and Plant Analysis, 29(11–14), 1491–1522. https://doi.org/10.1080/00103629809370045

Hansen, S. L., Trakooljul, N., Liu, H.-C., Moeser, A. J., & Spears, J. W. (2009). Iron transporters are differentially regulated by dietary iron, and modifications are associated with changes in manganese metabolism in young pigs. The Journal of Nutrition, 139(8), 1474–1479. https://doi.org/https://doi.org/10.3945/jn.109.105866

Hollander, D., & Kaunitz, J. D. (2020). The "Leaky Gut": Tight Junctions but Loose Associations? Digestive Diseases and Sciences, 65(5), 1277–1287. https://doi.org/10.1007/s10620-019-05777-2

Iida, A., Kemmochi, Y., Kakimoto, K., Tanimoto, M., Mimura, T., Shinozaki, Y., Uemura, A., Matsuo, A., Matsushita, M., & Miyamoto, K. (2013). Ferric Citrate Hydrate, a New Phosphate Binder, Prevents the Complications of Secondary Hyperparathyroidism and Vascular Calcification. American Journal of Nephrology, 37(4), 346–358. https://doi.org/10.1159/000348805

Jamaa, Z. I. M., Lhomme, P., Takhim, A., Sarehane, M., & Bouharroud, R. (2021). Growth performance, conversion and survival rates of *Tenebrio molitor* (Coleoptera: Tenebrionidae) reared on various livestock diets. https://doi.org/10.5281/zenodo.8045184

Jankauskienė, A., Aleknavičius, D., Kiseliovienė, S., Antanaitis, Š., Falkauskas, R., Šumskienė, M., Juknienė, I., & Kabašinskienė, A. (2024). The Influence of Different Sustainable Substrates on the Nutritional Value of *Tenebrio molitor* Larvae. Foods, 13(3). https://doi.org/10.3390/foods13030365

Janssen, R. H., Vincken, J.-P., van den Broek, L. A. M., Fogliano, V., & Lakemond, C. M. M. (2017). Nitrogen-to-Protein Conversion Factors for Three Edible Insects: *Tenebrio*, Alphitobius diaperinus, and *Hermetia illucens*. Journal of Agricultural and Food Chemistry, 65(11), 2275–2278. https://doi.org/10.1021/acs.jafc.7b00471

Keena, M. A. (2022). Effects of Dietary Iron Quantities and Sources on *Lymantria dispar* (Lepidoptera: Erebidae) Survival and Development. Environmental Entomology, 51(4), 806–814. https://doi.org/10.1093/ee/nvac043

Kieling, M., Franke, K., Heinz, V., & Aganovic, K. (2023). Relationship between substrate

composition and larval weight: a simple growth model for black soldier fly larvae. Journal of Insects as Food and Feed, 9(8), 1027–1036. https://doi.org/https://doi.org/10.3920/JIFF2022.0096

Kim, J. C., Wilcock, P., & Bedford, M. R. (2018). Iron status of piglets and impact of phytase superdosing on iron physiology: A review. Animal Feed Science and Technology, 235, 8–14. https://doi.org/https://doi.org/10.1016/j.anifeedsci.2017.11.001

Kim, S., Kim, H. G., Lee, K., Yoon, H., & Kim, N. (2016). Effects of Brewer's spent grain (BSG) on larval growth of mealworms, *Tenebrio molitor* (Coleoptera: Tenebrionidae). International Journal of Industrial Entomology, 32, 41–48. https://doi.org/10.7852/ijie.2016.32.1.41

Lalander, C., Diener, S., Zurbrügg, C., & Vinnerås, B. (2019). Effects of feedstock on larval development and process efficiency in waste treatment with black soldier fly (*Hermetia illucens*). Journal of Cleaner Production, 208, 211–219. https://doi.org/https://doi.org/10.1016/j.jclepro.2018.10.017

Latunde-Dada, G. O., Yang, W., & Vera Aviles, M. (2016). *In vitro* iron availability from insects and sirloin beef. Journal of Agricultural and Food Chemistry, 64(44), 8420–8424. https://doi.org/10.1021/acs.jafc.6b03286

Liu, C., Masri, J., Perez, V., Maya, C., & Zhao, J. (2020). Growth Performance and Nutrient Composition of Mealworms (*Tenebrio molitor*) Fed on Fresh Plant Materials-Supplemented Diets. Foods, 9(2). https://doi.org/10.3390/foods9020151

Lönnerdal, B. (2010). Calcium and iron absorption–mechanisms and public health relevance. International Journal for Vitamin and Nutrition Research. Internationale Zeitschrift Fur Vitamin- Und Ernahrungsforschung. Journal International de Vitaminologie et de Nutrition, 80(4–5), 293–299. https://doi.org/10.1024/0300-9831/a000036

Meadows, N. J., Grainger, S. L., Ruse, W., Keeling, P. W., & Thompson, R. P. (1983). Oral iron and the bioavailability of zinc. British Medical Journal, 287(6398), 1013–1014. https://doi.org/10.1136/bmj.287.6398.1013

Middleton, M., Olivares, M., Espinoza, A., Arredondo, M., Pizarro, F., & Valenzuela, C. (2021). Exploratory Study: Excessive Iron Supplementation Reduces Zinc Content in Pork without Affecting Iron and Copper. Animals, 11(3). https://doi.org/10.3390/

anil1030776

Missirlis, F. (2021). Regulation and biological function of metal ions in *Drosophila*. Current Opinion in Insect Science, 47, 18–24. https://doi.org/https://doi.org/10.1016/j.cois.2021.02.002

Missirlis, F., Holmberg, S., Georgieva, T., Dunkov, B. C., Rouault, T. A., & Law, J. H. (2006). Characterization of Mitochondrial Ferritin in *Drosophila*. Proceedings of the National Academy of Sciences of the United States of America, 103(15), 5893–5898. http://www.jstor.org.ezproxy.library.wur.nl/stable/30050196

Mwangi, M. N., Oonincx, D. G. A. B., Hummel, M., Utami, D. A., Gunawan, L., Veenenbos, M., Zeder, C., Cercamondi, C. I., Zimmermann, M. B., van Loon, J. J. A., Dicke, M., & Melse-Boonstra, A. (2022). Absorption of iron from edible house crickets: a randomized crossover stable-isotope study in humans. The American Journal of Clinical Nutrition, 116(4), 1146–1156. https://doi.org/https://doi.org/10.1093/ajcn/nqac223

Mwangi, M. N., Oonincx, D. G. A. B., Stouten, T., Veenenbos, M., Melse-Boonstra, A., Dicke, M., & Van Loon, J. J. A. (2018). Insects as sources of iron and zinc in human nutrition. Nutrition Research Reviews, 31(2), 248–255. https://doi.org/10.1017/S0954422418000094

Neda, M., Milica, Z., Margarita, D., Brižita, Đ., Branimir, R., Svetlana, I., & Nevena, I. (2022). Magnesium supplementation and iron status among female students: the intervention study. Journal of Medical Biochemistry, 41(3), 316–326. https://doi.org/10.5937/jomb0-33898

Nguyen, T. T. X., Tomberlin, J. K., & Vanlaerhoven, S. (2013). Influence of resources on *Hermetia illucens* (Diptera: Stratiomyidae) larval development. Journal of Medical Entomology, 50(4), 898–906. https://doi.org/10.1603/ME12260

Oonincx, D. G. A. B., Laurent, S., Veenenbos, M. E., & van Loon, J. J. A. (2019). Dietary enrichment of edible insects with omega 3 fatty acids. Insect Science, 27(3), 500–509. https://doi.org/10.1111/1744-7917.12669

Parlasca, M. C., & Qaim, M. (2022). Meat consumption and sustainability. Annual Review of Resource Economics, 14, 17–41. https://doi.org/10.1146/annurev-resource-111820-032340

Rebora, M., Salerno, G., Piersanti, S., Saitta, V., Morelli Venturi, D., Li, C., & Gorb, S. (2023). The armoured cuticle of the black soldier fly *Hermetia illucens*. Scientific Reports, 13(1),

22101. https://doi.org/10.1038/s41598-023-49549-5

Rumbos, C. I., Oonincx, D. G. A. B., Karapanagiotidis, I. T., Vrontaki, M., Gourgouta, M., Asimaki, A., Mente, E., & Athanassiou, C. G. (2022). Agricultural by-products from Greece as feed for yellow mealworm larvae: circular economy at a local level. Journal of Insects as Food and Feed, 8(1), 9–22. https://doi.org/10.3920/JIFF2021.0044

Schönfeldt, H. C., & Hall, N. G. (2011). Determining iron bio-availability with a constant heme iron value. Journal of Food Composition and Analysis, 24(4), 738–740. https://doi.org/https://doi.org/10.1016/j.jfca.2011.01.002

Seyedalmoosavi, M. M., Mielenz, M., Schleifer, K., Görs, S., Wolf, P., Tränckner, J., Hüther, L., Dänicke, S., Daş, G., & Metges, C. C. (2023). Upcycling of recycled minerals from sewage sludge through black soldier fly larvae (*Hermetia illucens*): Impact on growth and mineral accumulation. Journal of Environmental Management, 344, 118695. https://doi.org/https://doi.org/10.1016/j.jenvman.2023.118695

Seyedalmoosavi, M. M., Mielenz, M., Veldkamp, T., Daş, G., & Metges, C. C. (2022). Growth efficiency, intestinal biology, and nutrient utilization and requirements of black soldier fly (*Hermetia illucens*) larvae compared to monogastric livestock species: a review. Journal of Animal Science and Biotechnology, 13(1), 31. https://doi.org/10.1186/s40104-022-00682-7

Szudzik, M., Starzyński, R. R., Jończy, A., Mazgaj, R., Lenartowicz, M., & Lipiński, P. (2018). Iron Supplementation in Suckling Piglets: An Ostensibly Easy Therapy of Neonatal Iron Deficiency Anemia. Pharmaceuticals, 11(4). https://doi.org/10.3390/ph11040128

Taylor, C. W. (1985). Calcium Absorption by the Midgut of the Blowfly, Calliphora Vicina. Journal of Experimental Biology, 114(1), 551–561. https://doi.org/10.1242/jeb.114.1.551

Terra, W. R., & Ferreira, C. (2020). Evolutionary trends of digestion and absorption in the major insect orders. Arthropod Structure & Development, 56, 100931. https://doi.org/https://doi.org/10.1016/j.asd.2020.100931

Thabet, R., Rouault, J.-D., Ayadi, H., & Leignel, V. (2016). Structural analysis of the subunit of Na+/K+ ATPase genes in invertebrates. Comparative Biochemistry and Physiology Part B: Biochemistry and Molecular Biology, 196–197(11–18). https://doi.org/https://doi.org/10.1016/j.cbpb.2016.01.007

Thiex, N., Novotny, L., & Crawford, A. (2012). Determination of Ash in Animal Feed: AOAC Official Method 942.05 Revisited. Journal of AOAC International, 95(5), 1392–1397. https://doi.org/10.5740/jaoacint.12-129

Thompson, B. A. V, Sharp, P. A., Elliott, R., & Fairweather-Tait, S. J. (2010). Inhibitory Effect of Calcium on Non-heme Iron Absorption May Be Related to Translocation of DMT-1 at the Apical Membrane of Enterocytes. Journal of Agricultural and Food Chemistry, 58(14), 8414–8417. https://doi.org/10.1021/jf101388z

Tolkien, Z., Stecher, L., Mander, A. P., Pereira, D. I. A., & Powell, J. J. (2015). Ferrous sulfate supplementation causes significant gastrointestinal side-effects in adults: A systematic review and meta-analysis. Plos One, 10(2). https://doi.org/10.1371/journal.pone.0117383

van Huis, A., Rumpold, B. A., van der Fels-Klerx, H. J., & Tomberlin, J. K. (2021). Advancing edible insects as food and feed in a circular economy. Journal of Insects as Food and Feed, 7(5), 935–948. https://doi.org/10.3920/JIFF2021.x005

Weko, M. R., Bao, F., Ega, M. E., Mia, H., Una, K. S. I., Viana, M., Wale, L., Nalle, C. L., Burithnaban, Y. M., Lema, A. T., Helda, & Asrul. (2023). Nutrient Profile Black Soldier Fly Larvae (Hermetia Illucence): Effect Of Feeding Substrate And Harvested Time. Biotopia, 30(3), 297–307. https://doi.org/10.11598/btb.2023.30.3.1903

Wu, G., Ye, G., Hu, C., & Cheng, J.-A. (2006). Accumulation of cadmium and its effects on growth, development and hemolymph biochemical compositions in Boettcherisca peregrina larvae (Diptera: Sarcophagidae). Insect Science, 13(1), 31–39. https://doi.org/https://doi.org/10.1111/j.1744-7917.2006.00065.x

Wu, N., Wang, X., Xu, X., Cai, R., & Xie, S. (2020). Effects of heavy metals on the bioaccumulation, excretion and gut microbiome of black soldier fly larvae (*Hermetia illucens*). Ecotoxicology and Environmental Safety, 192, 110323. https://doi.org/https://doi.org/10.1016/j.ecoenv.2020.110323

CHAPTER

04

Forged in Iron: Molecular Insights into Iron Tolerance in *Hermetia illucens*

T. First[1], H. Walt[2], V. Ciaravolo[3], S. Arena[3], A. Scaloni[3], F. Missirlis[4], F. Meyer[2], F. G. Hoffmann[2], J. J.A. Van Loon[5], D. Oonincx[6], V. Fogliano[1] and M. Mishyna[1]

[1]Wageningen University and Research, Food Quality and Design group, 6708 Wageningen, the Netherlands; [2]Department of Biochemistry, Nutrition, and Health Promotion, 39762 MS Mississippi State University, Mississippi State, MS, USA; [3]Proteomics, Metabolomics and Mass Spectrometry Laboratory, ISPAAM, National Research Council, 80055 Portici, Italy; [4]Department of Physiology, Biophysics and Neuroscience, Center for Research and Advanced Studies (Cinvestav), 07360 Mexico City, Mexico; [5]Wageningen University and Research, Laboratory of Entomology, 6708 Wageningen, the Netherlands; [6]Wageningen University and Research, Animal Nutrition Group, 6708 Wageningen, the Netherlands;

Under review

Abstract

Black soldier fly (BSF) larvae are increasingly valued as a sustainable source of proteins and essential minerals in animal feed and potentially food, yet their physiological response to substrate iron fortification is poorly defined. Here, integrated transcriptomic, proteomic, and tissue iron detection approaches were used to characterize responses of BSF larvae reared on diets containing 323 (control), 1,255, and 6,970 mg Fe/kg dry matter (DM). Larval growth at day 12 was unaffected, while prepupal emergence after 15 days showed a statistically non-significant increase at the highest iron level, suggesting only subtle developmental effects. Prussian blue staining showed a dose-depended iron accumulation in the midgut epithelium, consistent with known insect iron responsive regions of entoferritin-based sequestration. An elevated iron signal in the peritrophic matrix indicated a complementary defensive barrier. Multi-omics profiling revealed oxidative stress responses, suppression of mitochondrial and translational pathways, and activation of exoskeleton biosynthesis. Entoferritin levels rose by ~70% for both protein subunits despite modest transcript changes, pointing to a post-transcriptional regulation mechanism. These results suggest a gut-centered "accumulate-and-store" physiological strategy enabling BSF larvae to tolerate high dietary iron. This entoferritin-based high iron accumulation capacity highlights the potential of this insect as a sustainable source of bioavailable iron in feeds.

1. Introduction

There is an increasing need for climate-resilient and bioavailable sources of dietary iron for food and feed alike (Byrne & Murphy, 2022; Wang *et al.*, 2024). Iron bioavailability in food is influenced by multiple factors, including its chemical form, whether it is bound to proteins, and the presence of absorption enhancers or inhibitors in the food matrix (Piskin *et al.*, 2022). For instance, the edible insect ferritin (entoferritin) is an iron binding protein that is hypothesized to increase iron bioavailability (First *et al.*, 2023). It is a spherical, hollow protein complex composed of 24 subunits that can hold thousands of iron atoms, typically assembled in a 1:1 ratio of heavy and light chains (FerHCH and FerLCH, respectively) (Pham & Winzerling, 2010).

Several edible insect species are proposed as novel protein and fat sources as well as suppliers of essential micronutrients, including dietary iron (Mwangi *et al.*, 2018). Among these, the black soldier fly (BSF, *Hermetia illucens*) is the most established species in the feed industry, valued for their larvae ability to efficiently convert organic waste into high-quality biomass (Siva Raman *et al.*, 2022). Notably, BSF larvae contain

considerable iron levels, of around 300 mg/kg Dry Matter (DM) under typical rearing conditions, and have demonstrated the capacity to accumulate heavy metals, including iron (First *et al.*, 2024; Wu *et al.*, 2006; Wu *et al.*, 2020).

Iron is an essential nutrient for all living organisms, but its redox properties make it potentially toxic at high concentrations, as it can catalyze the formation of reactive oxygen species (ROS) via mechanisms such as the Fenton reaction (Dixon & Stockwell, 2014). Despite this potential toxicity, we have recently showed that BSF larvae can tolerate and accumulate exceptionally high levels of dietary iron without adverse physiological effects. BSF larvae were reared on diets with iron concentrations ranging from 323 to 6,637 mg/kg DM, covering both typical feed iron levels and concentrations considered extreme (First *et al.*, 2024). For example, five days of exposure to 10 mM ferric ammonium citrate is lethal to *Drosophila melanogaster* (Bonilla-Ramirez *et al.*, 2011). When reared on 6,637 mg Fe/kg DM, the BSF larvae accumulated up to three times more iron and exhibited increased calcium levels, with no negative impacts on survival rate, larval weight, fat and protein content, or the molecular weight of major soluble proteins (First *et al.*, 2024). How BSF larvae can accumulate and tolerate such extreme iron loads remains unclear. A role for entoferritin is suggested (First *et al.*, 2024), but also specific biochemical tolerance mechanisms could be activated.

The aim of this study was to investigate the mechanisms by which BSF larvae accumulate and regulate increased dietary iron content, in the context of BSF larvae used as food and feed. Specifically, transcriptomic and proteomic analyses were employed to examine molecular changes in iron-fortified larvae. In addition, imaging and relative quantification of larval intestine of the BSF were conducted.

2. Methods

1. Larvae rearing and collection

Black soldier fly larvae were reared under controlled conditions at 27 °C and 70% relative humidity, in the dark. Rearing procedures were based on First *et al.* (2024), with minor modifications to feed moisture content, as well as rearing and sampling timelines, depending on the analysis.

Dry chicken feed (Kuikenopfokmeel no. 1, Kasper FaunaFood, the Netherlands) was sieved using a 1.0 mm to homogenize particle size of the dry substrate. Ferric ammonium

citrate (FAC; CAS 1185-57-5; Merck, Darmstadt, Germany) was dissolved in water to prepare solutions of 12.5, and 125mM, corresponding to final substrate concentrations of 323 (Control, i.e. no fortification), 1,255, and 6,970 mg Fe/kg DM, respectively. Diets were prepared by mixing 200 g of dry feed with 320 mL of the respective FAC solutions (1:1.6 feed-to-water ratio), yielding 520 g of wet feed per container.

A total of 0.2 g of BSF eggs (Protix, Bergen op Zoom, the Netherlands) were introduced to 520 g of wet, FAC-free feed. Larvae were reared on this control diet for five days. Then, larvae were separated from the substrate by sieving, counted, and assigned to treatments. For each treatment, 200 five-day-old larvae were transferred to new rearing containers (15.5 × 10.5 × 6 cm) containing 520 g of wet feed prepared with the corresponding FAC concentration. Each treatment was conducted in quadruplicate. Two days after exposure, four larvae per replicate were collected, flash frozen in liquid nitrogen, and stored at –80 °C for mRNA extraction. On day 7 since the start of the exposure, all remaining larvae were harvested, flash frozen in liquid nitrogen, and stored at –80 °C for protein and mRNA analyses.

To assess pre-pupation, an additional cohort of five-day-old larvae was reared on iron-supplemented diets for twelve consecutive days. For each treatment (Control, 12.5, and 125 mM FAC), 200 larvae were placed in rearing containers with 520 g of wet feed with the corresponded FAC fortification. All treatments were reared in triplicate. At the end of the period, larvae were harvested, sieved, and separated into larvae and pre-pupae based on external morphology, as darkened and hardened lighter larvae were counted as pre-pupas. All individuals were counted, and their biomass was measured to validate developmental stage separation, as pre-pupae are significantly lighter than earlier instar larvae (Georgescu *et al.*, 2020).

For iron cluster localization, larvae were reared using the same procedure but were switched to FAC-free feed on day 7 to avoid excess iron in the larval gut. These larvae were collected on day 8, sieved and freshly dissected following a sacrifice using CO_2 exposure.

2. Tissue Prussian Blue (iron) Staining

Larvae reared on control diet for 24 h after the end of iron treatments were harvested. Dissections were performed in phosphate-buffered saline (PBS, pH 7.2), at room temperature. Whole-body staining was initially performed using Prussian blue solution (2% w/v potassium ferrocyanide [KFe(CN)] and 2% hydrochloric acid mixed

in 1:1 ratio) for 10 min in dark conditions to localize iron deposits. Samples were subsequently washed in PBS to remove excess staining reagent.

Following whole-body staining, gut tissues were dissected and stained separately under the same conditions. This targeted approach was guided by the initial whole-body results to refine the localization of iron deposits.

Tissue imaging was performed using an Olympus SZX12 stereomicroscope equipped with a Euromex sCMEX-20 digital camera. Images were acquired and processed using ImageFocus software.

3. mRNA and Protein extraction

mRNA extraction was conducted by Novogene Europe (Cambridge, UK). Total RNA was isolated from frozen BSF larvae using TRIzol reagent (Invitrogen, USA), following the manufacturer's instructions with slight modifications. Two to three frozen whole larvae were ground in liquid nitrogen and 50 mg of the larvae were homogenized in 1 mL of TRIzol. After chloroform extraction and phase separation, the aqueous layer was collected, and RNA was precipitated using isopropanol. The pellet was then washed with 75% ethanol and dissolved in RNase-free water. RNA concentration and quality were evaluated with an Agilent 5400 system (Agilent, USA). All steps were carried out under RNase-free conditions.

For protein extraction, each frozen BSF larvae was subjected to a preliminary wash with 70% ethanol to remove potential surface contaminants, followed by three consecutive washes with PBS (137 mM NaCl, 2.7 mM KCl, 8.1 mM NaHPO·2HO, 1.76 mM KHPO) at a 1:10 weight-to-volume ratio, supplemented with EDTA-free protease inhibitor tablets. A RIPA buffer, composed of 25mM Tris-HCl (pH 7.6), 150 mM NaCl, 1% NP-40, and 1% sodium deoxycholate was used for protein extraction. The freeze dried larvae were homogenized on ice using an Ultraturrax at 30,000 rpm for 20 seconds, followed by a 30-second pause, for five repetitions. The homogenized samples were then left on ice for 1 hour following sonication for 5 minutes with 2-minute pauses on ice, which was repeated three times. The resulting crude extracts were centrifuged at 13,000 × g for 20 minutes at 4 °C. Protein concentration in the supernatants was determined using Pierce BCA Protein Assay™ kit (Thermo Scientific, Rockford, IL, USA). An aliquot containing 70 µg of protein from each sample was subjected to electrophoresis on a 12% SDS-PAGE gel under reducing conditions, and the gels were stained with Coomassie Brilliant Blue G-250 to verify the extraction protocol.

Aliquots of 150 g was reduced, alkylated in the dark, and precipitated by adding six volumes of cold acetone to remove interfering substances for shotgun analysis. After precipitation, the samples were centrifuged at 8,000 × g for 10 minutes at 4 °C, and the resulting protein pellets were air-dried. Each sample was digested with freshly prepared trypsin (1:50 enzyme/protein ratio) in 50 mM TEAB buffer at 37 °C overnight. The resulting peptides from each protein sample were quantified using the Pierce™ BCA Peptide Assay Kit (Thermo Scientific, Rockford, IL, USA). Subsequently, 30 g of peptides per sample were labeled using the TMTsixteenplex™ Isobaric Label Reagent Set (Thermo Fisher Scientific, USA). After 1h of reaction, 8 L of 5% w/v hydroxylamine was added to each tube and mixed for 15 min to stop the derivatization reaction. For a series of comparative experiments, the labeled peptide mixtures were mixed in equal molar ratios and dried in vacuo under rotation. Then, TMT-labeled peptide mixtures were suspended in 0.1% trifluoroacetic acid and fractionated using the Pierce™ High pH Reversed Phase Peptide Fractionation Kit (Thermo-Fisher Scientific, USA) to remove unbound TMT reagents and reduce sample complexity, according to the manufacturer's instructions. After fractionation, eight TMT-labeled peptide fractions were collected, dried under vacuum, and finally reconstituted in 0.1% formic acid for subsequent mass spectrometric analysis. All mRNA extraction and peptide extraction were conducted in biological quadruplicates.

4. Peptide Mass Spectrometry

Peptide mixtures were analyzed in technical triplicate by means of a nanoLC-ESI-Q-Orbitrap-MS/MS platform consisting of an Vanquish- Neo nano-chromatography system (Thermo Fisher Scientific) interfaced to a Exploris 480 mass spectrometer through an easy-spray ion source (Thermo Fisher Scientific, USA). Peptides were loaded on an EASY-Spray C18 column (150 mm × 75 m ID, 2 m particles, 100 Å pore size) (Thermo Fisher Scientific, USA), and eluted with a gradient of solvent B (19.92/80/0.08 v/v/v water/acetonitrile/formic acid) in solvent A (99.9/0.1 v/v water/formic acid), at a flow rate of 250 nL/min. The gradient of solvent B started at 6%, increased to 31% over 120 min, increased to 50% over 5 min, increased to 95% over 5 min and remained at 95% for 4 min, and finally returned to 6% for equilibrating step. The mass spectrometer operated in data-dependent mode, using a full scan range (m/z 400-1600, resolution of 60,000 @200 m/z), followed by MS/MS scans of the 20 most abundant ions. MS/MS spectra were acquired in a dynamic scan m/z range, using a normalized collision energy of 38%, a Normalized AGC Target (%) of 200, a maximum injection target of 105 ms, and a resolution of 45000 @200 m/z. The dynamic exclusion value was set to 25 s.

5. Transcriptomics

Universal Illumina adapter sequences were trimmed from the reads using Cutadapt v3.5 (Martin, 2008). Next, low-quality bases were removed using Trimmomatic v0.39 with the options SLIDINGWINDOW:4:15 MINLEN:30 (Bolger *et al.*, 2014). Read quality after processing was checked using fastqc v.0.11.9 (Andrews, 2010). Transcript abundances were quantified using Salmon v.0.14.1 (Patro *et al.*, 2017). First, a salmon index was made using the BSF reference transcripts and the BSF genome (GCF_905115235.1) as "decoy" sequences. Next, transcript abundance was quantified for each sample using salmon in "quant" mode, allowing the library orientation to be determined automatically and the –validateMappings flag implemented. Transcript abundances were imported to R using tximport v1.26.1 for differential expression analysis using DESeq2 v1.38.3 (Love *et al.*, 2014; Soneson *et al.*, 2015). Overall gene expression patterns were visualized using principal component analysis via the plotPCA function in DESeq2 on gene expression counts that had undergone variance-stabilizing transformation. Differential expression analysis was conducted at the gene level. Differentially expressed genes between each treatment within each time point were found using the Wald test with the Benjamini-Hochberg method to correct for multiple comparisons (as implemented in DESeq2). Genes were considered differentially expressed if they had an adjusted p-value less than 0.05. Differentially expressed genes across the samples were visualized using ComplexHeatmap v2.22.0 with hierarchical clustering for both rows and columns (Gu *et al.*, 2016). Venn diagrams were generated using ggVennDiagram v1.5.2 in R (Gao *et al.*, 2024).

To determine the over-represented functions in the differentially expressed genes, the BSF reference proteome associated with GCF_905115235.1 was functionally annotated using eggNOG mapper v2.1.9 in diamond mode (Cantalapiedra *et al.*, 2021). Gene ontology (GO) term enrichment analysis was conducted with ClusterProfiler v4.14.4 using the enricher function incorporating the "BH" method to adjust p-values for multiple comparisons. GO terms were considered "enriched" under a p-value cutoff of 0.05. Redundant enriched GO terms were clustered and assigned to parent terms using rrvgo based on the "rel" algorithm (Sayols, 2023). Significant p-values were negative log10 transformed and the term with the highest score was used as the representative "parent" term after clustering by semantic similarity (similarity threshold = 0.75). The *D. melanogaster* orgdb annotation (org.Dm.eg.db) was used as the GO database for annotations.

To locate entoferritin subunit iron response elements (IREs), ferritin subunit gene (LOC119652653 and LOC119652654) mRNA transcripts were downloaded from NCBI.

IREs in ferritin transcripts were predicted using the SIREs v3.0 web server with default settings (Suárez-Quintana *et al.*, 2025).

To determine the homology of BSF ribosomal L1 domain-containing protein 1 (RSL1D1) to vertebrate RSL1D1 proteins, a phylogenetic analysis was conducted. A selection of vertebrate, arthropod, and cnidarian (outgroup) protein gene models were downloaded from NCBI using biomartr v.1.0.7 (Drost & Paszkowski, 2017) and made into a protein BLAST database. Next BLASTp was used to align BSF, human, and *D. melanogaster* RSL1D1 amino acid sequences to the custom metazoan database with a minimum evalue of 1e-5. The longest isoforms from the resulting protein sequences were retrieved from NCBI using datasets v.17.3.0 (O'Leary *et al.*, 2024). All protein sequences were aligned using MAFFT v.7.490 incorporating the L-INS-i algorithm and the resulting alignment was trimmed with trimal v.1.2 using the gappyout option (Capella-Gutiérrez *et al.*, 2009; Katoh & Standley, 2013). A phylogeny was inferred from the trimmed alignment using IQ-TREE v.2.0.7 employing automatic model selection through ModelFinder (Kalyaanamoorthy *et al.*, 2017; Minh *et al.*, 2020). Support values are shown as ultrafast bootstrap with 1000 replicates (Hoang *et al.*, 2018).

6. Proteomics

All MS and MS/MS raw data files per sample were merged for protein identification using Proteome Discoverer v.3.1 software (Thermo Fisher Scientific, USA), allowing database searching using Mascot v. 2.4.2 algorithm (Matrix Science) according to a shotgun proteomic approach. Database searching was performed with the following criteria: *Hermetia* protein sequence database (downloaded from UniProtKB and including 17615 entries); carbamidomethylation at Cys and TMTpro 16plex modification at Lys and peptide N-terminus as fixed modifications; oxidation at Met, pyroglutamate formation at N-terminal Gln, phosphorylation at Ser/Thr/Tyr, and deamidation at Asn/Gln as variable modifications. The mass tolerance of the parent peptide was set to ± 10 ppm and ± 0.05 Da for MS/MS fragments. Trypsin was set as the proteolytic enzyme and the maximum number of missed cleavages was limited to 2.

Hierarchical clustering and PCA analysis were used to assess dimensionality reduction projections (DRPs). Both the heatmap and PCA were generated using Proteome Discoverer 3.1 and based on normalized abundance data. The heatmap was created using the Euclidean distance function, complete linkage method, and scaling after clustering. In both analyses, biological replicates are shown, and the mass spectrometry analysis was performed with three technical replicates. Functional annotation of

DRPs and network inference analysis were performed using STRING software with confidence score cutoff value of 0.4. Due to limited functional annotation in the BSF protein database, homologous polypeptide sequences from Insecta were used as a reference database.

7. Integrative omics analysis

Transcriptome-proteome integration analysis was conducted using DIABLO within the mixOmics v.6.30.0 R package. DIABLO is a supervised N-integration method that uses multiblock partial least squares-discriminant analysis (PLS-DA) to assess the correlation between two omics datasets (Singh *et al.*, 2019). Transformed counts using the variance stabilizing method implemented in DESeq2 were used as input for the transcriptomic data, while protein abundance per replicate was used as input for the proteomic data. A weight of 0.92 was used in the experimental design and was chosen by conducting a PLS regression analysis between the transcriptomic and proteomic data. Two components were chosen for the final sparse PLS-DA (sPLS-DA) model. The optimal number of variables used for the final sPLS-DA model was found using the tune.block.splsda function with 4 folds and 10 repeats. This returned 20 and 10 variables for the transcriptome dataset, and 25 and 5 variables as optimal for the proteomic dataset. Similarity between the datasets in two-dimensional overlapping space was visualized using the plotArrows function. Correlations between the components were found using the plotDiablo function, and loadings (i.e. which variables contribute the most separation between groups) were found using the plotLoadings function.

3. Results

1. Stable larval growth under iron supplementation with signs of accelerated pre-pupation

Twelve-day-old BSF larvae reared for 7 days on medium (12.5mM) or high (125mM) iron-enriched diets showed no difference in body weight compared to the control group, with mean values consistently ranging between 230 and 240 mg per larva (Figure 4.1 A). When five-day-old larvae were reared for 12 days on iron-supplemented diets, a mild ($P > 0.1$), dose-dependent increase in pre-pupation rate was observed, from 30% to 37% (Figure 4.1 B).

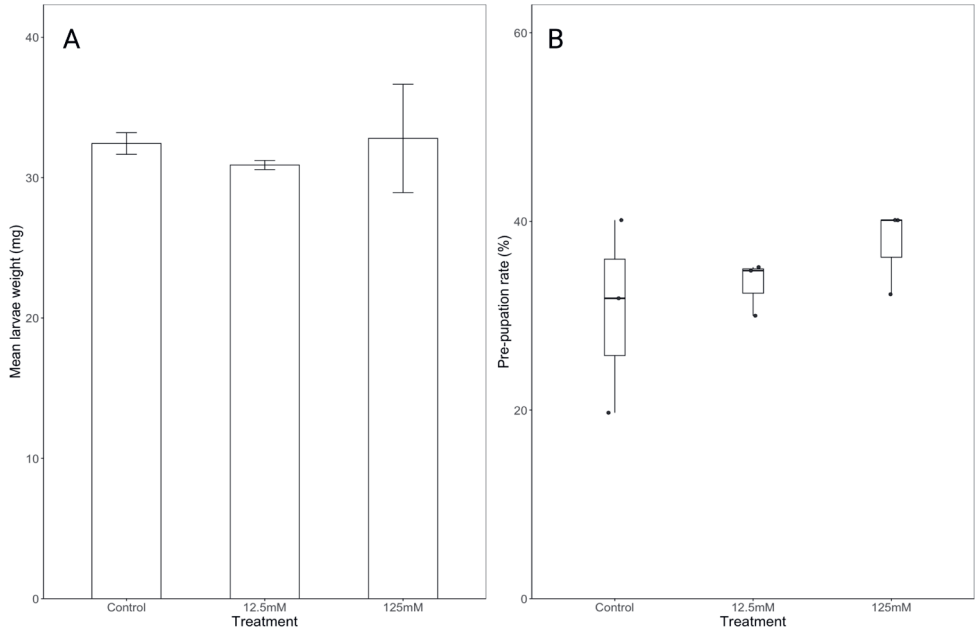


Figure 4.1. (A) Mean of BSF larvae weight (mg) after 7 days of exposure to different iron treatments. (B) Pre-pupation rate (%) of BSF larvae 12 days after exposure to the different iron treatments. No statistically significant differences were observed between the groups.

2. Iron accumulation localized to the anterior midgut and posterior midgut as the primary storage sites

Iron storage of larvae reared on the control diet was compared to that of larvae reared on medium (12.5mM) and high (125mM) iron diets. A dose-dependent increase in Prussian blue staining intensity was observed in the Posterior midgut and anterior midgut regions, as defined by Bonelli *et al.* (2020), indicating elevated iron accumulation (Figure 4.2). In contrast, no iron signal was detected in whole dissected larvae, isolated fat bodies, or extracted exoskeletons, regardless of the dietary treatment, suggesting no novel iron storing locations were found in iron fortified BSF larvae.

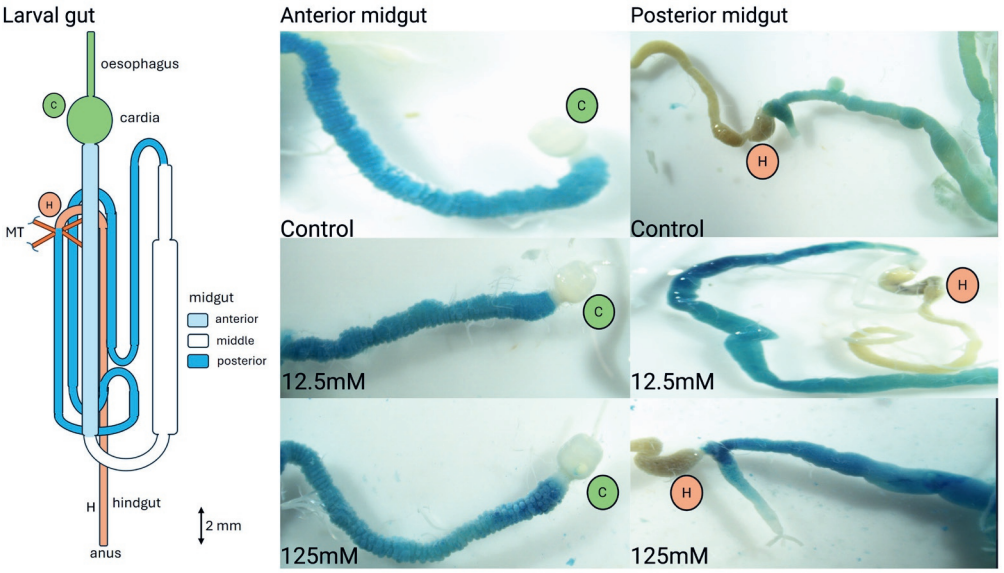


Figure 4.2. Prussian blue staining of the black soldier fly larva midgut under different dietary iron conditions. On the left, schematic drawing of the larval gut showing the subdivision of the entire gut, including the subdivision inside the midgut into anterior (light blue), middle (white), posterior (blue) regions, and Malpighian tubules (MT) as defined by Bonelli *et al.* (2019). Oesophagus and cardia constitute the foregut. In the center, images of anterior midgut, starting right after the cardia (C). On the right, images of the posterior midgut segment, showing the part until the start of the hindgut (H). Iron accumulation is visualized by Prussian blue staining in larvae reared for six days on control, medium (12.5mM), or high (125mM) iron diets, followed by 24 h on a control diet prior to dissection.

3. Peritrophic matrix acts as a dose-responsive iron-binding barrier

The peritrophic matrix (PM) was stained with Prussian blue. No iron signal was

detected in the larvae reared on the control diet, while the fortified larvae presented a dose-dependent increase in iron stain intensity (Figure 4.3).

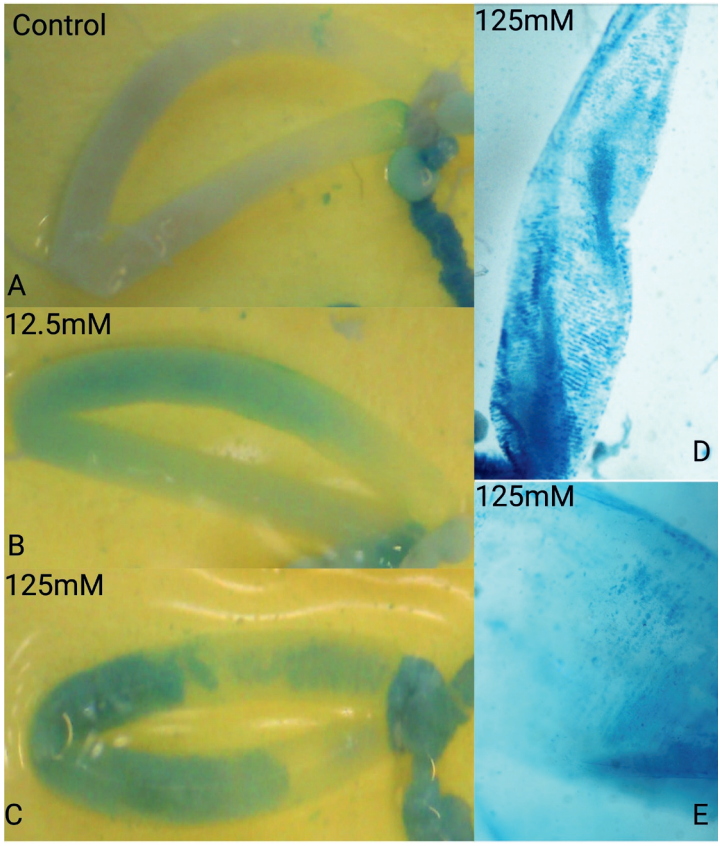


Figure 4.3. Peritrophic matrix of black soldier fly larvae stained with Prussian blue (A) reared on control, (B) medium (12.5mM) and (C) high (125mM) iron diets. (D and E) Zoomed in images of the Peritrophic membrane of larvae reared on the high (125mM) iron diet after staining with Prussian blue. Larvae were reared on the iron-enriched substrate for six days following a switch to control diet 24 hours prior to dissection.

4. Time-dependent transcriptomic shifts between treatments separate early defense suppression from later cuticle and oxidative stress activation

The transcriptomic analysis yielded 10,838 expressed genes in all the BSF larvae (Table 4.S1).

A total of 299 of these genes were differentially expressed on day 2, and 791 genes were differentially expressed on day 7 between the treatments (Figure 4.4). Principal component analysis (PCA) revealed more distinct overall expression patterns on day 7 compared to day 2, with the high (125mM) iron treatment group forming a separate cluster primarily along principal component 2 (Figure 4.4 A–B). Consistent with the PCA results, the high (125mM) iron group on day 7 also clustered separately based on the differentially expressed genes using hierarchical clustering (Figure 4.4 D). In contrast, hierarchical clustering of the differentially expressed genes on day 2 showed that the control group was distinct from both iron-fortified groups (Figure 4.4 C). Pairwise comparisons between treatment groups further revealed that on day 2, the medium (12.5mM) iron treatment group showed the greatest transcriptomic differences from the control, accounting for 270 out of the 299 differentially expressed genes identified on that day. Fewer differentially expressed genes were detected in the comparison between the high (125mM) iron and control groups (60 genes), and only two differentially expressed genes were identified between the high (125mM) and medium (12.5mM) iron groups on day 2 (Figure 4.4 E). In contrast, on day 7, the medium (12.5mM) iron group exhibited minimal differences relative to the control group, while the high (125mM) iron group displayed extensive transcriptomic changes compared to both the medium (12.5mM) iron and control groups (Figure 4.4 F).

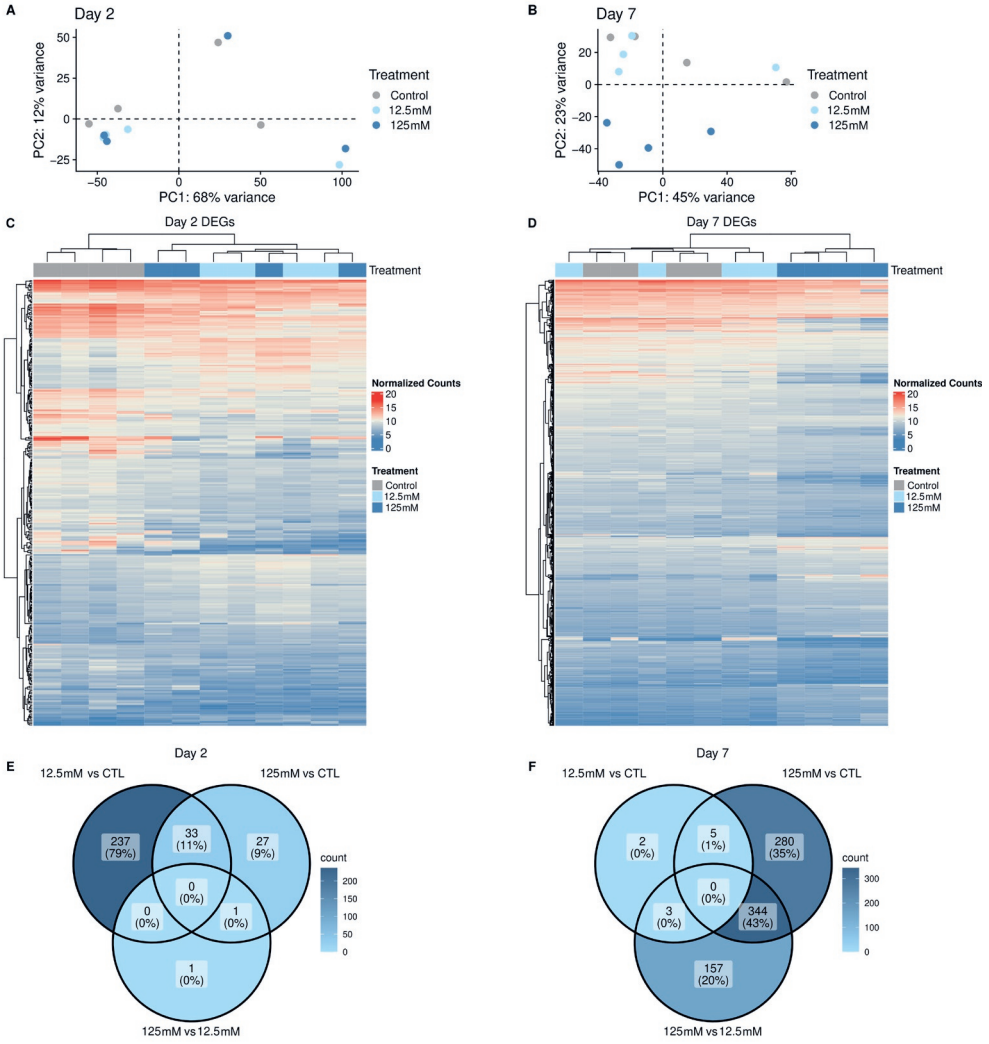


Figure 4.4. Differential transcriptomic analysis of iron-fortified black soldier fly larvae after two days (A, C, E) and seven days (B, D, F) of exposure to control, medium (12.5mM), and high (125mM) iron treatments. (A,B) Principal Component Analysis (PCA) of mRNA abundance data of the control (CTL), medium (12.5mM) and high (125mM) iron treatments. (C,D) Hierarchical heatmap of protein expression profiles in larvae fed a control (CTL) diet (grey), medium (12.5mM) iron (light blue), and high (125mM) iron (blue). The analysis was performed on normalized protein abundance data. Columns represent biological replicates; rows represent individual protein groups. Color scale indicates relative expression levels (blue = downregulation; red = upregulation). (E,F) Venn diagrams showing the overlap of significantly differentially expressed protein groups among treatments. Each circle represents one iron treatment: Control (CTL), Medium (12.5mM) and high (125mM) iron. The numbers indicate proteins uniquely or jointly differentially expressed in response to the respective treatments.

Functional enrichment analysis of the differentially expressed genes revealed limited functional over-representation on day 2, but substantial enrichment on day 7 (Figure 4.5). On day 2, Gene Ontology (GO) terms related to defense responses and protein folding were significantly enriched. Genes associated with defense responses included predicted detoxification-related cytochrome P450s (LOC119647124, LOC119651341, LOC119651369, LOC119652925, LOC119653044, and LOC119653068), small heat shock proteins (LOC119650070, LOC119650378, and LOC119650380), and lysozymes (LOC119654083, LOC119654085, LOC119654694, and LOC119654730), all of which were down-regulated. The enrichment in protein folding–related terms was primarily driven by multiple down-regulated genes encoding small heat shock proteins (Figure 4.5 A). By contrast, day 7 showed a broader range of enriched biological processes. Notably, genes involved in chitin-based metabolic processes, including cuticle and trachea development, were strongly over-represented. Additionally, several genes associated with the response to toxic substances were differentially expressed, including three predicted animal heme peroxidases (LOC119651583, LOC119659891, and LOC119659737), suggesting a physiological response to iron-induced oxidative stress (Figure 4.5 B).

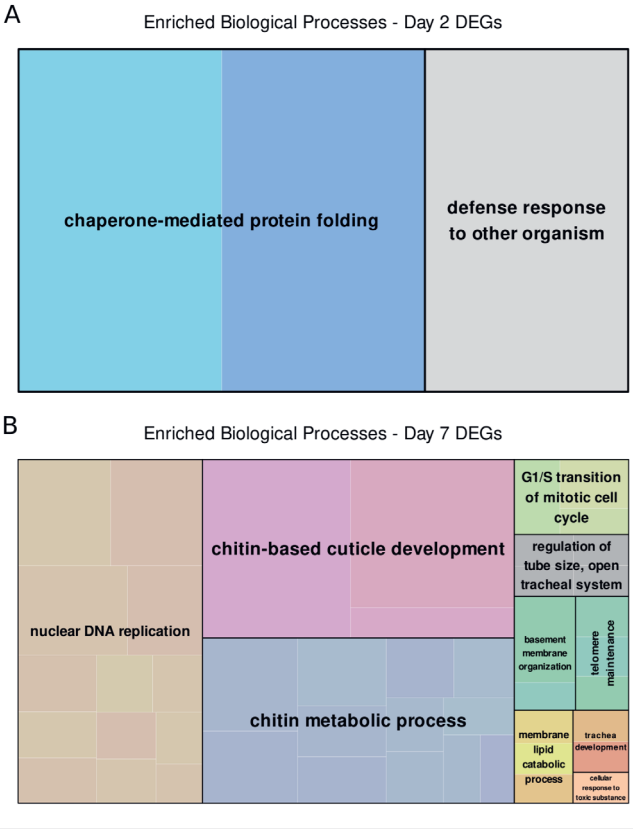


Figure 4.5. Functional enrichment of differentially expressed genes. (A) Day 2 and (B) Day 7. Enriched GO terms (p-adjusted < 0.05) were found using ClusterProfiler with BH corrections for multiple testing. GO terms were assigned to representative "parent terms" using rrvgo. The size of the boxes corresponds to the "score" of the parent term which is equal to the –log10 of its adjusted p-value.

5. Conserved IRE-mediated regulation of ferritin expression in BSF

The main known driver for ferritin regulation is the binding of iron-responsive element-binding proteins (IRP) to iron-responsive element (IRE) in the ferritin's mRNA 5 prime UTR region (Torti & Torti, 2002). To investigate if this same type of regulation is affecting ferritin expression in BSF, SIREs prediction tool was used to predict which BSF entoferritin transcripts contain IREs. Both Fer1HCH and Fer2LCH transcripts were found to contain IREs (Figure 4.6). In the gene encoding for ferritin's light chain (Fer2LCH), two of the three transcript variants (XM_038056904 and XM_038056903) have high-quality predicted IREs (SIRE score 7.5/8) with canonical IRE loop motifs

and only one mismatch (C-A) (Figure 4.6). The two Fer2LCH transcripts containing an IRE, accounted for the majority of Fer2LCH expression, with XM_038056903 making up for around 97% and XM_038056904 making up for about 2% overall (Table 4.1). Additionally, the only transcript encoded by BSF's ferritin heavy chain gene (Fer1HCH) also has a high-quality predicted IRE (SIRE score 7.5/8). However, instead of a C-A mismatch, Fer1HCH has a G-U pairing, resulting in lower predicted free energy (-11.2 kcal/mol) than Fer2LCH (-4.8 kcal/mol) (Figure 4.6).

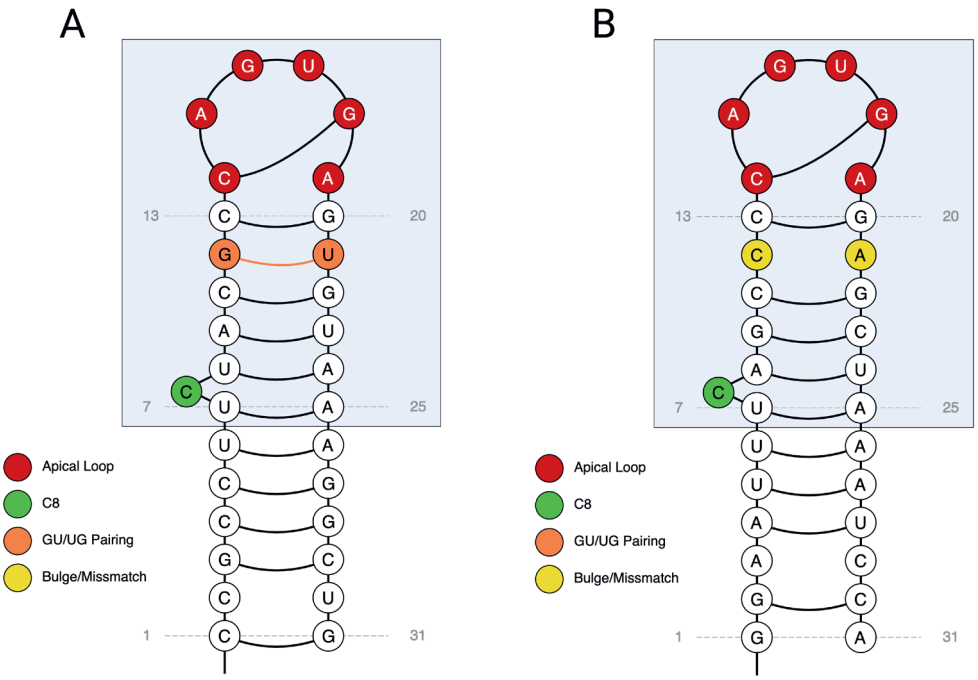


Figure 4.6. Predicted iron-responsive element structures found in the mRNA of ferritin subunits in black soldier fly larvae. (A) The heavy chain subunit IRE predicted mRNA and (B) the light chain subunit IRE predicted mRNA. Both IREs were predicted with high confidence using the SIREs v3.0 web server with default settings. Created in SIREs (Version 3.0).

Table 4.1. Overall Isoform Percentages of Fer2LCH and IRE Prediction

Transcript	Isoform Percentage	Predicted IRE
XM_038056903	97%	Yes
XM_038056904	2%	Yes
XM_038056905	1%	No

Phylogenetic analysis confirmed the homology of BSF ribosomal L1 domain-containing 1 (RSL1D1) to other arthropod and vertebrate candidate homologs, as the ancestral branch connecting these two lineages has 100% bootstrap support (Figure 4.S1). After these two lineages diverged, RSL1D1 orthologs were retained as single-copy genes, with the exception of the sandfly which has a lineage-specific duplication. In the arthropod side of the tree, closely related taxa form the expected monophyletic clades, however, the overall branching pattern is not consistent with previous phylogenomic studies in arthropods (Misof *et al.*, 2014; Su *et al.*, 2024). This is reflected by several lowly-supported branches, possibly due to limited sampling.

6. Proteomic changes under high (125mM) iron treatments reveal stress defense activation, suppression of energy metabolism and translation, and modulation of chitin-associated pathways

Proteomic analysis yielded a total of 2489 proteins (Table 4.S2). Of these, 170 were differentially represented between samples (Figure 4.7). The largest number of changes was observed in the high (125mM) iron vs control comparison, which included 122 differentially represented proteins. Among these, 95 proteins were unique to this comparison, 10 proteins were also differentially expressed in the medium (12.5mM) iron vs control comparison, and 22 proteins overlapped with the high (125mM) vs medium (12.5mM) iron treatments comparison. The medium (12.5mM) iron vs control comparison included 19 unique proteins, and the high (125mM) vs medium (12.5mM) iron comparison included 16 unique proteins. Two proteins were common in all three comparisons (Figure 4.7 C). The heatmap revealed distinct clustering of samples based on iron fortification, indicating clear differences in protein expression profiles among the control, medium (12.5mM) and high (125mM) iron treatments (Figure 4.7 A). Over representation of numerous proteins was observed in the high (125mM) iron group, while the medium (12.5mM) iron group larvae exhibited an intermediate protein representation between the control and high (125mM) iron conditions. This was supported by the PCA protein analysis of the proteomic data, where three of the four

high (125mM) iron replicates clustered in the positive PC1 and PC2 quadrant, reflecting a pronounced shift in protein expression. Control replicates clustered tightly near the origin, consistent with minimal variation and a baseline expression profile. The medium (12.5mM) iron replicates were more broadly distributed (Figure 4.7 B).

Key over-represented proteins belonged to pathways associated with iron homeostasis (e.g., entoferritin, transferrin), oxidative stress mitigation (e.g., glutathione S-transferase GstE7, cystathionine beta-synthase Cbs), innate immune activation (e.g., croquemort crq, calmodulin Cam), and cytoskeletal remodeling (e.g., tropomyosin, coactosin-like protein CG6891, Jupiter). These modulations reflect cellular strategies aimed at sequestration of excess iron, detoxification of ROS, immune defense, and preservation of structural integrity. Over-representation of cytochrome P450 enzymes (e.g., Cyp4d2, Cyp6a14) further supports the activation of detoxification pathways, while increased expression of coatomer subunit zeta (zetaCOP) and CHK kinase-like proteins (CG10562) suggests an early activation of vesicular trafficking and stress signaling processes. Conversely, a marked under-representation of mitochondrial respiratory chain components (ND-PDSW, ND-MLRQ, ND-23, ND-B18, ND-30, COX5A) indicates suppression of oxidative phosphorylation, likely aimed at limiting ROS production. In parallel, the repression of ribosomal proteins and translation factors (RpL27A, RpL36A, RpL0, RpL4, RpL32, RpL35, RpL38, RpS12, RpL10Ab, RpL40, and the initiation/elongation factors eIF3A, eIF3B, eIF4B, eIF5, eEF1delta) suggests a broad inhibition of ribosome assembly and translational activity. Additional under-represented proteins include enzymes involved in lipid metabolism (ceramide 1-phosphate binding CG30392, hydroxysteroid dehydrogenase-like protein 2 CG5590, beta hydroxy acid dehydrogenase 1 Had1, acetyl-CoA C-acyltransferase ScpX, 3-hydroxyacyl-CoA dehydrogenase Mtpalpha), nitrogen metabolism (glutamine synthetase Gs1, glycine N-methyltransferase Gnmt), and RNA processing (nucleolar protein 56 Nop56, RNA-binding protein squid sqd), reflecting broad metabolic reprogramming under iron overload (Table 4.S2, Figure 4.7).

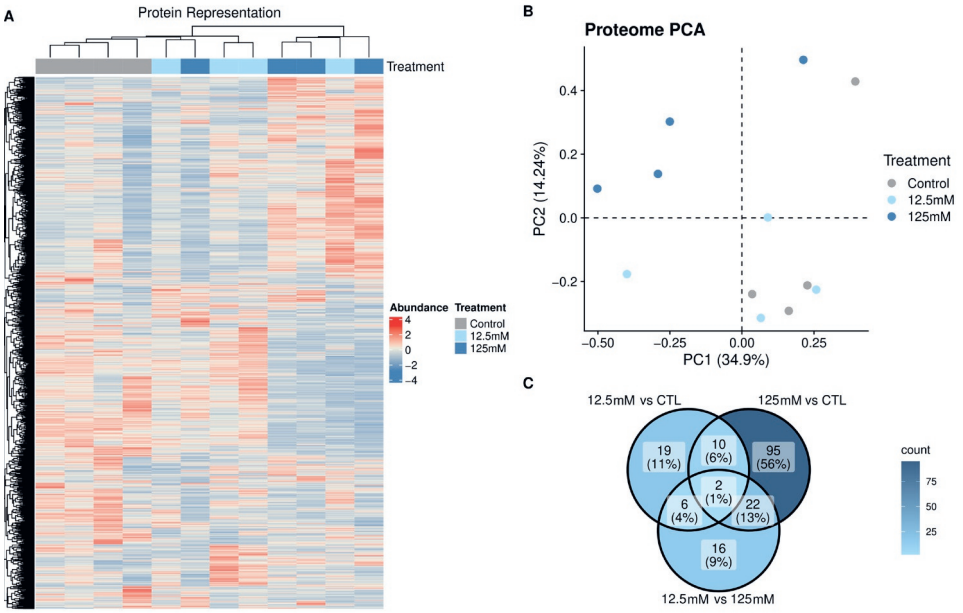


Figure 4.7. Differential proteomic analysis of iron fortified black soldier larvae at day 7. (A) Hierarchical heatmap of protein abundance profiles in larvae fed a control diet (grey), medium (12.5mM) iron (light blue), and high (125mM) iron (blue). The analysis was performed on normalized protein abundance data. Columns represent biological replicates; rows represent individual protein groups. Color scale indicates relative expression levels (blue = downregulation; red = upregulation). (B) Principal Component Analysis (PCA) of protein abundance data of the control, medium (12.5mM) and high (125mM) iron treatments. (C) Venn diagram showing the overlap of significantly differentially expressed protein groups among treatments. Each circle represents one iron treatment: Control (CTL), Medium (12.5mM) and high (125mM) iron. The numbers indicate proteins uniquely or jointly differentially expressed in response to the respective treatments.

The STRING-based protein–protein interaction (PPI) network presented in Figure 4.8, built from proteins differentially represented in BSF larvae reveals several densely interconnected functional modules. The largest hub centers on translation and general protein metabolism, where numerous ribosomal subunits (RpL/RpS nodes) interlink tightly with canonical initiation and elongation factors (eIF3 subunits, eIF4B, eIF5, eEF1), indicating coordinated regulation of protein synthesis under augmented dietary iron supply. Additionally, pathways related to iron transport (e.g., Fer1HCH, Tsf1) and oxidoreductase activity were markedly integrated, consistent with the modulation of iron homeostasis and redox balance affected by excess iron. Notably, proteins involved in nucleobase compound metabolism (e.g., Nop56, SC35, Prp8, AdS) formed a distinct but functionally connected module associated with RNA processing, ribonucleoprotein complex assembly, and mRNA splicing. Their close association with translation-related proteins suggests a tightly regulated continuum from RNA maturation to

active translation. Peripheral but connected clusters involve innate immune effectors, lipid metabolism enzymes, and chitin-based cuticle development proteins, indicating broader immunometabolic and developmental consequences.

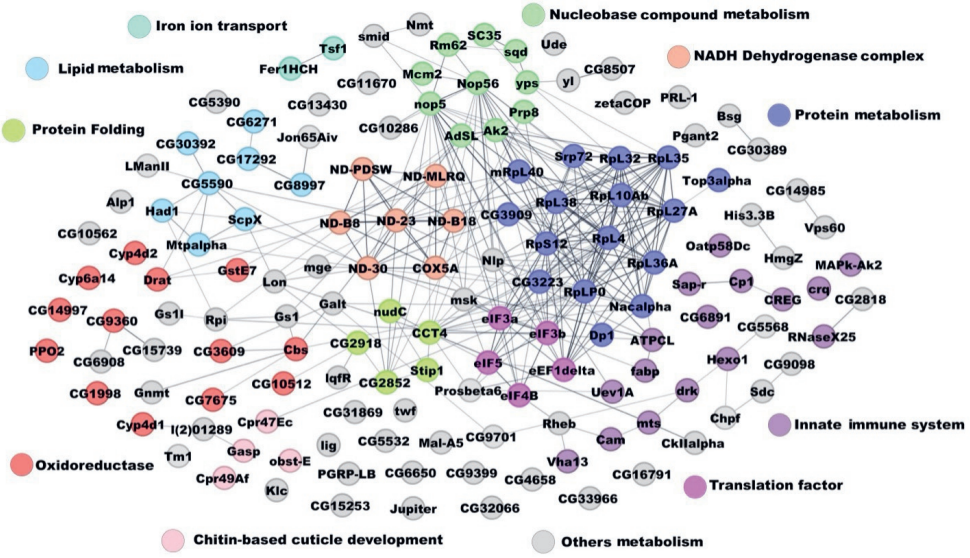


Figure 4.8. Cytoscape-based protein–protein interaction network of differentially expressed proteins in BSF larvae exposed to high (125mM) iron treatment. The network was constructed using STRING data and visualized with Cytoscape. Nodes represent proteins that were significantly over- or under-represented in the high (125mM) iron group compared to control (adjusted p-value < 0.05), and edges represent predicted functional or physical associations. This network reveals highly interconnected modules reflecting key cellular responses to iron overload, including iron sequestration, oxidative stress management, translational repression, immune activation, cytoskeletal stabilization, and metabolic adaptation.

7. Integrative omics confirms coordinated molecular changes, with cuticle and oxidative stress pathways driving treatment separation

Integrative analysis of the transcriptomic data and the proteomic data using DIABLO revealed that the two datasets were highly correlated, with an overall correlation coefficient of 0.92 (Figure 4.9 A). When plotting the overlayed sparse partial least squares-discriminant analysis (sPLS-DA) results in two dimensions, the transcriptomic data and proteomic data form three clusters by treatment group and corresponding replicates fall closely together on the coordinate plane (Figure 4.9 A). In the first sPLS-DA component, we observed a high correlation (correlation coefficient = 0.99) between the

transcriptomic and proteomic datasets along with clear separation between the high (125mM) iron treatment and the control treatment (Figure 4.9 B). Next, which variables (i.e. genes and proteins) are most important to cause this separation were investigated. Consistent with the differential expression analysis results, many of these genes were involved in cuticle formation, while oxidation related proteins such as cytochrome c oxidase and ribosomal protein L3 where amongst the main drivers for treatment separation (Figure 4.9 C). The two omics datasets were also highly correlated in the second s-PLS-DA component (correlation coefficient = 0.98). However, component 2 mainly separated the medium (12.5mM) iron treatment from the other groups (Figure 4.9 D). Similar to the first component, the genes and proteins driving this separation were not the same between the transcriptomic and the proteomic data (Figure 4.9 E).

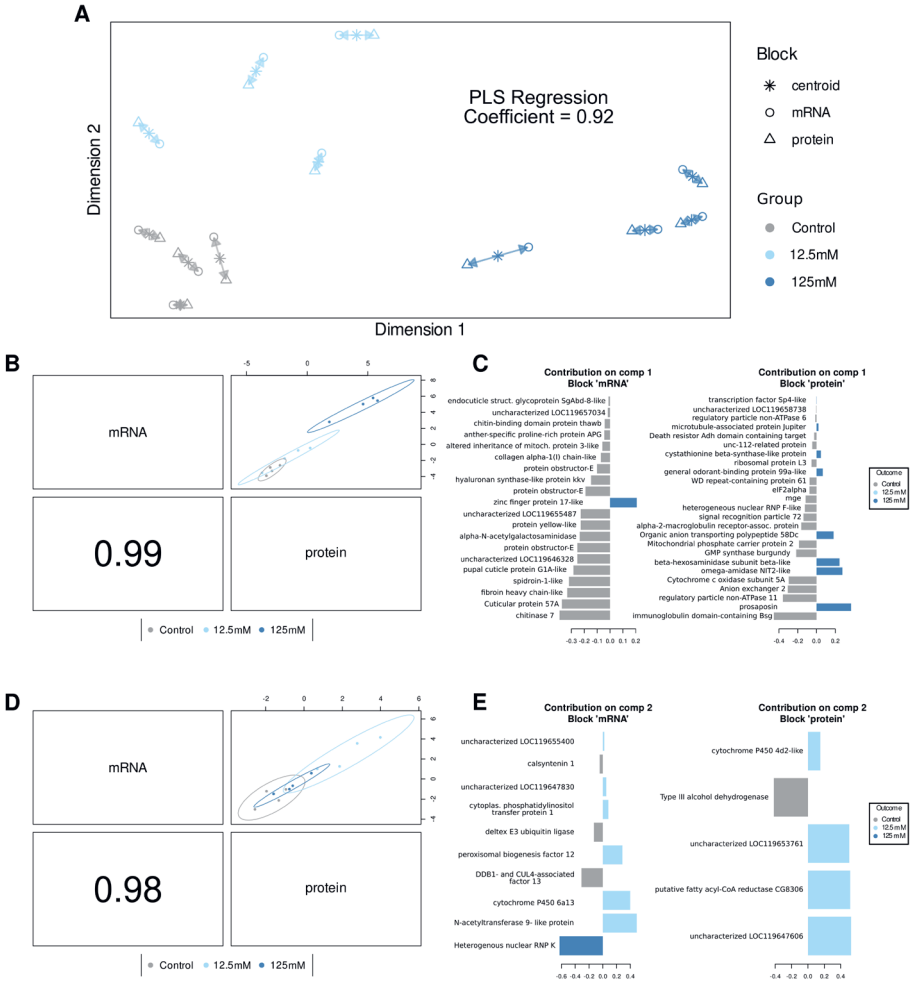


Figure 4.9. Integrative analysis of transcriptomic and proteomic data using DIABLO. (A) Block sPLS-DA plotted on two dimensions shows high degree of similarity between the transcriptomic and proteomic datasets. (B) Correlation of transcriptomic and proteomic datasets in sPLS-DA component 1. (C) Loading plots of the highest contributing genes and proteins to separation between groups. Component 1 primarily separated the control group from the high (125mM) iron group. (D) Correlation of transcriptomic and proteomic datasets in sPLS-DA component 2. (E) Loading plots of the highest contributing genes and proteins to separation between groups. Component 1 primarily separated the control group from the medium (12.5mM) iron group.

8. Entoferritin, ferritin, transferrin, IRP1, and RSL1D1 reflect iron homeostasis adjustments under increasing iron conditions

In addition to the broader omics analyses, the focus shifted to key genes and proteins involved in iron homeostasis (Figure 4.10). Larvae reared on the high (125mM) iron treatment showed a significant increase in entoferritin protein levels, with Fer1HCH and Fer2LCH subunits increasing by ~75% and ~70%, respectively. No significant change in entoferritin subunit mRNA levels was observed at day 2, while mild ($P > 0.1$), dose-dependent increases appeared by day 7. IRP1 expression was lower in high (125mM) iron larvae at day 7, accompanied by a mild ($P > 0.1$) decrease in IRP1 protein abundance for both iron treatments. RSL1D1 expression at day 2 was significantly elevated in both iron treatments compared to the control, with increases of ~320% for medium (12.5mM) iron group and ~350% for the high (125mM) iron group. Transferrin mRNA showed no significant difference at day 2, but at day 7 it was significantly higher in high (125mM) iron group than in the control (~210%) and medium (12.5mM) iron group (~120%). Protein abundance of transferrin in the high (125mM) iron group at day 7 followed the same pattern, with increases of ~140% compared to control and ~110% compared to the medium (12.5mM) iron. Malvolio (Mlv), the insect homolog of Divalent Metal Transporter 1 (DMT1), was detected at all time points, with no significant treatment-related differences, though temporal increases occurred across treatments (Table 4.S1). However, Mlv was not detected in the proteomic analysis.

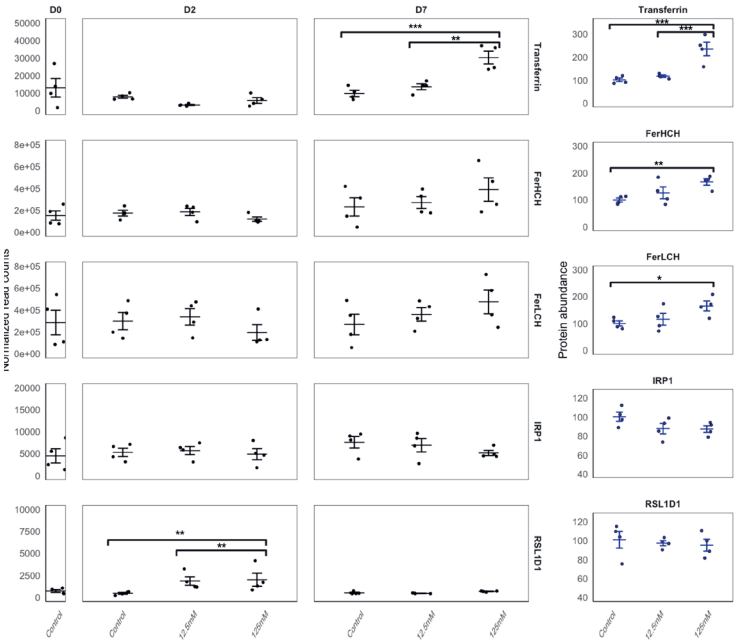


Figure 4.10. Gene expression and protein abundancy of proteins directly involved in iron homeostasis in iron fortified BSF larvae. Mrna expression is shown for day 0 (left), day 2 (center), and day 7 (right), while protein representation are shown in the rightmost panels (day 7). Y-axis scales are adjusted individually per gene to reflect differences in expression range. Asterisks indicate statistically significant differences between treatment groups based on DESeq2 analysis ($p < 0.1$ = *, $p < 0.05$ = **, $p < 0.005$ = ***); absence of asterisks indicates no significant difference.

4. Discussion

Consistent with the findings of First *et al.* (2024), BSF larvae showed no significant differences in body weight across treatments (Figure 4.1), maintaining stable growth under dietary iron concentrations considerably higher than those typically applied in excess iron exposure experiments on other insect species (Bonilla-Ramirez *et al.*, 2011; First *et al.*, 2024; Wagers *et al.*, 2024). Furthermore, larvae exposed to medium (12.5mM) iron exhibited mRNA expression profiles indistinguishable from controls by the final harvest day, suggesting effective transcriptional recovery at moderate iron levels. This contrasts with other insect species, where substantially lower iron concentrations have been shown to disrupt development or reduce survival (Bonilla-Ramirez *et al.*, 2011; First *et al.*, 2024; Wagers *et al.*, 2024), and highlights the BSF larvae unique physiological adaptations for tolerating high dietary iron.

Prussian blue staining revealed a dose-dependent increase in iron deposits, localized to the anterior and posterior midgut across all dietary treatments (Figure 4.2). No stain was detected in fat bodies, whole larvae, or exoskeletons, indicating that storage is restricted to the gut even under high (125mM) iron exposure. This localization aligns with previously reported anterior and posterior iron regions in the black soldier fly larval midgut (Bonelli *et al.*, 2020). The fact that iron accumulation was confined to this established storage site suggests that BSF larvae rely on the same pathway under increasing iron, most likely entoferritin-based sequestration, rather than recruiting novel storage mechanisms (Gorman, 2022). Previous work has shown that BSF larvae reared on standard chicken feed (~320 mg/kg iron) accumulate ~370 mg/kg in their bodies (First *et al.*, 2024), far surpassing the 71–131 mg/kg typically observed in *Drosophila* species larvae (Massie *et al.*, 1985; Sadraie & Missirlis, 2011). In line with this greater accumulation capacity, BSF larvae in this study displayed much stronger iron staining in the midgut compared to the weaker staining reported for *Drosophila* species. Moreover, the iron region of *Drosophila* is usually confined to the anterior midgut and does not include the posterior midgut (Bettedi *et al.*, 2011; Sadraie & Missirlis, 2011; N. Wu *et al.*, 2020). These differences highlight the enhanced ability of BSF larvae to accumulate iron and suggest a potential evolutionary adaptation to a metal-rich environments.

In addition to storage within the midgut, iron aggregates were also detected in the peritrophic matrix of larvae reared on iron-fortified diets, but not in controls (Figure 4.3). PM is a chitinous, semi-permeable layer that lines the insect gut lumen and acts as a protective barrier between ingested food and the gut epithelium (Lin *et al.*, 2021; Orozimbo *et al.*, 2025). In blood-feeding insects, free heme and iron can bind to the PM, reducing their pro-oxidant activity and limiting ROS formation (Orozimbo *et al.*, 2025). A proteomic analysis of BSF larva has identified both ferritin and transferrin in its PM (Lin *et al.*, 2021). Taken together, these findings suggest that, in addition to its barrier function, the BSF PM may contribute to iron handling and oxidative stress mitigation under high-iron conditions through the activation of mechanisms analogous to those described in blood-feeding insects.

While iron accumulation was localized to the midgut and somatic growth remained unaffected, both transcriptomic and proteomic data indicate that BSF larvae undergo substantial physiological adjustments under iron fortification. These adjustments extend beyond iron storage itself and involve pathways and proteins linked to oxidative stress regulation, mitochondrial respiration, ribosomal structure and function, translation factors, and exoskeletal development (Figures 4.5 and 4.8). Integration of the transcriptomic and proteomic data demonstrated strong agreement, with replicates clustering by treatment in both datasets (Figure 4.9). This clustering indicates that the

responses observed are not limited to isolated regulatory processes but instead reflect coordinated, system-wide remodeling under dietary iron stress. Dimension 1, the strongest driver in the DIABLO analysis, clearly separated the high-iron diet group from both the control and the medium (12.5mM) iron groups (Figure 4.9 A), highlighting that the most pronounced physiological reprogramming occurs under high (125mM) iron exposure.

The observed oxidative stress responses likely result from excess dietary iron increasing the pool of free iron available to larvae, which in turn promotes the generation of ROS via the Fenton reaction. These responses may represent cellular protective mechanisms aimed at mitigating ROS-induced damage. Iron exposure can impair mitochondrial function primarily through ROS-mediated pathways, which is in line with the observed reduction in abundance of ribosomal proteins under iron-fortified conditions (Zheng *et al.*, 2018). This agrees with the multi-omics results, where ribosomal and cytochrome proteins were among the strongest contributors to treatment separation (Figure 4.9 B), reflecting the central role of energy metabolism and translational machinery in the high-iron response. The increased iron has decreased larval ribosomal protein levels (Figure 4.8), potentially through direct binding of free iron to ribosomal proteins, leading to their destabilization and degradation (Smethurst *et al.*, 2020).

Beyond oxidative stress, multi-omics analyses revealed that chitin- and cuticle-associated transcripts were major drivers of treatment clustering (Figure 4.10 A). Consistently, DEG patterns of exoskeleton development pathways, together with the over expression of chitin-related proteins, indicated disruption of normal cuticle formation (Figures 4.5 and 4.8). In line with these findings, First *et al.,* (2024) reported that BSF larvae reared on a high-iron diet (6,637 mg/kg DM Fe) accumulated up to 25% more calcium compared to controls (323 mg/kg DM Fe) and developed limited black lesions on their exoskeletons, suggesting impaired cuticle development under iron stress. Calcium is a critical component of BSF cuticle development, where it is biomineralized primarily as calcium carbonate (CaCO) across life-stage specific structures (Rebora *et al.*, 2023). Altogether, these results suggest that excessive dietary iron disrupts cuticle homeostasis through oxidative stress, leading to structural remodeling and increased calcium deposition.

Calcium dynamics are not restricted to cuticle integrity but also indicate developmental progression, as content increase across successive instars to support sclerotization prior to pupation (Liu *et al.*, 2017). A mild ($P > 0.1$), dose-dependent increase in pre-pupate emergence was observed under iron fortification (Figure 4.2), suggesting a potential increase in development timing. Transcriptomic data supports this interpretation, with

hexamerin being the most strongly up-regulated transcript under high (125mM) iron on day 7 (Table 4.S1). Hexamerin is an amino acid storage protein typically stockpiled just before metamorphosis in holometabolous insects (Burmester & Scheller, 1999). Hexamerin protein abundance was numerically ~50% higher in the high (125mM) group as opposed to the control, although the difference was not statistically significant ($P > 0.1$) due to variability among biological replicates (Table 4.S2). Moreover, intracellular iron trafficking via transferrin and entoferritin to the prothoracic gland is essential for insect hormone production and developmental progression. A lack of transferrin or entoferritin has been shown to hinder iron signaling in the prothoracic gland (Soltani *et al.*, 2024), and whether the increased abundance of these proteins observed here (Figure 4.10) may advance the onset of iron signaling remains to be confirmed. Collectively, these observations point to accelerated developmental processes in BSF larvae exposed to high iron. However, neither the present data (Figure 4.1) nor a previous one (First *et al.*, 2024) showed an effect of dietary iron on larval fresh weight at harvest, suggesting that such a developmental shift is subtle. Larger-scale studies spanning the full life cycle are needed to determine whether iron supplementation can enhance developmental rates in BSF production systems.

The patterns observed in entoferritin, IRP1, RSL1D1, transferrin and Malvolio transcripts and protein abundance changes, reveal that BSF larvae rely on multiple regulatory mechanisms to cope with high dietary iron (Figure 4.10). Entoferritin, the predominant intracellular iron storage protein in insects (First *et al.*, 2023; Missirlis *et al.*, 2006), increased significantly at the protein level under high (125mM) iron conditions, while mRNA levels showed mild ($P > 0.1$), statistically insignificant changes. This divergence between transcript and protein abundance indicates that ferritin synthesis is regulated primarily at the post-transcriptional stage.

The reduction of IRP1 abundance detected under both iron conditions likely diminishes IRP–IRE binding, leaving ferritin mRNAs accessible for ribosomal translation (Figure 4.10). In mammals, IRPs binding to IREs in ferritin mRNAs prevents ribosomal assembly and translation. Under iron-replete conditions, cytosolic free iron binds to IRP1, promoting the formation of an iron–sulfur cluster that converts the protein into a cytosolic aconitase enzyme and abolishes its RNA-binding capacity. This conformational change, followed by degradation or repurposing of IRPs, frees the IRE and allows ferritin translation to proceed (Georgieva *et al.*, 2002; Meyron Holtz *et al.*, 2004; Nichol & Winzerling, 2002). Similar post-transcriptional control has been described in Manduca sexta, whereas the IRP/IRE interaction has been demonstrated to affect entoferritin heavy chain subunit translation (Zhang *et al.*, 2001). IRE motif analysis supports this regulatory framework. Both FerHCH and FerLCH transcripts

contained predicted IRE stem-loop structures (Figure 4.6). Messenger RNAs of ferritin light chain containing IREs, as well as various loop mutations, are well characterized and conserved in mammals (Luscieti *et al.*, 2013). This is a novel finding for a dipteran as IREs in the light chain were only reported in lepidopterans (Gorman, 2022; Missirlis *et al.*, 2007; Pham *et al.*, 1996). A light chain isoform lacking an IRE was also detected under high-iron conditions, which could bypass IRP-mediated repression and allow translation even when IRP1 levels are high (Lind *et al.*, 1998). However, given the predominance of the IRE-containing isoform (Table 4.1), its overall contribution to ferritin output is likely small. Together, these features suggest that BSF entoferritin regulation integrates canonical IRP/IRE control with isoform variation to adjust storage capacity in response to dietary iron.

Another potential indirect regulator of iron metabolism is RSL1D1, an mRNA-binding protein involved in various cellular processes including apoptosis, proliferation, and senescence. In mammals, RSL1D1 binds to ferritin heavy chain mRNA, stabilizing the transcript and protecting it from degradation. Knockdown of RSL1D1 in human colorectal cancer cells reduced ferritin heavy chain mRNA levels, while its presence extended mRNA stability over time (Jin *et al.*, 2023). In the current study, RSL1D1 expression rose sharply early after iron exposure before returning to baseline (Figure 4.10), which might increase the stability of heavy chain transcripts across the rearing period and in turn contribute to higher ferritin abundance. Phylogenetic analysis indicates that RSL1D1 is a conserved, single copy ortholog across vertebrates and arthropods, supporting a potentially shared role in ferritin regulation among these groups (Figure 4.S1). However, a functional confirmation of the occurrence of RSL1D1 in insects is needed to confirm this hypothesis.

Transferrin, an extracellular iron transporter in insects (Geiser & Winzerling, 2012), showed a delayed but significant increase at both the mRNA and protein levels by day 7 in the high-iron treatment (Figure 10). It is established that transferrin gene expression in insects is regulated primarily at the transcriptional level (Geiser & Winzerling, 2012). Consistent with this, in BSF we observed a close correspondence between transcript and protein abundance, in contrast to entoferritin (Figure 4.10). The observed concomitant up-regulation of transferrin gene expression and over-representation of the protein may reflect an increased requirement for iron absorption and transport under prolonged exposure. In mosquitoes, transferrin expression is influenced by the chemical form of dietary iron, with inorganic sources often leading to suppression (Harizanova *et al.*, 2005). The opposite pattern in BSF may be linked to adaptation to a non-blood detritus-type diet in which inorganic iron is a consistent dietary component. However, given its relatively low abundance compared to entoferritin, transferrin is

unlikely to make a major contribution to BSF iron bioavailability.

Malvolio (Mvl), the insect homolog of DMT1, functions as a divalent metal transporter that facilitates the uptake of iron and other transition metals across cellular membranes (Bettedi *et al.*, 2011). In contrast to transferrin, Mvl, showed no significant iron-fortification related changes in expression, indicating that BSF larvae do not appear to reduce dietary iron uptake under increased iron conditions (Table 4.S1). In mammals, DMT1 downregulation under iron overload is mediated in part through interaction with Nedd4 family-interacting protein 1, which promotes its degradation (Howitt *et al.*, 2009). In insects, however, regulatory pathways for Mvl are uncharacterized, and no expression patterns indicative of such regulation were detected. Instead, BSF larvae seem to maintain uptake capacity and rely on entoferritin storage as their primary protective strategy.

Overall, these findings suggest an entoferritin based "accumulate and store" approach to dietary iron through a mild ($P > 0.1$) entoferritin induction mRNA transcription increase, IRP1 repression, potential RSL1D1-mediated transcript stabilization, and increased transferrin expression to meet iron transport needs. The previously reported ~250% increase in total iron content (First *et al.*, 2024), compared to only ~70% increases in entoferritin subunits in this study implies a higher iron-to-entoferritin ratio under high-iron conditions. Such disproportionate loading could affect ferritin stability (Irimia-Dominguez *et al.*, 2020; Ruiyang Ji Mingyang Sun, 2023; Srivastava *et al.*, 2023), potentially reducing iron bioavailability, though this requires further investigation.

In conclusion, black soldier fly larvae tolerate a substantial level dietary iron, with larval mass unaffected and only a mild ($P > 0.1$), dose-dependent increase in pre-pupate emergence, suggesting that developmental shifts are subtle. Multi-omics integration revealed coordinated remodeling under iron fortification, including oxidative stress signatures, repression of mitochondrial and translational activity, and strong activation of chitin- and cuticle-associated pathways. Iron localized to the gut epithelium and peritrophic matrix, but not the fat body or exoskeleton, pointing to an "accumulate-and-store" strategy in which entoferritin serves as the primary sequestration site. Entoferritin subunits increased markedly at the protein level despite modest transcript changes, indicating post-transcriptional regulation. Decreased IRP1 abundance, predicted IREs, early RSL1D1 induction, and delayed transferrin upregulation further suggest fine-tuned control of uptake, storage, and transport. This mechanism enables larvae to withstand high iron exposure without impairing growth. From a food and feed perspective, the entoferritin-based 'accumulate-and-store' strategy observed here suggests that iron-fortified larvae could provide a source of highly bioavailable iron. The

soluble and stable nature of ferritins, particularly entoferritin, supports their potential as effective vehicles for dietary iron fortification, a strategy already demonstrated in ferritin-fortified plant models (Lönnerdal, 2007; Masuda *et al.*, 2012). Insects may offer additional advantages, as entoferritin is larger and potentially more water-soluble due to its secreted nature (First *et al.*, 2023), and the magnitude of total iron accumulation in fortified BSF larvae is substantially higher than that typically achieved in plant systems (First *et al.*, 2024; Masuda *et al.*, 2012). However, comparison with previously reported whole-larval iron accumulation suggests a high iron-to-entoferritin ratio, with possible consequences for protein stability and nutrient bioavailability. Future research should quantify iron speciation, resolve regulatory nodes such as RSL1D1, and evaluate whether controlled fortification can enhance larval development, improve production efficiency. This information will definitively strengthen the role of BSF as a sustainable source of bioavailable iron.

Reference:

Andrews, S. (2010). FastQC: a quality control tool for high throughput sequence data. Babraham Bioinformatics. 2010. https://www.bioinformatics.babraham.ac.uk/projects/fastqc/

Bettedi, L., Aslam, M. F., Szular, J., Mandilaras, K., & Missirlis, F. (2011). Iron depletion in the intestines of Malvolio mutant flies does not occur in the absence of a multicopper oxidase. Journal of Experimental Biology, 214(6), 971–978. https://doi.org/10.1242/jeb.051664

Bolger, A. M., Lohse, M., & Usadel, B. (2014). Trimmomatic: a flexible trimmer for Illumina sequence data. Bioinformatics, 30(15), 2114–2120. https://doi.org/10.1093/bioinformatics/btu170

Bonelli, M., Bruno, D., Brilli, M., Gianfranceschi, N., Tian, L., Tettamanti, G., Caccia, S., & Casartelli, M. (2020). Black Soldier Fly Larvae Adapt to Different Food Substrates through Morphological and Functional Responses of the Midgut. International Journal of Molecular Sciences, 21(14). https://doi.org/10.3390/ijms21144955

Bonilla-Ramirez, L., Jimenez-Del-Rio, M., & Velez-Pardo, C. (2011). Acute and chronic metal exposure impairs locomotion activity in *Drosophila* melanogaster: a model to study Parkinsonism. Biometals : An International Journal on the Role of Metal Ions in Biology, Biochemistry, and Medicine, 24(6), 1045–1057. https://doi.org/10.1007/s10534-011-9463-0

Burmester, T., & Scheller, K. (1999). Ligands and receptors: common theme in insect storage protein transport. Die Naturwissenschaften, 86(10), 468–474. https://doi.org/10.1007/s001140050656

Byrne, L., & Murphy, R. A. (2022). Relative Bioavailability of Trace Minerals in Production Animal Nutrition: A Review. Animals: An Open Access Journal from MDPI, 12(15). https://doi.org/10.3390/ani12151981

Cantalapiedra, C. P., Hernández-Plaza, A., Letunic, I., Bork, P., & Huerta-Cepas, J. (2021). eggNOG-mapper v2: Functional Annotation, Orthology Assignments, and Domain Prediction at the Metagenomic Scale. Molecular Biology and Evolution, 38(12), 5825–5829. https://doi.org/10.1093/molbev/msab293

Capella-Gutiérrez, S., Silla-Martínez, J. M., & Gabaldón, T. (2009). trimAl: a tool for automated alignment trimming in large-scale phylogenetic analyses. Bioinformatics (Oxford, England), 25(15), 1972–1973. https://doi.org/10.1093/bioinformatics/btp348

Dixon, S. J., & Stockwell, B. R. (2014). The role of iron and reactive oxygen species in cell death. Nature Chemical Biology, 10(1), 9–17. https://doi.org/10.1038/nchembio.1416
Drost, H.-G., & Paszkowski, J. (2017). Biomartr: genomic data retrieval with R. Bioinformatics, 33(8), 1216–1217. https://doi.org/10.1093/bioinformatics/btw821

First, T., Fogliano, V., & Mishyna, M. (2023). Entoferritin: An innovative iron source for human consumption. Journal of Functional Foods, 108, 105711. https://doi.org/https://doi.org/10.1016/j.jff.2023.105711

First, T., Van Haeften, A. J., Oonincx, D. G. A. B., Van Loon, J. J. A., Fogliano, V., & Mishyna, M. (2024). Strike while the iron is hot: unravelling the impact of dietary iron on two edible insects. Journal of Insects as Food and Feed, 11(7), 1187–1200. https://doi.org/https://doi.org/10.1163/23524588-00001422

Gao, C.-H., Chen, C., Akyol, T., Dusa, A., Yu, G., Cao, B., & Cai, P. (2024). ggVennDiagram: Intuitive Venn diagram software extended. IMeta, 3(1), e177. https://doi.org/https://doi.org/10.1002/imt2.177

Geiser, D. L., & Winzerling, J. J. (2012). Insect transferrins: Multifunctional proteins. Biochimica et Biophysica Acta - General Subjects, 1820(3), 437–451. https://doi.org/https://doi.org/10.1016/j.bbagen.2011.07.011

Georgescu, B., Struți, D., Păpuc, T., Ladoși, D., & Boaru, A. (2020). Body weight loss of black soldier fly *Hermetia illucens* (Diptera: Stratiomyidae) during development in non-feeding stages: implications for egg clutch parameters. European Journal of Entomology, 117(216–225), 216–225. https://doi.org/10.14411/eje.2020.023

Georgieva, T., Dunkov, B. C., Dimov, S., Ralchev, K., & Law, J. H. (2002). *Drosophila melanogaster* ferritin: cDNA encoding a light chain homologue, temporal and tissue specific expression of both subunit types. Insect Biochemistry and Molecular Biology, 32(3), 295–302. https://doi.org/https://doi.org/10.1016/S0965-1748(01)00090-X

Gorman, M. J. (2022). Iron homeostasis in Insects. Annual Review of Entomology, 68. https://doi.org/doi.org/10.1146/annurev-ento-040622-092836

Gu, Z., Eils, R., & Schlesner, M. (2016). Complex heatmaps reveal patterns and correlations in multidimensional genomic data. Bioinformatics, 32(18), 2847–2849. https://doi.org/10.1093/bioinformatics/btw313

Harizanova, N., Georgieva, T., Dunkov, B. C., Yoshiga, T., & Law, J. H. (2005). Aedes aegypti transferrin. Gene structure, expression pattern, and regulation. Insect Molecular Biology, 14(1), 79–88. https://doi.org/https://doi.org/10.1111/j.1365-2583.2004.00533.x

Hoang, D. T., Chernomor, O., von Haeseler, A., Minh, B. Q., & Vinh, L. S. (2018). UFBoot2: Improving the Ultrafast Bootstrap Approximation. Molecular Biology and Evolution, 35(2), 518–522. https://doi.org/10.1093/molbev/msx281

Howitt, J., Putz, U., Lackovic, J., Doan, A., Dorstyn, L., Cheng, H., Yang, B., Chan-Ling, T., Silke, J., Kumar, S., & Tan, S.-S. (2009). Divalent metal transporter 1 (DMT1) regulation by Ndfip1 prevents metal toxicity in human neurons. Proceedings of the National Academy of Sciences of the United States of America, 106(36), 15489–15494. https://doi.org/10.1073/pnas.0904880106

Irimia-Dominguez, J., Sun, C., Li, K., Muhoberac, B. B., Hallinan, G. I., Garringer, H. J., Ghetti, B., Jiang, W., & Vidal, R. (2020). Cryo-EM structures and functional characterization of homo- and heteropolymers of human ferritin variants. Scientific Reports, 10(1), 20666. https://doi.org/10.1038/s41598-020-77717-4

Jin, Y., Zhao, L., Wang, S., Zhang, X., Quan, J., Lin, Z., & Piao, J. (2023). RSL1D1 knockdown induces ferroptosis and mediates ferrous iron accumulation in senescent cells by inhibiting FTH1 mRNA stability. Carcinogenesis, 44(2), 129–142. https://doi.org/10.1093/carcin/bgad012

Kalyaanamoorthy, S., Minh, B. Q., Wong, T. K. F., von Haeseler, A., & Jermiin, L. S. (2017). ModelFinder: fast model selection for accurate phylogenetic estimates. Nature Methods, 14(6), 587–589. https://doi.org/10.1038/nmeth.4285

Katoh, K., & Standley, D. M. (2013). MAFFT multiple sequence alignment software version 7: improvements in performance and usability. Molecular Biology and Evolution, 30(4), 772–780. https://doi.org/10.1093/molbev/mst010

Lin, Y.-B., Rong, J.-J., Wei, X.-F., Sui, Z.-X., Xiao, J., & Huang, D.-W. (2021). Proteomics and ultrastructural analysis of *Hermetia illucens* (Diptera: Stratiomyidae) larval peritrophic matrix. Proteome Science, 19(1), 7. https://doi.org/10.1186/s12953-021-00175-x

Lind, M. I., Ekengren, S., Melefors, Ö., & Söderhäll, K. (1998). *Drosophila* ferritin mRNA: alternative RNA splicing regulates the presence of the iron-responsive element. Federation of European Biochemical Societies Letters, 436(3), 476–482. https://doi.org/https://doi.org/10.1016/S0014-5793(98)01186-7

Liu, X., Chen, X., Wang, H., Yang, Q., ur Rehman, K., Li, W., Cai, M., Li, Q., Mazza, L., Zhang, J., Yu, Z., & Zheng, L. (2017). Dynamic changes of nutrient composition throughout the entire life cycle of black soldier fly. Plos one, 12(8), e0182601-. https://doi.org/10.1371/journal.pone.0182601

Lönnerdal. (2007). The Importance and Bioavailability of Phytoferritin-Bound Iron in Cereals and Legume Foods. International Journal for Vitamin and Nutrition Research, 77(3), 152–157. https://doi.org/10.1024/0300-9831.77.3.152

Love, M. I., Huber, W., & Anders, S. (2014). Moderated estimation of fold change and dispersion for RNA-seq data with DESeq2. Genome Biology, 15(12), 550. https://doi.org/10.1186/s13059-014-0550-8

Luscieti, S., Tolle, G., Aranda, J., Campos, C. B., Risse, F., Morán, É., Muckenthaler, M. U., & Sánchez, M. (2013). Novel mutations in the ferritin-L iron-responsive element that only mildly impair IRP binding cause hereditary hyperferritinaemia cataract syndrome. Orphanet Journal of Rare Diseases, 8, 30. https://doi.org/10.1186/1750-1172-8-30

Martin, M. (2008). Cut adapt removes adapter sequences from high-throughput sequencing reads. European Molecular Biology Network. (Vol. 17, Issue 1, p. 10). https://cir.nii.ac.jp/crid/1370004237564985735.bib?lang=en

Massie, H. R., Aiello, V. R., & Williams, T. R. (1985). Iron accumulation during development and ageing of *Drosophila*. Mechanisms of Ageing and Development, 29(2), 215–220. https://doi.org/https://doi.org/10.1016/0047-6374(85)90020-X

Masuda, H., Ishimaru, Y., Aung, M. S., Kobayashi, T., Kakei, Y., Takahashi, M., Higuchi, K., Nakanishi, H., & Nishizawa, N. K. (2012). Iron biofortification in rice by the introduction of multiple genes involved in iron nutrition. Scientific Reports, 2, 543. https://doi.org/10.1038/srep00543

MeyronHoltz, E. G., Ghosh, M. C., Iwai, K., LaVaute, T., Brazzolotto, X., Berger, U. V, Land, W., OllivierreWilson, H., Grinberg, A., Love, P., & Rouault, T. A. (2004). Genetic ablations of iron regulatory proteins 1 and 2 reveal why iron regulatory protein 2 dominates iron

homeostasis. The European Molecular Biology Organization Journal, 23(2), 386-395–395. https://doi.org/https://doi.org/10.1038/sj.emboj.7600041

Minh, B. Q., Schmidt, H. A., Chernomor, O., Schrempf, D., Woodhams, M. D., von Haeseler, A., & Lanfear, R. (2020). IQ-TREE 2: New Models and Efficient Methods for Phylogenetic Inference in the Genomic Era. Molecular Biology and Evolution, 37(5), 1530–1534. https://doi.org/10.1093/molbev/msaa015

Misof, B., Liu, S., Meusemann, K., Peters, R. S., Donath, A., Mayer, C., Frandsen, P. B., Ware, J., Flouri, T., Beutel, R. G., Niehuis, O., Petersen, M., Izquierdo-Carrasco, F., Wappler, T., Rust, J., Aberer, A. J., Aspöck, U., Aspöck, H., Bartel, D., … Zhou, X. (2014). Phylogenomics resolves the timing and pattern of insect evolution. Science, 346(6210), 763–767. https://doi.org/10.1126/science.1257570

Missirlis, F., Holmberg, S., Georgieva, T., Dunkov, B. C., Rouault, T. A., & Law, J. H. (2006). Characterization of Mitochondrial Ferritin in Drosophila. Proceedings of the National Academy of Sciences of the United States of America, 103(15), 5893–5898. http://www.jstor.org.ezproxy.library.wur.nl/stable/30050196

Missirlis, F., Kosmidis, S., Brody, T., Mavrakis, M., Holmberg, S., Odenwald, W. F., Skoulakis, E. M. C., & Rouault, T. A. (2007). Homeostatic Mechanisms for Iron Storage Revealed by Genetic Manipulations and Live Imaging of *Drosophila* Ferritin. Genetics, 177(1), 89–100. https://doi.org/10.1534/genetics.107.075150

Mwangi, M. N., Oonincx, D. G. A. B., Stouten, T., Veenenbos, M., Melse-Boonstra, A., Dicke, M., & van Loon, J. J. A. (2018). Insects as sources of iron and zinc in human nutrition. Nutrition Research Reviews, 31(2), 248–255. https://doi.org/DOI: 10.1017/S0954422418000094

Nichol, H., & Winzerling, J. (2002). Structured RNA upstream of insect cap distal iron responsive elements enhances iron regulatory protein-mediated control of translation. Insect Biochemistry and Molecular Biology, 32(12), 1699–1710. https://doi.org/https://doi.org/10.1016/S0965-1748(02)00110-8

O'Leary, N. A., Cox, E., Holmes, J. B., Anderson, W. R., Falk, R., Hem, V., Tsuchiya, M. T. N., Schuler, G. D., Zhang, X., Torcivia, J., Ketter, A., Breen, L., Cothran, J., Bajwa, H., Tinne, J., Meric, P. A., Hlavina, W., & Schneider, V. A. (2024). Exploring and retrieving sequence and metadata for species across the tree of life with NCBI Datasets. Scientific Data, 11(1), 732. https://doi.org/10.1038/s41597-024-03571-y

Orozimbo, K. B. da S., Tauil, D. da S. G., Licurgo, A. M., Moreira, F. F., Araújo, J. da S., Bertonceli, M. A. A., Seabra, S. H., Machado, O. L. T., & Lemos, F. J. A. (2025). Structural and Functional Analysis of Hemoglobin Binding to the Peritrophic Matrix During Blood Digestion in Aedes aegypti. Insects, 16(2). https://doi.org/10.3390/insects16020116

Patro, R., Duggal, G., Love, M. I., Irizarry, R. A., & Kingsford, C. (2017). Salmon provides fast and bias-aware quantification of transcript expression. Nature Methods, 14(4), 417–419. https://doi.org/10.1038/nmeth.4197

Pham, D. Q. D., & Winzerling, J. J. (2010). Insect ferritins: Typical or atypical? Biochimica et Biophysica Acta - General Subjects, 1800(8), 824–833. https://doi.org/10.1016/j.bbagen.2010.03.004

Pham, D. Q.-D., Zhang, D., Hufnagel, D. H., & Winzerling, J. J. (1996). Manduca sexta hemolymph ferritin: cDNA sequence and mRNA expression. Gene, 172(2), 255–259. https://doi.org/https://doi.org/10.1016/0378-1119(96)00012-1

Piskin, E., Cianciosi, D., Gulec, S., Tomas, M., & Capanoglu, E. (2022). Iron Absorption: Factors, Limitations, and Improvement Methods. American Chemical Society Omega, 7(24), 20441–20456. https://doi.org/10.1021/acsomega.2c01833

Rebora, M., Salerno, G., Piersanti, S., Saitta, V., Morelli Venturi, D., Li, C., & Gorb, S. (2023). The armoured cuticle of the black soldier fly *Hermetia illucens*. Scientific Reports, 13(1), 22101. https://doi.org/10.1038/s41598-023-49549-5

Ruiyang Ji Mingyang Sun, J. Z. C. L. G. Z. (2023). Effects of heat treatment on the structure, digestive property, and absorptivity of holoferritin. In Food Innovation and Advances (Vol. 2, Issue FIA-2023-0005, p. 28). https://doi.org/10.48130/FIA-2023-0005

Sadraie, M., & Missirlis, F. (2011). Evidence for evolutionary constraints in *Drosophila* metal biology. Biometals : An International Journal on the Role of Metal Ions in Biology, Biochemistry, and Medicine, 24(4), 679–686. https://doi.org/10.1007/s10534-011-9420-y

Sayols, S. (2023). rrvgo: a Bioconductor package for interpreting lists of Gene Ontology terms. MicroPublication Biology, 2023. https://doi.org/10.17912/micropub.biology.000811

Singh, A., Shannon, C. P., Gautier, B., Rohart, F., Vacher, M., Tebbutt, S. J., & Lê Cao, K.-A. (2019). DIABLO: an integrative approach for identifying key molecular drivers

from multi-omics assays. Bioinformatics, 35(17), 3055–3062. https://doi.org/10.1093/bioinformatics/bty1054

Siva Raman, S., Stringer, L. C., Bruce, N. C., & Chong, C. S. (2022). Opportunities, challenges and solutions for black soldier fly larvae-based animal feed production. Journal of Cleaner Production, 373, 133802. https://doi.org/https://doi.org/10.1016/j.jclepro.2022.133802

Smethurst, D. G. J., Kovalev, N., McKenzie, E. R., Pestov, D. G., & Shcherbik, N. (2020). Iron-mediated degradation of ribosomes under oxidative stress is attenuated by manganese. The Journal of Biological Chemistry, 295(50), 17200–17214. https://doi.org/10.1074/jbc.RA120.015025

Soltani, S., Webb, S. M., Kroll, T., & King-Jones, K. (2024). *Drosophila* Evi5 is a critical regulator of intracellular iron transport via transferrin and ferritin interactions. Nature Communications, 15(1), 4045. https://doi.org/10.1038/s41467-024-48165-9

Soneson, C., Love, M. I., & Robinson, M. D. (2015). Differential analyses for RNA-seq: transcript-level estimates improve gene-level inferences. F1000Research, 4, 1521. https://doi.org/10.12688/f1000research.7563.2

Srivastava, A. K., Scalcione, L. J., Arosio, P., & Bou-Abdallah, F. (2023). Hyperthermostable recombinant human heteropolymer ferritin derived from a novel plasmid design. Protein Science, 32(1), e4543. https://doi.org/https://doi.org/10.1002/pro.4543

Su, Z.-H., Sasaki, A., Minami, H., & Ozaki, K. (2024). Arthropod Phylotranscriptomics With a Special Focus on the Basal Phylogeny of the Myriapoda. Genome Biology and Evolution, 16(9), evae189. https://doi.org/10.1093/gbe/evae189

Suárez-Quintana, C., Navarro-Padilla, M., Chorostecki, U., & Sanchez, M. (2025). SIREs 3.0, an improved RNA prediction tool for iron-responsive elements. Nucleic Acids Research. https://doi.org/10.1093/nar/gkaf390

Torti, F. M., & Torti, S. V. (2002). Regulation of ferritin genes and protein. Blood, 99(10), 3505–3516. https://doi.org/10.1182/blood.v99.10.3505

Wagers, M. L., Starks, A., Nadolski, J., Bierbower, S. M., Altenburg, S., Schryer, B., & Cooper, R. L. (2024). Examining the effect of iron (ferric) on physiological processes: Invertebrate models. Comparative Biochemistry and Physiology Part C: Toxicology &

Pharmacology, 278, 109856. https://doi.org/https://doi.org/10.1016/j.cbpc.2024.109856
Wang, L., Liang, D., Huangfu, H., Shi, X., Liu, S., Zhong, P., Luo, Z., Ke, C., & Lai, Y. (2024). Iron Deficiency: Global Trends and Projections from 1990 to 2050. Nutrients, 16(20). https://doi.org/10.3390/nu16203434

Wu, G., Ye, G., Hu, C., & Cheng, J.-A. (2006). Accumulation of cadmium and its effects on growth, development and hemolymph biochemical compositions in Boettcherisca peregrina larvae (Diptera: Sarcophagidae). Insect Science, 13(1), 31–39. https://doi.org/https://doi.org/10.1111/j.1744-7917.2006.00065.x

Wu, N., Wang, X., Xu, X., Cai, R., & Xie, S. (2020). Effects of heavy metals on the bioaccumulation, excretion and gut microbiome of black soldier fly larvae (*Hermetia illucens*). Ecotoxicology and Environmental Safety, 192, 110323. https://doi.org/https://doi.org/10.1016/j.ecoenv.2020.110323

Zhang, D., Albert, D. W., Kohlhepp, P., D-Pham, D. Q., & Winzerling, J. J. (2001). Repression of Manduca sexta ferritin synthesis by IRP1/IRE interaction. Insect Molecular Biology, 10(6), 531–539. https://doi.org/10.1046/j.0962-1075.2001.00293.x

Zheng, Q., Zhao, Y., Guo, J., Zhao, S., Fei, C., Xiao, C., Wu, D., Wu, L., Li, X., & Chang, C. (2018). Iron overload promotes mitochondrial fragmentation in mesenchymal stromal cells from myelodysplastic syndrome patients through activation of the AMPK/MFF/Drp1 pathway. Cell Death & Disease, 9(5), 515. https://doi.org/10.1038/s41419-018-0552-7

CHAPTER

05

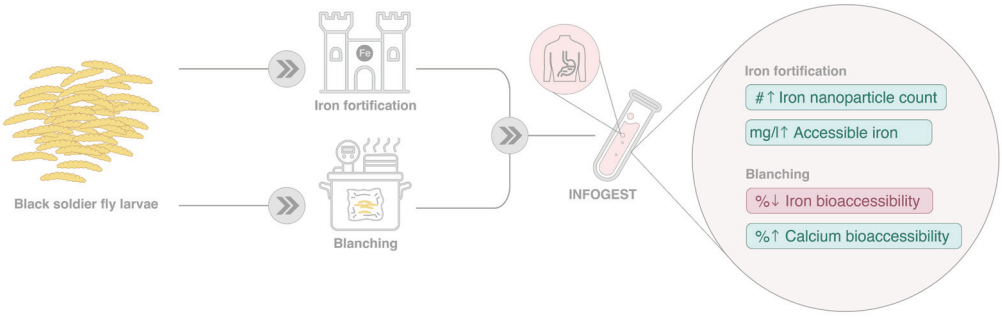
Built by Iron, Changed by Heat: Mineral Bioaccessibility in Iron-Fortified and Processed *Hermetia illucens* larvae

T. First[1], Joelin de Boer[1]; Miguel Gomez-Sanchez[2,3]; Carlos López-Portugués[2,3]; Jorg Bettmer[2,3]; Maria Montes-Bayón[2,3]; Dennis G.A.B. Oonincx[4], Vincenzo Fogliano[1] and Maryia Mishyna[1]

[1]Wageningen University and Research, Food Quality and Design group, 6708 Wageningen, the Netherlands; [2]Department of Physical and Analytical Chemistry, Faculty of Chemistry, University of Oviedo, 33006 Oviedo, Spain; [3]Health Research Institute of Asturias (ISPA), Central University Hospital of Asturias, 33011 Oviedo, Spain; [4]Animal Nutrition Group, Wageningen University and Research, De Elst 1, 6708 WD Wageningen, the Netherlands;

DOI:
https://doi.org/10.1016/j.foodchem.2026.148923

Graphical Abstract



Abstract

Black soldier fly larvae (BSFL) are a promising source of dietary minerals for food and feed. This study quantified the bioaccessibility of iron, calcium, zinc, and magnesium in BSFL reared on iron-fortified diets (269–7803 mg Fe/kg) and subjected to thermal processing. Iron fortification increased larval iron content and the number of naturally occurring iron nanoparticles (~45 nm), consistent with entoferritin-mediated storage. Although iron bioaccessibility decreased from ~50% to ~25% with fortification, the concentration of soluble iron released after *in vitro* digestion increased from 0.08 to 0.20 mg/mL, increasing total bioaccessible iron content. Thermal processing showed nutrient-specific effects: blanching reduced iron bioaccessibility, likely via entoferritin denaturation, but enhanced calcium and zinc bioaccessibility by disrupting mineral storage structures. Overall, these results demonstrate that iron-fortified BSFL can increase the absolute amount of bioaccessible iron despite reduced fractional bioaccessibility, underscoring their potential as a mineral-rich ingredient for food and feed.

1. Introduction

The mainstream livestock-based protein industry, which includes both meat and dairy-based production, is a major contributor to greenhouse gas emissions. It also places significant pressure on land, freshwater, and energy resources. These environmental demands are becoming increasingly unsustainable and pose a growing threat to global ecological and societal stability (Parlasca & Qaim, 2022). At the same time, animal and dairy products remain the most bioavailable sources of dietary protein, both for direct human consumption and for animal feed (Ajomiwe *et al.*, 2024). Importantly, they also provide the most bioavailable forms of iron and calcium, two of the most widespread micronutrient deficiencies worldwide (Carpenter & Mahoney, 1992; Gardner *et al.*, 2023; Guéguen & Pointillart, 2000; Shlisky *et al.*, 2022). Notably, iron deficiency is also the most prevalent micronutrient deficiency in young, farmed pigs (Friendship *et al.*, 2021). This dual challenge of environmental constrain and nutritional reliance points to the urgent need for alternative protein sources that are both sustainable and capable of addressing key nutrient gaps.

In this frame, edible insects have been proposed as a sustainable alternative protein source for both food and feed (van Huis *et al.*, 2021). The black soldier fly (BSF, *Hermetia illucens*) has become a leading candidate in the alternative feed sector, due to its efficient conversion of agricultural waste into protein-rich biomass with low resource

demands (Siva Raman *et al.*, 2022). Although not currently consumed, these attributes also position BSF larvae as a promising candidate for future use as a food ingredient in human diets (Bessa *et al.*, 2020). Beyond its protein content, black soldier fly larvae also provide significant amounts of iron and calcium (First *et al.*, 2024; Zulkifli *et al.*, 2022). To strengthen the larvae's potential as a novel mineral source, it was demonstrated that iron levels in the larvae could be fortified through substrate manipulation, increasing from 362 mg/kg Dry Matter (DM) to 999 mg/kg DM Fe. Moreover, iron fortification was accompanied by an increase in calcium content from 26.5 to 31.9 g/kg when substrate dietary iron level increased from 300 mg/kg to 6600 mg/kg (First *et al.*, 2024). However, current understanding of trace mineral bioavailability in this species remains limited, especially under conditions of iron fortification.

To understand the nutritional relevance of BSF larvae iron fortification, this study investigated mineral bioaccessibility. Bioaccessibility is defined as the soluble fraction of a nutrient available for absorption in the gut after digestion, relative to its total amount in the ingested material. The bioaccessibility of trace elements such as iron and calcium is strongly influenced by the species of the mineral, the compounds it is bound to, and the composition of the surrounding matrix (Manzoor *et al.*, 2024). Processing methods such as blanching or pasteurization, which are often required by food safety regulations in edible insects (European Commission Health and Food Safety Directorate General, 2024), can significantly affect nutrient availability by altering mineral solubility, binding structures, or matrix composition (Cilla *et al.*, 2019). The effect of boiling on mineral bioaccessibility has been previously tested in two harvested insects, *Eulepida mashona* and *Henicus whellani*. Blanching for 30 or 60 minutes was found to reduce iron and zinc bioaccessibility in both species. In contrast, calcium bioaccessibility increased in *Eulepida mashona* but decreased in *Henicus whellani* following boiling (Manditsera *et al.*, 2019). However, the commonly applied several minutes blanching procedure used for farmed insects (Bessa *et al.*, 2021; Borremans *et al.*, 2020; Son *et al.*, 2023) has not yet been tested for its effect on mineral bioaccessibility in any farmed species. The iron bioaccessibility of insect-based ingredients are largely influenced by the behavior of entoferritin, a large, water-soluble iron-binding protein containing a ferrihydrite iron core (First *et al.*, 2023).

Data on mineral bioaccessibility in farmed edible insects remains limited. Recently, Machado *et al.* (2024) investigated the bioaccessibility of iron in two commonly consumed edible insect species, house crickets (*Acheta domesticus*) and yellow mealworms (*Tenebrio molitor*). This study was accompanied with the analysis of iron nanoparticles (NP) content and its relation to iron bioaccessibility. Differences in the size and quantity of iron NPs can reflect distinct iron storage patterns among organisms.

Variations in iron NP size and content can affect bioavailability by influencing solubility, redox state, and intestinal absorption (Kumari & Chauhan, 2021). Moreover, in the iron-fortified BSF larvae, such data are essential for identifying the form in which the accumulated iron is stored and for evaluating its potential nutritional value. The yellow mealworm showed significantly higher iron bioaccessibility, despite both species being rich in chitin, a known inhibitor of iron absorption, and exhibited lower levels of iron NPs compared to house crickets (Karthikeyan *et al.*, 2005; Machado *et al.*, 2024). These results lead the hypothesis that iron nanoparticle content may act as an indicator of iron bioaccessibility. However, no analysis of iron NPs in black soldier fly larvae had been previously performed.

Using an *in vitro* digestion model, this study evaluated the bioaccessibility of four essential minerals, iron (Fe), calcium (Ca), zinc (Zn), and magnesium (Mg), in black soldier fly larvae, and assessed the effects of iron fortification and thermal processing on their bioaccessibility. In addition, the study investigated the effect of iron fortification on the formation of iron nanoparticles in the larvae and their relationship to iron solubility during digestion.

2. Methods

2.1 Insect rearing and processing

Insect rearing and feed preparation followed the protocol described by First *et al.* (2024) with minor modifications to moisture content, harvesting time, and the number of larvae per container. Commercial chicken feed (Kuikenopfokmeel no. 1, Kasper FaunaFood, the Netherlands) was sieved through a 1 mm kitchen strainer and mixed with water at a 1:1.6 (w:v) ratio to prepare the BSF feed. Dietary iron levels were modified by supplementing the water with ferric ammonium citrate to final concentrations of 0 mM (control), 12.5 mM, and 125 mM, corresponding to iron contents of 269, 1151, and 7803 mg/kg DM of the feed, respectively. Ferric ammonium citrate has been documented to increase the BSF larvae iron accumulation without adverse effects on growth or yield (First *et al.*, 2024).

Approximately 0.2 g of BSF eggs (Protix, Bergen op Zoom, the Netherlands) were introduced to 520 g of wet feed in rearing containers (15.5 × 10.5 × 6 cm). Five days post-hatching, larvae weighing 3 to 5 mg were harvested, washed and using a sieve with 1mm pore size, and separated into groups of 200. These were transferred to insect pots

(125 × H114 mm, mesh pore size 300 µm, Megaview Science, Taiwan) containing 440 g of wet feed corresponding to the dietary treatments. After six days on the treatment diets, all larvae were switched to the control diet for one day, until harvest. Following one day of feeding on the control feed, the larvae were harvested, washed, counted and weighted. All treatments were performed in triplicate.

For each replicate, 15 g of larvae were placed in vacuum-sealed bags to prevent leaching during blanching and subsequently blanched in boiling water (100 °C) for 120 seconds. All larvae were then flash-frozen in liquid nitrogen. Frozen larvae were homogenized using a CryoMill® 6775 (SPEX SamplePrep, NJ, USA) under automatic liquid nitrogen cooling (3 min pre-cool, 3.5 min run, 1 min cool time), with three cycles at 15 cps.

2.2 *In vitro* mineral bioaccessibility

To assess the effect of blanching on protein solubility, cryomilled freeze-dried larvae were extracted in phosphate-buffered saline (PBS, pH 7.5). From each replicate 10 mg of sample was suspended in 1 mL PBS and vortexed to ensure proper dispersion. The suspension was incubated at room temperature for 1 hour under continuous shaking, followed by centrifugation at 15,000 × g for 10 minutes. The resulting supernatant was collected, and protein concentration was quantified using the Pierce BCA Protein Assay (Thermo Fisher Scientific, USA).

An *in vitro* digestion assay was performed on dried BSF larvae reared under different dietary iron treatments. For each iron treatment, both blanched and unblanched larvae were assessed in biological triplicate, except for the 12.5 mM unblanched group, which was analyzed in duplicate due to a technical fault. The assay followed the standardized INFOGEST protocol (Brodkorb *et al.*, 2019), with minor modifications. The chemical reagents used in the simulated digestion model across the three phases were purchased from Sigma Aldrich (Sigma Chemical Co., St. Louis, Mo) and were prepared in bulk, the composition is elaborated on table S2. Nutri Whey™ Isolate (WPI) R, 90% protein content (Friesland campina, Amersfoort, Netherlands) was used as a reference protein source, and a water blank served as a negative control. The digestion procedure simulated physiologically relevant oral, gastric, and intestinal phases.

For the oral phase, 1 g of prepared BSF larvae powder was combined with 1.6 mL simulated salivary fluid (SSF), 0.01 mL of 0.3 M CaCl, and 0.39 mL Milli-Q water, yielding a final volume of 4 mL. No salivary amylase was included in this step.

In the gastric phase, the oral bolus was mixed with 3.2 mL simulated gastric fluid (SGF), and the pH was adjusted to 3.0 using 5.0 M HCl to represent a physiological postprandial condition. Pepsin (P7012, Sigma Aldrich, Burlington, USA, Activity = 4014 U/mg solid) was added to achieve a final enzymatic activity of 2000 U/mL. An additional 2 µL of 0.3 M CaCl was included, and the volume was adjusted to 8 mL with Milli-Q water. Samples were incubated at 37 °C with continuous shaking at 30 rpm for 2 hours. Gastric lipases were omitted.

For the intestinal phase, 5 mL of simulated intestinal fluid (SIF) was added to the gastric chyme, and the pH was adjusted to 7.0 using 5.0 M NaOH. Then, 16 µL of 0.3 M CaCl was added. Bile and pancreatin (B3883, P7545, Sigma Aldrich, Burlington, USA, Activity = 5.59 U/mg solid) were added to reach final concentrations of 10 mM bile salts and 100 U/mL trypsin (T0303, Sigma Aldrich, Burlington, USA) activity, respectively. The total volume was adjusted to 16 mL with Milli-Q water, and samples were incubated at 37 °C with shaking at 30 rpm for another 2 hours. At the end of digestion, samples were centrifuged at 10,000 × g for 30 minutes at 4 °C. The supernatants were collected and stored at –80 °C until analysis of mineral content and degree of hydrolysis.

To assess the mineral bioaccessibility, the mineral content of the supernatant analyzed from the *in vitro* digestion was divided by the total mineral content of the starting mineral and converted into percentage, as presented in equation (1):

$$\textit{Mineral bioaccessibility}\ (\%) = \left[\frac{\textit{Supernatant mineral content (mg)}}{\textit{Staring material mineral content (mg)}}\right] 100 \qquad (1)$$

Equation 5.1. Mineral bioaccessibility calculation.

2.3 Mineral analysis

Mineral quantification of the BSF larvae and the digesta was performed by the Soil Chemistry Laboratory of Wageningen University (CBLB, Wageningen University and Research, the Netherlands), similar to First *et al.* (2024). For the whole BSF larvae, approximately 300 mg of freeze-dried insect material, or 15ml of digested supernatant were digested using a mixture of concentrated nitric acid (HNO) and hydrochloric acid (HCl). Samples were subjected to microwave-assisted digestion, after which hydrogen peroxide (HO) was added, and the heating step was repeated to ensure complete oxidation of organic matter. Following digestion, the suspension was allowed to

settle to separate undissolved silica particles. The resulting supernatant was collected and analyzed for elemental composition using Inductively Coupled Plasma Atomic Emission Spectroscopy (ICP-AES; Thermo iCAP 6500 DV, Thermo Fisher Scientific, USA). Mineral content was quantified comparing the samples to certified standards (WEPAL, Wageningen, The Netherlands). All mineral concentrations are reported on a dry matter basis in units of mg/kg or g/kg. All analyzed minerals were above the protocol detection limit, provided in table S1.

2.4 Iron nanoparticle analysis

A mechanical lysis method adapted from a recent study (Álvarez-Fernández García *et al.*, 2020) was employed to preserve iron-accumulating proteins of the homogenized freeze-dried larvae, using 500 m glass beads (850 mg) mixed with 1 mL resuspended sample. The mixture underwent 10 min ultrasonic treatment (Ultrasons, J.P. Selecta S.A., Spain) and 5 min vertexing (V05 Vortex, Labbox Labware SI, Spain), repeated twice for optimal disruption. Lysates were filtered through a Millex™ hydrophilic PTFE 0.20 m syringe filter (MilliporeSigma, Darmstadt, Germany) and diluted for analysis: 1:1000 (control), 1:2000 (12.5 mM), and 1:5000 (125 mM) for sp-ICP-MS, and 1:2 for HPLC-ICP-MS. This protocol was used as the standard sample preparation for all nanoparticle analyses. All treatments were analyzed in biological triplicates.

In preparation for the single particle inductively coupled plasma mass spectrometry (sp-ICP-MS), all solutions and suspensions were prepared in water (18.2 MΩ cm) purified in a PURELAB flex 3 system (ELGA VEOLIA, Lone End, United Kingdom). The ICP-MS instrument was operated with 99.999% Alphagaz Argon (Air Liquide, Valladolid, Spain) and hydrogen (from Air Liquide) was used in the reaction cell of the instrument. The elemental iron standard solution (1000 mg L–1) was from Merck (Darmstadt, Germany), ammonium acetate (≥97%) was purchased from Fisher Scientific (Madrid, Spain). Glass beads of 500 µm diameter (BioSpec Products, Bartlesville, OK, USA) were obtained from Sigma Aldrich (St Louis, MO, USA).

All measurements were performed on the iCAP MTX ICP-MS (Thermo Fisher Scientific, USA, Bremen, Germany) selecting the 57Fe isotope in the single quadrupole mode using hydrogen as collision gas. Specific operating conditions of different measurement modes can be found in Table S3. For single particle experiments, the instrument was fitted with a High Efficiency Sample Introduction System (Glass Expansion, Weilburg, Germany) that consists of a High Efficiency MicroMist™ Nebulizer with an inner capillary tube of 110 m and a high efficiency spray chamber with a microjet gas adapter

that was designed to improve transport efficiency of nanoparticles using a sheath gas flow. Solutions and sample suspensions were pumped to the ICP-MS at a flow rate of 10 L min–1 using the syringe pump Fusion 100X (Chemix Inc., Stafford, Texas, EE. UU.) fitted with a 1 mL Hamilton syringe (Hamilton, Reno, NV, USA). To convert the counts of 57Fe for each event to mass of Fe (mdt), the intensity is related to the signal given by a calibration curve constructed using ionic iron standard solutions measuring 57Fe as well. This conversion includes the transport efficiency of the sample introduction system (Equation 2) that was determined using a gold nanoparticle standard suspension (LGCQC5050, LGC Standards, Middlesex, UK) of certified particle number concentration (Pace *et al.*, 2011).

$$m_{dt} = n \times c \times dt \times f \qquad (2)$$

Equation 5.2. Calculated mass of the element (Fe) on each particle (mdt) as a function of the transport efficiency (TE), the intensity of the particle event (I), the dwell time (dt), the sample flow (F) and the slope of the calibration curve with ionic standards.

The NP sizes (assuming spherical shapes) were obtained using the mass of iron obtained from the calibration curve, the atomic mass of iron, and the density and molecular mass of the iron containing species that forms the NP (Equation 3). Iron NPs are assumed to be present as ferrihydrite (5Fe2O3·9H2O), the most common Entoferritin iron mineral form (Pham & Winzerling, 2010).

$$V_{NP} = \frac{m_{Fe} \, x \, M_{Ferrihydrite}}{M_{Fe} \, x \, \rho_{Ferrihydrite}} \qquad (3)$$

Equation 5.3. Calculation of the volume of a NP, where m_{Fe} is the mass of iron present in each NP, $M_{Ferrihydrite}$ the molecular mass of the ferrihydrite, MFe the atomic mass of iron and $\rho_{Ferrihydrite}$ the density of the ferrihydrite.

Assuming that the NPs are spherical, with the equation that describes the volume of a sphere we can obtain the diameter of each nanoparticle (Equation 4), and that is the value given in the results.

$$d = 2x \sqrt[3]{\frac{3x\,V_{NP}}{4\,\pi}} \quad (4)$$

Equation 5.4. Calculation of the diameter of a NP assuming that it is spherical.

The data was acquired using time-resolved analysis mode at a dwell time of 100 s. The data was further processed by the SPCal software v1.4.5 and OriginPro 8 (Northampton, MA, USA).

High-Performance Liquid Chromatography coupled with Inductively Coupled Plasma Mass Spectrometry (HPLC-ICP-MS) was performed for chromatographic separations using a size exclusion column (SuperdexTM 200 Increase 10/300 GL, GE Healthcare, Uppsala, Sweden). This type of column proved to be versatile for the separation of differently sized proteins and in some cases, of small nanoparticles (Separation range between 10 kDa and 600 kDa). The chromatographic system 1260 Series (Agilent Technologies, Tokyo, Japan) was used at a flow rate of 0.7 mL min–1 with a mobile phase containing a 50 mM ammonium acetate (>98%, Sigma Aldrich, Darmstadt, Germany) buffer (pH 7.0). A sample volume of 50 L was used in each analysis. The exit of the column was connected in series to a UV-Vis detector that measured the absorption at 280 and 380 nm and then to the ICP-MS equipped with a Savillex C-Flow PFA nebulizer and a cyclonic quartz spray chamber (provided by Thermo Fisher Scientific, USA, Bremen, Germany).

For further characterization of the biogenic iron containing NPs, images were taken in high resolution transmission electron microscope (HR-TEM) MET JEOL JEM-2100F (Tokyo, Japan) at 200 kV. A small volume (150 L) of the lysed and filtrated sample suspensions were deposited on the Cu grids and introduced into the instruments after evaporation of the solvent. Following the TEM picture (Fig S1), Energy Dispersive X-ray Spectroscopy (EDX) was applied on the unidentified particles to provide relative quantification of their given minerals.

2.5 Statistical analysis

Statistical analyses were conducted using RStudio (version 1.3.1073). One-way ANOVA was performed to assess bioaccessibility differences among treatments for both iron fortification levels and blanching conditions and iron NPs content and sizes. Tukey's Honestly Significant Difference (HSD) post-hoc test was applied only to iron fortification groups to determine pairwise differences, with a significance threshold of

= 0.05. For blanching effects on solubility and bioaccessibility, statistical significance between blanched and non-blanched samples was indicated using asterisk notation: $P < 0.05$ = *, $P < 0.005$ = **, $P < 0.0005$ = ***; the absence of asterisks denotes no significant difference ($P > 0.05$).

3. Results and discussion

3.1 Iron fortification

Increasing the dietary iron content did not affect larval weight or survival in BSF larvae reared on iron-fortified substrates (Table 5.1), consistent with previous findings (First *et al.*, 2024). Larval iron content increased in a dose-dependent manner, ranging from 183 mg/kg DM to 832 mg/kg DM in response to elevated dietary iron levels (Table 5.2), which align with the previously reported iron increase from 362 mg/kg DM to 999 mg/kg DM through substrate fortification (First *et al.*, 2024). Calcium levels mean were mildly increased with iron supplementation (From 20.5 to 21.6 g/kg DM, Table 5.2), albeit to a lesser extent than previously reported (First *et al.*, 2024). No negative trend was observed in larval zinc content (84 mg/kg in the control DM to 91 mg/kg DM in the 125mM larvae, Table 5.2), despite prior evidence that iron inhibits zinc absorption in BSF larvae (First *et al.*, 2024). Notably, larval copper levels significantly increased when larvae were exposed to 12.5 mM and 125 mM treatment comparing to control (17 to 20 mg/kg DM). This increase aligns with the established role of copper as an essential cofactor in ferroxidase enzymes, which catalyze the oxidation of Fe^{2+} to Fe^{3+} during iron absorption in insects (Mandilaras *et al.*, 2013).

Blanching did not affect the content of all tested mineral of the larvae across treatments. This was likely due to the vacuum blanching method used in this study, which minimized contact with water and thus limited the leaching of trace minerals, as shown in similar food preparation methods (Rondanelli *et al.*, 2017).

Table 5.1. Survival rate and average weight of black soldier fly (BSF) larvae reared on diets with varying iron content with standard deviation per treatment. No statistically significant differences were observed between treatments ($P > 0.05$).

Treatment	Larval weight (mg)	Survival rate (%)
Control (269 Fe mg/kg DM)	240 ± 9.3	83 ± 0.05
12.5 mM (1151 Fe mg/kg DM)	231 ± 7.2	84 ± 0.01
125 mM (7803 Fe mg/kg DM)	226 ± 19.3	87 ± 0.05

Table 5.2. Mineral composition of larvae reared on diets with increasing levels of iron from ferric ammonium citrate with standard deviation per treatment. Different letters indicate significant differences ($P < 0.05$); mean groups without letters are not significantly different ($P > 0.05$). Mean groups lacking letters are not significantly different.

Treatment	Blanching	Fe (mg/kg)	Ca (g/kg)	Zn (mg/kg)	Mg (g/kg)	Cu (mg/kg)	K (g/kg)	P (g/kg)
Control (269 Fe mg/kg DM)	Non blanched	183 ± 11 a	20.6 ± 1.6	86 ± 2.0	2.7± 0.06	17 ± 0.4 a	10.7 ± 0.2	7.6 ± 0.5
	Blanched	188 ± 10 a	20.5 ± 6.6	84 ± 2.0	2.6 ± 0.03	17 ± 0.4 a	10.5 ± 0.1	7.3 ± 0.3
12.5 mM (1151 Fe mg/kg DM)	Non blanched	372 ± 39 b	21.3 ± 4.7	82 ± 0.5	2.8 ± 0.05	20 ± 0.6 b	11 ± 0.2	7.9 ± 0.2
	Blanched	372 ± 39 b	21.5 ±1.7	81 ± 3.0	2.7 ± 0.1	20 ± 0.8 b	11 ± 0.3	7.8 ± 0.4
125 mM (7803 Fe mg/kg DM)	Non blanched	771 ± 51 c	21.6 ± 1.6	89 ± 8.0	2.7 ± 0.2	20 ± 0.9 b	11.1 ± 0.8	8.1± 0.9
	Blanched	832 ± 40 c	22.5 ± 1.0	91 ± 4.0	2.7 ± 0.1	20 ± 0.1 b	11.1 ± 0.4	8.1± 0.5

3.2. Mineral Bioaccessibility

3.2.1. Iron

Unlike mammalian ferritins, entoferritin functions as the predominant soluble iron transporter in insects. At the same time, it also serves as the primary iron storage compartment within the insect body (Pham & Winzerling, 2010). In response to elevated iron levels, gut cells can increase ferritin accumulation in the Golgi apparatus and other vesicular structures. This phenomenon typically occurs in a region of the anterior midgut referred to as the "iron region", which had also been identified as the primary iron storage region in BSF larvae (Bonelli *et al.*, 2020; Pham & Winzerling, 2010).

ICP-MS data corresponding the measurements by single particle ICP-MS showed in Figure 1 (A-B) indicated that the number of detected Fe nanoparticles increased in a dose dependent manner, while iron ferrihydrite NPs diameter remained consistent at ~45 nm across treatments. These sizes substantially exceed the ~7 nm mineral core of entoferritin (Kim *et al.*, 2001), which could be ascribed to aggregates obtained during sample preparation. Given that iron bioaccessibility differed significantly among fortification levels, suggesting minimal changes in native entoferritin structure, the comparable iron NP aggregates are likely affected by the mechanical lysis and filtration steps of the nanoparticle preparation. However, further research should extract and evaluate these aggregates to confirm entoferritin based clusters. Size exclusion chromatography (SEC) further supported this interpretation, as the earliest eluting peak above 600 kDa contained detectable iron and matched the expected size range of large iron-accumulating proteins such as entoferritin (Figure 2). Energy-dispersive X-ray spectroscopy (EDX) confirmed strong signals for iron, which were significantly higher in the particles found in the larvae with 125mM compared to the two other dietary treatments (Figure 3), reinforcing the identification of iron NPs. The consistent size of iron NPs with a NPs increased content, combined with the SEC and EDX results, indicate that entoferritin-mediated storage remained the dominant mechanism of iron sequestration in BSF larvae, irrespective of iron fortification.

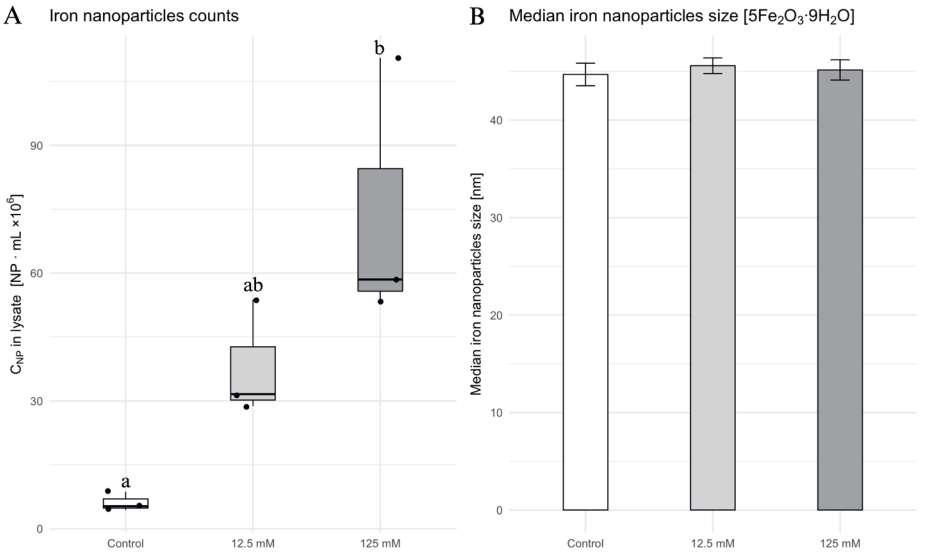


Figure 5.1. Iron nanoparticle concentration of iron fortified BSF larvae (A) and the iron nanoparticles median size of iron fortified BSF larvae, assuming that the NPs are ferrihydrites (5Fe2O3·9H2O). Iron nanoparticle concentrations are extrapolated from the events detected in the ICP-MS measurements (Figure S2-S4). Different letters indicate significant differences ($P < 0.05$).

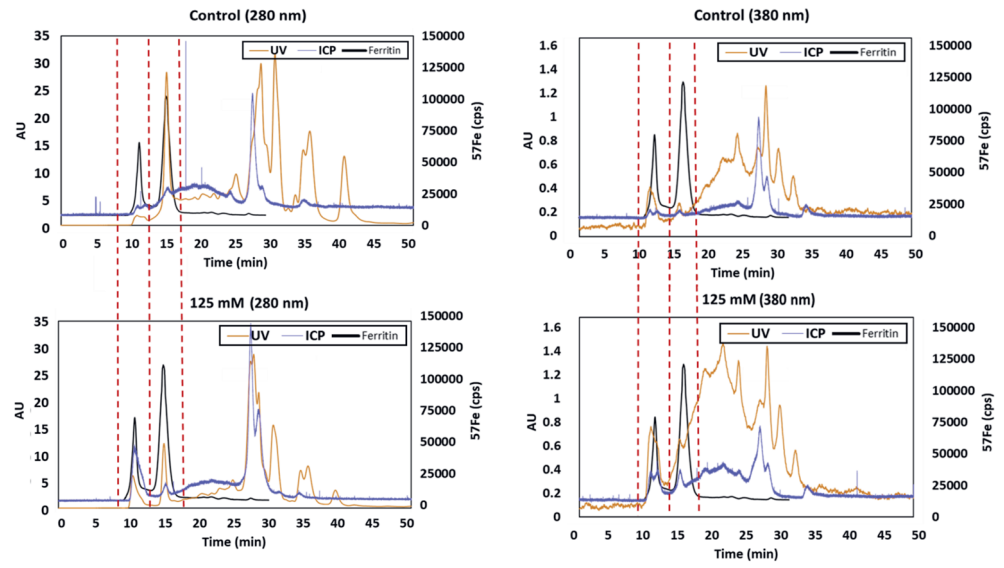


Figure 5.2. Chromatograms comparing retention times of horse spleen ferritin (Detection of 57Fe by ICP-MS) with control and 125 mM supplemented larvae (Detection of 57Fe by ICP-MS and absorbance at 280 nm and 380 nm), showing the coelution of characteristic peaks of ferritin with peaks of the samples.

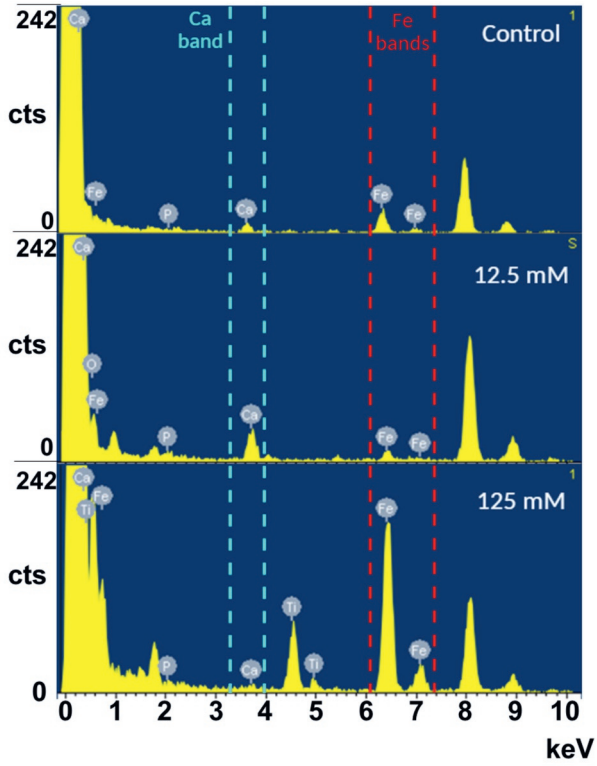


Figure 5.3. EDX spectra of the control, 12.5 mM and 125 mM treated larvae. The red boundaries represent the expected areas of which iron picks should be detectable, while the blue boundaries represent the area in which calcium is detectable.

Data on iron bioaccessibility for the differently fortified BSF larvae are shown in Figure 4A. The iron storage mechanism is similar across all fortification treatments, however, bioaccessibility percentage data show a significant, dose-dependent decrease with increasing fortification. Mammalian ferritin has an iron storage capacity of approximately 4,500 iron atoms per complex, although under physiological conditions it typically stores around 1,000 to 1,500 atoms (Kell & Pretorius, 2014; Macara *et al.*, 1972). The iron-holding capacity of entoferritin is not yet known. However, its substantially higher molecular weight compared to mammalian ferritin (~670 and ~440 KDa, respectively) suggests that it may be capable of storing a larger amount of iron. Given that both ferritins mineralize iron in a similar manner, it can be assumed that entoferritin, like its mammalian counterpart, generally operates below its maximum capacity, storing only a fraction of its potential load (First *et al.*, 2023). In mammals, iron overload can result in overloading ferritin with iron that has been shown to impair its

structural and thermal stability and solubility, which may negatively affect digestibility (Irimia-Dominguez *et al.*, 2020; Ruiyang Ji Mingyang Sun, 2023; Srivastava *et al.*, 2023). First *et al.* (2024) reported a threefold increase in iron content in fortified larvae. In the current study, a 400% increase in iron content was observed in the fortified BSF larvae. It can be hypothesized that this iron increase may not be fully matched by a proportional rise in entoferritin content, due to regulatory limits on its expression or synthesis. Further investigation is needed to confirm the iron to entoferritin ratio shifts under iron fortification. The observed decrease in iron bioaccessibility in fortified larvae may be explained by an increased iron to entoferritin ratio, potentially reducing entoferritin digestibility and iron in the bioaccessible supernatant fraction. Although iron bioaccessibility was lower with increasing iron supplementation, the iron concentration in the digesta significantly increases in a dose-depended manner, and more than doubled under the 125 mM treatment, from 0.08 mg/ml to 0.2 mg/ml of iron (Figure 4B). This was primarily due to the high initial iron content in the fortified larvae, which compensated the reduced bioaccessibility, suggesting that iron fortification in BSF larvae can improve the insect as an iron source. However, the implications of increased luminal iron on gut microbiota warrant evaluation, as unabsorbed soluble iron can promote pathogenic overgrowth. Yet, assuming most iron in BSF larvae is entoferritin-bound, it may behave similarly to ferritin-based iron supplements, which have been shown to maintain intestinal integrity and avoid dysbiosis compared with soluble iron salts (Yang *et al.*, 2025).

The blanching of the larvae significantly lowered both total digested iron and iron bioaccessibility across all treatments. Although the physiochemical behavior of entoferritin under heat pressure is not well studied, these results were expected. Under blanched conditions, proteins, including entoferritin can degrade, lose function, aggregate and precipitate (Ruiyang Ji Mingyang Sun, 2023). This hypothesis aligns with the visible decrease of over 40% of protein solubility after blanching across all fortification levels (Table S4). Heat stress degradation and precipitation of entoferritin following blanching are likely key factors contributing to the observed decrease in iron bioaccessibility, regardless of the level of iron fortification. Nevertheless, further spatial localization, and entoferritin relative quantification under heat treatments are required to confirm whether iron bioavailability in BSF larvae is predominantly governed by entoferritin-bound iron.

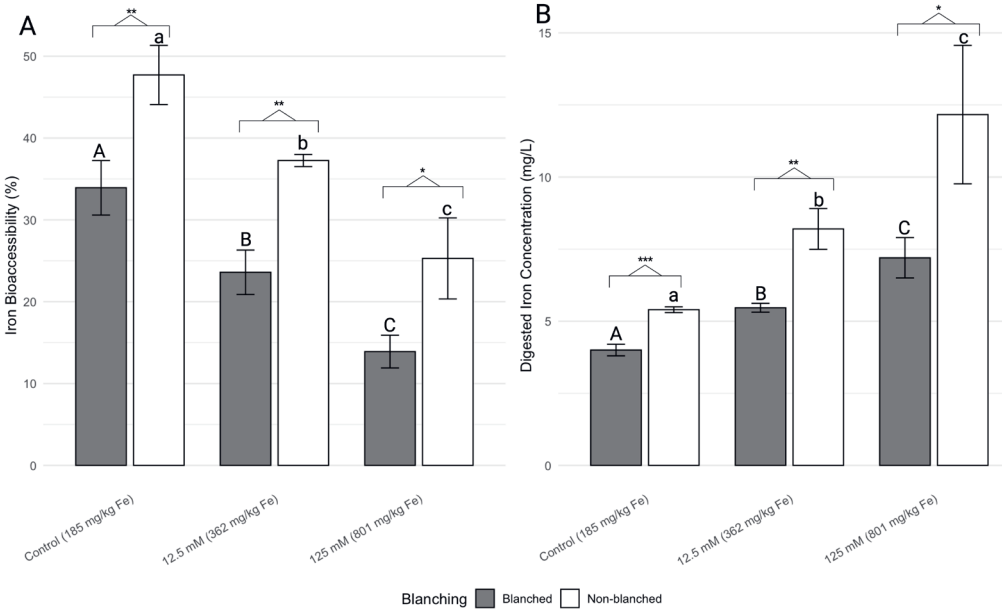


Figure 5.4. Iron bioaccessibility, expressed as percentages (%) (A) and digested iron concentration expressed in mg/L (B) of iron-fortified black soldier fly larvae. The iron concentrations listed in the treatment column correspond to the measured iron content of the differently treated larvae. Different letters indicate statistically significant differences among treatments ($P < 0.05$), with lowercase letters refer to non-blanched larvae, while uppercase letters refer to blanched larvae. Asterisks denote statistically significant differences between blanched and non-blanched samples ($P < 0.05$ = *, $P < 0.005$ = **, $P < 0.0005$ = ***); the absence of asterisks indicates no significant difference ($P > 0.05$).

3.2.2. Calcium

No differences in calcium bioaccessibility were observed among the non-blanched, iron-fortified larvae. The 12.5 mM group had the lowest bioaccessibility, while the 125 mM group had the highest (27.2%). A significant, yet small, decrease in calcium bioaccessibility was seen in the blanched samples, from 58.3% to 54% (Table 2). Despite this small reduction, the total amount of calcium digested remained similar, as the iron-fortified larvae contained more calcium prior to digestion. In BSF larvae, most calcium is found in a calcium carbonate granule which is stored in two specialized Malpighian tubules known as lime glands. These glands provide a physiological environment that facilitates the precipitation and accumulation of amorphous calcium carbonate during the feeding stages. As larvae develop, the stored calcium is mobilized and used primarily for cuticle hardening during molting and pupation. In the exoskeleton, calcium within

the exoskeleton exists in a more dispersed, organically bound state, integrated into the epicuticle and exocuticle layers through biomineralization (Rebora *et al.*, 2023). In the scope of iron fortification, it was shown that with an increased dietary iron in the BSF larvae diet, there is a significant increase in the calcium bioaccumulation. It has also been reported, that BSF exposed to excess dietary iron might exhibit dark lesions on the exoskeleton. This led to the hypothesis that the increased calcium content of the iron fortified larvae is accumulated in order to maintain exoskeletal structure and function under the high iron environment (First *et al.*, 2024). The given lack of changes in calcium accessibility regardless of iron fortification level, suggests that although calcium is accumulated to address exoskeletal development challenges under high iron conditions, the substantial calcium reserves in the lime glands may overshadow the contribution of the exoskeleton to overall bioaccessibility.

Interestingly, blanched larvae exhibited significantly higher calcium bioaccessibility compared to non-blanched larvae, with the 12.5 mM group increasing from 10.3% to 53.7% upon blanching (Table 2). A previous study investigating mineral digestibility in BSF larvae fed to mountain frogs reported a twofold increase in calcium digestibility when the larvae were crushed. It was hypothesized that this physical disruption of the exoskeleton led to the release of calcium from both storage and the chitin mineral protein matrix (Dierenfeld & King, 2008). In the current study, all samples were homogenized prior to digestion, providing a consistent baseline of mechanical disruption. The blanching process likely introduced further structural breakdown, especially of the lime glands residues, as indicated by the marked increase in calcium bioaccessibility. While direct physical confirmation is still needed, these findings imply that ground, thermally treated BSF larvae are preferable over live larvae when the goal is to enhance calcium absorption. These insights underscore the nutritional relevance of BSF larvae as a calcium source, and highlight the importance of processing in optimizing their use in feed formulation and food applications.

3.2.3. Zinc

Similar to calcium, blanching of the unfortified larvae and those reared on the 12.5 mM diet resulted in a significant increase in zinc bioaccessibility, from 22.5% to 50.1% and from 26.3% to 40.1%, respectively (Table 2). In insects, zinc is stored in specialized organelles known as zinc storage granules, which are localized specifically within the principal epithelial cells of the Malpighian tubules. In comparison to calcium, which is stored in larger granules (0.4 to over 10 µm) distributed across both principal and secondary cells, zinc granules are typically smaller (approximately 1 µm) and more spatially restricted (Rebora *et al.*, 2023; Tejeda-Guzmán *et al.*, 2018). Based on these

differences, it can be assumed that the increase in zinc bioaccessibility following blanching is related to structural disruption of zinc storage granules, similar to the mechanism proposed for calcium. However, this effect was not observed in larvae reared on the high iron diet. In this group, zinc bioaccessibility significantly decreased upon blanching, from 38.6% to 28.9%. Zinc absorption is known to be inhibited by iron due to competition at shared transport mechanisms (First *et al.*, 2024; Pérès *et al.*, 2001). It is therefore hypothesized that zinc homeostasis was disrupted in larvae reared on the high iron diet due to competitive interactions, leading to reduced accumulation or destabilization of zinc granules in the Malpighian tubules. Consequently, blanching may have a limited effect on zinc bioaccessibility in this group, as fewer zinc-containing granules were present to be disrupted.

These trends contrast with previous findings on boiling effects in *Eulepida mashona* and *Henicus whellani*, where zinc bioaccessibility increased. This discrepancy may be explained by the lower zinc content in those species (43 and 50 mg/kg DM, respectively), suggesting that zinc storage systems may be present to a lesser extent and thus less affected by thermal disruption (Manditsera *et al.*, 2019). This contradiction highlights species-specific differences in zinc storage and mobilization and reinforces the need for physicochemical confirmation of zinc granule localization, composition and structural behavior under heat stress in black soldier fly larvae.

With respect to the effect of iron fortification on zinc bioaccessibility, larvae reared on 125 mM diet exhibited significantly higher zinc bioaccessibility under non-blanched conditions compared to those reared on the control and 12.5 mM diets. In contrast, under blanched conditions, iron fortification resulted in a dose-dependent decrease in zinc bioaccessibility. Based on the hypothesis that high dietary iron interferes with the proper formation of zinc granules, it is likely that in non-blanched larvae reared on the 125mM diet, zinc was more diffusely distributed outside of the storage system within the Malpighian tubules, and therefore more bioaccessible.

3.2.4. Magnesium

Iron fortification of the larvae had no significant effect on magnesium bioaccessibility in either blanched or non-blanched treatments. In previous studies on meat, sous-vide cooking, comparable to the vacuum blanching approach applied in this study, was shown to enhance magnesium bioaccessibility (da Silva *et al.*, 2017). However, this effect was not observed in the BSF larvae, likely due to the already high magnesium bioaccessibility (>95%) across all treatments, leaving limited potential for further improvement.

Table 5.2. Mineral bioaccessibility (%) of iron-fortified black soldier fly larvae with standard deviation per treatment. Different letters indicate statistically significant differences among treatments ($P < 0.05$), with lowercase letters refer to non-blanched larvae, while uppercase letters refer to blanched larvae; mean groups sharing the same letter are not significantly different ($P > 0.05$). Asterisks denote statistically significant differences between blanched and non-blanched samples ($P < 0.05$ = *, $P < 0.005$ = **, $P < 0.0005$ = ***); the absence of asterisks indicates no significant difference ($P > 0.05$). Mean groups lacking letters or asterisks are not significantly different.

Treatment	Blanching	Fe (%)	Ca (%)	Zn (%)	Mg (%)
Control (269 Fe mg/ kg DM)	Non blanched	47.7 ± 3.6 a**	21.3 ± 5.4***	22.49 ± 4.4 a**	95.8 ± 3.5
	Blanched	33.9 ± 10.0 A	58.3 ± 0.8 A	50.1 ± 4.6 C	95 ± 0.7
12.5 mM (1151 Fe mg/ kg DM)	Non blanched	37.2 ± 0.7 a**	10.3 ± 0.5***	26.3 ± 0.2 a**	97.7 ± 1.6
	Blanched	23.6 ± 2.7 B	53.7 ± 2.0 B	40.1 ± 5.2 B	96.6 ± 1.7
125 mM (7803Fe mg/ kg DM)	Non blanched	25.3 ± 4.9 c*	27.2 ± 15.0*	38.6 ± 3.2 b**	95.4 ± 6.0
	Blanched	13.9 ± 2.0 C	54.0 ± 0.6 B	28.9 ± 1.4 A	96.6 ± 2.7

4. Conclusion

This study provides an integrated assessment of trace mineral bioaccessibility and iron nanoparticle formation in iron-fortified black soldier fly larvae. It also evaluates the effects of thermal processing on mineral bioaccessibility. Iron fortification led to a dose dependent increase in larval iron content and iron nanoparticle events, while nanoparticle diameter remained consistent (~45 nm), and chromatographic profiles confirmed the presence of high molecular weight (>600 KDa) iron protein complexes. Together, these findings indicate that entoferritin based iron sequestration persists as the primary storage mechanism even under high iron fortification. Despite the percentage of bioaccessible iron decrease with fortification, the total digestible iron increased, supporting the nutritional efficacy of fortification strategy. Blanching

significantly impaired iron bioaccessibility, likely due to heat-induced denaturation of Entoferritin. However, the effects of increased luminal iron on intestinal microbiota and related inflammatory or oxidative processes should be examined, noting that BSF iron is assumed to be largely entoferritin-bound. Live BSF larvae may be legally used as feed for all livestock species in the EU, excluding ruminants, following the 2024 clarification by the European Commission's PAFF Committee, under Regulation (EC) 767/2009 (EU, 2024; EU, 2009). Within this regulatory framework and the findings provided in this study, live, non-blanched iron-fortified BSF larvae could serve as a novel and enhanced source of iron for livestock nutrition.

Oppositely, blanching enhanced calcium and zinc bioaccessibility, probably by disrupting mineral storage structures such as lime glands and zinc granules. Magnesium bioaccessibility remained unaffected and consistently high.

Overall, the results highlight how iron fortification and thermal processing differentially impact the nutritional profile of BSF larvae, and support the potential of live, iron-fortified larvae as a sustainable, mineral-rich ingredient for animal feed. Moreover, these findings showcase the potential of processed BSF larvae as a mineral-rich food ingredient, with enhanced calcium availability, for future food applications.

Acknowledgements

The authors thank Protix (Bergen op Zoom, the Netherlands) for providing the black soldier fly eggs. Thanks are also extended to Dr. Alaa Adawy from the Department of Physics and the Unit of Electron Microscopy and Nanotechnology (SCTs), University of Oviedo (Oviedo, Spain), for performing the HRTEM and EDX analyses. Appreciation is further extended to Ciske Slothouber, Yeongbin Kim, Rutger Brouwer, Yifan Zhang, and Lucas Bozzo for their assistance in counting larvae during the experimental setup. Finally, the authors thank MSc Marjanne Verhoeven for preparing the *in vitro* digestion solutions. We also acknowledge the financial support of this study by the Spanish MICINN (Spanish Ministry for Science and Innovation and Universities; Grant Numbers MCIU22-PID2021-123854OB-I00 and PID2022-137222OB-I00) and Principado de Asturias/Sekuens (Grant Number: IDE/2024/000742).

Funding sources

This work was supported by the Topsector Agri & Food (TKI, The Netherlands) Green sector prize [Prize number: LWV21293].

References

Ajomiwe, N., Boland, M., Phongthai, S., Bagiyal, M., Singh, J., & Kaur, L. (2024). Protein Nutrition: Understanding Structure, Digestibility, and Bioavailability for Optimal Health. Foods (Basel, Switzerland), 13(11). https://doi.org/10.3390/foods13111771

Álvarez-Fernández García, R., Corte-Rodríguez, M., Macke, M., LeBlanc, K. L., Mester, Z., Montes-Bayón, M., & Bettmer, J. (2020). Addressing the presence of biogenic selenium nanoparticles in yeast cells: analytical strategies based on ICP-TQ-MS. The Analyst, 145(4), 1457–1465. https://doi.org/10.1039/C9AN01565E

Bessa, L. W., Pieterse, E., Marais, J., Dhanani, K., & Hoffman, L. C. (2021). Food Safety of Consuming Black Soldier Fly (*Hermetia illucens*) Larvae: Microbial, Heavy Metal and Cross-Reactive Allergen Risks. Foods (Basel, Switzerland), 10(8). https://doi.org/10.3390/foods10081934

Bessa, L. W., Pieterse, E., Marais, J., & Hoffman, L. C. (2020). Why for feed and not for human consumption? The black soldier fly larvae. Comprehensive Reviews in Food Science and Food Safety, 19(5), 2747–2763. https://doi.org/https://doi.org/10.1111/1541-4337.12609

Bonelli, M., Bruno, D., Brilli, M., Gianfranceschi, N., Tian, L., Tettamanti, G., Caccia, S., & Casartelli, M. (2020). Black Soldier Fly Larvae Adapt to Different Food Substrates through Morphological and Functional Responses of the Midgut. International Journal of Molecular Sciences, 21(14). https://doi.org/10.3390/ijms21144955

Borremans, A., Bußler, S., Sagu, S. T., Rawel, H., Schlüter, O. K., & Leen, V. C. (2020). Effect of Blanching Plus Fermentation on Selected Functional Properties of Mealworm (*Tenebrio molitor*) Powders. Foods (Basel, Switzerland), 9(7). https://doi.org/10.3390/foods9070917

Brodkorb, A., Egger, L., Alminger, M., Alvito, P., Assunção, R., Ballance, S., Bohn, T., Bourlieu-Lacanal, C., Boutrou, R., Carrière, F., Clemente, A., Corredig, M., Dupont, D., Dufour, C., Edwards, C., Golding, M., Karakaya, S., Kirkhus, B., Le Feunteun, S., … Recio, I. (2019). INFOGEST static *in vitro* simulation of gastrointestinal food digestion. Nature Protocols, 14(4), 991–1014. https://doi.org/10.1038/s41596-018-0119-1

Carpenter, C. E., & Mahoney, A. W. (1992). Contributions of heme and nonheme iron to human nutrition. Critical Reviews in Food Science and Nutrition, 31(4), 333–367. https://doi.org/10.1080/10408399209527576

Cilla, A., Barberá, R., López-García, G., Blanco-Morales, V., Alegría, A., & Garcia-Llatas, G. (2019). 7 - Impact of processing on mineral bioaccessibility/bioavailability. In F. J. Barba, J. M. A. Saraiva, G. Cravotto, & J. M. Lorenzo (Eds.), Innovative Thermal and Non-Thermal Processing, Bioaccessibility and Bioavailability of Nutrients and Bioactive Compounds 209–239. Woodhead Publishing. https://doi.org/https://doi.org/10.1016/B978-0-12-814174-8.00007-X

da Silva, F. L. F., de Lima, J. P. S., Melo, L. S., da Silva, Y. S. M., Gouveia, S. T., Lopes, G. S., & Matos, W. O. (2017). Comparison between boiling and vacuum cooking (sous-vide) in the bioaccessibility of minerals in bovine liver samples. Food Research International, 100, 566–571. https://doi.org/https://doi.org/10.1016/j.foodres.2017.07.054

Dierenfeld, E. S., & King, J. (2008). Digestibility and Mineral Availability of Phoenix Worms, *Hermetia illucens*, Ingested by Mountain Chicken Frogs, Leptodactylus fallax. Journal of Herpetological Medicine and Surgery, 18(3), 100–105. https://doi.org/10.5818/1529-9651.18.3-4.100

EFSA. (2024). Live insects in animal feed: what European Regulation says (and what it does not).

European Union. (2009). Regulation (EC) No 767/2009 of the European Parliament and of the Council of 13 July 2009 on the placing on the market and use of feed, amending European Parliament and Council Regulation (EC) No 1831/2003 and repealing Council Directive 79/373/EEC, Commission Directive 80/511/EEC, Council Directives 82/471/EEC, 83/228/EEC, 93/74/EEC, 93/113/EC and 96/25/EC and Commission Decision 2004/217/EC (Text with EEA relevance).

First, T., Fogliano, V., & Mishyna, M. (2023). Entoferritin: An innovative iron source for human consumption. Journal of Functional Foods, 108, 105711. https://doi.org/https://doi.org/10.1016/j.jff.2023.105711

First, T., Van Haeften, A. J., Oonincx, D. G. A. B., Van Loon, J. J. A., Fogliano, V., & Mishyna, M. (2024). Strike while the iron is hot: unravelling the impact of dietary iron on two edible insects. Journal of Insects as Food and Feed, 11(7), 1187–1200. https://doi.org/https://doi.org/10.1163/23524588-00001422

Friendship, R., Seip, V., & Amezcua, R. (2021). A comparison of 4 iron supplementation protocols to protect suckling piglets from anemia. The Canadian Veterinary Journal = La Revue Veterinaire Canadienne, 62(1), 55–58. https://www.ncbi.nlm.nih.gov/pubmed/33390600

Gardner, W. M., Razo, C., McHugh, T. A., Hagins, H., Vilchis-Tella, V. M., Hennessy, C., Taylor, H. J., Perumal, N., Fuller, K., Cercy, K. M., Zoeckler, L. Z., Chen, C. S., Lim, S. S., Aali, A., Abate, K. H., Abd-Elsalam, S., Abdurehman, A. M., Abebe, G., Abidi, H., ... Kassebaum, N. J. (2023). Prevalence, years lived with disability, and trends in anaemia burden by severity and cause, 1990-2021: findings from the Global Burden of Disease Study 2021. The Lancet Haematology, 10(9), e713–e734. https://doi.org/10.1016/S2352-3026(23)00160-6

Guéguen, L., & Pointillart, A. (2000). The Bioavailability of Dietary Calcium. Journal of the American College of Nutrition, 19(sup2), 119S-136S. https://doi.org/10.1080/07315724.2000.10718083

Irimia-Dominguez, J., Sun, C., Li, K., Muhoberac, B. B., Hallinan, G. I., Garringer, H. J., Ghetti, B., Jiang, W., & Vidal, R. (2020). Cryo-EM structures and functional characterization of homo- and heteropolymers of human ferritin variants. Scientific Reports, 10(1), 20666. https://doi.org/10.1038/s41598-020-77717-4

Karthikeyan, G., Andal, N. M., & Anbalagan, K. (2005). Adsorption studies of iron(III) on chitin. Journal of Chemical Sciences, 117(6), 663–672. https://doi.org/10.1007/BF02708296

Kell, D. B., & Pretorius, E. (2014). Serum ferritin is an important inflammatory disease marker, as it is mainly a leakage product from damaged cells. Metallomics, 6(4), 748–773. https://doi.org/10.1039/c3mt00347g

Kim, B. S., Lee, C. S., Yun, C. Y., Yeo, S. M., Park, W. M., & Kim, H. R. (2001). Characterization and immunological analysis of ferritin from the hemolymph of Galleria mellonella. Comparative Biochemistry and Physiology Part A: Molecular & Integrative Physiology, 129(2), 501–509. https://doi.org/https://doi.org/10.1016/S1095-6433(01)00287-2

Kumari, A., & Chauhan, A. K. (2021). Iron nanoparticles as a promising compound for food fortification in iron deficiency anemia: a review. Journal of Food Science and Technology, 59(9), 3319–3335. https://doi.org/10.1007/s13197-021-05184-4

Macara, I. G., Hoy, T. G., & Harrison, P. M. (1972). The formation of ferritin from apoferritin. Kinetics and mechanism of iron uptake. The Biochemical Journal, 126(1), 151–162. https://doi.org/10.1042/bj1260151

Machado, I., Priede, A. S., Rodríguez, M. C., Heath, D., Heath, E., Kouřimská, L., Kulma,

M., Bettmer, J., & Montes-Bayón, M. (2024). Bioaccessibility of trace elements and Fe and Al endogenic nanoparticles in farmed insects: Pursuing quality sustainable food. Food Chemistry, 458, 140229. https://doi.org/https://doi.org/10.1016/j.foodchem.2024.140229

Mandilaras, K., Pathmanathan, T., & Missirlis, F. (2013). Iron Absorption in *Drosophila melanogaster*. Nutrients, 5(5), 1622–1647. https://doi.org/10.3390/nu5051622

Manditsera, F. A., Luning, P. A., Fogliano, V., & Lakemond, C. M. M. (2019). Effect of domestic cooking methods on protein digestibility and mineral bioaccessibility of wild harvested adult edible insects. Food Research International, 121, 404–411. https://doi.org/https://doi.org/10.1016/j.foodres.2019.03.052

Manzoor, M. F., Ali, A., Ain, H. B. U., Kausar, S., Khalil, A. A., Aadil, R. M., & Zeng, X.-A. (2024). Bioaccessibility mechanisms, fortification strategies, processing impact on bioavailability, and therapeutic potentials of minerals in cereals. Future Foods, 10, 100425. https://doi.org/https://doi.org/10.1016/j.fufo.2024.100425

Pace, H. E., Rogers, N. J., Jarolimek, C., Coleman, V. A., Higgins, C. P., & Ranville, J. F. (2011). Determining Transport Efficiency for the Purpose of Counting and Sizing Nanoparticles via Single Particle Inductively Coupled Plasma Mass Spectrometry. Analytical Chemistry, 83(24), 9361–9369. https://doi.org/10.1021/ac201952t

Parlasca, M. C., & Qaim, M. (2022). Meat consumption and sustainability. Annual Review of Resource Economics, 14, 17–41. https://doi.org/10.1146/annurev-resource-111820-032340

Pérès, J.-M., Bureau, F., Neuville, D., Arhan, P., & Bouglé, D. (2001). Inhibition of zinc absorption by iron depends on their ratio. Journal of Trace Elements in Medicine and Biology, 15(4), 237–241. https://doi.org/https://doi.org/10.1016/S0946-672X(01)80039-0

Pham, D. Q. D., & Winzerling, J. J. (2010). Insect ferritins: Typical or atypical? Biochimica et Biophysica Acta - General Subjects, 1800(8), 824–833. https://doi.org/10.1016/j.bbagen.2010.03.004

Rebora, M., Salerno, G., Piersanti, S., Saitta, V., Morelli Venturi, D., Li, C., & Gorb, S. (2023). The armoured cuticle of the black soldier fly *Hermetia illucens*. Scientific Reports, 13(1), 22101. https://doi.org/10.1038/s41598-023-49549-5

Rondanelli, M., Daglia, M., Meneghini, S., Di Lorenzo, A., Peroni, G., Faliva, M. A., & Perna,

S. (2017). Nutritional advantages of sous-vide cooking compared to boiling on cereals and legumes: Determination of ashes and metals content in ready-to-eat products. Food Science & Nutrition, 5(3), 827–833. https://doi.org/10.1002/fsn3.469

Ruiyang Ji Mingyang Sun, J. Z. C. L. G. Z. (2023). Effects of heat treatment on the structure, digestive property, and absorptivity of holoferritin. In Food Innovation and Advances, 2(0005), 28. https://doi.org/10.48130/FIA-2023-0005

Shlisky, J., Mandlik, R., Askari, S., Abrams, S., Belizan, J. M., Bourassa, M. W., Cormick, G., Driller-Colangelo, A., Gomes, F., Khadilkar, A., Owino, V., Pettifor, J. M., Rana, Z. H., Roth, D. E., & Weaver, C. (2022). Calcium deficiency worldwide: prevalence of inadequate intakes and associated health outcomes. Annals of the New York Academy of Sciences, 1512(1), 10–28. https://doi.org/https://doi.org/10.1111/nyas.14758

Siva Raman, S., Stringer, L. C., Bruce, N. C., & Chong, C. S. (2022). Opportunities, challenges and solutions for black soldier fly larvae-based animal feed production. Journal of Cleaner Production, 373, 133802. https://doi.org/https://doi.org/10.1016/j.jclepro.2022.133802

Son, J., Park, S. H., Jung, H. J., You, S. J., & Kim, B. G. (2023). Effects of Drying Methods and Blanching on Nutrient Utilization in Black Soldier Fly Larva Meals Based on *in vitro* Assays for Pigs. Animals : An Open Access Journal from MDPI, 13(5). https://doi.org/10.3390/ani13050858

Srivastava, A. K., Scalcione, L. J., Arosio, P., & Bou-Abdallah, F. (2023). Hyperthermostable recombinant human heteropolymer ferritin derived from a novel plasmid design. Protein Science, 32(1), e4543. https://doi.org/https://doi.org/10.1002/pro.4543

Tejeda-Guzmán, C., Rosas-Arellano, A., Kroll, T., Webb, S. M., Barajas-Aceves, M., Osorio, B., & Missirlis, F. (2018). Biogenesis of zinc storage granules in *Drosophila melanogaster*. Journal of Experimental Biology, 221(6), jeb168419. https://doi.org/10.1242/jeb.168419

van Huis, A., Rumpold, B. A., van der Fels-Klerx, H. J., & Tomberlin, J. K. (2021). Advancing edible insects as food and feed in a circular economy. Journal of Insects as Food and Feed, 7(5), 935–948. https://doi.org/10.3920/JIFF2021.x005

Zulkifli, N. F. N. M., Seok-Kian, A. Y., Seng, L. L., Mustafa, S., Kim, Y.-S., & Shapawi, R. (2022). Nutritional value of black soldier fly (*Hermetia illucens*) larvae processed by different methods. PLOS ONE, 17(2), e0263924-. https://doi.org/10.1371/journal.pone.0263924

Supplementary Information

Table S1. Mineral analysis lower detection limits. Data provided by the Soil Chemistry Laboratory of Wageningen University (CBLB, Wageningen University and Research, the Netherlands)

Mineral	Fe	Ca	Zn	Mg	Cu	K	P
Lower detection limit (mg/kg)	60	150	5	50	0.6	3	1

Table S2. Volumes of electrolyte stock solutions and final electrolyte concentrations of simulated digestion fluids (SSF, SGF, and SIF)

Salt solution added	Stock conc. (g/L)	Stock conc. (M)	SSF (pH 7) mL stock for 0.4 L	Final conc. in SSF (mM)	SGF (pH 3) mL stock for 0.4 L	Final conc. in SGF (mM)	SIF (pH 7) mL stock for 0.4 L	Final conc. in SIF (mM)
KCl	37.3	0.5	15.1	12.1	6.9	5.5	6.8	5.4
KH_2PO_4	68	0.5	3.7	3.0	0.9	0.72	0.8	0.64
$NaHCO_3$[a]	84	1	6.8	10.9	12.5	20.0	42.5	68.0
NaCl	117	2	-	-	11.8	37.8	9.6	30.7
$MgCl_2(H_2O)_6$	30.5	0.15	0.5	0.12	0.4	0.096	1.1	0.26
$(NH_4)CO_3$*	48	0.5	0.06	0.048	0.5	0.40	-	-
HCl	–	6	0.09	0.88	1.3	12.5	0.7	6.7
$CaCl_2(H_2O)_2$[b]	44.1	0.3	0.025	1.2	0.005	0.12	0.04	0.48

Table S3. Operating conditions of the iCAP MTX ICP-MS in different measurement modes.

Parameter	
RF Power [W]	1550
Coolant gas flow [L min^{-1}]	14.0
Auxiliary gas flow [L min^{-1}]	0.8
Carrier gas flow [L min^{-1}]	0.8
Sheath gas flow [L min^{-1}]	0.31
Cell gas flow [mL min^{-1}]	0.31
Q1 bias [V]	0
Qcell bias [V]	-5.94
Q3 bias [V]	-12.0
Q3 masses [u]	57 ($^{57}Fe^{+}$)
Single particle mode	
Dwell time [µs]	100
Sample flow rate [mL min^{-1}]	0.01
Analysis time [s]	60
HPLC-ICP-MS	
Dwell time [ms]	100
Sample flow rate [mL min-1]	0.7
Analysis time [min]	60

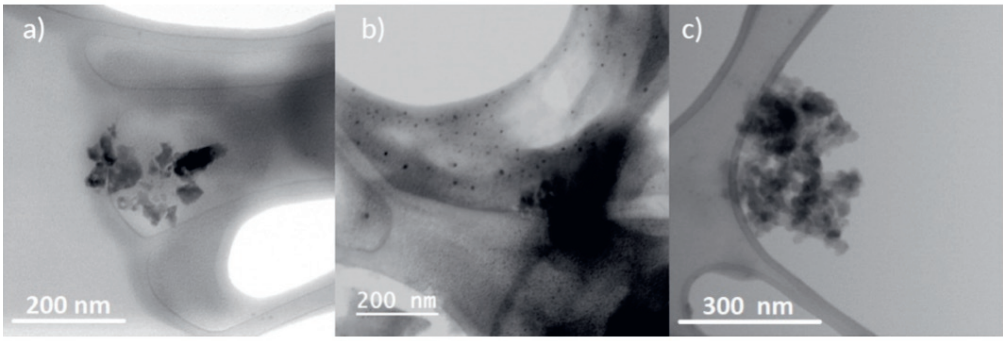


Figure S1. Images obtained from the HR-TEM analysis of the control (a), 12.5 mM (b) and 125 mM (c) sample.

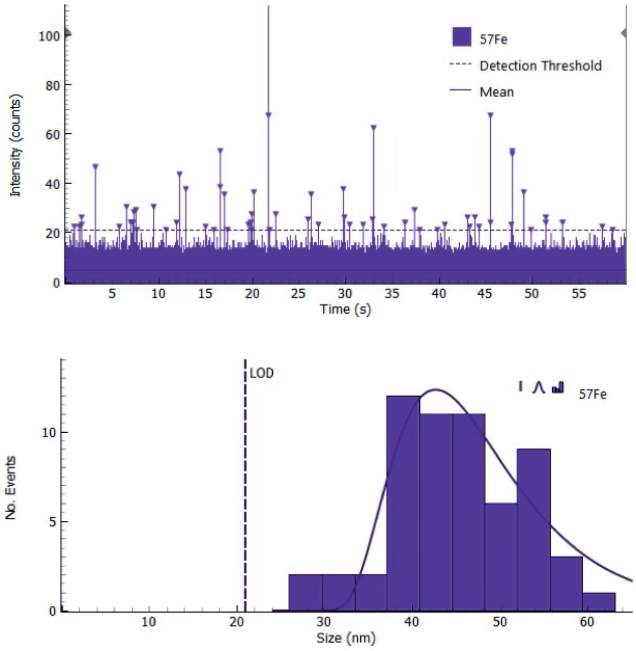


Figure S2. Single particle ICP-MS results from a control sample after 1:1000 dilution. A) Time-resolved analysis. B) Histogram of the resulting sizes (Bin size: 3 nm).

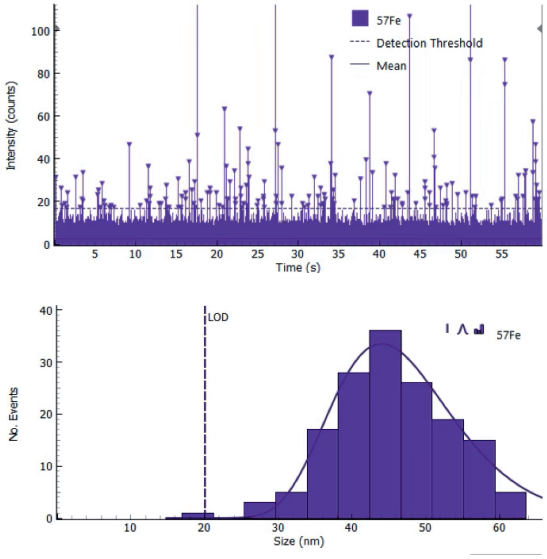


Figure S3. Single particle ICP-MS results from a 12.5 mM treatment, sample after a 1:2000 dilution. A) Time-resolved analysis. B) Histogram of the resulting sizes (Bin size: 4 nm).

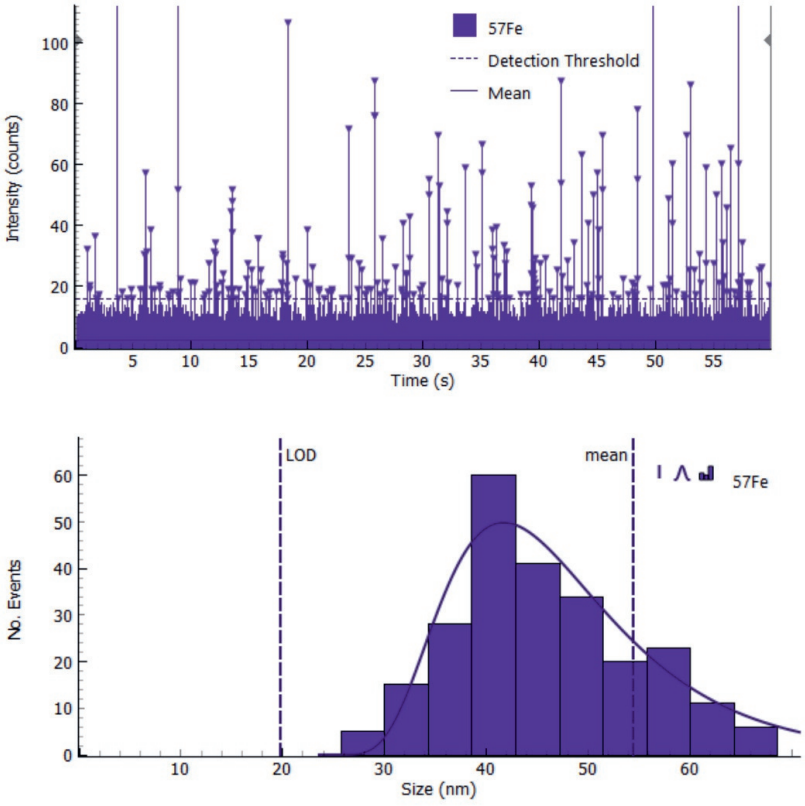


Figure S4. Single particle ICP-MS results from a 125 mM treatment, sample after 1:5000 dilution. A) Time-resolved analysis. B) Histogram with the resulting sizes (Bin size: 4nm).

Table S4. Soluble protein content (mg/ml) of cryomilled freeze dried iron fortified black soldier fly larvae, before and after blanching with standard deviation per treatment. The solubilized proteins are sourced in 10mg of cryomilled freeze dried larvae in 1ml of PBS buffer (Ph7.5). Asterisks denote statistically significant differences between blanched and non-blanched samples ($P < 0.0005 = ***$).

Mineral Soluble protein content (mg/ml)	Control	12.5 mM	125 mM
Non blanched	1.6***± 0.02	1.7***± 0.2	1.9***± 0.1
Blanched	0.9± 0.01	1± 0.05	1± 0.06

CHAPTER

06

General Discussion

1. Main findings

Edible insects have previously been proposed as a novel source of dietary iron, primarily due to two factors, their rapidly growing interest as a sustainable protein source over the past decade, and their relatively high absolute iron content (Mwangi *et al.*, 2018). However, little is known about the absorption and storage form of iron, bioavailability for both animals and humans and potential to manipulate dietary iron in edible insect species. This PhD thesis therefore aimed to elucidate the source and bioavailability of iron in edible insects, focusing on the black soldier fly (BSF) larvae. The research further explored iron biofortification strategies and evaluated their potential to enhance iron content and bioavailability, thereby contributing to sustainable solutions for mitigating iron deficiency in both humans and animals.

In this thesis, BSF larvae were identified as a successful animal model capable of iron biofortification through dietary intervention. By altering the iron concentration in the rearing substrate, BSF larvae were shown to effectively accumulate and regulate iron levels, providing a biological route for iron enrichment. The baseline iron content in BSF larvae already exceeded that of conventional iron sources, including beef and fortified cereals, and fortification further amplified these levels, resulting in an exceptionally iron-rich biomass (Figure 6.1).

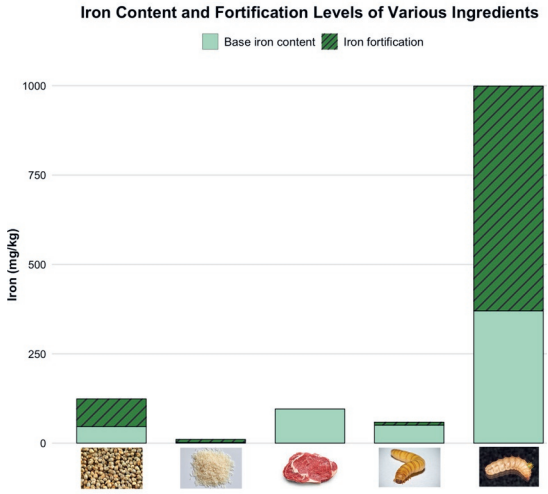


Figure 6.1. Iron content and degree of successful iron biofortification in various food ingredients. Stacked bars represent the total iron concentration (mg/kg DM) for each ingredient, divided into base iron content (light green) and additional iron gained through biofortification (dark green with stripes). Iron biofortification of the plant samples are achieved by either classical breeding or genetic modification, while insect iron biofortification was achieved through substrate manipulation. There are no successful reports of iron biofortification of meats. From left to right: finger millet, rice, beef steak, lesser mealworm larva, and black soldier fly larva. Data adapted from (Boonyaves *et al.*, 2017; First *et al.*, 2024; Teklu *et al.*, 2023).

Iron biofortification experiments established the BSF larvae as a viable model for iron enrichment, providing a foundation for continued investigation into underlying mechanisms and nutritional and processing effects. The main outcomes of this thesis are described below and summarized in Table 6.1. **Chapter 2** reviewed the biology of entoferritin in the context of a dietary iron source. The chapter highlighted entoferritin as a nutritionally relevant iron carrier, characterized by high iron storage capacity, solubility, and stability. Compared to ferritins in plants and animals, entoferritin is larger and naturally water-soluble, making it a distinct and understudied form. Evidence from related ferritins indicates that ferritin-bound iron can be absorbed through mechanisms different from classical non-heme uptake and is less affected by inhibitors such as phytates and polyphenols. The review concluded that entoferritin warrants systematic consideration as a distinct dietary iron source and called for further research which includes iron speciation, entoferritin characterization, and nutritional availability. **Chapter 3** examined the feasibility of insect iron biofortification by rearing the lesser mealworm and the black soldier fly larvae on iron-supplemented substrates. Both species increased their body iron content in response to dietary enrichment, but their tolerance and physiological responses differed markedly. Black soldier fly larvae exhibited a threefold increase in body iron content without reductions in growth or survival, while the iron concentration in the substrate was ten times higher than that used for yellow mealworms. In contrast, yellow mealworm larvae showed decreased survivability under elevated iron conditions. In black soldier fly, iron enrichment was accompanied by moderate co-accumulation of calcium, while both species exhibited a reduction in zinc levels. These findings established the black soldier fly as a promising model for animal-based iron biofortification through substrate manipulation. **Chapter 4** investigated the molecular responses of BSF larvae to iron biofortification using an integrated transcriptomic and proteomic approach combined with tissue-level iron localization. The analyses revealed an increase of about 70% in entoferritin abundancy, largely achieved through post-transcriptional regulation involving iron-responsive proteins such as IRP1 and RSL1D1. System-level responses also linked iron handling to cuticle-associated processes and oxidative stress responses. Dissection and staining showed that fortified iron was predominantly localized in the gut, supporting the view that larvae rely on entoferritin-based compartmentalization to tolerate high mineral loads. This chapter provided mechanistic insight into how BSF can serve as an effective fortification platform. **Chapter 5** addressed the effects of thermal processing and iron biofortified on mineral bioaccessibility in BSF larvae using an *in vitro* digestion model and mineral nanoparticle analysis. The results demonstrated that fortified larvae provided significantly more digestible iron compared to controls. However, under high iron conditions, the relative fraction of bioaccessible iron decreased, likely due to an increased iron-to-entoferritin ratio that reduced entoferritin solubility. Iron nanoparticle characterization showed that fortification and processing influenced

nanoparticle abundance but not size, suggesting that BSF relies on a consistent storage mechanism that scales with iron content, further supporting the entoferritin-based iron accumulation hypothesis presented in **Chapter 4**. Blanching reduced iron solubility, which may indicate partial **entoferritin destabilization**, while calcium solubility and bioaccessibility increased after blanching, underscoring mineral-specific effects of thermal treatment. Overall, iron-fortified BSF larvae represent a promising source of bioavailable dietary iron.

Table 6.1. Overview of thesis chapters, including core research questions, experimental approaches, and main findings.

Chapter	Core question	Experimental approach	Key findings
2. Entoferritin: An innovative iron source for human consumption	Is entoferritin nutritionally relevant and distinct from other ferritins?	Literature review.	· Entoferritin is larger and naturally water-soluble compared with plant/animal ferritins · Ferritin-bound iron uptake? is less affected by phytates/polyphenols and may use alternative uptake routes · Entoferritin presents untapped opportunities as a novel iron source
3. Strike while the iron is hot: Unravelling the impact of dietary iron on two edible insects	How does substrate iron dosing affect edible insects?	Rearing on iron-supplemented substrates, insect parameter analysis, nutritional facts analysis.	· BSF tolerated and accumulated high dietary iron while lesser mealworm showed a survivability decline at iron levels an order of magnitude lower · Calcium accumulated in BSF in an iron dose-dependent manner · Zinc concentration decreased in both species
4. Forged in iron: Molecular insights into iron tolerance in *Hermetia illucens*	What molecular response does iron fortification lead to in the black soldier fly larvae?	Transcriptomics, proteomics, larvae dissection and iron staining.	· Entoferritin abundancy increased by ~70%, driven primarily by post-transcriptional regulation involving IRP1 · Transcriptional and proteomic changes associated with cuticle and exoskeletal processes

Chapter	Core question	Experimental approach	Key findings
5. Built by iron, Changed by heat: Mineral bioaccessibility in iron-fortified and processed *Hermetia illucens* larvae	How does iron fortification and thermal stability affect the mineral bioavailability of the black soldier fly larvae?	*In vitro* mineral bioaccessibility, iron nanoparticle analysis.	· Fortified larvae provided significantly more digestible iron · Blanching reduced iron solubility consistent with entoferritin destabilization · Iron nanoparticles showed similar size but greater abundance with fortification · Calcium bioaccessibility increased after blanching

2. Dietary iron considerations of an entoferritin-based systems

The multi-layer omics analyses and tissue dissections described in Chapter 4, together with the iron nanoparticle characterization presented in Chapter 5, demonstrate that iron biofortification of BSF larvae is based on an entoferritin system for iron storage. Ferritin absorption differs fundamentally from that of heme iron and other inorganic iron sources. Studies in humans and animals have shown that ferritin uptake is not affected by the presence of heme or FeSO, indicating that ferritin follows an independent absorption pathway that does not rely on the Haem Carrier Protein 1 (HCP1) or Divalent Metal Transporter-1 (DMT1) pathways. Instead, ferritin appears to be absorbed, at least in part, as an intact protein complex through enterocytes in the duodenum and upper small intestine. Saturable binding patterns observed in intestinal cell models fed with plant ferritin support a receptor-mediated process. In rats, ferritin-based iron, was shown not only to be absorbed through digestion, but was also incorporated in the body iron pool at a slower rate, strengthening the hypothesis of a distinct iron absorption pathway (Theil *et al.*, 2012). While the specific receptor for non-mammalian ferritin remains unknown, studies on plant ferritin indicate that endocytosis involves clathrin-coated vesicle formation coordinated by the adaptor protein AP2, suggesting that a similar pathway could also operate for entoferritin (Kalgaonkar & Lönnerdal, 2008). A potential candidate in this context is the scavenger receptor class A member 5 (SCARA5), which has been shown to interact with the light-chain subunit of mammalian ferritin and is expressed in intestinal epithelium (Mendes-Jorge *et al.*, 2014). It could therefore represent a part of the missing link in ferritin absorption from non-mammalian sources. Entoferritins tend to be glycosylated on their light-chain units, a modification that might interfere with receptor recognition or binding efficiency

(Pham & Winzerling, 2010). If ferritins do not survive the digestive tract intact, the released iron may still enter via DMT1, but evidence from *in vitro* and *in vivo* models suggests that a substantial fraction of ferritin can endure gastrointestinal conditions long enough to be taken up as a macromolecular complex (Perfecto *et al.*, 2018). Notably, no studies have been dedicated to validating dietary ferritin-based iron absorption patterns in economically relevant livestock, and further research is required.

Ferritin-bound iron is also considerably less affected by antinutritional factors than other non-heme iron sources. Because the iron remains mineralized within the protein shell until degradation inside enterocytes, it is protected from inhibitors such as phytates, polyphenols, and chitin (Lönnerdal, 2007). This point is particularly relevant for insect-based foods, which naturally contain a high amount of chitin. When compared to published work on iron bioaccessibility of mushroom-based burgers, which are similarly high in chitin, the bioaccessible fraction of the BSF larvae presented in Chapter 5 is considerably higher than that reported for mushroom systems, both in the untreated larvae (≈50%) and after thermal processing (≈35%), compared with the mushroom-based samples (≈0–25%). Conversely, the mushroom-based burger study reported that both the polyphenol:iron and phytate:iron ratios were too low to substantially influence mineral bioaccessibility, indicating that inhibitory effects from these compounds are minimal in that system (Luz *et al.*, 2024). In BSF larvae, polyphenols are present at a much lower levels (Camperio *et al.*, 2025; Luz *et al.*, 2024), providing easier comparison as neither matrix is meaningfully influenced by polyphenols or phytates. However, it should be noted that *in vitro* bioaccessibility outcomes can vary substantially across different methodologies, and comparisons between studies should be interpreted with caution (Faubel *et al.*, 2023). In addition to this chitin-rich models comparison, chitin isolated from mealworms has been shown to exert minimal effects on iron solubility during digestion (Mwangi *et al.*, 2022), which further supports the role of an entoferritin-based system in stabilizing iron and protecting it from antinutritional factors under gastrointestinal conditions.

The significant increase in digestible iron in biofortified larvae shown in chapter 5, can be attributed to the entoferritin-based system, which facilitates iron solubility even at high levels of stored iron. However, iron biofortification in BSF larvae also introduces structural alterations that may influence entoferritin behavior. As the iron-to-ferritin ratio increases, ferritin can become less soluble and more prone to aggregation, which may lower the fraction of bioaccessible iron (Irimia-Dominguez *et al.*, 2020). In Chapters 3 and 5, iron levels increased by approximately 150–350% in the biofortified larvae, whereas in Chapter 4, entoferritin abundance increased by about 70% under similar iron fortification conditions. Notably, because the mineral content and protein

abundance were obtained using different rearing batches and distinct methodologies, the iron-to-entoferritin ratio should be interpreted with caution. Nevertheless, the magnitude of the observed differences indicates an increase in this ratio. This relationship suggests that, while ferritin synthesis responds to iron exposure, the degree of protein upregulation may not fully match the extent of iron accumulation, potentially leading to overloaded or aggregated ferritin structures. This trade-off is evident in the reduced bioaccessibility fraction of fortified larvae reported in Chapter 5, indicating that increased iron accumulation may come at the expense of solubility. However, when ferritins lose solubility due to iron overloading, processing or digestion, this does not necessarily mean that its iron core is released. The mineralized core can remain immobilized within the protein shell even when precipitated (Everett *et al.*, 2020; Muhoberac *et al.*, 2010), assumed to lower potential for oxidative stress or mucosal irritation compared to freely soluble iron salts, as the iron remains bound within the protein complex rather than contributing to oxidative stress or mucosal irritation. Evidence also supports the persistence of the mineral core structure in entoferritin following partial protein dissociation. In non-reducing SDS–PAGE, where disulfide bonds remain intact and only non-covalent interactions are disrupted, entoferritin subunits are partially separated. The semi-intact protein complex remains visible when stained for iron, indicating that the mineralized core is retained even after partial breakdown of the protein shell (Rosas-Arellano *et al.*, 2016). Additional supporting evidence was obtained from preliminary, unpublished work shown in Figure 6.2, in which entoferritin was purified from blanched lesser mealworms (Alphitobius diaperinus) using potassium bromide (KBr) density gradient centrifugation following the protocol of Gutiérrez *et al.* (2013). Aggregated and precipitated entoferritin appeared structurally intact under transmission electron microscopy (TEM).

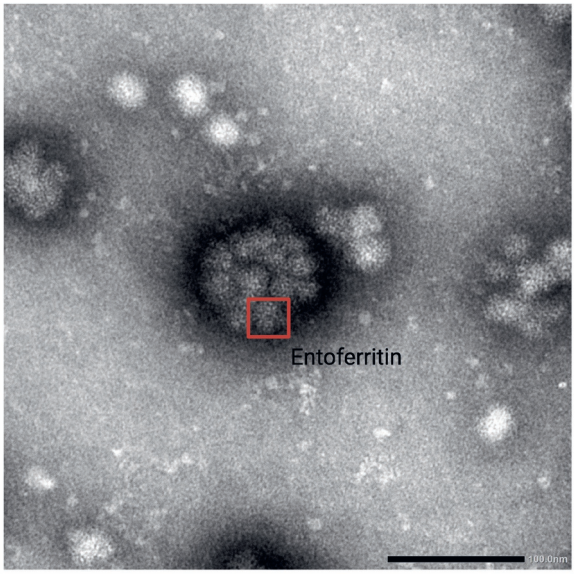


Figure 6.2. Transmission electron micrograph of purified entoferritin from blanched lesser mealworms *(Alphitobius diaperinus).* Samples were prepared and stained based on the protocol provided by Nocera *et al.* (2014). The red square marks an individual entoferritin complex within an aggregated cluster. Attached aggregates in the clusters are also assumed to be entoferritins. Scale bar = 100 nm.

At present, little is known about the detailed biochemical characteristics of entoferritin, and even less about those of BSF. Similarly, the effects of iron loading on ferritin structure and solubility in insects remain uncharacterized. However, based on what is known from mammalian and plant ferritins and the results provided in this thesis, it is reasonable to assume that the fundamental relationships between iron saturation, protein stability, and solubility are conserved. Understanding these relationships in BSF larvae will require further study of entoferritin stability during both processing and digestion, alongside the impact of iron loading under biofortification. Addressing these aspects will be essential for evaluating the nutritional potential of BSF ferritin and for translating these biochemical insights into practical applications for sustainable iron fortification.

3. Substrate factors influencing black soldier fly larvae iron uptake

Beyond the structural and stability-related aspects of entoferritin that affect the nutritional potential of BSF as an iron source, the mechanisms by which BSF larvae acquire and absorb iron from their substrates must also be considered. Similar to humans, non-heme iron absorption in insects occurs primarily via uptake of the

ferrous (Fe^{2+}) form. Most iron present in plant-based insect diets exists in the insoluble ferric (Fe^{3+}) form, which must be reduced before absorption can occur. FIRE (Ferric Iron Reductase) and FIRE-like enzymes have recently been identified as key catalysts of ferric iron (Fe^{3+}) reduction in the *Drosophila* gut (Soltani *et al.*, 2025), functioning analogously to duodenal cytochrome B (DCYTB) in mammals, which performs a similar role during dietary iron absorption. Malvolio (Mvl) transporter, the *Drosophila* homolog of DMT1, facilitates the transport of ferrous iron and other divalent metals from the gut lumen into enterocytes, particularly in the acidic midgut region, and is localized mainly to the plasma membrane of midgut cells. This represents the first step in intestinal dietary iron absorption in insects. As with non-heme iron uptake via DMT1 in humans, soluble ferrous iron in the insect gut must remain in the reduced state to prevent chelation or precipitation (Gorman, 2023). Consequently, substrate formulations intended for BSF iron fortification should aim to minimize anti-nutritional factors known to inhibit iron absorption in humans, such as phytates, tannins, and polyphenols (Piskin *et al.*, 2022), which may exert similar effects in insects. An example is that cooking pinto beans increased iron bioavailability in a Caco-2 cell model by reducing the concentration of procyanidins, a class of tannins known to inhibit iron absorption (Wiesinger *et al.*, 2021). One variable that may differentiate the understanding of iron-related anti-nutritional factors in mammals from that in BSF larvae is the role of the peritrophic matrix (PM) in defense against iron overload, as described in Chapter 4. The observation that iron binds to the PM under medium (12.5 mM) and high (125 mM) dietary iron conditions, but not under control conditions, suggests that the PM has both a threshold concentration at which iron binding begins and a finite capacity for iron retention. These characteristics may determine the bioavailability of dietary iron for absorption. Given that iron biofortification in insects is a novel concept and that the extent of iron manipulation achieved in BSF larvae is unprecedented, future research should investigate how substrate composition, processing, anti-nutritional factors and the PM, influence iron uptake and bioavailability. Translating these biochemical considerations into applied rearing strategies requires attention to the practical and regulatory dimensions of BSF feed formulation.

4. Integrating substrate design and regulation for iron fortification in BSF larvae

In both conventional livestock and insect farming, feed formulation largely concentrates on conversion efficiency, biomass yield, and macronutrient composition (Oonincx, van Broekhoven, *et al.*, 2015; Rauw *et al.*, 2025). Black soldier fly larvae production has followed this same trajectory, with most efforts directed toward maximizing protein output and waste conversion efficiency (Janssen *et al.*, 2017; Scala *et al.*, 2020). The

findings of this thesis demonstrate that BSF can also be deliberately enriched with minerals through substrate manipulation, pointing to the need for a broader outlook that integrates performance with nutritional enrichment. As shown in chapter 3, BSF larvae reared on unfortified chicken feed, already contains high levels of essential minerals, particularly iron, and larval feed formulation provides a means to further enhance this natural advantage. The experiments in this thesis focused on the larval physiological response to high dietary iron. To minimize experimental variability, the substrate composition was kept constant except for the iron salt concentration. While this approach enabled mechanistic insights, it limits industrial applicability, as such iron salts are already common as an iron supplementation for humans and as feed additives for target livestock species (Friendship *et al.*, 2021; Lorinczova *et al.*, 2021). Accordingly, future work should evaluate naturally iron rich substrates to determine whether similar levels of enrichment can be achieved under realistic production conditions.

Within the European context, as a "farmed animal" the use of BSF larvae for iron fortification is currently constrained by substrate regulations under Article 3(6) of Regulation (EC) No. 1069/2009, which permits rearing only on materials of vegetal origin and selected animal-derived by-products, notably fish waste and non-ruminant blood products (Meijer *et al.*, 2025; EU, 2019). As exemplified in Table 6.2, these exceptions are particularly relevant to iron fortification, as several approved substrates already contain appreciable iron levels. For instance, sugar beet pulp, abundant within the European Union, contains approximately 625 mg Fe/kg dry matter, making it one of the few plant-based side streams that combine high iron content with regulatory approval (Feed tables, 2024). Other vegetal residues such as cocoa pod husk and coconut coir waste also exhibit relatively high iron concentrations but scarcely available in Europe (Barrios-Rodríguez *et al.*, 2022; Patil *et al.*, 2018).

Table 6.2. Reported iron concentrations (mg/kg dry matter) in selected agricultural and animal-derived waste streams and by products that could serve as substrates for black soldier fly larvae rearing.

Category	Material/Stream	Iron Content (mg/kg DM)	Approved as insect feed in EU
Plant	Coconut coir waste	1,100 (Patil *et al.*, 2018)	Yes
	Sugar beet pulp	600 (Feed tables, 2024)	Yes
	Cocoa pod husk	600 (Barrios-Rodríguez *et al.*, 2022)	Yes
Animal	Fish scales (Chitala)	13,600 (Begum *et al.*, 2021)	Yes
	Chicken litter	5,700 (Ehlert, 2017)	No
	Cow manure	1,500 (Men *et al.*, 2020)	No
	Non ruminant blood meals (chicken, duck and pork)	1,400-1,800 (Csurka *et al.*, 2021)	Yes

Animal-derived side streams generally provide even higher iron concentrations. Fish scales, for example, can exceed 13,000 mg Fe/kg. A study demonstrated that using fish waste, including scales, as the sole substrate for BSF rearing is technically feasible but negatively affects larval survival and yield (Begum *et al.*, 2021). Nevertheless, this approach resulted in a high degree of iron fortification in the larvae, reaching approximately 800 mg Fe/kg DM in the BSF larvae yield. When fish waste was combined with other organic side streams, larval performance improved, and although the resulting iron concentration was somewhat lower, it remained substantial, at around 600 mg Fe/kg (Ogello *et al.*, 2025). While these results indicate strong potential for mineral enrichment, the mechanisms and optimal strategies for using fish waste and scales as substrates for iron biofortification are still not well understood. Regardless, utilization of such high-iron fish by-products is permitted under current EU regulations and remains largely underexploited (Coppola *et al.*, 2021; EU, 2019), despite their clear potential to contribute to iron enrichment in BSF larvae.

Another approved high iron feed are bloodmeals (EU, 2019). While rich in high-quality heme iron, bloodmeals are already extensively valorized in both animal and pet feed industries. Introducing BSF larvae as an intermediate step for utilizing blood meal

would be counterproductive, as it would convert readily bioavailable heme iron into entoferritin-based non-heme iron, while losing part of the original heme fraction in the process (Csurka *et al.*, 2021).

Among currently non-permitted by-products, chicken litter stands out as a particularly promising candidate for BSF rearing, containing approximately 5,700 mg Fe/kg. Managing chicken litter has become a major global concern, and BSF rearing has been proposed as an effective strategy for its reduction and valorization (Kullan *et al.*, 2025a). Black soldier fly has been proposed as an agent for chicken litter management. However, studies evaluating larval performance on chicken litter remain scarce and inconclusive. Some evidence suggests that the growth and survival of larvae reared on chicken litter are comparable to those reared on standard chicken feed (Broeckx *et al.*, 2021), while other studies report lower larval weight and pupation rates on this substrate (Schreven *et al.*, 2022). Yet, most research has focused on waste management applications, with limited attention to larval growth performance and nutritional outcomes (Kullan *et al.*, 2025b). For instance, previous studies have optimized the use of chicken litter through approaches such as fermentation and manipulation of substrate physical properties, resulting in a reduction of more than 75% in litter volume and the conversion of this major waste stream into two valuable products, insect biomass for feed and nutrient-rich frass for fertilizer (Rehman *et al.*, 2019). Further studies should investigate the fundamental biological responses of BSF larvae reared on chicken litter, including growth dynamics and nutrient composition. Notably, larvae generally perform better on fresh manure than on dried, rehydrated material (Broeckx *et al.*, 2021; Oonincx, van Huis, *et al.*, 2015; Schreven *et al.*, 2022). This advantage restricts opportunities for controlled manipulation of substrate composition in iron biofortification applications.

As mentioned above, chicken litter is not permitted as a feed ingredient for any livestock in the EU, including insects. This restriction primarily stems from concerns about pathogenic contamination (EU, 2009). To assess this risk, a recent study examined the microbial load of BSF larvae reared on chicken litter. Strains of *Escherichia coli* and *Staphylococcus spp.*, both of which include species with pathogenic potential, were detected in the larvae. However, the study also demonstrated that sun-drying and oven-drying treatments substantially reduced their abundance (Prudence *et al.*, 2025). Beyond microbial safety, an increasing trend of heavy metal contamination has been reported in poultry litter, with elevated concentrations of elements such as cadmium and lead. These contaminants often originate from feed, water, or soil polluted through industrial activities, including fossil fuel production, pesticide use, and chemical manufacturing (Aljohani, 2023). As BSF larvae can bioaccumulate metals from their substrate (Diener *et al.*, 2015), the use of chicken litter requires monitoring to ensure safety for feed or food applications.

In the scope of iron biofortification, one study reported approximately 400 mg Fe/kg in larvae reared directly on chicken manure, indicating that this substrate can naturally promote elevated iron levels compared to conventional feeds (Ogello *et al.*, 2025). However, there is still a general lack of understanding regarding the mechanisms and potential of chicken litter as a substrate for targeted iron fortification. Given its high iron content and abundance, employing BSF for the bioconversion of chicken litter could simultaneously enhance manure management and provide an iron-enriched feed source for pigs and aquaculture.

5. Black soldier fly thermal processing from a dietary iron perspective

Larval feed formulation highlights the potential of BSF larvae as a vehicle for iron enrichment. However, the nutritional value of the final ingredient also depends on post-harvest processing. Thermal treatments such as blanching, drying, or cooking are essential for microbial safety and shelf stability of insects, yet they influence mineral solubility and bioaccessibility (Borremans *et al.*, 2020; Manditsera *et al.*, 2019; Son *et al.*, 2023). Ferritins are generally considered thermally stable proteins. For example, mammalian ferritins with similar heavy-to-light chain ratios typically exhibit melting points above 100 °C (Srivastava *et al.*, 2023). Moderate heating between 60 °C and 80 °C, as shown for seed ferritins in the same study, can enhance ferritin stability and promote monodispersity. In contrast, exposure to higher temperatures (≥ 90 °C) induces structural rearrangements in seed ferritins, potentially reducing their solubility (Tang *et al.*, 2019). The thermal stability limits of entoferritin remain unknown, but evidence from entoferritin purification procedures suggests that these complexes can withstand temperatures up to approximately 75 °C, a condition often used during purification to denature less stable proteins (Wajnberg *et al.*, 2018).

In Chapter 5, *in vitro* digestion experiments revealed that boiling (≈ 100–105 °C) markedly reduced iron solubility and bioaccessibility in BSF larvae, suggesting that entoferritin complexes were destabilized and aggregated under these conditions. The larvae were vacuum cooked for two minutes, with a temperature exceeding this required by the European Food Safety Authority for approved edible insects such as the yellow mealworm, which specifies a minimum of 90 °C for two minutes for safe insect consumption (Turck *et al.*, 2021). Although not specifically approved yet, it has been shown that heating BSF larvae at 90 °C reduced main pathogen levels under the detection level while maintaining similar protein digestibility as the control groups (Campbell *et al.*, 2020). To optimize BSF as a dietary iron source, future research should

therefore determine how minimal thermal processing requirements affect iron digestibility, with particular attention to entoferritin stability.

Moreover, ferritin stability has been shown to decrease when the protein is heavily iron-loaded, as observed in mammalian systems (Irimia-Dominguez *et al.*, 2020). This aligns with the results of Chapter 5, where blanching reduced iron bioaccessibility by approximately 30% in control larvae and by about 45% in iron-fortified larvae (125 mM treatment). Hence, evaluating how moderate processing temperatures, around 90 °C, affect the digestibility of iron-biofortified BSF larvae will be essential for balancing microbial safety with nutritional retention.

From a feed application viewpoint, the thermal treatments effect of dietary iron can be avoided. Under EU regulation, it is possible to feed live BSF larvae as both feed and pet food (Meijer*et al.*, 2025; EU, 2019). Although *in vivo* confirmation is needed, live iron biofortified larvae can be fed to pigs and treated as iron enriched ingredient. However, while live BSF larvae can be used directly in feed, their application in food or shelf-stable products will necessarily involve thermal processing, making the effects of heat on entoferritin stability and mineral bioavailability unavoidable.

6. Prospects for iron-fortified black soldier fly larvae as a human food source

The use of BSF larvae as food for humans is currently neither permitted by regulation nor common in practice (European commission, 2025). One of the few documented examples of BSF consumption occurs in the Sabah region of Malaysia, where people traditionally consume raw BSF larvae (Chung *et al.*, 2002). Nonetheless, the same attributes that make BSF larvae an appealing and sustainable feed ingredient, such as high nutrient density, efficient bioconversion, and feedstock flexibility, also make it a promising candidate for future food applications (Ogello *et al.*, 2025; Weko *et al.*, 2023). In terms of consumer perception, willingness-to-try surveys in North America indicate that BSF-based foods are regarded with a level of acceptability comparable to more established edible insects such as mealworms and crickets (Higa *et al.*, 2021). Likewise, in Belgium, replacing 25% of the butter in waffle formulations with BSF larvae fat did not negatively affect consumer acceptance (Delicato *et al.*, 2020). These findings suggest that, although regulatory approval is still lacking, social and sensory barriers to BSF as food may be less restrictive than previously assumed. In addition to social acceptance, the nutritional relevance of BSF larvae, particularly in the context of dietary iron, provides another perspective on their potential as food.

In Zimbabwe, Mopane worms, traditionally consumed as food, have been incorporated into porridges to evaluate their potential as an iron source, illustrating the feasibility of using insect-derived ingredients to alleviate micronutrient deficiencies (Ledbetter *et al.*, 2024). Compared to the Mopane worm, which typically contain 40–80 mg/kg iron on a dry matter basis, iron-fortified BSF contained 300–1000 mg/kg (First *et al.*, 2024; Nemadodzi *et al.*, 2023). Iron biofortification of BSF through larval feed formulation therefore offers a practical route to create food ingredients with several-fold higher iron levels than those used in existing food fortification trials. Further research is required to evaluate the performance of BSF in fortified foods such as porridges, particularly in light of the discrepancies observed in iron bioavailability between mealworms and crickets in controlled studies. These studies showed that mealworm iron was absorbed at levels comparable to ferrous sulfate, whereas cricket iron was significantly less bioavailable, underscoring the need to evaluate the bioavailability of BSF-derived iron before its use in food fortification can be established (Hilaj *et al.*, 2022; Mwangi *et al.*, 2022). While live BSF larvae may serve directly as a fortified feed ingredient, human consumption will require processing for safety and acceptability (Rumpold & Schlüter, 2013). Building on the results of Chapter 5 and the thermal considerations discussed in subchapter 6.5, the key challenge is to identify milder processing methods to maximize iron bioavailability while maintaining microbial safety.

At the same time, processing effects extend beyond iron. As shown in Chapter 5, blanching at boiling temperatures markedly increased calcium bioaccessibility, likely due to the breakdown of lime glands during heating. Considering that iron biofortified BSF larvae also contain approximately 30 g Ca/kg DM, meaning that a 30 g portion of fresh larvae provides more calcium than a glass of milk containing 240 mg Ca (First *et al.*, 2024; Guéguen & Pointillart, 2000). This increase in calcium solubility during processing could substantially enhance their nutritional value. This highlights the need to optimize thermal treatments to ensure microbial safety while preserving entoferritin-bound iron and supporting the release of other nutritionally relevant minerals. Moreover, the incorporation of BSF into diverse food matrices should be assessed within this framework, as interactions with antinutritional factors can further influence mineral bioavailability (Samtiya *et al.*, 2020). Understanding how processing and matrix composition influence mineral bioavailability will be key to translating BSF larvae into reliable, biofortified food ingredients.

7. Rethinking the European edible insect industry

Approximately five years ago, the edible insect industry in the Global North was heralded as a future-proof, high-tech, and heavily funded sector, primarily envisioned

as a new source of sustainable human food. It was portrayed as a field poised for rapid industrialization, with visions of fully automated facilities managing everything from egg production to final consumer products under one roof. Large companies attracted hundreds of millions in venture capital, and optimistic forecasts predicted scalable manufacturing, "lights-off" fully automated factories, reducing costs while simultaneously achieving global sustainability goals and revolutionizing protein production (IPIFF, 2019).

However, over the past few years, the edible insect industry has faced severe structural and financial challenges. Rising substrate and labor costs, technological limitations, restricted legislative approval for human consumption, and limited public acceptance have collectively prevented farmed insects from becoming a mainstream food source. After a peak in 2021, it seems that the number of investments deals in the sector is gradually declining (Figure 6.3; Sagar Shah, 2024). It should be noted that the decline in investment observed since 2021 is not unique to the insect sector but is also evident across other alternative protein markets, including plant-based, fermentation-derived, and cultivated proteins (Anay Mridul, 2025). Major European companies such as Ÿnsect and Enorm have experienced significant setbacks, including funding shortages, high operational costs, and difficulties in reliably scaling biological production, leading to major layoffs and restructurings (Elaine Watson, 2025; Jane Byrne, 2025). As an example, the international Platform of Insects for Food and Feed (IPIFF) presented a report in 2019, which estimated that the European edible insect sector will produce 3-5 million tons of insect material annually. As it stands for 2024, the estimation is that by 2030, the European insect industry will produce between 221-500K tons of insect material annually (IPIFF, 2019; Sagar Shah, 2024). Reports indicate that high labor and electricity costs in Europe, substrate limitation and declining investor confidence have led to downsizing, suspended projects, and the offshoring of production to lower-cost regions (Rossi *et al.*, 2025; Ryba, 2024; Sagar Shah, 2024). While these constraints have slowed progress in Europe, the global insect industry follows a different trajectory, driven mainly by the Asia-Pacific region, which currently accounts for about 40% of market activity and is projected to expand further (Sepehr Achard, 2025).

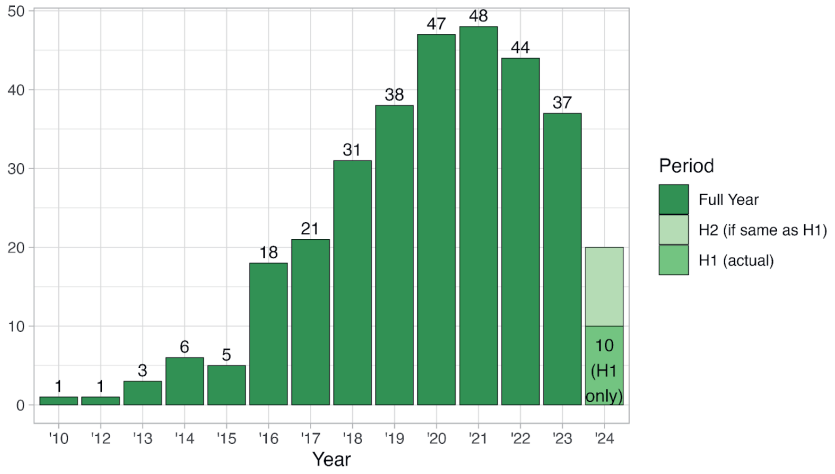


Figure 6.3. Annual investments into insect farming by number of announced deals. Published by Sagar Shah (2024).

Given these developments, there is currently no indication that insects as human food will have a substantial impact on the European food system in the foreseeable future. Furthermore, the addition of an extraction step to recover a specific molecule such as entoferritin would only be applicable under a standardized and automated large-scale production, which minimize rearing variability (Sun *et al.*, 2025; Voutilainen *et al.*, 2021). In contrast, the use of BSF larvae presents more immediate opportunities in addressing pressing challenges such as waste management and the environmental footprint of animal feed. For this potential to be realized, two key developments are necessary, a reduction in substrate costs through the broader use of BSF larvae for waste valorization, and advances in automation technology to reduce labor dependency and operational costs.

8. Global realignment of the farmed insect sector

An instructive example of a developing BSF industry can be found in China. Although increasing, labor costs there are considerably lower than in the EU, reducing the economic pressure to automate production (Liuyi *et al.*, 2023). Moreover, the climate, tropical and subtropical with high humidity, also provides a natural advantage, lowering energy requirements and creating ideal conditions for BSF rearing. The most critical regulatory distinction lies in substrate legislation. In China, BSF larvae are widely used

for waste management, including catering waste, and subsequently as animal feed, an approach that remains largely prohibited in the EU (Liu *et al.*, 2023; EU, 2009). A broader economic shift is also reshaping BSF applications in China, following trade tensions that led China to reduce soy imports from the United States (Klebanov, 2025), the local government is prioritizing catering waste as pig feed. Notably, edible insects are also mentioned as a focus feed for pigs (Cao & Thukral, 2025). As this practice expands, the need for BSF larvae as catering waste recyclers has diminished, leading to a shift toward rearing BSF on chicken manure. This shift is visible with specific research on the subject, related patents and example for industrial scale and small-scale plants in China and neighboring countries (Cai *et al.*, 2024; Ezra Cheung, 2024; Newsmarket, 2023; Zhao Heshan, 2016). This industrial shift will lead to the rearing of BSF larvae under high iron conditions, and the iron biofortification should be taken into consideration. Thus, the findings of this thesis should provide insights into substrate management strategies aimed at maximizing the micronutrient content of BSF larvae under such evolving production systems.

A smaller scale but equally relevant perspective can be found in sub-Saharan Africa. As in China, lower labor costs and favorable climatic conditions provide a natural advantage for BSF rearing. Most initiatives in this region focus on small-scale, circular agricultural systems. These typically involve using BSF larvae to process animal manure, particularly from poultry, thereby accelerating and improving fertilizer quality while generating larvae for use as animal feed (Mukonoweshuro & Callender, 2023; Shumo *et al.*, 2019; Zirp, 2022). Similarly, the shift toward utilizing BSF for manure management and lesser legislative constrains can benefit from a deeper understanding of iron biofortification mechanisms. Given the dual challenges of protein insufficiency and iron deficiency prevalent in many developing regions, iron-biofortified BSF larvae produced on readily available substrates could serve not only as animal feed but also as a promising, sustainable food ingredient for human consumption.

Taken together, these developments point to a global realignment of the farmed insect sector, from its early vision of supplying human food toward a more practical focus on waste valorization. Regions such as China and sub-Saharan Africa are already demonstrating how BSF rearing can integrate into local waste management systems, converting organic residues into insect biomass suitable for animal feed and potentially edible applications, along with nutrient-rich frass for fertilizer. These implementations also represent environments where BSF are increasingly reared on high-iron waste streams, particularly chicken manure, making the insights from this thesis on iron biofortification particularly relevant to their emerging production systems. In contrast, Europe's restrictive substrate regulations and high production

costs continue to limit progress, preventing the industry from realizing its potential as a circular waste-management solution. Advancing BSF production in Europe will ultimately depend on broadening substrate regulations and identifying opportunities for automation to lower labor costs, both of which are necessary for scaling the system under current economic and legislative conditions. In addition, the European Union's stringent novel food authorization process would pose a significant barrier to the future introduction of BSF-based foods. Obtaining approval typically requires several years of evaluation, often around five, and the resulting authorization can impose restrictions on producers, processing methods, and end-use specifications (EU, 2015). Given the high costs, regulatory and market uncertainties, and lengthy approval timelines, pursuing a novel food application for BSF would currently be a challenging and economically risky endeavor. Dedicated efforts, and dramatic shifts in the EU novel food approval systems are needed if it is to address human macro- and micronutrient needs.

9. Conclusions and future perspective

Edible insects have been proposed as promising alternative iron source due to their high iron content and sustainable advantages (Mwangi *et al.*, 2018). Among them, BSF larvae contain significant levels of iron under physiological conditions and represent the most economically feasible edible insect for large-scale and small-scale production alike (Ogello *et al.*, 2025; Seyedalmoosavi *et al.*, 2023). In this thesis, the potential for iron biofortification in BSF larvae through substrate manipulation was explored. The larvae were shown to more than triple their iron content via an entoferritin-based mechanism, without compromising survival, growth, or development time. Moreover, larvae reared on iron-enriched substrates provided significantly higher levels of digestible iron *in vitro* bioaccessibility assays. Because most of the accumulated iron was stored in entoferritin form, BSF-derived iron is expected to be both bioavailable and safer for consumption than commonly used inorganic iron salts (Karregat *et al.*, 2025).

This thesis established a mechanistic understanding of iron storage and demonstrated the feasibility of increasing larval iron content. Building on that, future research should assess how efficiently this iron is absorbed *in vivo* to determine its true nutritional potential. Both iron bioavailability and possible gut irritation should be evaluated in relevant models, particularly humans and pigs.

Furthermore, future studies should assess how effectively BSF larvae can absorb iron from less soluble sources and from substrates containing varying levels of anti-

nutritional factors. Fish waste and chicken litter as two promising substrates for waste valorization into iron-rich feed and food ingredients. Substrate processing methods and substrate combinations should be assessed from a biofortification perspective to maximize iron enrichment. Although the European Union currently prohibits the use of chicken litter as a substrate, fish waste offers an immediate, high-iron, and underutilized alternative that could be explored within existing regulations (EFSA, 2024). Given the processing losses observed in this thesis, the use of live BSF larvae may help retain iron bioavailability. Current EU regulations already permit the inclusion of live BSF larvae in livestock feed, and live iron-biofortified larvae should therefore be considered a practical option for delivering bioavailable iron without the post-harvest losses presented in this thesis.

Further characterization of entoferritin is essential to understand its structural stability, iron-loading capacity, and behavior during processing and digestion. Such insights will provide the basis for optimizing both iron biofortification and post-harvest handling strategies. While current findings indicate that thermal treatments can reduce iron bioaccessibility, particularly in iron-biofortified larvae, future research should focus on refining processing methods that maintain microbial safety while preserving entoferritin integrity and maximizing iron bioavailability. In addition, the bioavailability of iron from both fortified and unfortified BSF larvae should be evaluated in diverse food matrices to identify optimal integration strategies for feed and human food applications.

Finally, in regions where iron deficiency anemia is highly prevalent and access to heme-based iron sources such as meat is limited, there is an urgent need to identify new, locally sustainable alternatives. Sub-Saharan Africa, where above 60% of children suffer from iron deficiency anemia, exemplifies this challenge (Tesema *et al.*, 2021). In such contexts, iron-fortified BSF larvae reared on high-iron substrates could be integrated into human diets as a multifunctional food ingredient, providing not only high-quality protein and fat but also a valuable source of bioavailable iron. While such settings represent an immediate opportunity, BSF's development as a human food ingredient should also progress in other regions, given its potential to recycle organic waste into foods that provide both high-quality protein and dietary iron.

Reference:

Aljohani, A. S. M. (2023). Heavy metal toxicity in poultry: a comprehensive review. Frontiers in Veterinary Science, 10, 1161354. https://doi.org/10.3389/fvets.2023.1161354

Anay Mridul. (2025, May). What Do 2025's Investment Trends So Far Tell Us About Alternative Proteins? Green Queen. https://www.greenqueen.com.hk/alternative-protein-funding-investment-trends-q1-2025/

Barrios-Rodríguez, Y. F., Salas-Calderón, K. T., Orozco-Blanco, D. A., Gentile, P., & Girón-Hernández, J. (2022). Cocoa Pod Husk: A High-Pectin Source with Applications in the Food and Biomedical Fields. ChemBioEng Reviews, 9(5), 462–474. https://doi.org/ https://doi.org/10.1002/cben.202100061

Begum, M., Mzuam, M., & Satter, M. A. (2021). Nutritional profiling of selected fish's scales: An approach to determine its prospective use as a biomaterial. International Journal of Fisheries and Aquatic Studies, 9(3), 26–31.

Boonyaves, K., Wu, T.-Y., Gruissem, W., & Bhullar, N. K. (2017). Enhanced Grain Iron Levels in Rice Expressing an Iron-regulated Metal Transporter, Nicotianamine Synthase, and Ferritin. Frontiers in Plant Science, 8, 130. https://doi.org/10.3389/fpls.2017.00130

Borremans, A., Bußler, S., Sagu, S. T., Rawel, H., Schlüter, O. K., & Leen, V. C. (2020). Effect of Blanching Plus Fermentation on Selected Functional Properties of Mealworm (*Tenebrio molitor*) Powders. Foods, 9(7). https://doi.org/10.3390/foods9070917

Broeckx, L., Frooninckx, L., Slegers, L., Berrens, S., Noyens, I., Goossens, S., Verheyen, G., Wuyts, A., & Van Miert, S. (2021). Growth of Black Soldier Fly Larvae Reared on Organic Side-Streams. Sustainability, 13(23). https://doi.org/10.3390/su132312953

Cai, T., Ming, Y., Zhang, Y., & Zhang, Q. (2024). Unraveling the role of black soldier fly larvae in chicken manure conversion: Facilitating maturation and enhancing humification. The Science of the Total Environment, 952, 175952. https://doi.org/10.1016/j.scitotenv.2024.175952

Campbell, M., Ortuño, J., Stratakos, A. Ch., Linton, M., Corcionivoschi, N., Elliott, T., Koidis, A., & Theodoridou, K. (2020). Impact of Thermal and High-Pressure Treatments on the Microbiological Quality and *in vitro* Digestibility of Black Soldier Fly (*Hermetia illucens*) Larvae. Animals, 10(4). https://doi.org/10.3390/ani10040682

Camperio, J., Suarez, J. A., Simonton, J., Paresky, E., Parodi, J., & Benetti, D. D. (2025). Valorizing Organic Waste Through Black Soldier Fly Larvae (*Hermetia illucens*): A Sustainable Solution for Aquafeeds with Key Nutrients and Natural Bioactive Polyphenols. Sustainability, 17(5). https://doi.org/10.3390/su17051788

Cao, E., & Thukral, N. (2025, June). China's big feed shift to curb soybean imports, strain small farmers. Reuters. https://www.reuters.com/markets/commodities/chinas-big-feed-shift-curb-soybean-imports-strain-small-farmers-2025-06-18/

Chung, A. Y. C., Chey Vun Khen, C. V. K., Sining Unchi, S. U., & Momin Binti, M. B. (2002). Edible insects and entomophagy in Sabah, Malaysia. 56(2), 131–144. https://www.cabidigitallibrary.org/doi/full/10.5555/20033021703

Coppola, D., Lauritano, C., Palma Esposito, F., Riccio, G., Rizzo, C., & de Pascale, D. (2021). Fish Waste: From Problem to Valuable Resource. Marine Drugs, 19(2). https://doi.org/10.3390/md19020116

Csurka, T., Pásztor-Huszár, K., Tóth, A., Németh, C., & Friedrich, F. L. (2021). Animal blood, as a safe and valuable resource. 35, 41–47. https://www.cabidigitallibrary.org/doi/full/10.5555/20210461331

Delicato, C., Schouteten, J. J., Dewettinck, K., Gellynck, X., & Tzompa-Sosa, D. A. (2020). Consumers' perception of bakery products with insect fat as partial butter replacement. Food Quality and Preference, 79, 103755. https://doi.org/https://doi.org/10.1016/j.foodqual.2019.103755

Diener, S., Zurbrügg, C., & Tockner, K. (2015). Bioaccumulation of heavy metals in the black soldier fly, *Hermetia illucens* and effects on its life cycle. Journal of Insects as Food and Feed, 1(4), 261–270. https://doi.org/https://doi.org/10.3920/JIFF2015.0030

EFSA. (2024). Live insects in animal feed: what European Regulation says (and what it does not). https://ipiff.org/live-insects/

Ehlert, P. (2017). Agronomic effectivity of Poultry Litter Ash. Wageningen Environmental Research, Wageningen. https://www.bmcmoerdijk.nl/app/uploads/2022/02/Agronomic-Effectivity-of-Poultry-Litter-Ash-WUR-Alterra-BMC-Moerdijk.pdf

Elaine Watson. (2025, September). Ÿnsect wins more time to restructure under court-supervised process; Innovafeed's US plans 'very much alive.' Agfundernews. https://agfundernews.com/ynsect-wins-more-time-to-restructure-under-court-supervised-

process-innovafeeds-us-plans-very-much-alive

European commission. (2025, January). Approval of another insect/insect-derived food as a Novel Food. https://food.ec.europa.eu/food-safety/novel-food/authorisations/approval-insect-novel-food_en

Everett, J., Brooks, J., Lermyte, F., O'Connor, P. B., Sadler, P. J., Dobson, J., Collingwood, J. F., & Telling, N. D. (2020). Iron stored in ferritin is chemically reduced in the presence of aggregating A(1-42). Scientific Reports, 10(1), 10332. https://doi.org/10.1038/s41598-020-67117-z

Ezra Cheung. (2024). Will Hong Kong's only industrial-scale chicken waste treatment plant be forced to shut down? https://www.scmp.com/news/hong-kong/health-environment/article/3263272/will-hong-kongs-only-industrial-scale-chicken-waste-treatment-plant-be-forced-shut-downhttps://www.baguio.com.hk/upload/news_center/14/pdf2/SCMP_20240520_1716194812.pdf

Faubel, N., Cilla, A., Alegría, A., Barberá, R., & Garcia-Llatas, G. (2023). Overview of *in vitro* digestion methods to evaluate bioaccessibility of lipophilic compounds in foods. Food Reviews International, 39(9), 7126–7147. https://doi.org/10.1080/87559129.2022.2143520

Feed tables. (2024). Beet pulp, dried. Feed tables. https://www.feedtables.com/content/beet-pulp-dried

First, T., Van Haeften, A. J., Oonincx, D. G. A. B., Van Loon, J. J. A., Fogliano, V., & Mishyna, M. (2024). Strike while the iron is hot: unravelling the impact of dietary iron on two edible insects. Journal of Insects as Food and Feed, 11(7), 1187–1200. https://doi.org/https://doi.org/10.1163/23524588-00001422

Friendship, R., Seip, V., & Amezcua, R. (2021). A comparison of 4 iron supplementation protocols to protect suckling piglets from anemia. The Canadian Veterinary Journal = La Revue Veterinaire Canadienne, 62(1), 55–58. https://www.ncbi.nlm.nih.gov/pubmed/33390600

Gorman, M. J. (2023). Iron Homeostasis in Insects. Annual Review of Entomology, 68(Volume 68, 2023), 51–67. https://doi.org/https://doi.org/10.1146/annurev-ento-040622-092836

Guéguen, L., & Pointillart, A. (2000). The Bioavailability of Dietary Calcium. Journal of

the American College of Nutrition, 19(sup2), 119S-136S. https://doi.org/10.1080/07315724.2000.10718083

Gutiérrez, L., Zubow, K., Nield, J., Gambis, A., Mollereau, B., Lázaro, F. J., & Missirlis, F. (2013). Biophysical and genetic analysis of iron partitioning and ferritin function in *Drosophila melanogaster*. Metallomics, 5(8), 997–1005. https://doi.org/10.1039/c3mt00118k

Higa, J. E., Ruby, M. B., & Rozin, P. (2021). Americans' acceptance of black soldier fly larvae as food for themselves, their dogs, and farmed animals. Food Quality and Preference, 90, 104119. https://doi.org/https://doi.org/10.1016/j.foodqual.2020.104119

Hilaj, N., Zimmermann, M. B., Galetti, V., Zeder, C., Murad Lima, R., Hammer, L., Krzystek, A., Andlauer, W., & Moretti, D. (2022). The effect of dechitinization on iron absorption from mealworm larvae (*Tenebrio molitor*) flour added to maize meals: stable-isotope studies in young females with low iron stores. The American Journal of Clinical Nutrition, 116(4), 1135–1145. https://doi.org/https://doi.org/10.1093/ajcn/nqac210

IPIFF. (2019). The European insect sector today: challenges, opportunities and regulatory landscape. https://ipiff.org/wp-content/uploads/2019/12/2019IPIFF_VisionPaper_updated.pdf

Irimia-Dominguez, J., Sun, C., Li, K., Muhoberac, B. B., Hallinan, G. I., Garringer, H. J., Ghetti, B., Jiang, W., & Vidal, R. (2020). Cryo-EM structures and functional characterization of homo- and heteropolymers of human ferritin variants. Scientific Reports, 10(1), 20666. https://doi.org/10.1038/s41598-020-77717-4

Jane Byrne. (2025, May). Enorm rethinking insect production business model. AgTechNavigator. https://www.agtechnavigator.com/Article/2025/05/05/enorm-seeks-new-investors-to-relaunch-operations/

Janssen, R. H., Vincken, J.-P., van den Broek, L. A. M., Fogliano, V., & Lakemond, C. M. M. (2017). Nitrogen-to-Protein Conversion Factors for Three Edible Insects: *Tenebrio molitor*, Alphitobius diaperinus, and *Hermetia illucens*. Journal of Agricultural and Food Chemistry, 65(11), 2275–2278. https://doi.org/10.1021/acs.jafc.7b00471

Kalgaonkar, S., & Lönnerdal, B. (2008). Receptor-mediated uptake of ferritin-bound iron by human intestinal Caco-2 cells. The Journal of Nutritional Biochemistry, 20(4), 304–311. https://doi.org/10.1016/j.jnutbio.2008.04.003

Karregat, J. H. M., Meulenbeld, A., Quee, F. A., Novotny, V. M. J., Swinkels, D. W., van den Born, B.-J. H., Zaaijer, H. L., Twisk, J. W. R., & van den Hurk, K. (2025). Ferritin-guided iron supplementation as an alternative or complement to prolonged blood donation intervals (FORTE): a double-blind, randomised, controlled trial. The Lancet Haematology, 12(9), e694–e704. https://doi.org/10.1016/S2352-3026(25)00167-X

Klebanov, S. (2025, September). China buys zero soybeans from the US. Morning Brew. https://www.morningbrew.com/stories/2025/09/26/china-buys-zero-soybeans-from-the-us

Kullan, A. R. K., Suresh, A., Choi, H. L., Gabriel Neumann, E., & Hassan, F. (2025a). Bioconversion of Poultry Litter into Insect Meal and Organic Frasstilizer Using Black Soldier Fly Larvae as a Circular Economy Model for the Poultry Industry: A Review. Insects, 16(1). https://doi.org/10.3390/insects16010012

Kullan, A. R. K., Suresh, A., Choi, H. L., Gabriel Neumann, E., & Hassan, F. (2025b). Bioconversion of Poultry Litter into Insect Meal and Organic Frasstilizer Using Black Soldier Fly Larvae as a Circular Economy Model for the Poultry Industry: A Review. Insects, 16(1). https://doi.org/10.3390/insects16010012

Ledbetter, M., Wilkin, J. D., Mubaiwa, J., Angeline Manditsera, F., Macheka, L., Matiza Ruzengwe, F., Madimutsa, O. N., Chopera, P., Matsungo, T. M., Cottin, S. C., Stephens, E. W., Ranawana, V., & Fiore, A. (2024). Development of a nutritious cereal-based instant porridge by the incorporation of protein-rich insect powder – An example from Zimbabwe. Journal of Functional Foods, 112, 105957. https://doi.org/https://doi.org/10.1016/j.jff.2023.105957

Liu, T., Liu, H., Wei, G., Zhao, H., Gong, Y., Guo, X., & Zhang, Y. (2023). Comprehensive assessment of food waste treatment emission reduction in China: a life cycle perspective. Environmental Science and Pollution Research, 30(37), 87669–87684. https://doi.org/10.1007/s11356-023-28622-6

Liuyi, Y., Yunchan, Z., & Feirong, R. (2023). Does government investment push up manufacturing labor costs? Evidence from China. Humanities and Social Sciences Communications, 10(1), 694. https://doi.org/10.1057/s41599-023-02180-1

Lönnerdal, B. (2007). The importance and bioavailability of phytoferritin-bound iron in cereals and legume foods. International Journal for Vitamin and Nutrition

Research. Internationale Zeitschrift Fur Vitamin- Und Ernahrungsforschung. Journal International de Vitaminologie et de Nutrition, 77(3), 152–157. https://doi.org/10.1024/0300-9831.77.3.152

Lorinczova, H. T., Begum, G., Renshaw, D., & Zariwala, M. G. (2021). Acute administration of bioavailable curcumin alongside ferrous sulphate supplements does not impair iron absorption in healthy adults in a randomised trial. Nutrients, 13(7). https://doi.org/10.3390/nu13072300

Luz, G. M., Orlando, E. A., Rebellato, A. P., Greiner, R., & Pallone, J. A. L. (2024). Essential minerals and anti-nutritional compounds in plant-based burgers using the infogest *in vitro* digestion protocol. Journal of Food Composition and Analysis, 135, 106574. https://doi.org/https://doi.org/10.1016/j.jfca.2024.106574

Macwan, S., S. P. de Souza, T., Dunshea, F. R., DiGiacomo, K., & Suleria, H. A. R. (2023). Black soldier fly larvae (Hermetica illucens) as a sustainable source of nutritive and bioactive compounds, and their consumption challenges. Animal Production Science, 64(1), AN23192. https://doi.org/10.1071/AN23192

Manditsera, F. A., Luning, P. A., Fogliano, V., & Lakemond, C. M. M. (2019). Effect of domestic cooking methods on protein digestibility and mineral bioaccessibility of wild harvested adult edible insects. Food Research International, 121, 404–411. https://doi.org/https://doi.org/10.1016/j.foodres.2019.03.052

Meijer, N., Safitri, R. A., Tao, W., & Hoek-Van den Hil, E. F. (2025). Review: European Union legislation and regulatory framework for edible insect production – Safety issues. Animal, 19, 101468. https://doi.org/https://doi.org/10.1016/j.animal.2025.101468

Men, Y., Zheng, L., Zhang, L., Li, Z., Wang, X., Zhou, X., Cheng, S., & Bao, W. (2020). Effects of Adding Zero Valent Iron on the Anaerobic Digestion of Cow Manure and Lignocellulose. Frontiers in Bioengineering and Biotechnology, 8, 590200. https://doi.org/10.3389/fbioe.2020.590200

Mendes-Jorge, L., Ramos, D., Valença, A., López-Luppo, M., Pires, V. M. R., Catita, J., Nacher, V., Navarro, M., Carretero, A., Rodriguez-Baeza, A., & Ruberte, J. (2014). L-Ferritin Binding to Scara5: A New Iron Traffic Pathway Potentially Implicated in Retinopathy. Plos one, 9(9), e106974-. https://doi.org/10.1371/journal.pone.0106974

Muhoberac, B. B., Baraibar, M. A., & Vidal, R. (2010). Iron loading-induced aggregation and reduction of iron incorporation in heteropolymeric ferritin containing a mutant

light chain that causes neurodegeneration. Biochimica et Biophysica Acta, 1812(4), 544–548. https://doi.org/10.1016/j.bbadis.2010.10.010

Mukonoweshuro, T. F., & Callender, N. (2023, August). Green Protein: Farming Black Soldier Fly Larvae in Zimbabwe. World Bank Blogs. https://blogs.worldbank.org/en/africacan/green-protein-farming-black-soldier-fly-larvae-afe-zimbabwe

Mwangi, M. N., Oonincx, D. G. A. B., Hummel, M., Utami, D. A., Gunawan, L., Veenenbos, M., Zeder, C., Cercamondi, C. I., Zimmermann, M. B., van Loon, J. J. A., Dicke, M., & Melse-Boonstra, A. (2022). Absorption of iron from edible house crickets: a randomized crossover stable-isotope study in humans. The American Journal of Clinical Nutrition. https://doi.org/10.1093/ajcn/nqac223

Mwangi, M. N., Oonincx, D. G. A. B., Stouten, T., Veenenbos, M., Melse-Boonstra, A., Dicke, M., & Van Loon, J. J. A. (2018). Insects as sources of iron and zinc in human nutrition. Nutrition Research Reviews, 31(2), 248–255. https://doi.org/10.1017/S0954422418000094

Nemadodzi, L. E., Managa, G. M., & Prinsloo, G. (2023). The Use of Gonimbrasia belina (Westwood, 1849) and Cirina forda (Westwood, 1849) Caterpillars (Lepidoptera: Sarturniidae) as Food Sources and Income Generators in Africa. Foods, 12(11). https://doi.org/10.3390/foods12112184

Newsmarket. (2023, September). With black soldier flies, chicken manure disappears, and chickens still have insects to eat! A card box achieves a natural and odorless agricultural waste recycling. Newsmarket.

Nocera, T. M., Zeng, Y., & Agarwal, G. (2014). Distinguishing ferritin from apoferritin using magnetic force microscopy. Nanotechnology, 25(46), 461001. https://doi.org/10.1088/0957-4484/25/46/461001

Ogello, E. O., Outa, N. O., Muthoka, M., Juma, F., & Hoinkis, J. (2025). Optimizing Black Soldier Fly (*Hermetia illucens*) production: effects of substrate variation on biomass, nutritional quality, hatchability, fecundity, and frass quality. Frontiers in Sustainable Food Systems, Volume 9-2025. https://doi.org/10.3389/fsufs.2025.1621034

Oonincx, D. G. A. B., van Broekhoven, S., van Huis, A., & van Loon, J. J. A. (2015). Feed Conversion, Survival and Development, and Composition of Four Insect Species on Diets Composed of Food By-Products. PLOS ONE, 10(12), e0144601-. https://doi.org/10.1371/journal.pone.0144601

Oonincx, D. G. A. B., van Huis, A., & van Loon, J. J. A. (2015). Nutrient utilisation by black soldier flies fed with chicken, pig, or cow manure. Journal of Insects as Food and Feed, 1(2), 131–140. https://doi.org/https://doi.org/10.3920/JIFF2014.0023

Patil, S. S., Kasture, M. C., & Dhopavkar, R. V. (2018). Micro-nutrient Enriched Vermicompost by Coconut Coir Waste. Int. J. Curr. Microbiol. App. Sci, 7(06), 2352–2361. https://doi.org/10.20546/ijcmas.2018.706.281

Perfecto, A., Rodriguez-Ramiro, I., Rodriguez-Celma, J., Sharp, P., Balk, J., & Fairweather-Tait, S. (2018). Pea ferritin stability under gastric pH conditions determines the mechanism of iron uptake in Caco-2 cells. Journal of Nutrition, 148(8), 1229–1235. https://doi.org/10.1093/jn/nxy096

Pham, D. Q. D., & Winzerling, J. J. (2010). Insect ferritins: Typical or atypical? Biochimica et Biophysica Acta - General Subjects, 1800(8), 824–833. https://doi.org/10.1016/j.bbagen.2010.03.004

Piskin, E., Cianciosi, D., Gulec, S., Tomas, M., & Capanoglu, E. (2022). Iron Absorption: Factors, Limitations, and Improvement Methods. ACS Omega, 7(24), 20441–20456. https://doi.org/10.1021/acsomega.2c01833

Prudence, M., Ester, L., Joyce, M., Misheck, S., Mazuba, S., Todd, J., Ngawo, N., Phenny, M., & Mudenda, H. B. (2025). Bacteriological quality of fresh and processed black soldier fly *Hermetia illucens* larvae reared on chicken manure in Kitwe, Zambia. Microbiology Spectrum, 13(8), e00570-24. https://doi.org/10.1128/spectrum.00570-24

Rauw, W. M., Baumgard, L. H., & Dekkers, J. C. M. (2025). Review: Feed efficiency and metabolic flexibility in livestock. Animal, 19(1), 101376. https://doi.org/https://doi.org/10.1016/j.animal.2024.101376

Regulation (EC) No 767/2009 of the European Parliament and of the Council of 13 July 2009 on the Placing on the Market and Use of Feed, Amending European Parliament and Council Regulation (EC) No 1831/2003 and Repealing Council Directive 79/373/EEC, Commission Directive 80/511/EEC, Council Directives 82/471/EEC, 83/228/EEC, 93/74/EEC, 93/113/EC and 96/25/EC and Commission Decision 2004/217/EC (Text with EEA Relevance) (2009).

Regulation (EC) No 1069/2009 of the European Parliament and of the Council of 21 October 2009 Laying down Health Rules as Regards Animal by-Products and Derived

Products Not Intended for Human Consumption and Repealing Regulation (EC) No 1774/2002 (Animal by-Products Regulation) (2019).

Regulation (EU) 2015/2283 of the European Parliament and of the Council of 25 November 2015 on Novel Foods, Amending Regulation (EU) No 1169/2011 of the European Parliament and of the Council and Repealing Regulation (EC) No 258/97 of the European Parliament and of the Council and Commission Regulation (EC) No 1852/2001 (Text with EEA Relevance) (2015).

Rehman, K. ur, Ur Rehman, R., Somroo, A. A., Cai, M., Zheng, L., Xiao, X., Ur Rehman, A., Rehman, A., Tomberlin, J. K., Yu, Z., & Zhang, J. (2019). Enhanced bioconversion of dairy and chicken manure by the interaction of exogenous bacteria and black soldier fly larvae.
Journal of Environmental Management, 237, 75–83. https://doi.org/https://doi.org/10.1016/j.jenvman.2019.02.048

Rosas-Arellano, A., Vásquez-Procopio, J., Gambis, A., Blowes, L. M., Steller, H., Mollereau, B., & Missirlis, F. (2016). Ferritin Assembly in Enterocytes of *Drosophila melanogaster*. International Journal of Molecular Sciences, 17(2). https://doi.org/10.3390/ijms17020027

Rossi, G., Psarianos, M., Ojha, S., & Schlüter, O. K. (2025). Review: Insects as a novel feed ingredient: processing technologies, quality and safety considerations. Animal, 19, 101495. https://doi.org/https://doi.org/10.1016/j.animal.2025.101495

Rumpold, B. A., & Schlüter, O. K. (2013). Nutritional composition and safety aspects of edible insects. Molecular Nutrition & Food Research, 57(5), 802–823. https://doi.org/https://doi.org/10.1002/mnfr.201200735

Ryba, R. (2024). Offshoring insect farms may jeopardize Europe's food sovereignty. Global Sustainability, 7, e31. https://doi.org/DOI: 10.1017/sus.2024.35

Sagar Shah. (2024). Insect farming: investment trends and projected production capacity. https://rethinkpriorities.org/research-area/investments-into-insect-farming/?gad_source=1&gad_

Samtiya, M., Aluko, R. E., & Dhewa, T. (2020). Plant food anti-nutritional factors and their reduction strategies: an overview. Food Production, Processing and Nutrition, 2(1), 6. https://doi.org/10.1186/s43014-020-0020-5

Scala, A., Cammack, J. A., Salvia, R., Scieuzo, C., Franco, A., Bufo, S. A., Tomberlin, J. K., & Falabella, P. (2020). Rearing substrate impacts growth and macronutrient composition of *Hermetia illucens* (L.) (Diptera: Stratiomyidae) larvae produced at an industrial scale. Scientific Reports, 10(1), 19448. https://doi.org/10.1038/s41598-020-76571-8

Schreven, S. J. J., de Vries, H., Hermes, G. D. A., Zeni, G., Smidt, H., Dicke, M., & van Loon, J. J. A. (2022). Black Soldier Fly Larvae Influence Internal and Substrate Bacterial Community Composition Depending on Substrate Type and Larval Density. Applied and Environmental Microbiology, 88(10), e0008422. https://doi.org/10.1128/aem.00084-22

Sepehr Achard. (2025). Insect Farming's Role in Food Production. IGrow News. https://igrownews.com/insect-farming-a-sustainable-solution-to-global-protein-needs/

Seyedalmoosavi, M. M., Mielenz, M., Schleifer, K., Görs, S., Wolf, P., Tränckner, J., Hüther, L., Dänicke, S., Daș, G., & Metges, C. C. (2023). Upcycling of recycled minerals from sewage sludge through black soldier fly larvae (*Hermetia illucens*): Impact on growth and mineral accumulation. Journal of Environmental Management, 344, 118695. https://doi.org/https://doi.org/10.1016/j.jenvman.2023.118695

Shumo, M., Osuga, I. M., Khamis, F. M., Tanga, C. M., Fiaboe, K. K. M., Subramanian, S., Ekesi, S., van Huis, A., & Borgemeister, C. (2019). The nutritive value of black soldier fly larvae reared on common organic waste streams in Kenya. Scientific Reports, 9(1), 10110. https://doi.org/10.1038/s41598-019-46603-z

Soltani, S., Yan, M., Yu, Q., Abd Elhafiz, A., Pfriem, E., Webb, S. M., Kroll, T., Bahena Lopez, J. M., Missirlis, F., & King-Jones, K. (2025). New molecular components of high and low affinity iron import systems in *Drosophila*. Nature Communications, 16(1), 5662. https://doi.org/10.1038/s41467-025-60758-6

Son, J., Park, S. H., Jung, H. J., You, S. J., & Kim, B. G. (2023). Effects of Drying Methods and Blanching on Nutrient Utilization in Black Soldier Fly Larva Meals Based on *in vitro* Assays for Pigs. Animals: An Open Access Journal from MDPI, 13(5). https://doi.org/10.3390/ani13050858

Srivastava, A. K., Scalcione, L. J., Arosio, P., & Bou-Abdallah, F. (2023). Hyperthermostable recombinant human heteropolymer ferritin derived from a novel plasmid design. Protein Science: A Publication of the Protein Society, 32(1), e4543. https://doi.org/10.1002/pro.4543

Sun, S., Yu, Y., Jo, Y., Han, J. H., Xue, Y., Cho, M., Bae, S.-J., Ryu, D., Park, W., Ha, K.-T., & Zhuang, S. (2025). Impact of extraction techniques on phytochemical composition and bioactivity of natural product mixtures. Frontiers in Pharmacology, 16, 1615338. https://doi.org/10.3389/fphar.2025.1615338

Tang, J., Yu, Y., Chen, H., & Zhao, G. (2019). Thermal Treatment Greatly Improves Storage Stability and Monodispersity of Pea Seed Ferritin. Journal of Food Science, 84(5), 1188–1193. https://doi.org/https://doi.org/10.1111/1750-3841.14581

Teklu, D., Gashu, D., Joy, E. J. M., Lark, R. M., Bailey, E. H., Wilson, L., Amede, T., & Broadley, M. R. (2023). Impact of zinc and iron agronomic biofortification on grain mineral concentration of finger millet varieties as affected by location and slope. Frontiers in Nutrition, 10, 1159833. https://doi.org/10.3389/fnut.2023.1159833

Tesema, G. A., Worku, M. G., Tessema, Z. T., Teshale, A. B., Alem, A. Z., Yeshaw, Y., Alamneh, T. S., & Liyew, A. M. (2021). Prevalence and determinants of severity levels of anemia among children aged 6–59 months in sub-Saharan Africa: A multilevel ordinal logistic regression analysis. PLOS ONE, 16(4), e0249978-. https://doi.org/10.1371/journal.pone.0249978

Theil, E. C., Chen, H., Miranda, C., Janser, H., Elsenhans, B., Núñez, M. T., Pizarro, F., & Schümann, K. (2012). Absorption of Iron from Ferritin Is Independent of Heme Iron and Ferrous Salts in Women and Rat Intestinal Segments. The Journal of Nutrition, 142(3), 478–483. https://doi.org/10.3945/jn.111.145854

Turck, D., Bohn, T., Castenmiller, J., De Henauw, S., Hirsch-Ernst, K. I., Maciuk, A., Mangelsdorf, I., McArdle, H. J., Naska, A., Pelaez, C., Pentieva, K., Siani, A., Thies, F., Tsabouri, S., Vinceti, M., Cubadda, F., Frenzel, T., Heinonen, M., Marchelli, R., … Knutsen, H. K. (2021). Safety of frozen and dried formulations from whole yellow mealworm (*Tenebrio molitor* larva) as a novel food pursuant to Regulation (EU) 2015/2283. EFSA Journal, 19(8), e06778. https://doi.org/https://doi.org/10.2903/j.efsa.2021.6778

Voutilainen, E., Pihlajaniemi, V., & Parviainen, T. (2021). Economic comparison of food protein production with single-cell organisms from lignocellulose side-streams. Bioresource Technology Reports, 14, 100683. https://doi.org/https://doi.org/10.1016/j.biteb.2021.100683

Wajnberg, E., Alves, O. C., Perales, J., da Rocha, S. L. G., Ferreira, A. T., Cameron, L. C., Esquivel, D. M. S., & de Lourdes Barriviera, M. (2018). Ferritin from the haemolymph

of adult ants: an extraction method for characterization and a ferromagnetic study. European Biophysics Journal, 47(6), 641–653. https://doi.org/10.1007/s00249-018-1293-3

Weko, M. R., Bao, F., Ega, M. E., Mia, H., Una, K. S. I., Viana, M., Wale, L., Nalle, C. L., Burithnaban, Y. M., Lema, A. T., Helda, & Asrul. (2023). Nutrient Profile Black Soldier Fly Larvae (Hermetia Illucence): Effect Of Feeding Substrate And Harvested Time. Biotropia, 30(3), 297–307. https://doi.org/10.11598/btb.2023.30.3.1903

Wiesinger, J. A., Osorno, J. M., McClean, P. E., Hart, J. J., & Glahn, R. P. (2021). Faster cooking times and improved iron bioavailability are associated with the down regulation of procyanidin synthesis in slow-darkening pinto beans (Phaseolus vulgaris L.). Journal of Functional Foods, 82, 104444. https://doi.org/https://doi.org/10.1016/j.jff.2021.104444

Zhao Heshan. (2016). Chicken manure treatment method and system based on black soldier flies (Patent CN106070073A).

Zirp, zimbabwe. (2022, August). Buhera rural farmers turning household waste into value. Zimbabwe Idai Recovery Project. https://zirp-zimbabwe.org/news/buhera-rural-farmers-turning-household-waste-into-value/

Scientific Summary

Background and aim:

Iron deficiency remains one of the most prevalent micronutrient deficiencies worldwide, while sustainable and bioavailable iron sources are still limited. Edible insects, particularly Hermetia illucens (black soldier fly; BSF), have emerged as promising alternatives due to their high mineral content and efficient feed conversion. However, the mechanisms regulating iron uptake, storage, and utilization under elevated dietary iron conditions remain poorly understood. This thesis investigates how BSF larvae respond to increasing dietary iron levels, examining effects on larval physiology, nutritional composition, iron storage, and mineral bioaccessibility, providing insight into the potential of BSF as a sustainable iron source for animal feed and human food.

Methods:

A multidisciplinary framework was applied, combining literature research, controlled rearing experiments, omics analyses, histological localization, and digestion studies. **Chapter 2** reviewed entoferritin, the primary iron-binding protein in insects, describing its structure, function, and nutritional relevance. **Chapter 3** examined the effects of increasing dietary iron, supplied as ferric ammonium citrate, on growth, survival, and mineral composition of BSF and yellow mealworm larvae. **Chapter 4** combined transcriptomic and proteomic analyses to characterize the molecular response of BSF to elevated dietary iron, with parallel dissections to localize iron accumulation across larval tissues. **Chapter 5** applied an in vitro digestion model coupled with iron nanoparticle characterization to evaluate mineral bioaccessibility across biofortification levels and thermal processing conditions.

Results:

Chapter 2 reviewed entoferritin as the primary insect iron-binding protein, highlighting its high mineralization capacity, pH stability, and structural similarity to vertebrate ferritin, properties supporting its relevance as a bioavailable dietary iron source. In **Chapter 3**, increasing dietary iron produced a dose-dependent rise in BSF larval iron content, reaching nearly a threefold increase at the highest treatment level, without affecting larval growth, survival, or macronutrient composition. Calcium concentration increased by approximately 20% at the highest iron level. In contrast, yellow mealworm showed limited iron accumulation and reduced survival at far

lower iron concentrations, indicating substantially lower tolerance. **Chapter 4** revealed pronounced transcriptomic and proteomic shifts under elevated dietary iron, including approximately 70% increases in both entoferritin subunit abundances, driven by post-transcriptional regulatory mechanisms. Histological imaging localized iron clusters to the midgut across all biofortification levels, consistent with entoferritin-based sequestration. Additional pathway changes were observed in metal transport, oxidative stress response, and exoskeletal formation. **Chapter 5** demonstrated significantly higher digestible iron in biofortified larvae compared to controls. Iron nanoparticle characteristics remained consistent across treatments, indicating a conserved storage mechanism. Thermal processing reduced iron bioaccessibility while increasing calcium solubilization, demonstrating mineral-specific effects of blanching.

Conclusions:

This thesis demonstrates that BSF efficiently regulates and accumulates dietary iron without impairing growth or survival. Elevated dietary iron triggered coordinated molecular responses, including increased entoferritin abundance and activation of oxidative stress and metal transport pathways, accompanied by localized midgut iron storage. Digestion studies confirmed higher digestible iron in biofortified larvae, while thermal processing reduced iron bioaccessibility but enhanced calcium availability. These findings provide fundamental mechanistic knowledge supporting iron-biofortified BSF as a sustainable ingredient for animal feed and, in the future, human food.

Appendices

ACKNOWLEDGMENTS

The past 4.5 years have truly been a rollercoaster. Reaching the end of this journey would not have been possible without the support, guidance, and encouragement of many people, and I am deeply grateful to all of them. My sincere apologies to anyone I may unintentionally forget.

First and foremost, I would like to thank **my supervision team**. **Maryia**, our journey together started a long time ago. Beyond teaching me the fundamentals of food science and biochemistry, you gave me something far more valuable as a supervisor. No matter how crazy, naive, or overly ambitious my ideas were, I always felt that you had my back. You supported me through brainstorming, challenged me to think more critically, and provided me with the freedom and environment to carry out my experiments to the best of my ability. I will always cherish the many work trips we shared during this period. If I counted correctly, we visited five different countries together, with at least one more to come. Thank you for everything. I am very happy that I will remain here for now, and I hope we will continue working together in the years ahead. **Vincenzo**, thank you for opening the very first door for me five years ago. You believed in my idea from the beginning and helped polish it into something strong enough to pursue. By giving me the opportunity and supporting me in applying for the prize that ultimately funded this PhD, you made this journey possible. I am also deeply grateful for your scientific insight throughout these years, even during the times when I may not have listened as carefully as I should have, although melting only one machine is still a relatively good outcome. Beyond the PhD itself, your support for my trips to Mexico and your patience with the many complications I inevitably created were deeply appreciated. As this chapter closes, I am honored that you have opened yet another door for me to continue my journey at FQD. Thank you for your continued trust and belief in me.

I would also like to thank the people who may not have been official supervisors on paper, but in practice were essential mentors and guides along the way. **Dennis**, I always appreciated our small conversations in parking lots and inside the rearing chambers. You taught me how to properly rear insects, and this knowledge became the foundation that allowed my experiments to succeed. Without those skills, this PhD would not have been possible. Thank you for sharing your expertise and for always being willing to help. **Fanis**, our conversations began about four years ago, sparked by our shared fascination with iron binding proteins. This grew into a wonderful collaboration and several memorable and enjoyable days in the entomology lab. You helped me develop a more critical scientific mindset, and thanks to you, I am confident that I have become a better scientist. **Joop,** you have been part of my Wageningen journey since the very

beginning, during my MSc thesis. Thank you for your continuous support and interest in my work. Your deep expertise in entomology was an invaluable source of knowledge, and I am grateful for your willingness to share it.

My **international collaborators**, **Hunter** (our work together was so fun for me!), **Florencia** and **Federico** from team Mississippi, **Maria, Jorg, Carlos** and **Miguel** from team Oviedo, **Valentina, Simona** and **Andrea** from team Napoli, and **Fanis** from Mexico City, it was a privilege working with you. Our collaborations made this journey richer, more enjoyable, and truly international.

My **professional collaborators**, **Protifarm (Ynsect)** and **Protix,** thank you for your collaboration, support, and for helping translate science into real-world impact.

FQD, my second home. This group became so much more than just a workplace.

Corine and **Lisa**, thank you for making sure everything behind the scenes always runs smoothly. Thank you especially for always helping me with my weird requests, and obviously I have a lot.

The **technician crew,** past and present: **Erik, Frans, Jelle, Anastasia, Xandra, Christos, Marjanne, Jochem, Nienke, Charlotte** and **Geert**, you are the backbone of FQD. You keep these too busy labs alive.

All my colleagues at FQD, thank you for making this journey so fun and unforgettable.

To my **thesis students**, **David, Floor, Lin, Amée, Stephan, Jesper, Bart, Ciske** and **Dafni**, thank you, I have learned so much from you.

The **Mexico committee**, together we made the impossible happen and created an amazing trip. **Andrea**, I am sorry you had to go to a place without sourdough for two weeks. **Laura**, one day we will have guac on the beach again. **Danielle**, the cat queen, no one can compete with your coons. **Qing**, although it was way after the trip, we will always have baby metal. And finally **Jolien**, it must really annoy you that not only I am stronger than you, I am now officially more educated than you.

Obaid, Rutger, Lucas, Andrea and **Yifan**, *BOYS ARE WEAK!*

Teresa, although I still don't work for you, we are one step closer, we will get there!

The **X1114 family**, everchanging and everlasting, thank you for the constant support, chaos, and memories. **Diana**, you were the first to take me in and introduce me to the fun part of FQD, and I am sure we will stay good friends no matter where we end up. **Xuan**, you were an amazing replacement for Diana, love how we share the love for good foods and how you always help me and use your mafia power when needed. **Marianna**, the Aunt from abroad, I love every time we get to see each other. **Andrea**, Dr. IR. Cum Laude. POS. Son of a baker. Olive oil. You are so full of swag that David Zilber almost knows your name. **Marialena**, you are misunderstood and more bad than good, and I am sure you would kill for a comeback. Regardless, you are family to me, and thank you for everything. **Laura**, we had a lot of fun together, ate so much, and saw so many bands. I am sure you will always be a big part of my life, and *"don't worry about it"*.

To the outside WUR **friends from around the world**, thank you for always giving me energy, fun times and perspective!

Leia, Roy, Assaf and **Hans**, thank you for always being there for me and enjoying my amazing fun facts.

Rona, the most important one. Thank you for always being there for me and for being my partner in everything in life. This title is as much yours as it is mine.

Ima and **Aba**, thank you for giving me the confidence, support, and freedom to pursue what I wanted. You always made me feel proud of myself, and that means everything to me.

Again, thank you all and sorry for the hassle.

ABOUT THE AUTHOR



Tomer First was born on May 3, 1992, in Ramat Gan, Israel. He completed his BSc degree in Plant Agroecology at the Hebrew University of Jerusalem, Rehovot campus, in 2019. During his undergraduate studies, he developed a strong interest in sustainable food systems and alternative protein sources.

He then moved to the Netherlands to pursue a Master's degree in Plant Sciences, with a specialization in Entomology, at Wageningen University. During his MSc, he focused on edible insects through two thesis projects. His first MSc thesis, titled *"Behavioural bioassay of Hermetia illucens under stress conditions,"* investigated behavioural traits of black soldier fly larvae under environmental stress conditions and their interactions with substrates. His second thesis, titled *"Sensory analysis of cookies fortified by insects,"* evaluated the sensory profile and nutritional properties of cookies fortified with insect powders, as well as consumer perception of insect-based food products.

In 2021, he was awarded the TKI Green Sector Prize for his PhD proposal, which provided a full research scholarship to pursue doctoral studies in the Food Quality and Design group at Wageningen University. His PhD research focused on dietary iron in edible insects and strategies to manipulate iron content and bioavailability.

Following the completion of his PhD, Tomer started his postdoctoral research in the Food Quality and Design group at Wageningen University, where he continues to work on dietary iron and its manipulation in edible insects.

LIST OF PUBLICATIONS

This thesis

First, T., Fogliano, V., & Mishyna, M. (2023). Entoferritin: An innovative iron source for human consumption. Journal of Functional Foods, 108, 105711.

First, T., Van Haeften, A. J., Oonincx, D. G. A. B., Van Loon, J. J. A., Fogliano, V., & Mishyna, M. (2024). Strike while the iron is hot: unravelling the impact of dietary iron on two edible insects. Journal of Insects as Food and Feed, 11(7), 1187-1200.

First, T., de Boer, J., Gomez-Sanchez, M., López-Portugués, C., Bettmer, J., Montes-Bayón, M., Oonincx, D.G., Fogliano, V. and Mishyna, M., (2026). Built by Iron, changed by heat: Mineral bioaccessibility in iron-fortified and processed Hermetia illucens larvae. Food Chemistry, 148923.

This thesis (pre-print)

First, T., Walt, H., Ciaravolo, V., Arena, S., Scaloni, A., Missirlis, F., Meyer, F., Hoffmann, F.G., van Loon, J.J., Oonincx, D. and Fogliano, V., Forged in Iron: Molecular Insights into Iron Tolerance in *Hermetia illucens.*

Other Publications

Mishyna, M., Hirnet, J., Mancini, S., Grabowski, T.N., Nowacka, M., **First, T**., Kouřimská, L. and Kulma, M., (2025). Teaching about edible insects: design and insights from the summer school “Insects as food: From farm to fork”. Journal of Insects as Food and Feed, 1(aop), 1-12.

OVERVIEW OF COMPLETED TRAINING ACTIVITIES

Descipline-specific activities		
Name of the course/meeting	**Organizing institute (s)**	**Year**
Protein quality control for down-stream processes	EMBL	2022
ERRAZE @WUR event	ERRAZE	2022
Food proteins	VLAG	2024
IFW 2024	Singapore government/Nutrition technolo-gies/potenga	2024
Traditional foods for the future	WUR+Zambia university	2025
Ghent insect summer school	Ghent	2023

General courses		
Name of the course/meeting	**Organizing institute (s)**	**Year**
VLAG PhD week	VLAG	2022
Introduction to R	VLAG	2022
Career perspectives	WGS	2025
Mindful Productivity for scientists -Online	WGS	2025
Efficient Writing Strategies	WGS	2022

Assisting in teaching and supervision activities	
Code and name of the course	**Year**
Insects as Food and Feed (ENT21306) (Practicals)	2023
Insects as Food and Feed (ENT21306) (Case study)	2023

Other Activities	
Name	**Year**
PhD research proposal	2022
FQD champion colloquia	2022-2025
FQD colloquia	2022-2025
PhD trip	2024
Head of PhD trip committee	2022-2024

Layout by Tomer First and Rona David
Cover design by Tomer First and Rona David

Printed by ProefschriftMaken | www.proefschriftmaken.nl